Title
Water-Soluble BODIPY Dyes for Membrane Potential Imaging

Author
Franke, Jenna Marie

Publication Date
2019

Peer reviewed|Thesis/dissertation

Water-Soluble BODIPY Dyes for Membrane Potential Imaging

By
Jenna M. Franke

A dissertation submitted in partial satisfaction
of the requirements for the degree of

Doctor of Philosophy
in
Chemistry
in the
Graduate Division
of the
University of California, Berkeley

Committee in charge:
Professor Evan W. Miller, Chair
Professor Matthew B. Francis
Professor Richard H. Kramer

Spring 2019

Water-Soluble BODIPY Dyes for Membrane Potential Imaging

By Jenna M. Franke

Abstract

Water-Soluble BODIPY Dyes for Membrane Potential Imaging

By

Jenna M. Franke

Doctor of Philosophy in Chemistry
University of California, Berkeley
Professor Evan W. Miller, Chair

Fluorophores based on 4,4-difluoro-4-bora-3a,4a,-diaza-*s*-indacene (BODIPY) are used widely as biological probes and labeling agents because of their brightness and highly modifiable scaffold. This dissertation describes the design, synthesis, and characterization of a variety of BODIPY-based probes aimed towards membrane potential imaging. We first synthesized a probe based on a zwitterionic BODIPY, but found its synthesis to be challenging and not generalizable. We then designed and synthesized new water-soluble BODIPYs featuring an *ortho*-sulfonated *meso*-aromatic pendant ring and a range of 2,6-substituents: ethyl, hydrogen, carboxylate, amide, and cyano. The condensation methodology we developed is high-yielding (29-61% over three steps), installs the water-solubilizing sulfonate moiety in the same step the fluorophore is formed, and is amenable to pyrrole building blocks of a wide solubility and nucleophilicity range. This new BODIPY scaffold is water-soluble without the need for added detergent and displayed impressive quantum yields of fluorescence in the ϕ_{fl} = 0.70–0.99 range. These BODIPYs were functionalized with a lipophilic photo-induced electron transfer (PeT) donor to act as membrane-localized voltage-sensitive dyes, or VoltageFluors. Altering the 2,6-substituents allowed the voltage-sensitivity to be tuned, and in general we found the order of voltage sensitivity to be ethyl < hydrogen < carboxy < amide > cyano. 2,6-amido based VoltageFluor amide*m*H is the most voltage-sensitive BODIPY probe to date, with a 48% ΔF/F per 100 mV. Two other BODIPY VoltageFluors, TM*m*OMe and carboxy*m*OMe, display voltage sensitivities of 33 and 24% ΔF/F and were used to obtain real-time membrane potential dynamics from neurons and cardiomyocytes. In addition to these BODIPY VoltageFluors, we also report on additional strategies to increase the hydrophilicity of BODIPY, 2,6-chlorination methodologies, and alternate routes towards the VoltageFluor scaffold. Forming monoalkoxy BODIPYs by functionalizing the boron with an alcohol or adding a second *ortho*-sulfonate to the *meso*-pendant ring both increased hydrophilicity of BODIPY VoltageFluors and improved membrane localization. We found 2,6-chlorination of 1,3,5,7-tetramethyl BODIPY with the *ortho*-sulfonated *meso*-pendant ring could be accomplished with *N*-chlorosuccinimide or 1-chloro-1,2-benziodoxol-3-one, but the resulting 2,6-chloro BODIPY was highly susceptible to decomposition when exposed to aqueous conditions or slightly acidic conditions, such as silica gel chromatography. Finally, we developed two alternate routes to the VoltageFluor scaffold that complement the typical Heck coupling route. The first hinged on replacing the Heck coupling with a Suzuki coupling, and we synthesized two different boronate ester molecular wire Suzuki coupling partners. The second was a linear, bottom-up route, in which the entire VoltageFluor scaffold except the fluorophore is assembled, and then the fluorophore condensation is performed. Both routes are generalizable to a wide range of BODIPY and xanthene fluorophores. Together, these projects add valuable synthetic routes to a range of highly water-soluble BODIPY dyes that can be applied directly to voltage-sensitive dyes or more broadly for biological imaging.

Table of Contents

Acknowledgements……..ii

Chapter 1: Addressing BODIPY water solubility: zwitterionic BODIPY
Abstract……2
Introduction……..2
Results & Discussion……..3
Conclusion/Thoughts on Future Work……6
Figures & Schemes……...7
Experimental……..13
References...……...24

Chapter 2: New *ortho*-sulfonated BODIPYs for membrane potential imaging
Abstract……..……27
Introduction……..……..27
Results & Discussion……..28
Conclusion/Thoughts on Future Work……...……35
Figures & Schemes……...……...36
Experimental……..…50
References……..99

Appendix A: Improving hydrophilicity of ortho-sulfonated BODIPY dyes: monoalkoxy and disulfonated BODIPY VoltageFluors
Introduction...……...103
Results & Discussion……103
Conclusion/Thoughts on Future Work……...……..105
Figures & Schemes……...……...….106
Experimental……110
References……122

Appendix B: Chlorination attempts on 1,3,5,7-Tetramethyl *meta*-bromo (TM*m*Br) BODIPY
Introduction……..……124
Results & Discussion……124
Conclusion/Thoughts on Future Work……125
Figures & Schemes……...……....126
Experimental……...…128
References……132

Appendix C: Alternate routes towards BODIPY-based VoltageFluor scaffolds
Introduction……..……134
Results & Discussion……134
Conclusion/Thoughts on Future Work……...……..136
Figures & Schemes……...……137
Experimental……...……142
References……...……150

Acknowledgements

I would first like to thank Professor Evan Miller for being an amazing Ph.D. advisor. Even at the most challenging points during my graduate career, I always left my meetings with Evan feeling more confident in myself and optimistic about my project because of his advice and support. I don't think I could have chosen an advisor more dedicated to helping me achieve my goals and fostering a wonderful lab environment to work in.

Professor Matt Francis has also been a very accessible and supportive mentor to me since my rotation in his lab, and later serving as my qualifying exam chair and a member of my dissertation committee. Matt, thank you for our many discussions about graduate school, your advice on pursing a career in industry, and for always encouraging me.

The Miller lab is filled with great people, all extremely talented scientists, and each of them has supported me both scientifically and emotionally over the past 5 years. I want to acknowledge my incoming class—Steven Boggess, Julia Lazzari-Dean, Pei Liu, and Gloria Ortiz. It's been amazing to see our growth over the past 5 years, and I am excited to follow your success in the coming years.

Huge thanks to Team BODIPY—Ben Raliski, Steven Boggess, Rishi Kulkarni, and especially the three undergraduates I've had the privilege of working with on this project: Patrick Zhang, Divya Natesan, and Evan Koretsky. Your contributions and hard work have been so invaluable to this project and I've enjoyed collaborating with you all. To Divya—you started working with me at the most frustrating point of the BODIPY project, and I am so grateful that you stuck with it and with me for three years. Working with you every week and knowing I wasn't alone on the project kept me motivated, and we did finally get our chemistry to work! You are one of the most dedicated and diligent people I know, and I can't wait to see where medicine takes you. To Evan Koretsky—I am so glad we brought you onto this project a year ago. Your synthetic contributions and theoretical calculations added so much depth to the BODIPY manuscript, and your work ethic and ability to pick up the fluorophore chemistry so quickly always impressed me. I know you will be extremely successful in your future endeavors.

I would like to thank my B.A./M.S. mentors at Northwestern University, Professor Regan Thomson and Dr. Reed Larson. The synthetic foundation I built under your guidance was crucial to my Ph.D. success, as well as landing my dream job! Your continued support is very appreciated.

To my graduate school friends outside of the Miller lab, especially Rachel Bisiewicz, Helen Hobbs, and Rebekah Kitto, you helped me get through Phys Org problemsets, my qualifying exam, dissertation writing, and all the stress in between. Our girls' nights kept me sane, and I value your friendships so much! My long distance high school and college friends have also been a great support system for me—thank you for always lending an ear when I needed to vent.

Lastly, but most importantly, my entire family has been my rock throughout graduate school. To my parents, Janet and Steve, without your hard work and support, I never could have made it to where I am today. I am forever grateful for everything you have sacrificed for my education and your unconditional love. To my sisters, Cara and Megan, and my Grandma Betty, your unwavering belief in me helped me find the strength and persistence to finish strong. To my uncle, Dr. John Beals, without you as a chemist role model, I likely would not have ended up in chemistry in the first place. Your faith in me and encouragement to earn my Ph.D. was instrumental to my success. And finally, to my fiancé, James Judge—you believed in me when I doubted myself, and never failed to put things into perspective when I was overwhelmed with everything on my plate. I am so excited for all our post-Ph.D. adventures to come!

Chapter 1: Addressing BODIPY water solubility: zwitterionic BODIPY

Abstract

We report synthetic routes towards a zwitterionic boron dipyrromethene (BODIPY)-based voltage-sensitive dye. The routes that would have allowed installation of the zwitterionic groups last failed, requiring us to attempt palladium-catalyzed cross-coupling reactions on the challenging, zwitterionic fluorophore substrate. While small amounts of the product were detectible by LC-MS, the probe was never successfully isolated, and we instead pursued a more generalizable, synthetically tractable target.

Introduction

Voltage-sensitive dyes are important tools for probing the activity of individual neurons embedded within complex circuits.[1] They enable detailed studies on neuron network connectivity or activity changes due to neurological disease or pharmaceuticals. Voltage-sensitive small molecules are less invasive and can monitor many more cells at once than electrode-based methods such as patch-clamp electrophysiology, while still providing a very fast and sensitive read-out.

The Miller lab has developed fluorescent dyes with a novel voltage-sensitive photo-induced electron transfer (PeT) mechanism (**Figure 1.1**).[2] VoltageFluors consist of a polar fluorophore head and an electron rich aniline PeT donor connected by a phenylene vinylene molecular wire (**Figure 1.2**). The lipophilic wire inserts into the outer lipid bilayer of cells when loaded onto cultured cells or tissue, and the dye's fluorescence increases when cells depolarize, such as during a neuronal action potential. These spikes in fluorescence allow elucidation of cell firing frequency or connectivity of a large field of neurons when recorded with high-speed fluorescence microscopes.[3]

Previous VoltageFluors have utilized a variety of xanthene fluorophores including fluorescein, tetramethyl rhodamine, and silicon rhodamine.[3–5] Boron dipyrromethene fluorophores (BODIPY, **Figure 1.3**) are poised as a promising alternative for the VoltageFluor scaffold because they have higher quantum yield of fluorescence (ϕ_{fl}) than many xanthene fluorophores and more chemical modifications available than xanthene cores, useful for adjusting the HOMO/LUMO level of the chromophore, shifting the emission spectra, or attaching targeting moities.[6,7]

BODIPYs have been used extensively as photo-induced electron transfer (PeT)-based probes for biological imaging, typically as intracellular probes for pH, metal ions, or reactive oxygen/nitrogen/sulfur species.[8–11] One class of BODIPY voltage-sensitive dyes was recently reported by Benniston and coworkers, based on near-IR emitting distyryl BODIPY dyes.[12] The mechanism of voltage sensing of these molecules is not definitive, but similar to electrochromic voltage-sensitive dye di-4-ANEPPS, these BODIPY-based dyes have a high degree of charge-transfer character.[1,13] The % $\Delta F/F$ per 100 mV of these dyes is not reported, but the signal-to-noise ratios of these BODIPY VSDs are reported as being on par with di-4-ANEPPS for imaging the stomatogastric ganglion (STG) of the *Cancer pagurus* crab.

The PeT-based voltage-sensing mechanism employed by Miller lab voltage-sensitive dyes retains the fast response kinetics of electrochromic dyes like di-4-ANEPPS, but has the added benefits of higher voltage sensitivity and not altering membrane capacitance.[1,12,13] The design criteria for a BODIPY fluorophore suitable for PeT-based voltage sensing are the following: 1) the fluorophore head must be water-soluble to prevent aggregation, and 2) negatively charged to prevent internalization into cells 3) the BODIPY should have high ϕ_{fl} to provide maximum signal 4) photostability for longer imaging experiments 5) favorable rate of PeT between the aniline donor and BODIPY acceptor to impart high voltage sensitivity.

We envisioned using a reported zwitterionic water-soluble BODIPY and incorporating it into a photo-induced electron transfer (PeT)-based voltage-sensitive dye (**Figure 1.2**).[14] Ideally, the phenylene vinylene molecular wire would insert into the outer leaflet of the plasma membrane, anchored by the zwitterionic moieties. When cells are at their resting membrane potential, around –60 mV for neurons, the extracellular space has a net positive charge relative to the inside of the cell (**Figure 1.1**). In this state, photo-induced electron transfer from the aniline PeT donor to the BODIPY acceptor would be favored. When cells depolarize, such as during a neuronal or cardiac action potential, the membrane potential flips and the extracellular side of the cell is net negative, disfavoring the donation of an electron from the PeT donor. This slower rate of PeT during an action potential should cause the fluorescence of the BODIPY to increase, and these spikes of fluorescence could be used to monitor the frequency and shape of action potentials.[1]

In the absence of a PeT donor, a fluorophore can be excited with light, and then this energy is emitted as a photon (fluorescence) as the fluorophore returns to the ground state (**Figure 1.4a**). If a PeT donor is present within the same molecule or within a short enough distance, after the fluorophore is excited the PeT donor donates an electron to the vacancy in the fluorophore HOMO (**Figure 1.4b**). This forms a charge-separated state and prevents the excited electron from returning to the ground state via fluorescence. Instead, a non-radiative charge recombination recurs to return both the fluorophore and donor to the ground state. The rate of this non-radiative PeT affects the quantum yield of fluorescence (ϕ_{fl}) of the probe and its voltage sensitivity. The rate of PeT can be tuned by synthetically changing the fluorophore or molecular wire electron density.

Results & Discussion

Retrosynthetic analysis and initial routes towards zwitterionic BODIPY VoltageFluor

Our original retrosynthetic analysis for zwitterionic BODIPY VoltageFluor involved installing the zwitterionic groups last, because zwitterionic compounds often have limited solubility and are difficult to work with (**Figure 1.5**). The BODIPY and molecular wire can be disconnected via palladium-catalyzed cross coupling, and the BODIPY fluorophore can be synthesized from 4-bromobenzaldehyde and 3-ethyl-2,4-dimethyl-*1H*-pyrrole.

Beginning this route in the forward direction (**Scheme 1.1a**), 2 eq of 3-ethyl-2,4-dimethyl-*1H*-pyrrole were reacted with 4-bromobenzaldehyde in a TFA-catalyzed condensation to form a dipyrromethane.[15] The dipyrromethane was oxidized with DDQ, deprotonated with DIPEA, and the BF_2 group was chelated using $BF_3{\cdot}Et_2O$. I found that using toluene or toluene:hexanes as column eluent gave better separation than the reported DCM:hexanes eluent, and obtained the corresponding 2,6-diethyl BODIPY **1.4** in a 42% yield. A Heck coupling with molecular wire **1.5**, $Pd(OAc)_2$, $P(o\text{-}tol)_3$, DMF, and NEt_3 at 110°C overnight proceeded readily, affording Heck product **1.6** in a 71% yield.[2]

Despite the similarities between Grignard reaction on **1.6**, and reported substrate BODIPY **1.4**, we never observed conversion for the reaction between Heck product **1.6** and the Grignard reagent derived from 3-dimethylamino-1-propyne (**Scheme 1.1a**).[14] The first issue we encountered was that the 3-dimethylamino-1-propyne Grignard precursor was not dry enough, and the trace water was quenching the TurboGrignard reagent before the alkyne could be deprotonated. Filtering through alumina and storing over sieves sufficiently dried alkyne **1.7**, confirmed by a test Grignard reaction on 4-(dimethylamino)benzaldehyde. This test reaction also demonstrated that the aniline functional group, present on substrate **1.6** but not reported substrate **1.4**, posed no issue for the reaction.

The second issue with the Grignard reaction we encountered was that Heck product **1.6** was less soluble in THF than BODIPY **1.4**, which made transferring **1.6** into the reaction flask via syringe or cannula following the Grignard formation challenging. I tried three strategies to circumvent the solubility issue: 1) Used a greater volume of anhydrous THF to transfer Heck product **1.6**. 2) Heated the solution of **1.6** in THF to 60°C to increase solubility before transferring it to the reaction flask. 3) Swapped the order of addition—transferred Grignard solution to a solution of **1.6** in THF via cannula. No conversion to product was observed in any of these cases, and the unmodified starting material could be recovered after quenching the reaction with MeOH followed by flash chromatography. If substrate solubility is not the root issue, our other hypothesis is that perhaps the electron-rich aniline molecular wire made the boron of **1.6** less electrophilic than its BODIPY **1.4** precursor.

After we were unable to observe any conversion for the Grignard reaction on **1.6**, we decided to pursue the route outlined in **Scheme 1.1b**. If successful, this route would still allow installation of the sulfonate groups last. The Grignard reaction on BODIPY **1.4** proceeded as reported, yielding BODIPY with propynes **1.9** in a 57% yield.[14] The crude product was >95% pure by NMR following aqueous workup, so purification by flash chromatography was not necessary. BODIPY **1.9** was a much poorer Heck coupling substrate than its BODIPY **1.4** precursor, likely because the tertiary amines on the propyne groups can chelate the palladium catalyst and prevent oxidative addition of the bromine. I attempted increasing the concentration and the catalyst loading, but never saw any confirmed conversion by LC-MS. There was a slightly promising minor orange spot on the TLC with a R_f of ~0.5 in 7% MeOH in DCM eluent, but it did not look like product by NMR after isolation. The R_f of the starting material is 0.1 in this eluent, and typically we'd expect only a slight increase in R_f following the Heck coupling, supporting that this orange spot is likely due to an undesired side reaction and not the desired product.

Because BODIPY with propynes **1.9** turned out to be a poor Heck coupling substrate and there are not many protecting groups suitable for tertiary amines, we decided to alkylate the amines with 1,3-propanesultone **1.10** and attempt a Heck coupling on the resulting zwitterionic BODIPY **1.11** (**Scheme 1.1c**). The alkylation with 1,3-propanesultone worked well, affording a 77% yield of zwitterionic BODIPY **1.11**.[14] Despite the zwitterionic BODIPY's solubility in DMF, initial Heck couplings based on $Pd(OAc)_2$, P(*o*-tol)$_3$, and NEt_3 in DMF solvent showed no conversion to product (**Scheme 1.1c**). Screening Heck coupling parameters, including different solvents, catalysts, ligands, bases, and different equivalents/concentrations of each reagent requires copious amounts of starting material and rapid screen strategies such as GC/MS. Adding to the challenge, most substrates in methodology papers are relatively simple aromatics or perhaps more challenging heterocycles—nothing like the huge, zwitterionic fluorophore **1.11**, so identifying promising conditions from the literature was extremely difficult.

Synthesis of sulfonated ligand DTBPPS and subsequent cross-couplings

The only literature precedent we found for a palladium-catalyzed cross-coupling on a sulfonated BODIPY was reported by Nierth and coworkers in 2010 (**Scheme 1.2**).[16] Similar to the problem we were facing coupling zwitterionic BODIPY **1.11** with the hydrophobic molecular wire **1.5**, they noted that 'classical' reaction parameters for their Sonogashira coupling between their highly polar 2,6-sulfonated BODIPY and alkynyl anthracene failed. Swapping to hydrophilic ligand 3-(di-tert-butylphosphonium)-propane sulfonate (**DTBPPS**) led to appreciable product, eventually finding conditions that gave them a respectable 46% yield.

Inspired by the similarity between this reported Sonogashira coupling and our desired Heck coupling, I synthesized the DTBPPS ligand (**Scheme 1.3**). The di-tert-butylphosphine starting material is highly air-sensitive and pyrophoric, so I transferred the reagents to the flame-dried reaction flask in an inert atmosphere glovebox. Gram-scale alkylation of di-tert-butylphosphine with 1,3-propanesultone yielded 782 mg of DTBPPS in a 62% yield.[17] This zwitterionic ligand is reported to be relatively air and water-stable; it was stored in a desiccator and weighed out under air.

The hydrophilic DTBPPS phosphine ligand proved to be an improvement over P(*o*-tol)$_3$—simply switching the ligand and keeping the Heck conditions the same (molecular wire **1.5**, NEt_3, DMF, 110°C) we observed conversion to product **1.1** for the first time, 12% by LC-MS (**Table 1.1**, entry 1). There was still 63% unmodified starting material by LC-MS under these conditions, so we investigated whether an aqueous co-solvent would help improve our rate of oxidative addition.[18] No product was detected for 1:1 acetonitrile:water solvent, but toluene:water yielded similar results to the DMF conditions—43% unmodified starting material and 11% Heck product by LC-MS, with a small amount of dehalogenation (**Table 1.1**, entries 2-3).

Interestingly, we observed for both solvent systems that the zwitterionic BODIPY was not as water-soluble as we anticipated—it prefers to dissolve in alcohols over water. For this reason I tried 1:1:1 toluene:MeOH:water, and while it did greatly improve the solubility and reactivity of the zwitterionic BODIPY **1.11**, we observed 45% dehalogenation, 5% unmodified starting material, and no product by LC-MS (**Table 1.1**, entry 4). The palladium catalyst complex would be extremely sterically hindered and hydrophilic following oxidative addition of **1.11** (**Figure 1.6**). This steric hindrance, along with the poor solubility of hydrophobic molecular wire coupling partner **1.5** in water and MeOH, seem to disfavor the migratory insertion of the molecular wire for the Heck coupling to be productive. Instead, MeOH or water acts as a proton source and the BODIPY undergoes reductive elimination to form the dehalogenated product, the major product under these conditions.

Transmetallation of a boronic acid coupling partner in a Suzuki coupling tends to be faster than migratory insertion of an alkene in a Heck coupling. Suzuki couplings are also much more commonly run in polar protic solvents than Heck couplings.[18,19] For these reasons, we decided to try a Suzuki coupling on zwitterionic BODIPY **1.11**.

To convert the styryl moiety of molecular wire **1.5** into a boronic acid precursor, we turned to *N*-methyliminodiacetic acid (MIDA) boronates because of their improved bench stability compared to traditional boronic acids and esters.[20] Molecular wire **1.5** was converted into a MIDA boronate via a ruthenium-catalyzed olefin metathesis reaction with vinylboronic acid MIDA ester **1.12** (**Scheme 1.4**).[21] Only partial conversion to product was observed, and purification was very challenging—the product was insoluble in most organic solvents, and a mixture of *E* and *Z* olefin products was obtained. We were unable to fully separate the *E* and *Z* isomers, but the major isomer shows 4 trans olefin protons in the proton NMR spectrum (J = 16-18 Hz, NMR in **Experimental**) and the major isomer absorbs more strongly than the minor isomer at 350 and 400 nm, as we would expect for the all trans MIDA boronate **1.13**.

Only 15.4 mg (8% yield) of the MIDA boronate wire **1.13** was isolated, a major drawback compared to the Heck coupling route—synthesis of molecular wire **1.5** is very robust in comparison.[2] A small-scale Suzuki coupling under Burke "slow-release" conditions[20] (referring to the rate of hydrolysis of the MIDA ester to the free boronic acid) showed 19% conversion to product by LC-MS (based on 520 nm absorbance), though the reaction also showed many unidentifiable side products, similar to the Heck couplings attempted previously (**Figure 1.7**).

Conclusion & thoughts on future work

Zwitterionic BODIPY **1.11** was not as water-soluble as we anticipated, and the Grignard reaction necessary to install the water-solubilizing zwitterionic groups was finicky enough that we wanted a more generalizable, functional group tolerant approach that would allow electrophilic moieties to be installed on the 2,6-positions of the BODIPY to tune the rate of PeT between the aniline and fluorophore.

We wanted to use sulfonate(s) as the water-solubilizing group because they have proved very effective at helping VoltageFluors localize to cell membranes and they are inert in most chemical reactions.[3–5,22] 2,6-sulfonated BODIPYs are previously reported and have been used in biological probes (the product of **Scheme 1.2** is an example), but they are difficult to synthesize—the chlorosulfonic acid used to install the sulfonates at the 2,6-positions often causes decomposition of the fluorophore because BODIPYs are very acid-sensitive. Installing sulfonates at the 2,6-positions would also mean we would not be able to take advantage of the many synthetic modifications possible at those positions, a major drawback to optimizing BODIPY voltage-sensitive dyes. For these reasons, we decided to pursue a new water-solubilizing strategy for BODIPYs, which is discussed in **Chapter 2**.

Potential improvements to the synthetic route described in **Scheme 1.1a** include transferring Heck product **1.6** to the reaction flask using toluene instead of THF, since a toluene co-solvent should not affect the Grignard reaction. The best route to isolate desired zwitterionic VoltageFluor **1.1** would likely be scale up of the DTBPPS Heck coupling reaction in DMF (**Table 1.1**, entry 1). The Heck coupling would be low yielding, but molecular wire **1.5** and zwitterionic BODIPY **1.11** could be prepared on a gram scale relatively easily, whereas the preparation and purification of MIDA boronate wire **1.13** is much less robust.

Figures & Schemes

Figure 1.1 *Voltage Sensing by PeT mechanism*

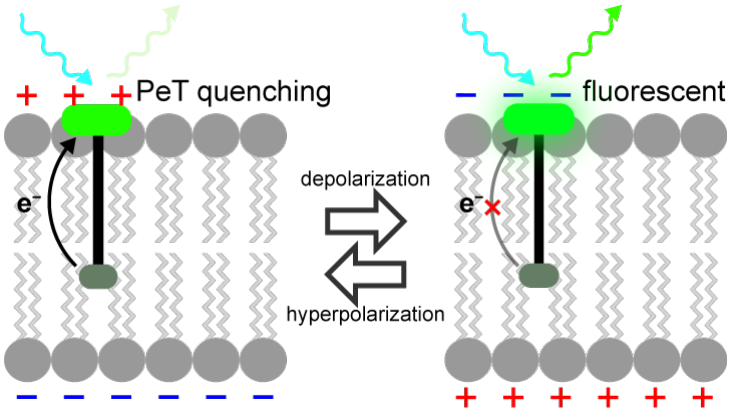

Figure 1.2 *Proposed BODIPY VoltageFluor structure*

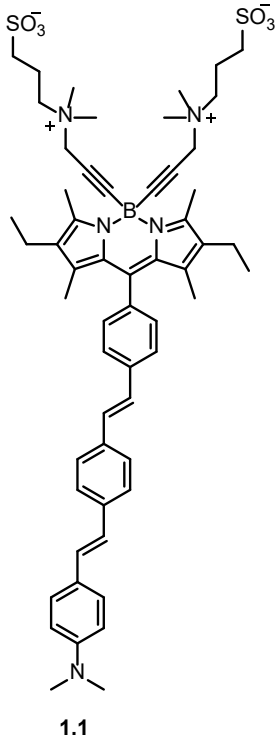

1.1

Water-solubilizing groups to keep probe in external leaflet of membrane

Fluorophore reporter

Hydrophobic molecular wire

Electron-rich aniline PeT donor

Figure 1.3 *BODIPY core & numbering nomenclature*

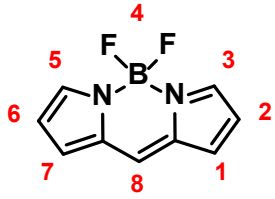

Figure 1.4 *Photo-induced electron transfer mechanism*

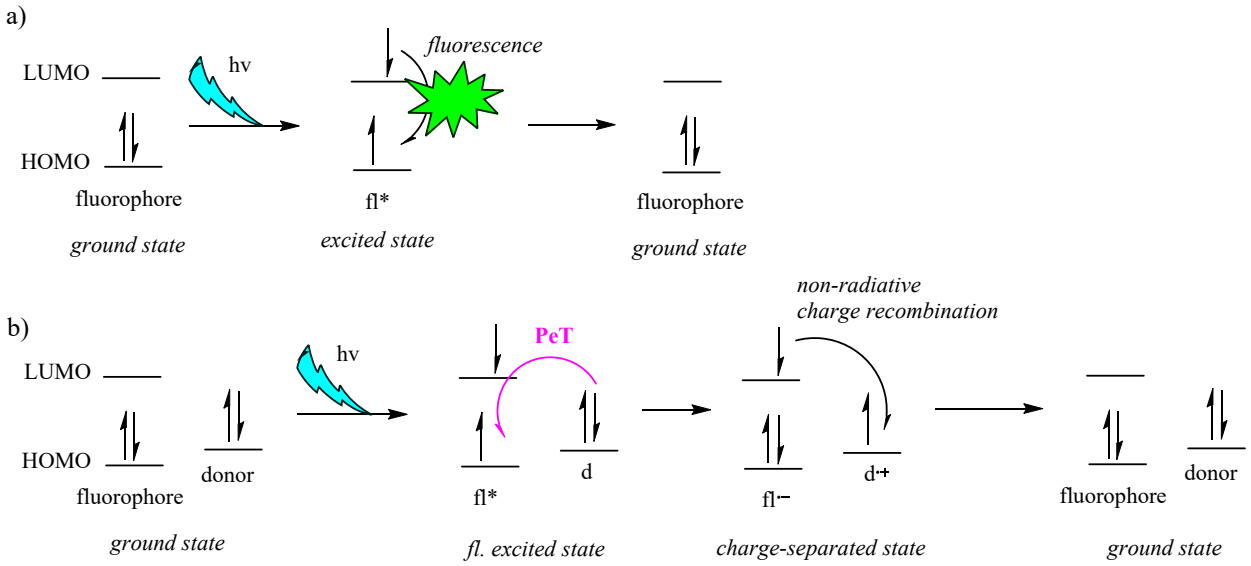

Figure 1.4 a) Fluorophore excitation and emission as fluorescence in the absence of a PeT donor. b) Photo-induced electron transfer mechanism when excited fluorophore is within range of a PeT donor.

Figure 1.5 *Retrosynthetic strategy towards zwitterionic BODIPY VoltageFluor*

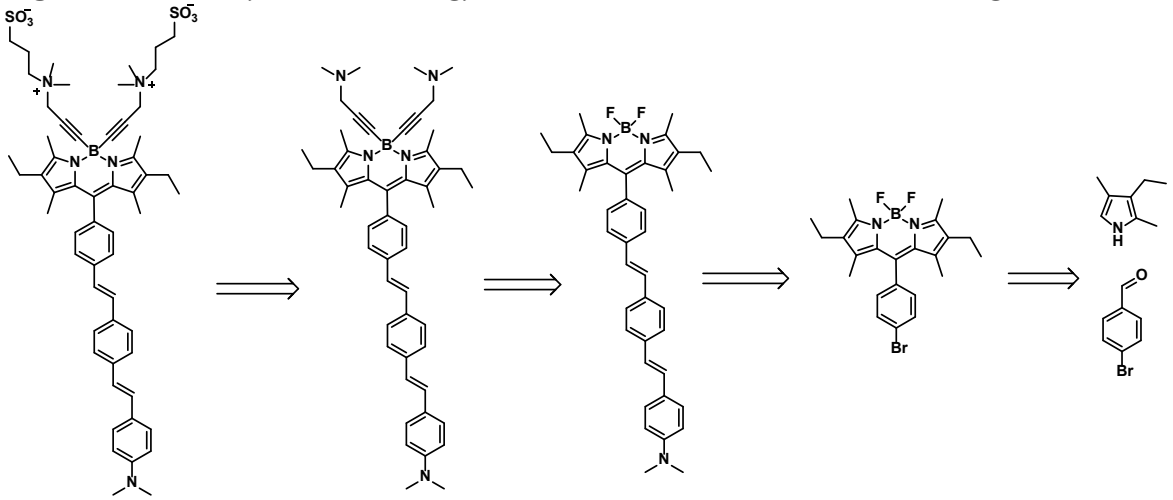

Scheme 1.1 *Routes attempted towards zwitterionic BODIPY VoltageFluor*

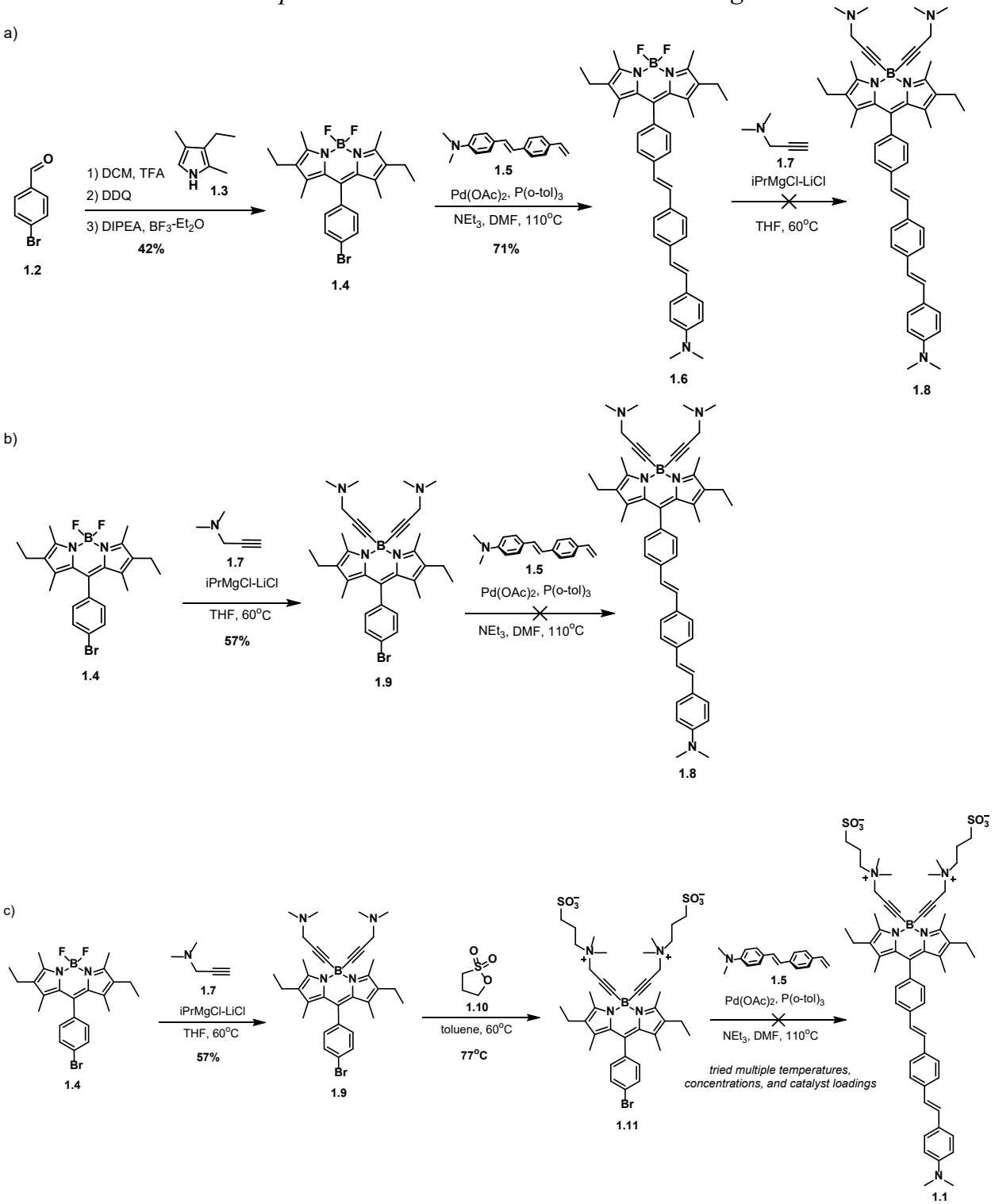

Scheme 1.2 *Literature precedent for cross-coupling on sulfonated BODIPY*[16]

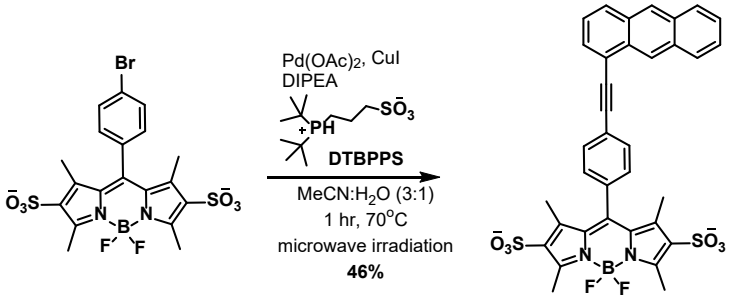

Scheme 1.3 *Synthesis of DTBPPS ligand*

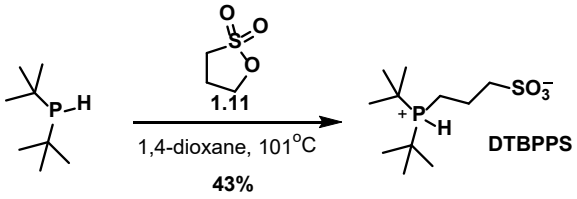

Table 1.1 *Heck coupling conditions screened with DTBPPS ligand*

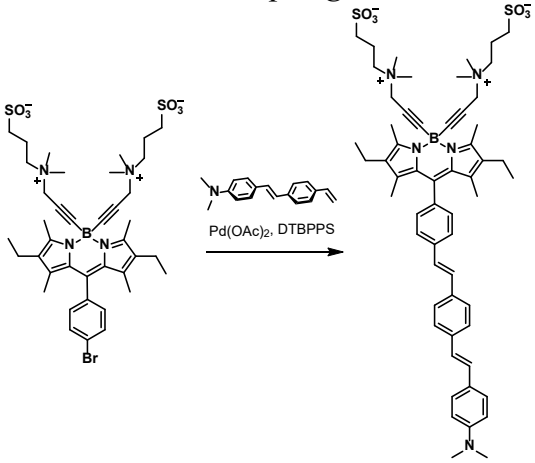

Entry	Solvent	Base	Temp (°C)	SM*	-Br*	Product*
1	DMF	NEt_3	110	63	6	12
2	1:1 ACN:H_2O	K_2CO_3	80	28	n.d.	n.d.
3	1:1 toluene:H_2O	K_2CO_3	70	43	7	11
4	1:1:1 toluene:MeOH:H_2O	K_2CO_3	70	5	45	n.d.
5	1:1 toluene:H_2O	$CsCO_3$	70	29	4	9
6	1:1 toluene:H_2O	K_2CO_3	85	3	10	3

*determined by % absorbance at 520 nm in LC-MS, n.d. = not detected.

Figure 1.6 *Proposed Heck catalyst complex following oxidative addition*

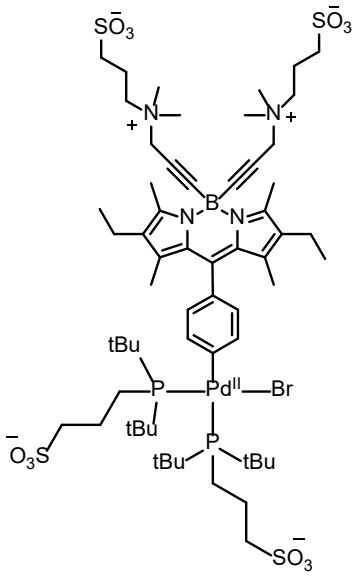

Scheme 1.4 *Suzuki coupling with MIDA boronate*

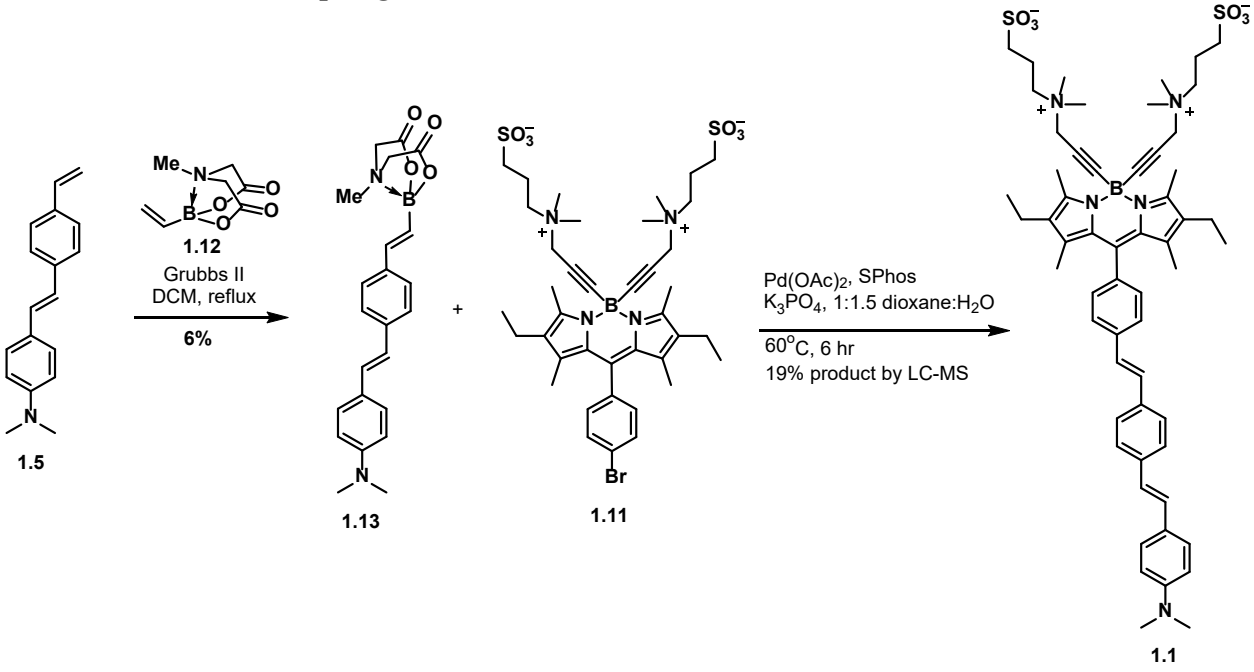

Figure 1.7 *LC-MS of crude Suzuki coupling on zwitterionic BODIPY*

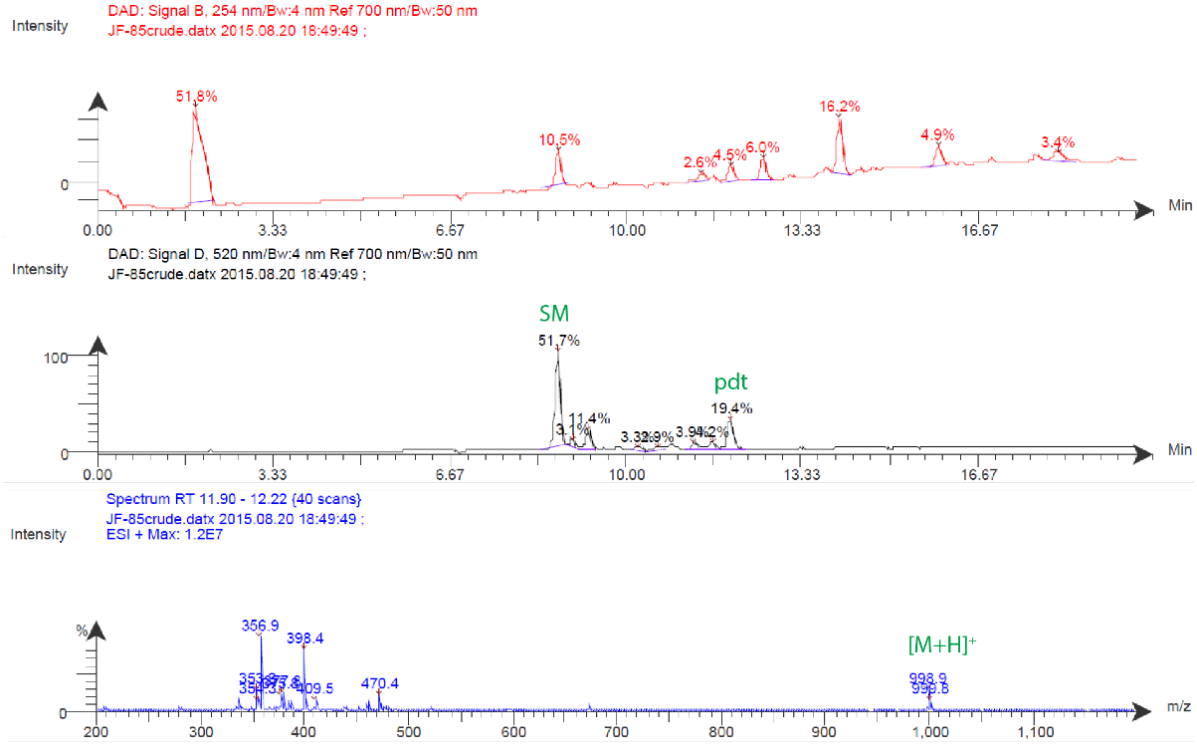

Experimental

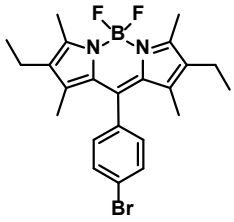

1.4

2,6-ethyl BODIPY(1.4)[15] 4-bromobenzaldehyde (500 mg, 2.7 mmol, 1 eq) was added to a flame-dried 250 mL round-bottom flask. Flask was evacuated and backfilled with N_2 3x, then anhydrous DCM (100 mL), 3-ethyl-2,4-dimethyl-*1H*- pyrrole (0.73 mL, 5.4 mmol, 2 eq) and TFA (4 drops) were added via syringe and reaction stirred under nitrogen atmosphere at rt 20 h. DDQ (613 mg, 2.7 mmol, 1 eq) was added and solution stirred 5 hr. DIPEA (5.6 mL, 32 mmol, 12 eq) then $BF_3{\cdot}Et_2O$ (5.3 mL, 43 mmol, 16 eq) were added via syringe and the solution became green fluorescent. After 10 min, reaction was quenched by addition of water, and organics were washed with H_2O (3 x 50 mL), brine (50 mL), dried over Na_2SO_4, and concentrated under reduced pressure. Flash chromatography on silica gel (toluene eluent) yielded the BODIPY **1.4** as a purple, green iridescent solid (519 mg, 42%).

^{1}H NMR (400 MHz, chloroform-d) δ 7.64 (*J* = 8.1 Hz, 2H), 7.18 (*J* = 8.0 Hz, 2H), 2.53 (s, 6H), 2.31 (q, *J* = 7.4 Hz, 4H), 1.32 (s, 6H), 0.99 (t, *J* = 7.5 Hz, 6H).

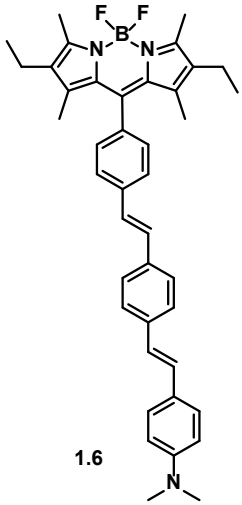

1.6

BODIPY with wire (1.6) To an oven-dried 25 mL Schlenk flask were added BODIPY **1.4**, molecular wire **1.5**, $Pd(OAc)_2$, and P(*o*-tol)$_3$. Flask was evacuated and backfilled with N_2 3x. DMF then NEt_3 were added via syringe, and reaction stirred at 110°C 21 h. Reaction was then cooled to rt, diluted with 20 mL DCM, washed with H_2O (2 x 25 mL), sat. aq. NH_4Cl (25 mL), brine (25 mL), then dried over Na_2SO_4 and concentrated under reduced pressure. Flash chromatography on silica gel (7:10 DCM:hex → 1:1 DCM:hex) yielded **1.6** as a red, green iridescent solid (96 mg, 71%).

^{1}H NMR (400 MHz, Chloroform-*d*) δ 7.64 (d, *J* = 8.4 Hz, 2H), 7.55 – 7.48 (m, 4H), 7.44 (d, *J* = 8.6 Hz, 2H), 7.28 – 7.24 (m, 2H), 7.19 (d, *J* = 10.0 Hz, 2H), 7.10 (d, *J* = 16.7 Hz, 1H), 6.93 (d, J = 16.4 Hz, 1H), 6.73 (d, J = 8.8 Hz, 2H), 3.00 (s, 6H), 2.55 (s, 6H), 2.31 (q, *J* = 7.4 Hz, 4H), 1.36 (s, 6H), 0.99 (t, *J* = 7.5 Hz, 6H). **^{19}F NMR** (400 MHz, Chloroform-*d*) δ 145.0 (q, *J* = 32.5 Hz, 2F split by boron).

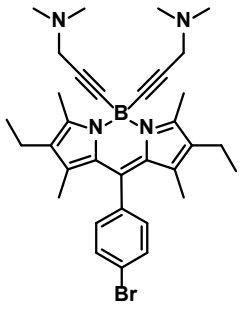

1.9

BODIPY with propynes (1.9)[14] 3-dimethylamino-1-propyne (182 µL, 1.7 mmol, 2.5 eq) was dissolved in anhydrous THF (4 mL) in a flame-dried 50 mL round-bottom flask. TurboGrignard (1.3 M, 1.19 mL) was added dropwise and reaction stirred at 60°C 2 h. BODIPY **1.4** (310 mg, 0.67 mmol) was transferred into the reaction flask with anhydrous THF (1.5 mL + 1.5 mL rinse) and the reaction stirred at 60°C for 1.5 hr. Reaction was then quenched with water (5 mL), poured into brine (50 mL), and extracted with DCM (2 x 50 mL). Combined organics were dried over Na_2SO_4 and concentrated under reduced pressure. The resulting orange, green iridescent product (225 mg, 57%) was clean and used without further purification. Product can be purified by flash chromatography on silica gel (1:9 MeOH:DCM eluent, isocratic) if needed.

^{1}H NMR (400 MHz, Methanol-d_4) δ 7.73 (d, *J* = 8.1 Hz, 2H), 7.26 (d, *J* = 8.0 Hz, 2H), 3.22 (s, 4H), 2.74 (s, 6H), 2.38 (q, *J* = 7.5 Hz, 4H), 2.30 (s, 12H), 1.36 (s, 6H), 0.99 (t, *J* = 7.5 Hz, 6H).

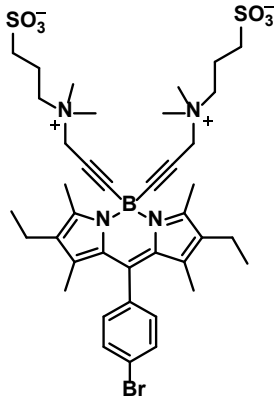

1.11

Zwitterionic BODIPY (1.11)[14] 1,3-propanesultone (77.2 mg, 0.63 mmol, 2 eq) was added to BODIPY with propynes **1.9** (185 mg, 0.32 mmol, 1 eq) in a 20 mL scintillation vial. Anhydrous toluene (6 mL) was added, vial was purged with N_2, then sealed with electrical tape and heated to 60°C 26 h. Reaction was transferred to a 50 mL falcon tube with toluene (as much as necessary to suspend the product solid) and centrifuged for 2 min. Toluene was decanted off with a pipette.

Cold ether (25 mL) was added and falcon tube was centrifuged again, then ether decanted. Resulting red pellet was transferred with MeOH to a round-bottom flask and concentrated under reduced pressure. Resulting solid was dissolved in a minimal amount of MeOH and pipetted into an Erlenmeyer flask filled with cold acetone (100 mL). Flask sat in an ice bath 1 h, then mixture was filtered over a Hirsch funnel and washed with cold acetone to yield zwitterionic BODIPY **1.11** as a red solid (202 mg, 77%).)

^{1}H NMR (400 MHz, Methanol-d_4) δ 7.75 (d, J = 8.0 Hz, 2H), 7.29 (d, J = 8.1 Hz, 2H), 4.30 (s, 4H), 3.63 – 3.55 (m, 4H), 3.14 (s, 12H), 2.83 (t, J = 6.8 Hz, 4H), 2.74 (s, 6H), 2.41 (q, J = 7.3 Hz, 4H), 2.21 (t, J = 12.0 Hz, 5H), 1.39 (s, 6H), 1.01 (t, J = 7.5 Hz, 6H).

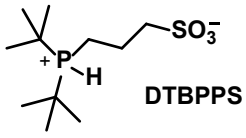

DTBPPS

3-(di-tert-butylphosphonium)-propane sulfonate (DTBPPS)[17] An oven-dried 25 mL round-bottom flask, vial of pre-weighed 1.3-propanesultone (580 mg, 4.75 mmol), ampoule of di-tert-butylphosphine (1g, 6.84 mmol), septum, and syringe were transferred into a glovebox. 1,3-propanesultone was transferred into the reaction flask, then anhydrous dioxane (4 mL) was added via syringe down the sides of the flask. The di-tert-butylphosphine was opened and transferred to the reaction flask via pipette followed by a rinse of the ampoule with dioxane (2 mL). Flask was capped with septum, removed from glovebox, and the septum was quickly replaced with an oven-dried reflux condenser. Reaction refluxed at 101°C 19 h. The white precipitate product was filtered and washed with THF (3 x 10 mL) and diethyl ether (3 x 10 mL). Drying in vacuo yielded **DTBPPS** as a white solid (782 mg, 62%).

^{1}H NMR (400 MHz, Deuterium Oxide) δ 3.06 (t, J = 7.0 Hz, 2H), 2.56 – 2.46 (m, 2H), 2.23 (q, J = 8.0 Hz, 2H), 1.48 (d, J = 16.8 Hz, 18H).

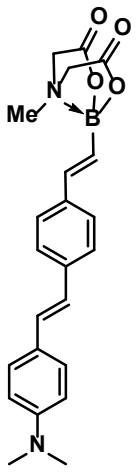

1.13

MIDA boronate wire (1.13)[21] To a flame-dried 10 mL Schlenk flask were added normal wire **1.5** (312 mg, 1.25 mmol), vinylboronic acid MIDA ester **1.12** (91.5 mg, 0.5 mmol), and Grubbs II (42.4 mg, 0.05 mmol). Flask was evacuated and backfilled with N_2 3x, then dissolved in anhydrous DCM (5 mL), fitted with a reflux condenser, and refluxed 24 h. After cooling to rt, Quadrasil AP was added and stirred for 15 min. Concentrated under reduced pressure, then dry loaded onto a column. Flash chromatography (DCM → 5% MeOH in DCM gradient) yielded MIDA boronate wire **1.13** as a yellow solid (15.4 mg, 8%).

^{1}H NMR (600 MHz, acetone-d_6) δ 7.51 – 7.43 (m, 6H), 7.15 (d, J = 16.2 Hz, 1H), 6.98 (d, J = 16.2 Hz, 1H), 6.93 (d, J = 18.3 Hz, 1H), 6.74 (d, J = 8.4 Hz, 2H), 6.33 (d, J = 18.1 Hz, 1H), 3.06 (s, 3H), 2.97 (s, 4H), 2.79 (s, 6H). **Analytical HPLC retention time of product**: 8.6 min (10-100% MeCN in water with 0.05% TFA additive).

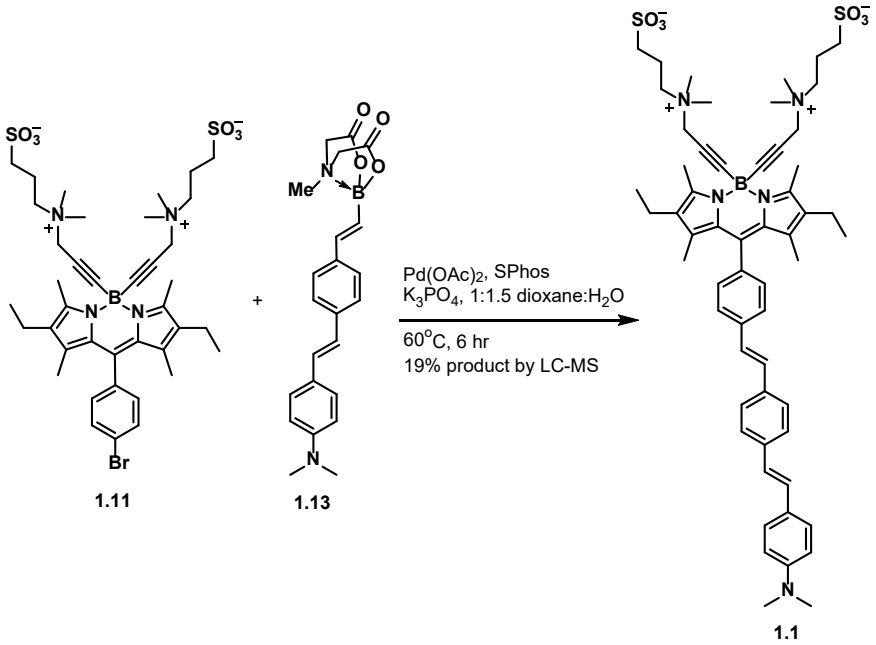

1.11 1.13 1.1

Suzuki with slow release conditions on Zwitterionic BODIPY[20] Zwitterionic BODIPY **1.11** **(**10 mg, 0.012 mmol), $Pd(OAc)_2$ (1 mg, 0.004 mmol), SPhos (3.7 mg, 0.009 mmol), and MIDA boronate wire **1.13** were added to a 4 mL dram vial. Dioxane (150 µL) and degassed aq K_3PO_4 (0.9M, 100 µL) were added, then vial cap was sealed with electrical tape and reaction was heated to 60°C 4.5 h. Filtering through celite with MeOH yielded a brownish, green fluorescent solution which was then concentrated under reduced pressure. Crude LC-MS showed around 19% conversion to product (**Figure 1.7**), but product was barely detectible by LC-MS after filtering and was never isolated. **Analytical HPLC retention time of product**: 11.9 min (10-100% MeCN in water with 0.05% TFA additive).

Compound NMR Spectra

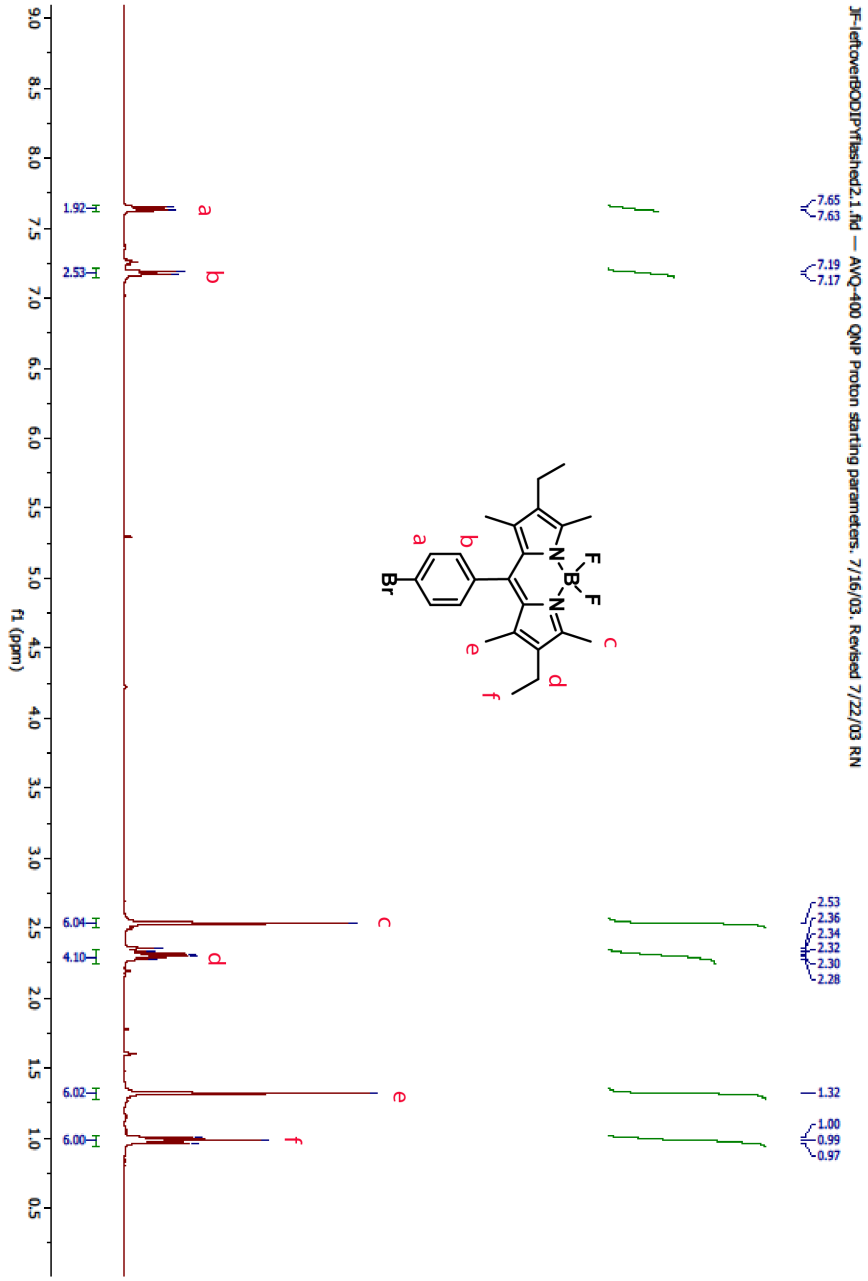

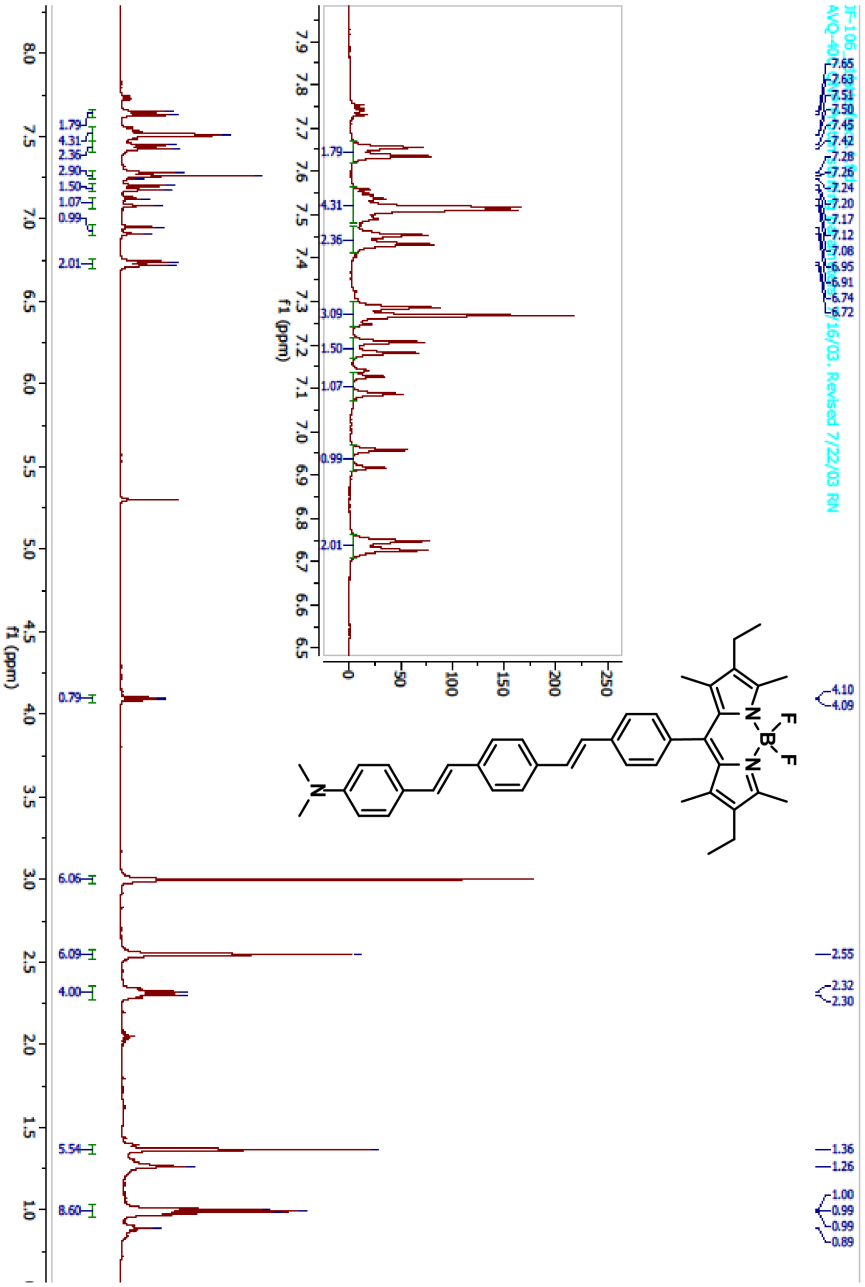
f1 (ppm)
1.79
4.31
2.36
2.90
1.50
1.07
0.99
2.01
0.79
6.06
6.09
4.00
5.54
8.60
3.09
4.10
4.09
2.55
2.32
2.30
1.36
1.26
1.00
0.99
0.99
0.89
N
B
F
F

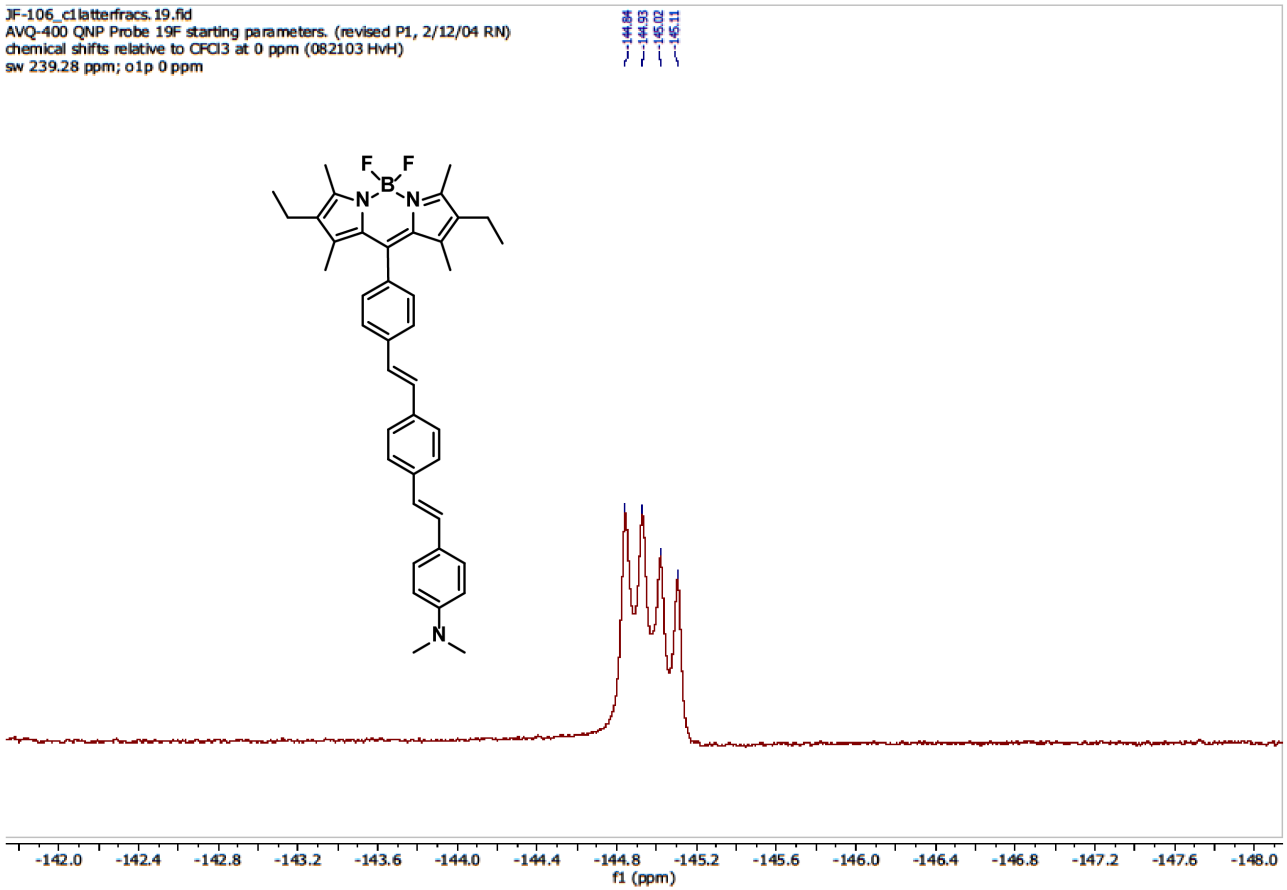
JF-106_c1latterfracs.19.fid
AVQ-400 QNP Probe 19F starting parameters. (revised P1, 2/12/04 RN)
chemical shifts relative to CFCl3 at 0 ppm (082103 HvH)
sw 239.28 ppm; o1p 0 ppm
-144.84
-144.93
-145.02
-145.11
F
F
B
N
N
N
-142.0
-142.4
-142.8
-143.2
-143.6
-144.0
-144.4
-144.8
-145.2
-145.6
-146.0
-146.4
-146.8
-147.2
-147.6
-148.0
f1 (ppm)

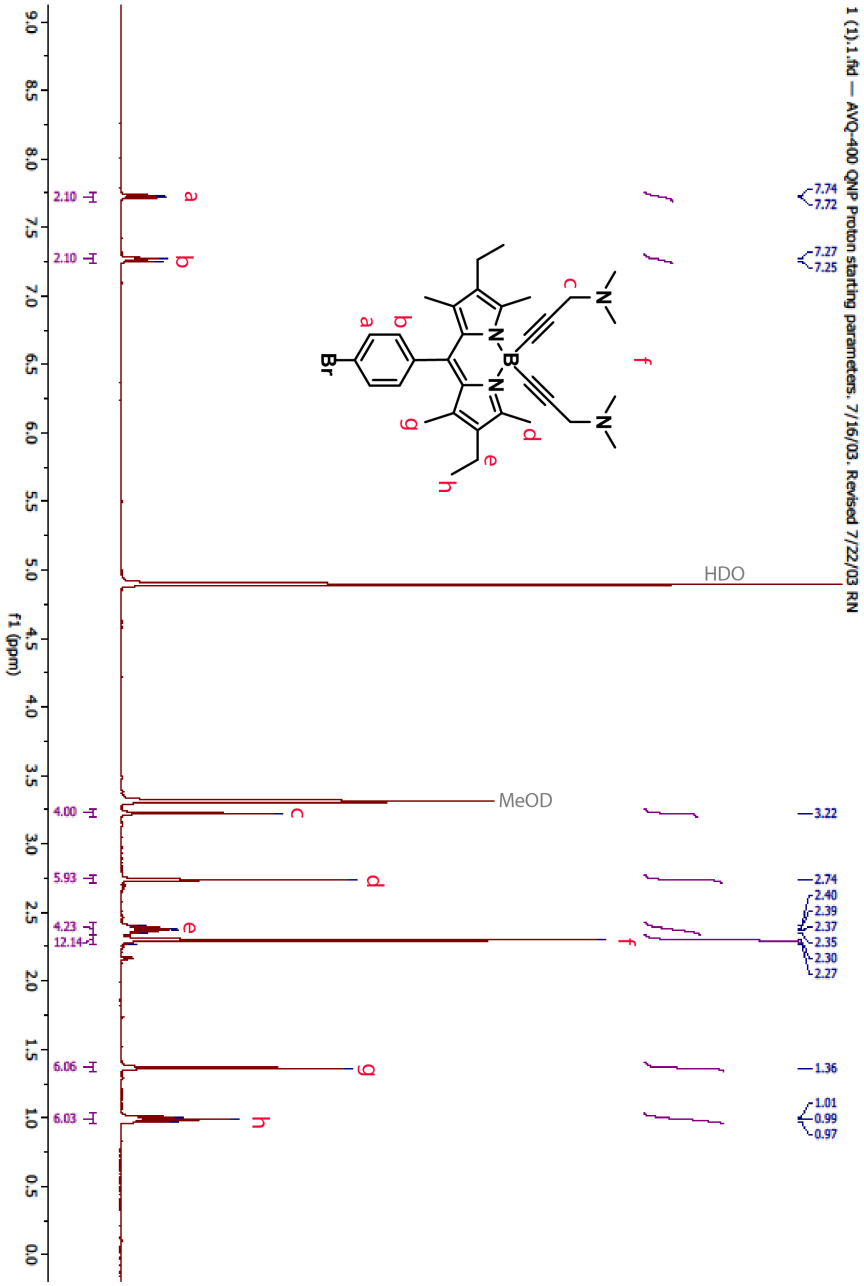
1 (1).1.fid — AVQ-400 QNP Proton starting parameters 7/16/03. Revised 7/22/03 RN
f1 (ppm)
HDO
MeOD
2.10
2.10
4.00
5.93
4.23
12.14
6.06
6.03
7.74
7.72
7.27
7.25
3.22
2.74
2.40
2.39
2.37
2.35
2.30
2.27
1.36
1.01
0.99
0.97
Br
N
B
N

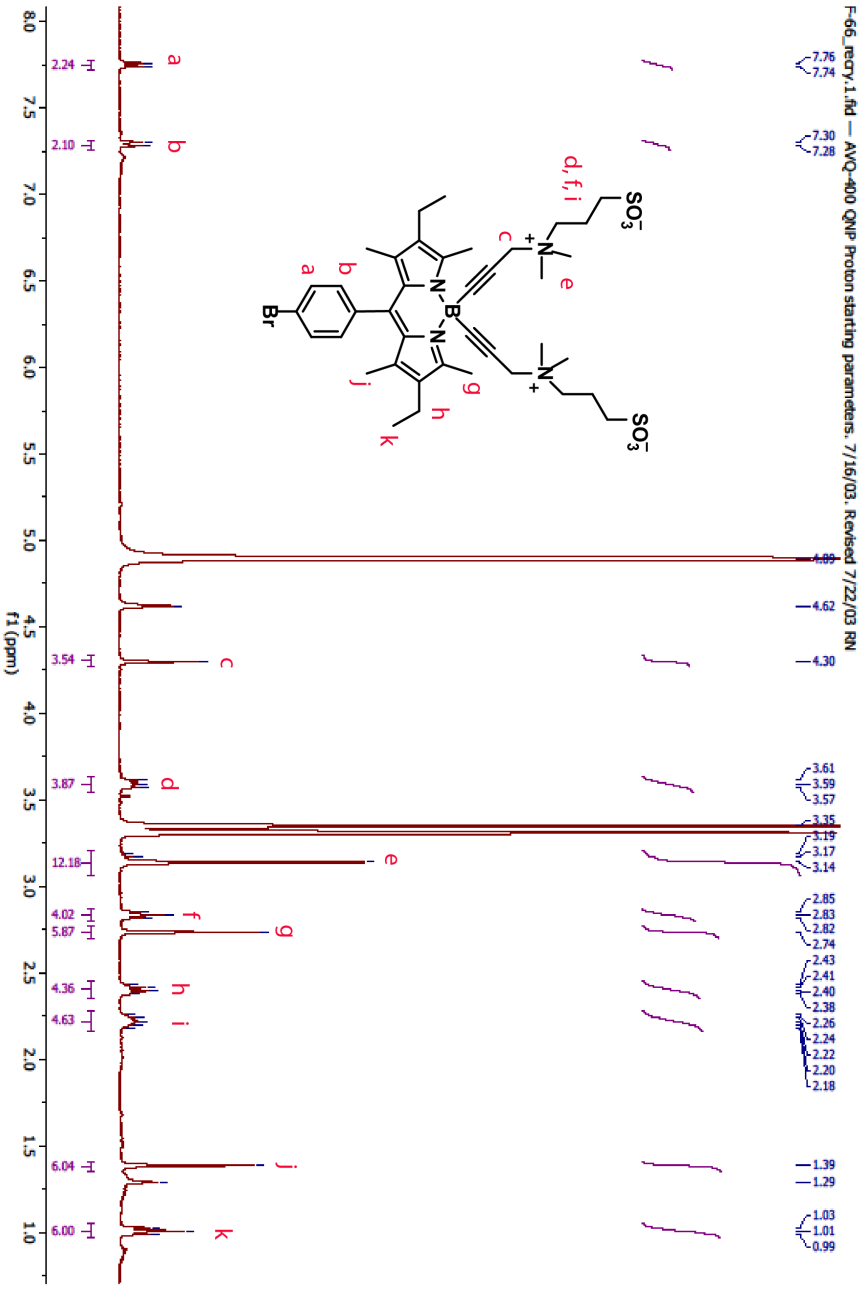
F-66_recry.1.fid — AVQ-400 QNP Proton starting parameters. 7/16/03. Revised 7/22/03 RN
f1 (ppm)
8.0
7.5
7.0
6.5
6.0
5.5
5.0
4.5
4.0
3.5
3.0
2.5
2.0
1.5
1.0
2.24
2.10
3.54
3.87
12.18
4.02
5.87
4.36
4.63
6.04
6.00
a
b
c
d
e
f
g
h
i
j
k
7.76
7.74
7.30
7.28
4.89
4.62
4.30
3.61
3.59
3.57
3.35
3.19
3.17
3.14
2.85
2.83
2.82
2.74
2.43
2.41
2.40
2.38
2.26
2.24
2.22
2.20
2.18
1.39
1.29
1.03
1.01
0.99
d, f, i
SO3−
SO3−
N+
N+
B
N
N
Br

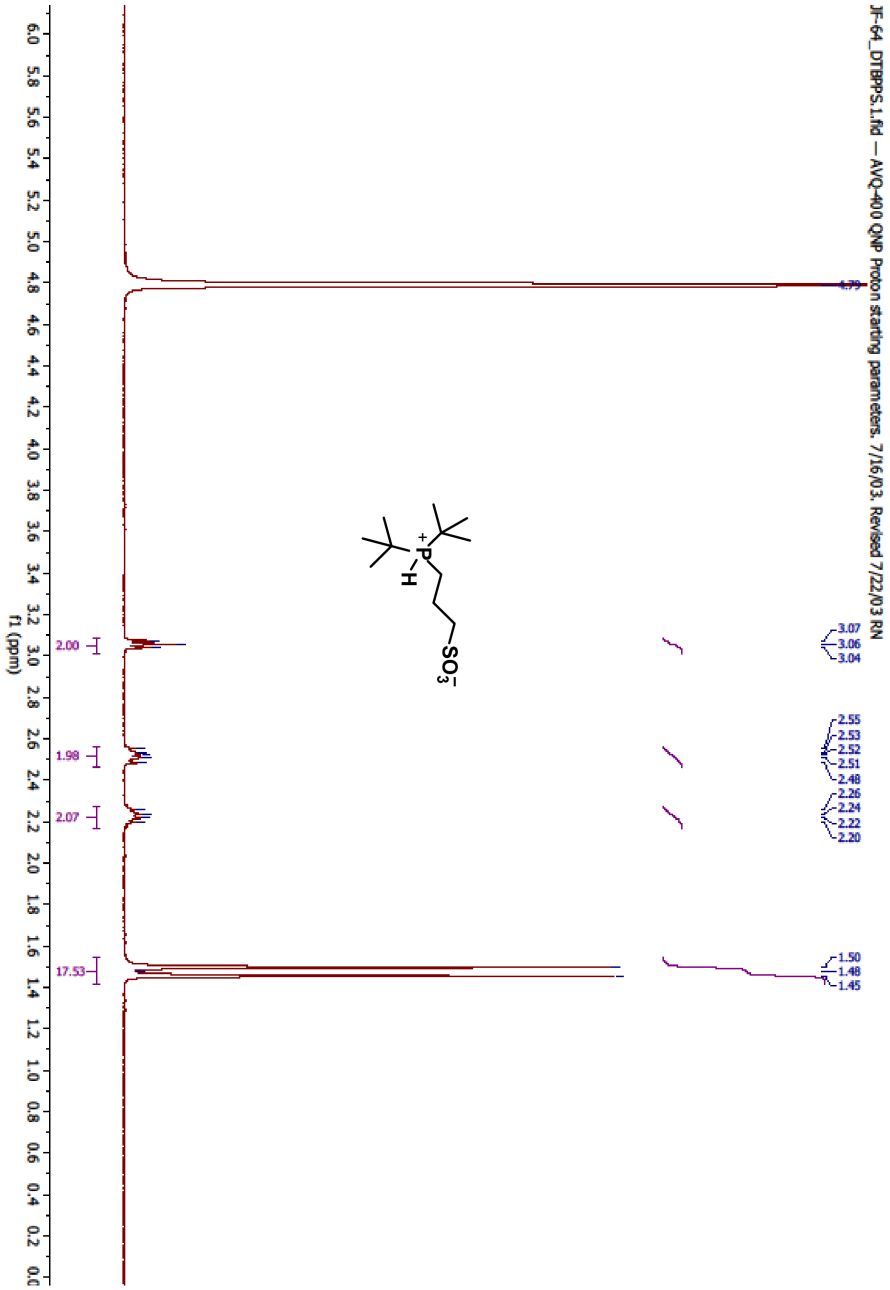
JF-64_DTBPPS.1.fid — AVQ-400 QNP Proton starting parameters. 7/16/03. Revised 7/22/03 RN
f1 (ppm)
2.00
1.98
2.07
17.53
4.79
3.07
3.06
3.04
2.55
2.53
2.52
2.51
2.48
2.26
2.24
2.22
2.20
1.50
1.48
1.45
P
H
SO3

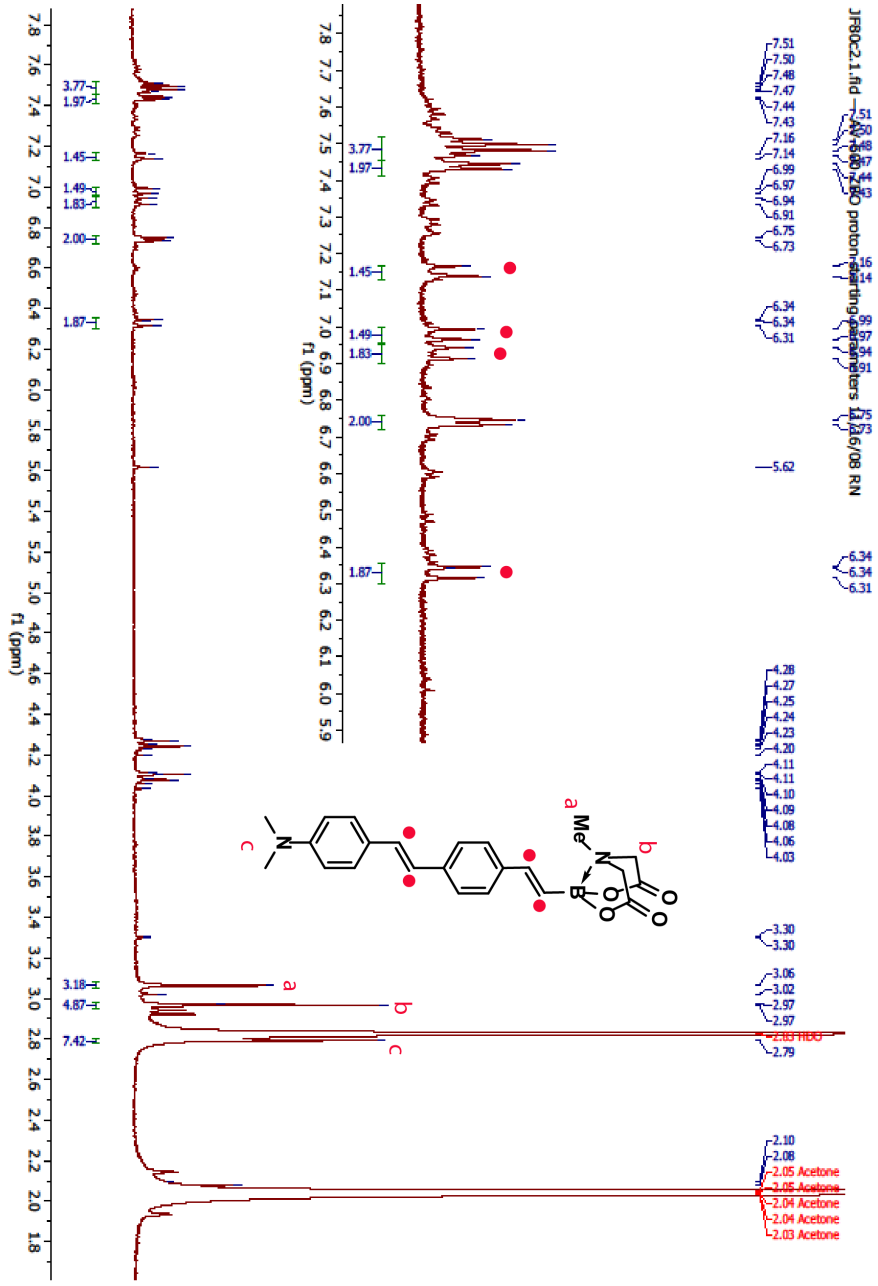
JF80c2.1.fid
f1 (ppm)
a
b
c
Me
B
O
N

References

(1) Miller, E. W. Small Molecule Fluorescent Voltage Indicators for Studying Membrane Potential. *Curr. Opin. Chem. Biol.* **2016**, *33*, 74–80.

(2) Miller, E. W.; Lin, J. Y.; Frady, E. P.; Steinbach, P. a; Kristan, W. B.; Tsien, R. Y. Optically Monitoring Voltage in Neurons by Photo-Induced Electron Transfer through Molecular Wires. *Proc. Natl. Acad. Sci. U. S. A.* **2012**, *109* (6), 2114–2119.

(3) Huang, Y. L.; Walker, A. S.; Miller, E. W. A Photostable Silicon Rhodamine Platform for Optical Voltage Sensing. *J. Am. Chem. Soc.* **2015**, *137* (33), 10767–10776.

(4) Woodford, C. R.; Frady, E. P.; Smith, R. S.; Morey, B.; Canzi, G.; Palida, S. F.; Araneda, R. C.; Kristan, W. B.; Kubiak, C. P.; Miller, E. W.; et al. Improved PeT Molecules for Optically Sensing Voltage in Neurons. *J. Am. Chem. Soc.* **2015**, *137* (5), 1817–1824.

(5) Deal, P. E.; Kulkarni, R. U.; Al-Abdullatif, S. H.; Miller, E. W. Isomerically Pure Tetramethylrhodamine Voltage Reporters. *J. Am. Chem. Soc* **2016**, *138*, 9085–9088.

(6) Loudet, A.; Burgess, K. BODIPY Dyes and Their Derivatives: Syntheses and Spectroscopic Properties. *Chem. Rev.* **2007**, *107*, 4891–4932.

(7) Ziessel, R.; Ulrich, G.; Harriman, A. The Chemistry of Bodipy: A New El Dorado for Fluorescence Tools. *New J. Chem.* **2007**, *31*, 496–501.

(8) Dodani, S. C.; He, Q.; Chang, C. J. A Turn-On Fluorescent Sensor for Detecting Nickel in Living Cells Synthesis of Nickelsensor-1 (NS1). *J. Am. Chem. Soc.* **2009**, *131*, 18020–18021.

(9) Miller, E. W.; Zeng, L.; Domaille, D. W.; Chang, C. J. Preparation and Use of Coppersensor-1, a Synthetic Fluorophore for Live-Cell Copper Imaging. *Nat. Protoc.* **2006**, *1* (2), 824–827.

(10) Kolemen, S.; Akkaya, E. U. Reaction-Based BODIPY Probes for Selective Bio-Imaging. *Coord. Chem. Rev.* **2018**, *354*, 121–134.

(11) Kowada, T.; Maeda, H.; Kikuchi, K. BODIPY-Based Probes for the Fluorescence Imaging of Biomolecules in Living Cells. *Chem. Soc. Rev* **2015**, *44*, 4953–4972.

(12) Sirbu, D.; Butcher, J. B.; Waddell, P. G.; Andras, P.; Benniston, A. C. Locally Excited State–Charge Transfer State Coupled Dyes as Optically Responsive Neuron Firing Probes. *Chem. - A Eur. J.* **2017**, *23* (58), 14639–14649.

(13) Fluhler, E.; Burnham, V. G.; Loew, L. M. Spectra, Membrane Binding, and Potentiometric Responses of New Charge Shift Probes. *Biochemistry* **1985**, *24*, 5749–5755.

(14) Niu, S. L.; Ulrich, G.; Ziessel, R.; Kiss, A.; Renard, P. Y.; Romieu, A. Water-Soluble BODIPY Derivatives. *Org. Lett.* **2009**, *11* (10), 2049–2052.

(15) Davies, L. H.; Wallis, J. F.; Probert, M. R.; Higham, L. J. Efficient Multigram Syntheses of Air-Stable, Fluorescent Primary Phosphines via Palladium-Catalyzed Phosphonylation of Aryl Bromides. *Synthesis,* **2014**, *46*, 2622–2628.

(16) Nierth, A.; Kobitski, A. Y.; Ulrich Nienhaus, G.; Jäschke, A. Anthracene-Bodipy Dyads as Fluorescent Sensors for Biocatalytic Diels Alder Reactions. *J. Am. Chem. Soc.* **2010**, *132* (8), 2646–2654.

(17) Brown, W. S.; Boykin, D. D.; Sonnier, M. Q.; Clark, W. D.; Brown, F. V.; Shaughnessy, K. H. Sterically Demanding, Zwitterionic Trialkylphosphonium Sulfonates as Air-Stable Ligand Precursors for Efficient Palladium-Catalyzed Cross-Couplings of Aryl Bromides and Chlorides. *Synthesis,* **2008**, *12*, 1965–1970.

(18) Yun Cho, S.; Kyu Kang, S.; Hee Ahn, J.; Du Ha, J.; Choi, J.-K. Suzuki Reaction of Cyclopenta[d][1,2]Oxazine in Aqueous Solvent with Water-Soluble Phosphine Ligand. *Tetrahedron Lett.* **2006**, *47*, 5237–5240.

(19) Miyaura, N.; Suzuki, A. Palladium-Catalyzed Cross-Coupling Reactions. *Chemistry* **1995**, *95* (1), 2457–2483.

(20) Knapp, D. M.; Gillis, E. P.; Burke, M. D. A General Solution for Unstable Boronic Acids: Slow-

Release Cross-Coupling from Air-Stable MIDA Boronates. *J. Am. Chem. Soc.* **2009**, *131*, 6961–6963.
(21) Uno, B. E.; Gillis, E. P.; Burke, M. D. Vinyl MIDA Boronate: A Readily Accessible and Highly Versatile Building Block for Small Molecule Synthesis. *Tetrahedron* **2008**, *65*, 3130–3138.
(22) Kulkarni, R. U.; Vandenberghe, M.; Thunemann, M.; James, F.; Andreassen, O. A.; Djurovic, S.; Devor, A.; Miller, E. W. *In Vivo* Two-Photon Voltage Imaging with Sulfonated Rhodamine Dyes. *ACS Cent. Sci*. **2018**, *4*, 1371–1378.

Chapter 2: New *ortho*-sulfonated BODIPYs for membrane potential imaging

Portions of this work were performed in collaboration with the following persons:
Synthesis was assisted by Divya Natesan, Evan Koretsky, and Patrick Zhang
Theoretical calculations were performed by Evan Koretsky
Electrophysiology and imaging in neurons/cardiomyocytes assisted by Benjamin Raliski, Steven Boggess, and Dr. Rishikesh Kulkarni.

Abstract

Fluorophores based on the BODIPY scaffold are prized for their tunable excitation and emission profiles, mild syntheses, and biological compatibility. Improving the water-solubility of BODIPY dyes remains an outstanding challenge. The development of water-soluble BODIPY dyes usually involves direct modification of the BODIPY fluorophore core with ionizable groups or substitution at the boron center. While these strategies are effective for the generation of water-soluble fluorophores, they are challenging to implement when developing BODIPY-based indicators: direct modification of BODIPY core can disrupt the electronics of the dye, complicating the design of functional indicators; and substitution at the boron center can render the resultant BODIPY a poor substrate for the chemical transformations required to generate fluorescent sensors. In this study, we show that BODIPYs bearing a sulfonated aromatic group at the *meso* position provide a general solution for water-soluble BODIPYs. We outline the route to a suite of 5 new BODIPYs with 2,6-disubstitution patterns spanning a range of electron-donating and -withdrawing propensities. To highlight the utility of these new, sulfonated BODIPYs, we further functionalize them to access 13 new, BODIPY-based voltage-sensitive fluorophores. The best of these BODIPY VF dyes displays a 48% $\Delta F/F$ per 100 mV in mammalian cells. Two additional BODIPY VFs show good voltage sensitivity ($\geq$24% $\Delta F/F$) and excellent brightness in cells. These compounds can report on action potential dynamic in both mammalian neurons and human-derived cardiomyocytes. The ability to access a range of electron-donating and -withdrawing substituents in the context of a water soluble BODIPY fluorophore provides the ability to tune the electronic properties to access new fluorescent indicators.

Introduction

Synthetic chemistry has long been a source of colorful compounds whose ability to absorb light find application in far-ranging fields.[1–3] Fluorescent dyes find widespread use in the modern research laboratory, where features such as visible excitation and emission profiles, large molecular brightness values, and photostability are highly prized, along with biologically compatible properties like water-solubility. Since the late 19th century, xanthene dyes like fluoresceins[4] and rhodamines[5,6] offered a fertile source of inspiration as scaffolds for biologically-useful dyes and indicators.[7–9] More recently, BODIPY, or 4,4-difluoro-4-bora-3a,4a,-diaza-s-indacene, (**Scheme 2.1**) dyes have emerged as a versatile complement to xanthene dyes. Owing to the relatively mild reaction conditions for the generation of BODIPYs[10] relative to xanthenes, a number of flexible synthetic routes afford the opportunity to install a range of substituents directly to the BODIPY core to tune both the color and electronic properties of BODIPY dyes.

Since the initial report of BODIPY in 1968,[11] a proliferation of synthetic methods[10,12,13] and conceptual understanding enabled the application of BODIPYs to indicators for a number of important, biologically-relevant analytes and properties,[14,15] including pH,[16,17] cations like Na^+,[18] K^+,[19,20] Mg^{2+},[21] and Ca^{2+};[22,23] transition metals;[24–26] reactive oxygen[27] and nitrogen species,[28] electron transfer reactions,[29] and membrane viscosity.[30]

Because of the broad tunability of BODIPY-based scaffolds, we thought these fluorophores would make an excellent choice for incorporation into a molecular wire-based, photo-induced electron transfer (PeT) membrane potential sensing framework.[31] Previous work in our lab showed that tuning the relative electron affinities between a fluorescein-based reporter and electronically-orthogonal phenylenevinylene molecular wire voltage-sensing domain profoundly altered the

voltage sensitivities of fluorescein based dyes. However, the limited synthetic scope of sulfonated fluorescein only allowed access to a narrow range of substituents (H, F, Cl, Me).[32]

Here, we introduce new, water-soluble sulfonated BODIPYs with substituents ranging from highly electron donating (Et) to withdrawing (CN). We incorporate these sulfonated BODIPYs into a molecular wire voltage-sensing scaffold to provide the first examples of PeT-based voltage-sensitive BODIPYs. The most sensitive of these dyes displays a 48% ΔF/F per 100 mV in HEK cells, and two others possess ≥24% ΔF/F, making them useful for voltage sensing applications in both neurons and cardiomyocytes.

Results & Discussion

Design of water soluble BODIPYs

We prepared a total of 13 BODIPY-based Voltage-sensitive Fluorophores, or BODIPY-VF dyes. All the BODIPY compounds feature a common *ortho*-sulfonic acid substituted *meso* aromatic ring (8-position, **Scheme 2.1**) and substitution patterns at the 2,6-positions that include hydrogen, ethyl, carboxylate, amide, and cyano functionalities (**Scheme 2.1**). Our initial attempts to access BODIPY-based VoltageFluor indicators centered around the development of water-soluble 1,3,5,7-tetramethyl-2,6-diethyl BODIPY fluorophores. Ionizable groups, such as sulfonates or carboxylates, are essential for the proper orientation of VF-types dyes in cellular membranes.[33,34]

Initial attempts to introduce water-solubilizing groups centered on substitution at boron,[35–37] because modifications here have little influence on the overall optical properties of the dyes. However, in our hands, these modifications proved incompatible with many of the subsequent reaction conditions required for installation of voltage-sensing phenylenevinylene molecular wires. Functionalization of the 2,6-positions of the BODIPY core offered a route to the installation of water-solubilizing groups like sulfonates[38] or carboxylates,[39] but direct functionalization of the BODIPY core can profoundly alter redox properties, confounding the tuning of fluorophore redox potential[32,40] with installation of water solubilizing groups. One solution is to include a sulfonate on the *meso* aromatic ring (**Scheme 2.1**), which we hypothesized would improve solubility, be generalizable across a range of 2,6-substitution patterns on the BODIPY core, and aid in the proper orientation within cellular plasma membranes.

Synthesis of Et- and H- BODIPY VoltageFluors

Owing to the commercial availability of the 3-ethyl-2,4-dimethyl-*1H*-pyrrole precursors (kryptopyrrole), we first synthesized BODIPY **3** (**Scheme 2.2**) for use in subsequent coupling with phenylenevinylene molecular wires. The common sulfonated benzaldehyde precursor for the synthesis of phenyl-substituted BODIPYs, **1** (**Scheme 2.2**, and related isomer, **9**), was completely insoluble in CH_2Cl_2 and toluene, the most commonly used solvents for BODIPY condensations.[10,18,28,30,41–44] Polar solvents were screened for the TFA-catalyzed condensation of aldehyde **1** and kryptopyrrole **2** (**Scheme 2.2**) and DMF gave the best conversion to the dipyrromethane. Oxidation with DDQ to form the corresponding dipyrromethene followed by BF_2 chelation with boron trifluoride diethyl etherate ($BF_3 \cdot OEt_2$) in CH_2Cl_2 solvent gave novel *ortho*-sulfonated BODIPY **3** (Br *para* to BODIPY, **Scheme 2.2**) in 49% yield and **11** (Br *meta* to BODIPY, **Scheme 2.2**) in 33% yield. Novel BODIPY dyes with two *ortho*-sulfonates were also synthesized under similar conditions (**Appendix A**). Most water-soluble BODIPYs require

multiple synthetic steps to assemble,[35,38] but our condensation methodology yields water-soluble BODIPYs in a simple, one-pot sequence, and in equal or greater yields than the condensation of non-water-soluble BODIPY fluorophores.

A Pd-catalyzed Heck coupling between BODIPY **3** and substituted styrenes **4** and **5** gave two different 2,6-ethyl, *para* molecular wire BODIPY VoltageFluors: Et*p*H (**6**) and Et*p*OMe (**7**) in 92 and 25% isolated yield, respectively (**Scheme 2.2**). The naming convention represents the ethyl groups at the 2,6-positions, molecular wire *para* from the fluorophore, and the identity of the R_1 substituent. Derivatives with the molecular wire *meta* from the fluorophore were prepared via a similar route from BODIPY **11** (**Scheme 2.2**; Et*m*H **15**, 26% yield, and Et*m*OMe **16**, 29%). We also synthesized monoalkoxy 2,6-ethyl BODIPY VoltageFluors with improved water solubility and membrane staining.[45] These monoalkoxy BODIPYs had lower photostability and chemical stability than their difluoro precursors and were not pursued beyond the ethyl series. Synthetic and imaging details can be found in **Appendix A**.

Tetramethyl BODIPY VoltageFluors **17**-**19** (R = H) were prepared first by reacting 2,4-dimethyl-*1H*-pyrrole **10** with sulfonated aldehyde **9**, resulting in a 38% yield of *ortho*-sulfonated tetramethyl BODIPY **12**. Heck coupling with substituted styrene **4**, **13**, or **14** then gave TM*m*H (**17**), TM*m*Me (**18**), and TM*m*OMe (**19**) in 35-62% yield after silica gel chromatography (**Scheme 2.2**). An advantage of tetramethyl BODIPY is that the 2,6-positions can be readily functionalized through electrophilic aromatic substitution and radical reactions.[10] We chlorinated the 2,6-positions of tetramethyl BODIPY **12**, but the resulting 2,6-dichloro BODIPY was unstable and never successfully characterized. A discussion of this chemistry can be found in **Appendix B**.

Synthesis of CN-BODIPY VoltageFluor

Electron-withdrawing BODIPY derivatives provide a useful counterpoint to H- and ethyl-substituted BODIPYs and may produce lower levels of reactive $^1O_2$ than more electron-rich derivatives.[46] Synthesizing cyano VoltageFluor derivative **22** was more challenging than either H- or Et-substituted BODIPY VoltageFluors. Because of the poor nucleophilicity of 2,4-dimethyl-*1H*-pyrrole-3-carbonitrile (**20**), no reaction with sulfonated benzaldehyde **9** was observed in DMF solvent unless heated to 60 °C. The heated condensation resulted in only an 8% isolated yield of 2,6-cyano BODIPY **21**. Switching the solvent to a 2:3 DMF:CH_2Cl_2 mixture and adding an excess of TFA (100 µL, 6 equiv.) allowed the synthesis to proceed at room temperature and increased the isolated yield to 29% (**Scheme 2.3**).

BODIPY **21** appears less stable than 2,6-ethyl and tetramethyl BODIPYs **11** and **12**, possibly due to the lower effective charges on the dipyrromethene nitrogen atoms.[47] When subjected to the Pd-catalyzed Heck coupling conditions that afforded previous BODIPY VoltageFluors, cyano BODIPY **21** decomposed before any conversion was observed. Lowering the reaction temperature from 100 °C to 70 °C did not prevent decomposition. By exposing cyano BODIPY **21** to Heck reaction conditions and systematically removing single reaction components, we determined that the presence of trimethylamine (NEt_3) was initiating decomposition of BODIPY **21**. Replacing NEt_3 with inorganic bases (Cs_2CO_3, K_2CO_3) or bulky amine bases (1,8-bis(dimethylamino)naphthalene) resulted in scant improvement to the conversion product, and decomposition of **21** remained a problem. To circumvent the sensitivity of cyano BODIPY **21**, we attempted a base-free Heck coupling, relying only on the substituted aniline of styrene reactant **4** to buffer the HBr generated during the reaction. The resulting Heck coupling was low yielding (6%), but provided sufficient cyano*m*H **22** to purify and characterize.

Synthesis of carboxy- and amide-BODIPY VoltageFluors

The 2,6-carboxy VoltageFluor series was synthesized via two different routes. Initially, 2,6-dicarboxy BODIPY **32** was synthesized in a 49% yield from aldehyde **9** and 2,4-dimethylpyrrole-3-carboxylic acid **31** (**Scheme 2.4**), then subjected to the same base-free Heck coupling conditions as the cyano BODIPY, giving the 2,6-dicarboxylic acid VoltageFluor, carboxy*m*H (**28**) in a 6% yield after preparative thin layer chromatography (pTLC). Subsequent Heck couplings with the unprotected BODIPY **32** were unproductive, resulting in either unmodified starting material or decomposition. Heck couplings, Suzuki couplings, and an alternate bottom-up synthetic approach towards the dicarboxy VoltageFluors can be found in **Appendix C**. We suspected the carboxylates could be chelating the palladium catalyst and decided to switch to a protecting group approach, which would likely improve the Heck coupling and allow for more facile purification of intermediates by normal phase chromatography.

Benzyl ester protected pyrrole **23**[39] is less nucleophilic than its carboxylic acid precursor. We performed the BODIPY condensation in the same 2:3 DMF:CH_2Cl_2 solvent mixture that worked well for 2,6-cyano BODIPY, providing benzyl-protected BODIPY **24** in a 61% isolated yield (**Scheme 2.4**). Gratifyingly, benzyl-protected BODIPY **24** proceeded cleanly through Heck coupling, even in the presence of NEt_3, and benzyl-protected intermediates **26** and **27** were isolated in a 30 and 43% yield following column chromatography. Cleavage of the benzyl groups with Pd/C under hydrogen atmosphere also reduced one of the alkenes of the molecular wire, evidenced by a mass 2 m/z higher than the desired product and increased brightness of the resulting dye (**Figure 2.1**). A Birkofer reduction[48,49] with $Pd(OAc)_2$, Et_3SiH, NEt_3 in CH_2Cl_2 at room temperature gave the cleanest conversion to the free carboxylate carboxylate product with minimal over-reduction of the alkenes of the molecular wire. Carboxy*m*Me **29** and carboxy*m*OMe **30** were isolated in 31 and 14% yields after pTLC.

Glycyl-amido BODIPY VoltageFluors **35** and **36** were synthesized via Heck coupling between styrenes **4** or **13** and 2,6-amido BODIPY **34**—which was accessed in 82% yield from a HATU-mediated amide bond formation between dicarboxy BODIPY **32** and glycine methyl ester (**33**). Like benzyl-protected BODIPY **24**, the amide-substituted BODIPY **34** withstands the presence of NEt_3 in the Pd-catalyzed cross-coupling, which returns amide*m*H (**35**) and amide*m*Me (**36**) in 21 and 34% isolated yields, respectively (**Scheme 2.4**).

Spectroscopic characterization of sulfonated BODIPYs

The absorption and the emission of BODIPY fluorophores (**Figure 2.2**, **Table 2.1**) and VoltageFluors (**Figure 2.3**, **Table 2.2**) varied with the 2,6-substituents. Consistent with a Dewar formalism,[50–52] electron-withdrawing groups at the 2,6-positions result in a hypsochromatic shift (λ_{max} = 502 nm for cyano-BODIPY **21**) and electron donating groups like Et (BODIPY **3** and **11**) yield bathochromic shifts (λ_{max} = 530 nm). Emission trends mirror the absorption profiles, with the more electron-rich 2,6-ethyl BODIPY **3** and **11** emitting around 544 nm, and 2,6-cyano BODIPY **21**, the most electron-poor, emitting at 517 nm. The absorption and emission profiles of the complete BODIPY VF dyes closely match the spectra of the parent BODIPY fluorophores, with absorption profiles centered at 502 to 528 nm and the phenylene vinylene molecular wire absorbing near 400 nm (**Figure 2.3** and **Table 2.2**).

The *ortho*-sulfonated BODIPY fluorophores have impressive fluorescence quantum yields (ϕ_{fl}) of 0.70—0.99 (**Table 2.1**), but after the addition of the phenylene vinylene molecular wire the quantum yields drop dramatically, supporting the presence of PeT within the compounds (**Table**

2.2). In general, ϕ_{fl} decreased as the fluorophore electron density decreased, such as from Et*m*H **15** to TM*m*H **17**, and decreased further whenever the standard phenylene vinylene molecular wire **4** was replaced with more electron-rich methyl-substituted **13** or methoxy-substituted **14**. These variable wires provided a second strategy to tune the amount of PeT besides directly modifying the fluorophore.

Cellular characterization of BODIPY VF Dyes

The relative cellular brightness of BODIPY VoltageFluors in HEK 293T cells did not match the trend of ϕ_{fl} in cuvette. Despite having the highest ϕ_{fl}, BODIPY VF Et*p*H **6** was one of the dimmest dyes in cells (relative brightness in cells = 0.4), likely due to its poor solubility in aqueous buffer (HBSS) even in the presence of detergent (**Table 2.2, Figure 2.5a**). Et*m*H **15** was approximately 10x brighter than Et*p*H **6** (rel. brightness 4.4 vs 0.4). We suspect this jump is due to the molecular wire being *para* from the sulfonate (**15**) rather than *meta* (**6**), increasing the overall dipole moment and increasing polarity and water solubility. The link between water solubility and efficient membrane staining was further supported by 2,6-dicarboxy BODIPY VF dyes **28** – **30**. These VoltageFluors possessed the largest cellular brightness (rel. brightness up to 12x, **Table 2.2**, **Figure 2.4**). The three negative charges on these VoltageFluors rendered them extremely hydrophilic. Carboxy VoltageFluors prefer to dissolve in water over any organic solvent, despite their relatively greasy phenylene vinylene molecular wire. This water-solubility proved to be advantageous for staining cell membranes—they were the brightest BODIPY VF dyes in HEK cells (**Table 2.2, Figure 2.5d**), including probes that displayed greater ϕ_{fl} in cuvette such as Et*p*H **6**, Et*m*H **15**, or TM*m*H **17**.

The photostability of BODIPY VFs was tested in HEK293T cells and compared to two dichlorofluorescein-based VoltageFluors commonly used by our lab, VF2.1Cl and FVF 2 (**Figure 2.4b**).[31,53] Photostability allows longer imaging experiments and is also correlated with decreased phototoxicity.[54] Based on the Nagano group's work designing photostable BODIPYs,[46] we would expect the BODIPYs to be photostable in the order Amide*m*H > TM*m*OMe > carboxy*m*OMe > Et*m*H. we were not sure how they would compare to our dichlorofluorescein-based VoltageFluors. Amide*m*H was the most photostable VoltageFluor tested—it did not photobleach after 6 minutes of constant illumination, and displayed significant negative photobleaching, which can be a result of the molecular wire bleaching before the BODIPY reporter. Amide*m*H is the most photostable green-emitting voltage-sensitive dye synthesized by our lab to date. VF2.1Cl and TM*m*OMe were in a similar range of photostability, bleaching less than 10% after 2 minutes of constant illumination. Et*m*H and FVF2 showed very similar rates of photobleaching, both bleaching about 35% after 2 minutes and 70-80% after 6 minutes. We were disappointed to see that carboxy*m*OMe bleached the fastest out of all the VoltageFluors—it lost half of its fluorescence after 1 minute of constant illumination, and 80% of its fluorescence after 2 minutes. Despite the photobleaching, carboxy*m*OMe is still a good candidate for voltage imaging because of its bright membrane staining and robust voltage response—it starts at a much higher level of fluorescence than the other BODIPY VoltageFluors and would be the best candidate for short periods of voltage imaging.

Voltage Sensitivity of BODIPY VF Dyes

After confirming BODIPY VoltageFluors localize to the cell membrane, we next investigated their voltage sensitivity using whole cell voltage-clamp electrophysiology in tandem with epifluorescence microscopy. We stepped the membrane potential of a single HEK cell stained with 2 μM BODIPY VoltageFluor from a holding potential of -60 mV to ±100 mV while recording

dye fluorescence intensity. 2,6-ethyl BODIPY VF dyes (**6**, **7**, **15**, and **16**) demonstrated little to no voltage sensitivity. BODIPYs **6** and **7**, with a *para* molecular wire configuration, show no voltage sensitivity, while BODIPYs Et*m*H (**15**) and Et*m*OMe (**16**) with *meta* molecular wire configuration display modest voltage sensitivities of 1.5 and 5 % ΔF/F per 100 mV (**Table 2.2**).

We hypothesized replacing the 2,6-ethyl BODIPY with progressively more electron-poor BODIPYs would increase PeT and therefore increase % ΔF/F. Gratifyingly, we see a 67% increase in voltage sensitivity from Et*m*H **16** to TM*m*H **17**, from 1.5 to 2.5 % ΔF/F (**Table 2**). Strengthening the aniline's electron-donating ability through addition of a methyl or methoxy group further increased the voltage-sensitivity to 6.2 % for TM*m*Me **18** and 33 % ΔF/F for TM*m*OMe **19**. Even-more electron-deficient cyano BODIPY VF **22** displayed extremely low cellular brightness (**Table 2.2**, **Figure 2.5c**) and required increasing both illumination intensity and camera exposure time in order to obtain a reasonable estimate of its voltage sensitivity, which was low: 3.8 % ΔF/F per 100 mV (**Table 2**, **Figure 2.5c**) While cyano BODIPY VF **22** was slightly more voltage sensitive than its analogous precursors, Et*m*H **15** and TM*m*H **17**, its extremely low cellular brightness prohibited further use as a voltage-sensitive dye in cells.

We then evaluated the 2,6-carboxy and amide BODIPY series, hoping to find an electronic "sweet spot" between the tetramethyl and cyano series. The carboxy VoltageFluors carboxy*m*H **28**, carboxy*m*Me **29**, and carboxy*m*OMe **30** had voltage sensitivities of 4.4%, 9.9%, and 24% ΔF/F per 100 mV, respectively. While dicarboxy BODIPY VF dyes display a similar range of voltage sensitivities to their tetramethyl precursors, the most striking quality of the dicarboxy VoltageFluors was their cellular brightness—they were 5-12x brighter compared to the cellular fluorescence intensity of TM*m*OMe **19** (**Table 2.2**). The *in vitro* fluorescence quantum yields of the carboxy VoltageFluors are slightly lower than the tetramethyl VoltageFluors, so this striking increase in brightness is likely due to increased hydrophilicity and cell loading efficiency. We found that amide-substituted BODIPY VF **35** (amide*m*H) possess voltage sensitivity 10x greater than the corresponding carboxy*m*H **28**, with a fractional sensitivity of 48% ΔF/F per 100 mV in HEK cells (compared to 4.4% for carboxy*m*H **28**). Introduction of a more electron-rich molecular wire (methyl substitution) results in a loss of voltage sensitivity for amide*m*Me **36**, which displays only nominal voltage sensitivity (5.1% ΔF/F per 100 mV).

Functional Imaging

We evaluated the ability of BODIPY VF dyes to report on voltage dynamics in electrically excitable cells: mammalian neurons and stem cell-derived cardiomyocytes. Three BODIPY VoltageFluors stood out as good candidates for functional imaging: TM*m*OMe BODIPY VF **19** and amide*m*H BODIPY VF **35** because of their high ΔF/F (33 and 48%, respectively), and carboxy*m*OMe BODIPY VF **30** because of its combination of brightness (7x brighter than TM*m*OMe and amide*m*H, **Figure 2.4**) and good sensitivity (24% ΔF/F).

When cultured rat hippocampal neurons were stained with BODIPY VFs, we determined that TM*m*OMe and amide*m*H were too dim at 2 ms exposure time to capture evoked neuronal action potentials from single neurons. Carboxy*m*OMe, on the other hand, displayed bright, membrane-localized staining in neurons isolated from rat hippocampi (**Figure 2.6b**). Carboxy*m*OMe **30** responded to electrically-evoked neuronal action potentials (**Figure 2.6c** and **d**).

We also evaluated the performance of the three BODIPY VF dyes in human induced pluripotent stem cell-derived cardiomyocytes (hiPSC-CMs). Unlike neurons, cardiomyocytes beat synchronously, allowing action potentials to be reliably analyzed from a small field of view rather

than single cells. We were able successfully image action potentials from hiPSC-CMs using TM*m*OMe, carboxy*m*OMe, and amide*m*H (**Figure 2.7**). TM*m*OMe showed the least associated phototoxicity among the BODIPYs tested, reliably reporting cardiac action potentials for short recordings (10 seconds of constant illumination, **Figure 2.8**), however a decrease in the amplitude and increase in the length of the cardiac action potentials were observed for longer periods of imaging for both TM*m*OMe and fluorescein-based control VF2.1Cl, suggesting slight phototoxic effects on the hiPSC-CMs (**Figure 2.9**).

Discussion

We designed, synthesized, and tested 13 new BODIPY VoltageFluors. We choose 2,6-ethyl BODIPY as a starting point because of its precedent in other biological probes[14,24,29] and its slightly red-shifted spectral properties relative to fluorescein. When the initial probes most analogous to our original VoltageFluor VF2.1Cl, Et*p*H (**6**) and Et*p*OMe (**7**), proved to not be voltage-sensitive, we decided to try moving the molecular wire to the *meta* position, as this had a positive effect on both brightness and voltage sensitivity with previously tested tetramethyl rhodamine VoltageFluors.[33,55] Both *meta* isomers Et*m*H (**15**) and Et*m*OMe (**16**) showed improved brightness and voltage sensitivity compared to *para* isomer, we decided to synthesize all future derivatives as the *meta* isomer. While Et*m*H (**15**) and Et*m*OMe (**16**) were voltage sensitive with 1.5 and 5.4 % ΔF/F per 100 mV, empirically we find that at least a 10% ΔF/F per 100 mV in HEK cells is required for effective use in either neuronal or cardiomyocyte systems.[53]

Small structural changes to the fluorophore or molecular wire electron density dramatically alter ΔF/F, especially for fluorescein-based VoltageFluors.[32,34] Inspired by this and the synthetic versatility of the BODIPY fluorophore, we decided to incorporate progressively more electron-poor BODIPY fluorophores to see if the voltage sensitivity could be improved. The tetramethyl BODIPY VoltageFluors supported our hypothesis that increasing the ΔG_{PeT} would increase voltage sensitivity. The more electron-poor tetramethyl BODIPY VFs TM*m*H (**17**), TM*m*Me (**18**), and TM*m*OMe (**19**) outperformed the more electron-rich 2,6-ethyl BODIPY VF series with respect to voltage sensitivity (**Table 2.2**) and photostability in cells under extended illumination (**Figure 2.4**). TM*m*OMe (**19**) stood out as a good candidate for biological imaging because of its excellent membrane staining, robust voltage sensitivity (33 % ΔF/F per 100 mV), and linear fluorescent response to changes in membrane potential (**Figure 2.5b**).

Decreasing the electron density of BODIPY VF dyes by replacing the 2,6 positions with cyano groups results in an indicator with prohibitively low voltage sensitivity (3.8% ΔF/F per 100 mV) and extremely low cellular brightness (**Figure 2.5c**). Electron withdrawing substituents such as carboxylates and amides were an attractive choice, both because their electron withdrawing character is lower than that of –CN, and because amides and carboxylates allow for the opportunity of subsequent functionalization for improved cellular localization and/or targeting.[54,56]

Dicarboxy and amide BODIPY VF dyes were more challenging to synthesize than their ethyl, hydrogen or cyano congeners, but gave indicators with cellular brightness up to an order of magnitude higher than any other probe, in the case of the carboxy BODIPY VFs (**28-30**). The voltage sensitivity of the carboxy BODIPY VF dyes and the tetramethyl BODIPY VF dyes were similar: 2.5 or 4.4% ΔF/F for TM*m*H (**17**) and carboxy*m*H (**28**); 6.2 or 9.9% ΔF/F for TM*m*Me (**18**) and carboxy*m*Me (**29**); and 33 or 24% ΔF/F for TM*m*OMe (**19**) and carboxy*m*OMe (**30**).

We were not expecting the amide BODIPY VoltageFluor (**35**) to be drastically different from its carboxy precursors, but the change in voltage sensitivity was dramatic—compared to the

4.4 % ΔF/F of carboxy*m*H, just changing the carboxylates to amides gave amide*m*H 48 % ΔF/F, a tenfold increase (**Table 2.2**, **Figure 2.5e**). Amide*m*H was not as bright as the dicarboxy series (**Figure 2.4**), possibly due to the lack of additional negative charges. Amide*m*Me **36**, like cyano*m*H **22**, displayed a lower voltage sensitivity than amide*m*H, suggesting that amide*m*H is close to the ideal rate of PeT to optimize the voltage sensitivity, and increasing the rate of PeT any further is detrimental to the voltage sensitivity.

The voltage sensitivity of the BODIPY VF dyes correlates with the electron-withdrawing character of the 2,6-substitution pattern in the BODIPY fluorophore. More electron-withdrawing substituents increase voltage sensitivity in the order of -Et < -H < -CO_2H < -CONHR > -CN. The extremely electron-withdrawing character of nitrile substitution makes for a poorly sensitive BODIPY VF. We find that calculated values of HOMO energies for the BODIPY fluorophores—lacking the molecular wire—correlate extremely well with either *meta* or *para* Hammett constants (σ_m or σ_p), validating the use of tabulated Hammett constants for analysis of the relative electron density of a particular BODIPY fluorophore (**Figure 2.10a,b**). Correlation between calculated HOMO energies and σ_m or σ_p values is best when evaluating neutral BODIPYs (Et, H, CONHR, or CN), with correlation coefficients (R^2) >0.99 for both σ_m and σ_p compared to HOMO. If carboxy-substituted BODIPYs are included, the correlation (R^2) between HOMO level and Hammett parameter drops to 0.92 (σ_m) and 0.78 (σ_p) (**Figure 2.10a,b**).

The average ΔF/F for a class of BODIPY fluorophore (R = Et, H, CO_2H, CONHR, or CN) displays a parabolic relationship with published Hammett constants (either σ_m or σ_p, **Figure 2.10c**), with maximum voltage sensitivity at around σ = 0.2 - 0.4. BODIPY VF dyes that have very large and negative ΔG_{PeT}, either by a combination of electron deficient fluorophores (R = CN) with mildly donating anilines (R = H) as in the case of BODIPY VF **22**, or by with moderately withdrawing fluorophores (R = CONHR) with electron-rich anilines (R = Me) in the case of amide*m*Me BODIPY **36**, will have low voltage sensitivity. These results suggest that amide*m*H **36** occupies a "sweet spot" of PeT to optimize the voltage sensitivity for BODIPY VoltageFluors, and any further lowering of the fluorophore HOMO (such as amide BODIPY to cyano BODIPY) or raising the HOMO of the aniline PeT donor (unsubstituted aniline to methyl-substituted aniline) is detrimental to the voltage sensitivity.

Despite its impressive 48% ΔF/F in HEK cells, amide*m*H BODIPY **36** has some downsides compared to its dicarboxy precursors. It is 5-12x dimmer in HEK293T cells than the dicarboxy VoltageFluors, despite *in vitro* ϕ_{fl} being in the range of 0.03—0.07 for both dicarboxy and amide BODIPY VoltageFluors. We suspect this relative dimness is a cell loading issue, and the dicarboxy BODIPY VoltageFluors load much more efficiently into cells compared to TM*m*OMe or amide*m*H because of their two additional negative charges, increasing their water solubility and amphiphilicity.

The other downside we discovered is that while the amide BODIPY VoltageFluor is very photostable, it tends to internalize into HEK293T cells if under continuous illumination for more than a minute (**Figure 2.11**). We did not observe this internalization for our VF2.1Cl and FVF 2 controls or any other BODIPY VoltageFluors in HEK293T cells and were able to continuously illuminate for 6 minutes without internalization. Amide*m*H was the most photostable BODIPY VoltageFluor and was also more photostable than one of our best fluorescein-based indicators, VF2.1Cl, so improving upon these weaknesses could make amide*m*H a great tool for voltage imaging.

Current work is underway to synthesize amide*m*H with terminal carboxylates instead of methyl esters to see if this improves the probe's brightness. We first attempted to hydrolyze the

methyl esters of amide*m*H by incubating the probe with pig liver esterase (PLE) for 1-3 hours at 37°C.[57] Unfortunately, amide*m*H did not seem to be a good substrate for PLE—we observed mostly unmodified starting material. We also attempted a saponification with 10 equivalents of aqueous NaOH, but observed an intractable mixture of more polar products. The BODIPY fluorophore's sensitivity to acid and base was a major reason we chose benzyl protecting groups for the synthesis of the dicarboxy VoltageFluors, and this protecting group strategy could also be applied to make the amide BODIPY VoltageFluor more water-soluble (**Scheme 2.5**).

Conclusion & Future Work

We designed, synthesized, and tested 13 new BODIPY voltage-sensitive fluorophores. The most sensitive, amide*m*H BODIPY VF **36** at 48% ΔF/F per 100 mV, is the most sensitive BODIPY-based voltage indicator to date.[58,59] Two other indicators developed in this study, TM*m*OMe BODIPY VF **19**, with its slightly lower sensitivity (33% ΔF/F per 100 mV), but good brightness, and carboxy*m*OMe BODIPY VF **30**, which retains good voltage sensitivity (24% ΔF/F per 100 mV) and exceptional brightness (~7x brighter than **19** or **36**) proved to be useful tools for functional imaging in neurons or cardiomyocytes. We discovered that the voltage sensitivity of BODIPY VoltageFluors display a parabolic relationship to Hammett constants, both σ_p and σ_m, and utilized the synthetic versatility of the BODIPY fluorophore to systematically increase the voltage sensitivity of these indicators.

Future work to improve BODIPY VFs could include increasing the brightness of amide*m*H by synthesizing a derivative with terminal carboxylates (**Scheme 2.5**) and decreasing the dye's phototoxicity by appending a triplet state quencher, such as cyclooctatetraene (COT),[60–62] on the dye scaffold. Amide*m*H's excellent photostability would make it a great candidate for targeted dual-color imaging with red/NIR VoltageFluors,[63] and terminal carboxylates would also be useful synthetic handles to attach targeting substrates.[56] Cellular membrane loading of TM*m*OMe could also be improved, potentially by adding water-solubilizing moieties to the BODIPY boron with established methodologies,[35,37] since substitution at boron should not drastically affect the dye's excellent voltage sensitivity.

Figures & Schemes

Scheme 2.1 *Design of H_2O-soluble BODIPYs*

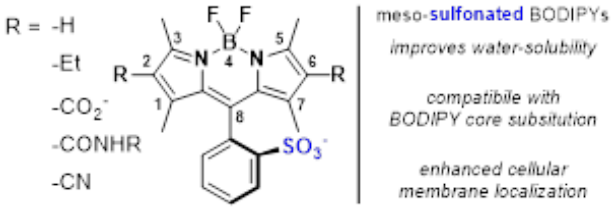

Scheme 2.2 *Synthesis of Ethyl and Tetramethyl VoltageFluors*

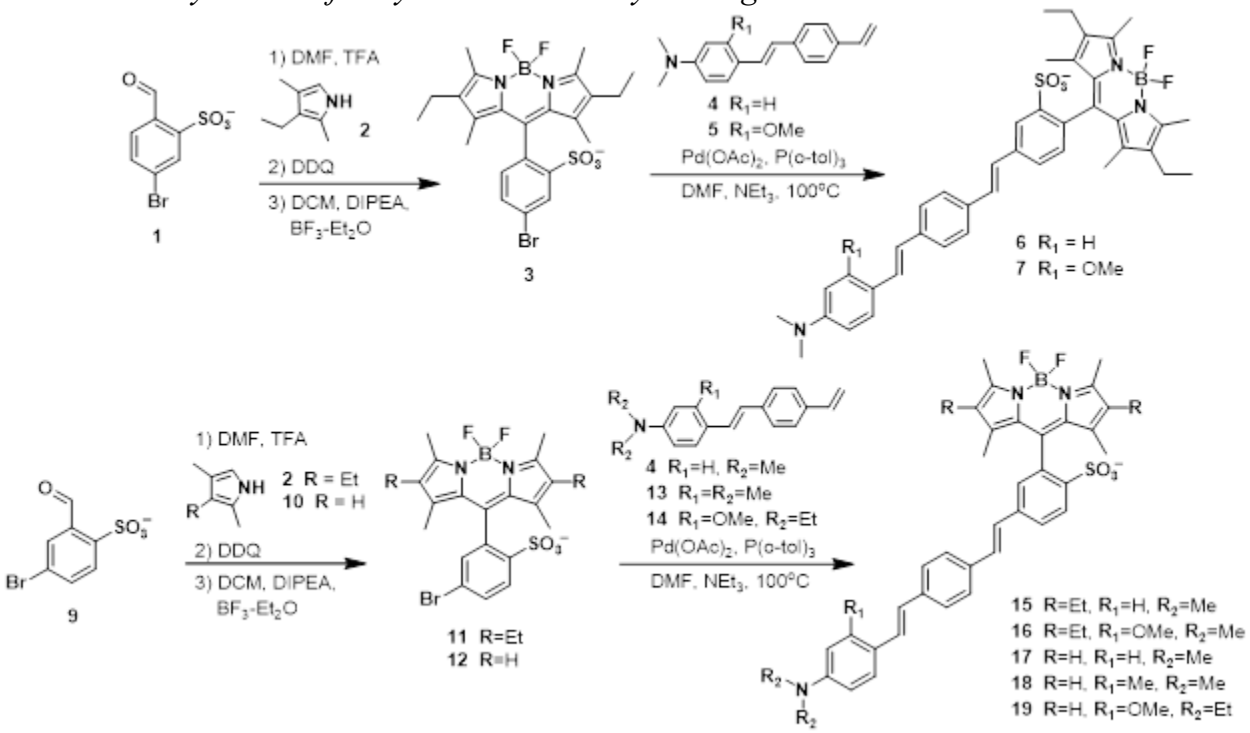

Scheme 2.3 *Synthesis of CN-BODIPY VoltageFluor*

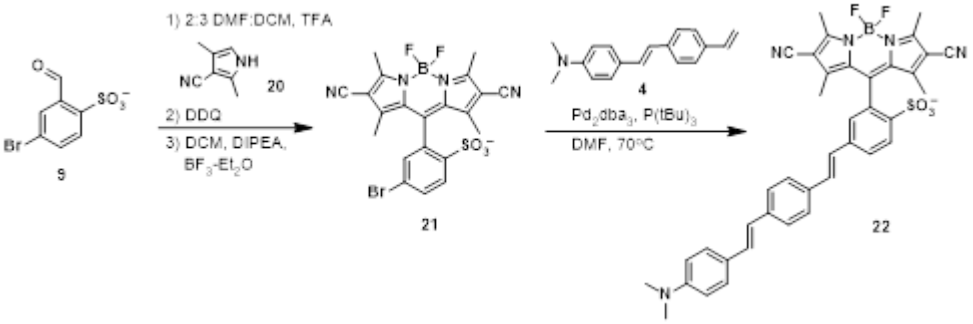

Scheme 2.4 *Synthesis of Carboxy and Amide VoltageFluors*

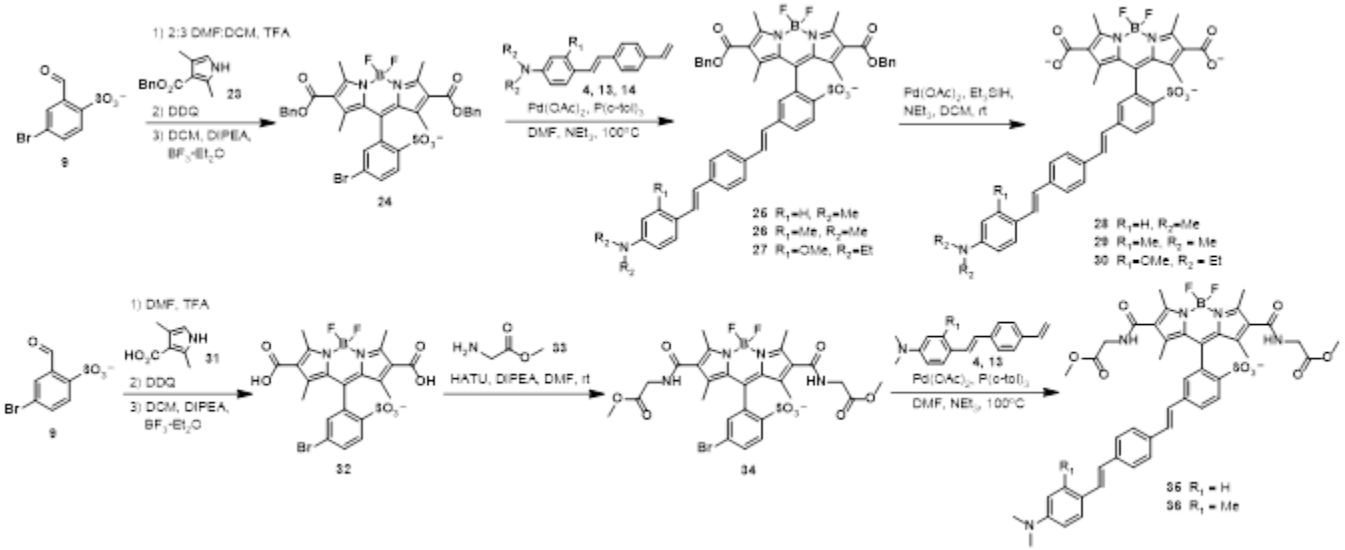

Scheme 2.5 *Proposed route to amidemH with terminal carboxylates*

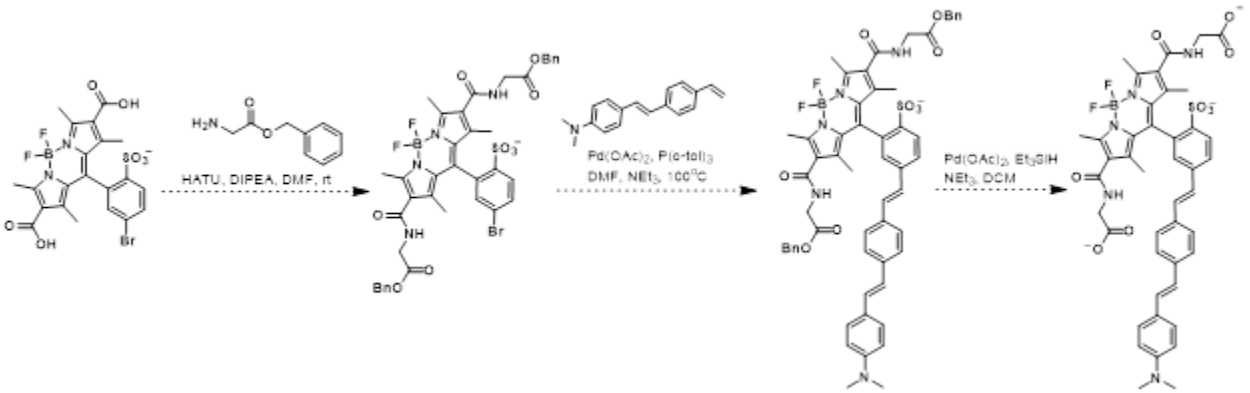

Figure 2.1 *Over-reduction by Pd/C and H_2*

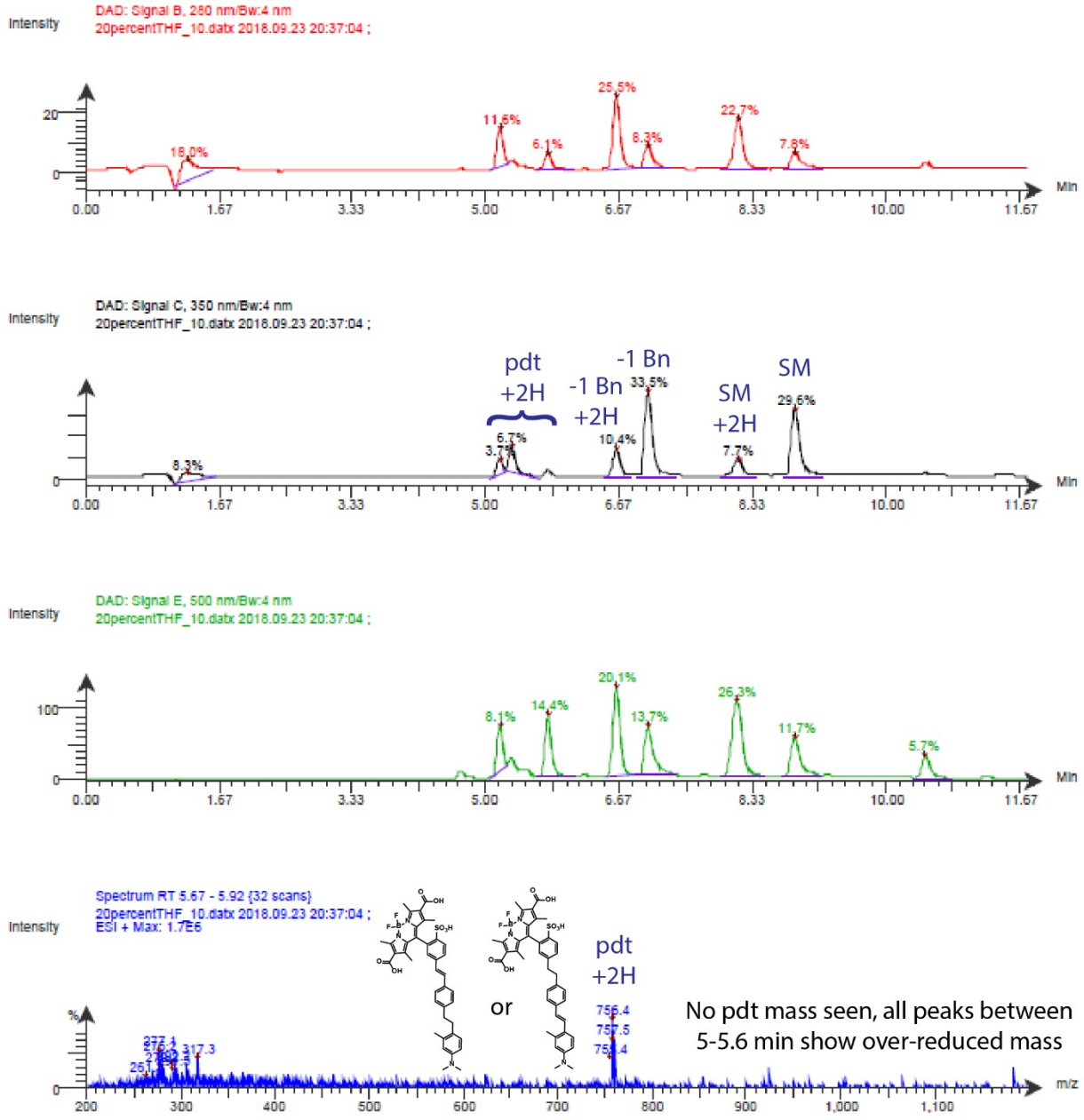

Figure 2.1. LC-MS of treating OBn*m*Me **26** with 20 mol% Pd/C under hydrogen atmosphere. While one benzyl group is successfully cleaved with only partial over-reduction of the molecular wire, no doubly deprotected product was obtained. All peaks between 5-6 min displayed 756 m/z, corresponding to cleaving both benzyl groups and reducing an alkene.

Figure 2.2 *Normalized absorption and emission spectra of ortho-sulfonated BODIPYs*

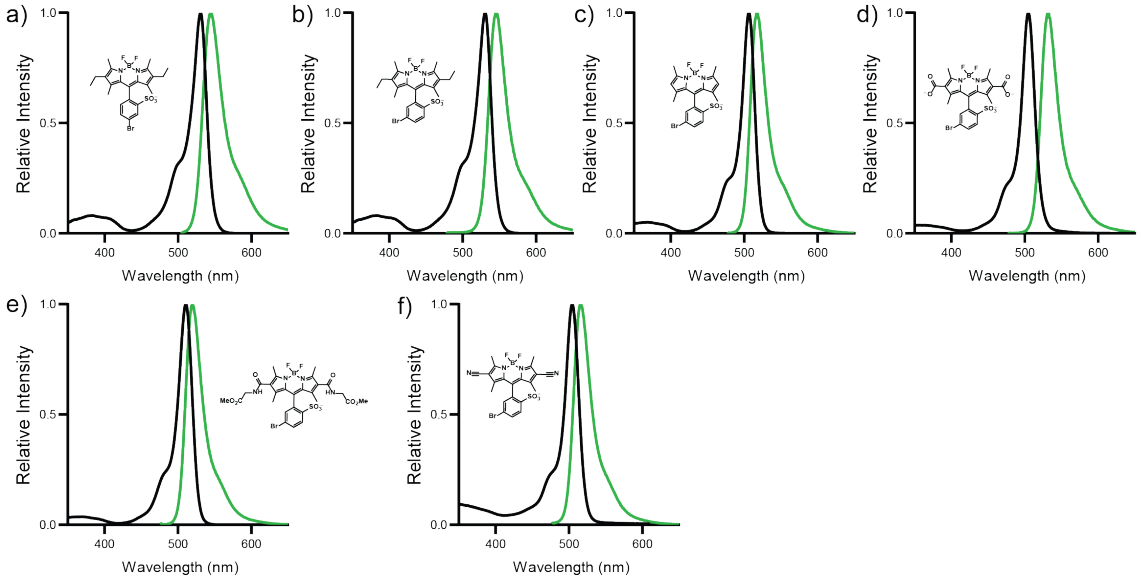

Figure 2.2 Absorption and emission spectra of **a)** Et*p*Br **3**, **b)** Et*m*Br **11**, **c)** TM*m*Br **12**, **d)** Carboxy*m*Br **32**, **e)** Amide*m*Br **34**, and **f)** CN*m*Br **21** *ortho*-sulfonated BODIPYs. Spectra were acquired in PBS pH 7.4 with 1 μM dye.

Table 2.1 *Spectroscopic properties of ortho-sulfonated BODIPYs*

	R	λ_{max} abs [a]	λ_{max} em [a]	ε (M^{-1} cm^{-1})[b]	ϕ_{fl}[a]
3	Et	530	544	53000	0.72
11	Et	530	545	60000	0.70
12	H	503	515	70000	0.99
32	CO_2H	517	532	77000	0.95
34	$CONHCH_2CO_2Me$	507	519	84000	0.92
21	CN	502	517	41000	0.93

a acquired in PBS pH 7.4. b acquired in ethanol.

Figure 2.3 *Normalized absorption and emission spectra of BODIPY VoltageFluors*

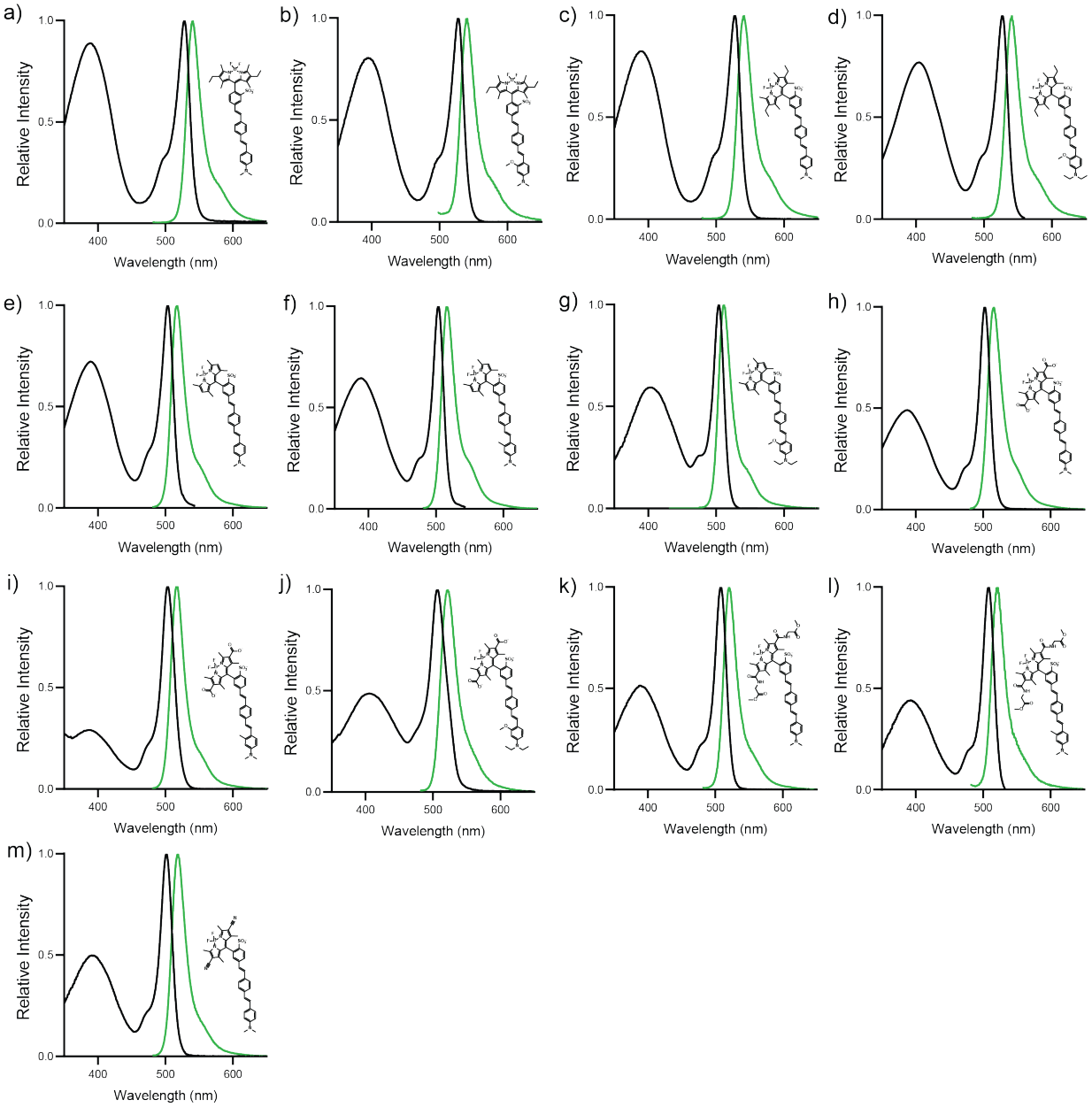

Figure 2.3 Absorption and emission spectra of **a)** Et*p*H, **b)** Et*p*OMe, **c)** Et*m*H, **d)** Et*m*OMe, **e)** TM*m*H, **f)** TM*m*Me, **g)** TM*m*OMe, **h)** carboxy*m*H, **i)** carboxy*m*Me, **j)** carboxy*m*OMe, **k)** amide*m*H, **l)** amide*m*Me, and **m)** cyano*m*H BODIPY VoltageFluors. Spectra were acquired in ethanol with 1 μM dye.

Table 2.2 *Properties of BODIPY VoltageFluors*

	Name	R	R_1	isomer	λ_{max} abs[a]	λ_{max} em[a]	ϕ_{fl}[a]	% $\Delta F/F$[bc]	Cell brightness[cd]
6	Et*p*H	Et	H	*para*	528	541	0.14	0	0.43 ± 0.02[f]
7	Et*p*OMe	Et	OMe	*para*	527	541	0.07	0	0.76 ± 0.03[f]
15	Et*m*H	Et	H	*meta*	528	541	0.15	1.8 ± 0.1	4.4 ± 0.3[f]
16	Et*m*OMe	Et	OMe	*meta*	527	541	0.05	5.4 ± 0.6	0.60 ± 0.03[f]
17	TM*m*H	H	H	*meta*	503	518	0.11	2.5 ± 0.1	0.62 ± 0.08
18	TM*m*Me	H	Me	*meta*	504	517	0.07	6.2 ± 0.4	1.5 ± 0.2
19	TM*m*OMe	H	OMe	*meta*	504	512	0.05	33 ± 0.7	1.0 ± 0.1
28	carboxy*m*H	COOH	H	*meta*	503	516	0.07	4.4 ± 0.2	12 ± 2
29	carboxy*m*Me	COOH	Me	*meta*	503	517	0.03	9.9 ± 0.4	5.1 ± 0.9
30	carboxy*m*OMe	COOH	OMe	*meta*	509	522	0.06	24 ± 0.5	7.1 ± 0.8
35	amide*m*H	$CONHCH_2CO_2Me$	H	*meta*	508	521	0.06	48 ± 2	1.0 ± 0.1
36	amide*m*Me	$CONHCH_2CO_2Me$	Me	*meta*	509	521	0.03	5.1 ± 0.4	1.0 ± 0.1
22	cyano*m*H	CN	H	*meta*	502	519	0.08	3.8[e]	0.34 ± 0.002

a Determined in ethanol. **b** Per 100 mV depolarization. **c** Determined in HEK cells. **d** Relative to TMmOMe **19**. **e** Increased exposure time and light intensity required to make measurement. **f** Pluronic F-127 (0.01%) used during loading

Figure 2.4 *Relative brightness of BODIPY VoltageFluors in HEK293T cells*

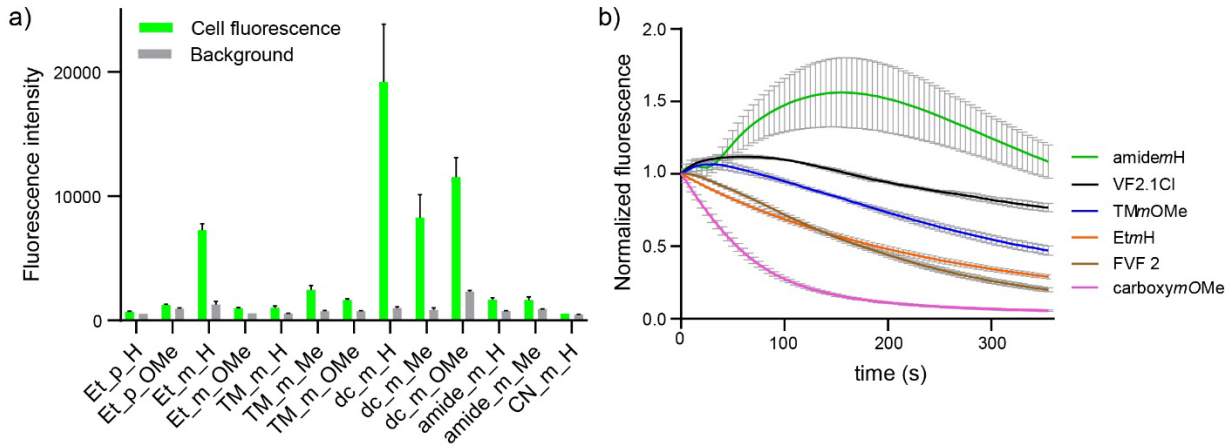

Figure 2.4 a) Average background-subtracted fluorescence intensity of BODIPY VoltageFluors in HEK293T cells for n = 3 images. Cells were loaded with 1 µM of each dye, and images acquired with teal LED/100 ms exposure time. b) Relative photobleaching over 6 minutes of constant illumination of 1 µM BODIPY VoltageFluors as well as 1 µM of two dichlorofluorescein-based voltage indicators, VF2.1Cl and FVF 2.[31,53]

Figure 2.5a *Cellular characterization of ethyl-substituted BODIPY VF dyes* ***6****,* ***7****,* ***15****,* ***16***

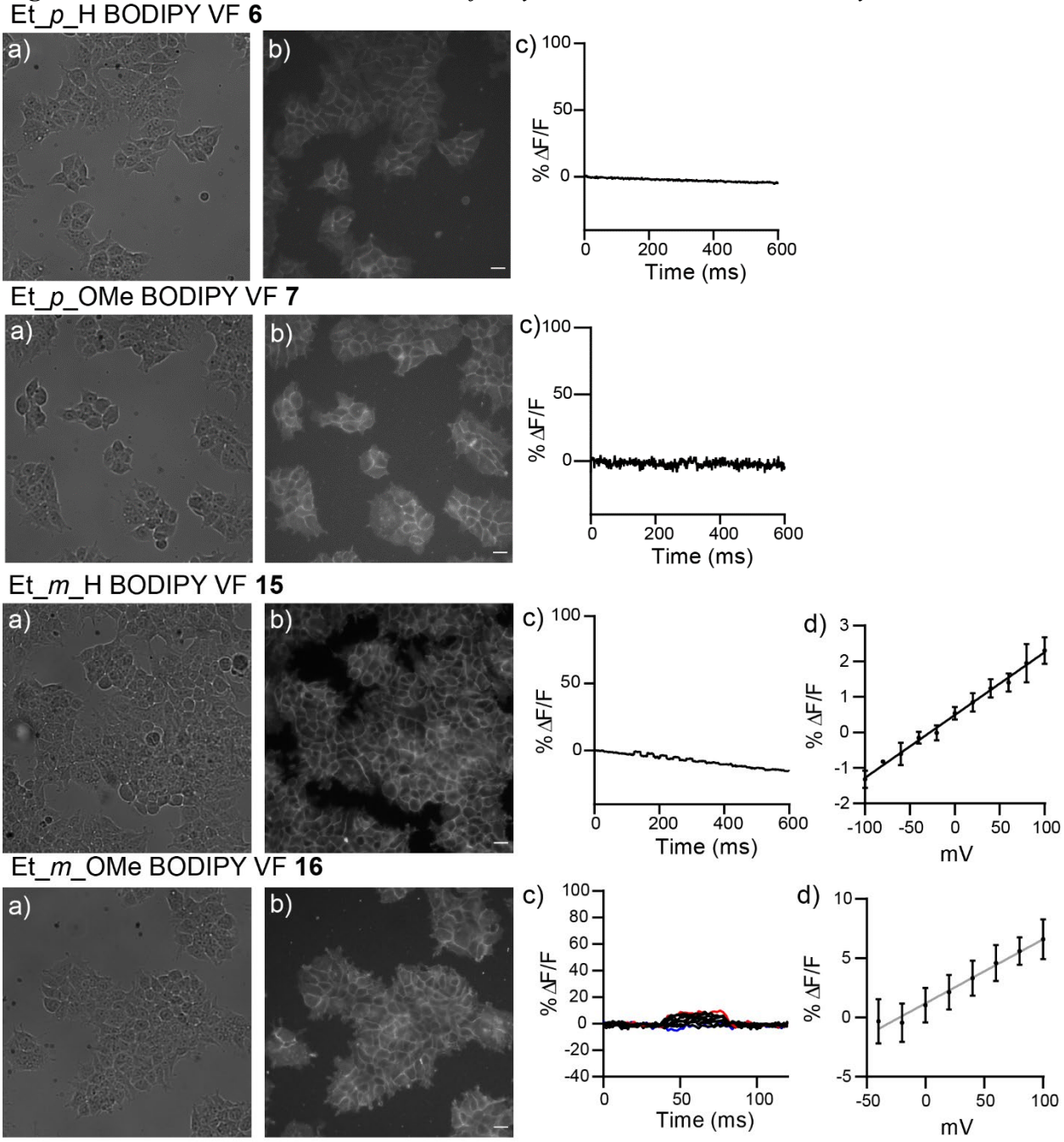

Figure 2.5a. Cellular characterization of ethyl-substituted BODIPY VF dyes Et*p*H **6**, Et*p*OMe **7**, Et*m*H **15**, and Et*m*OMe **16**. HEK293T cells stained with 1 µM BODIPY VF are visualized under **a)** transmitted light and **b)** widefield fluorescence microscopy. Fluorescence images are adjusted to allow membrane staining to be seen. Scale bars are 20 µm. **c)** Plot of fractional change in fluorescence (ΔF/F) vs. time for hyper- and depolarizing steps (±100 mV in 20 mV increments) from a holding potential of -60 mV in a single HEK cell under whole-cell voltage-clamp mode. BODIPY VoltageFluors with < 5% ΔF/F are shown as unconcatenated, non-bleach corrected traces. All plots are scaled from -40 to 100% ΔF/F to facilitate comparison of voltage sensitivity. **d)** Plot of fractional change in fluorescence (ΔF/F) vs. final membrane potential. Data represent the mean ΔF/F, ± S.E.M., for a minimum of n = 3 separate cells. Grey line is the line of best fit.

Figure 2.5b *Cellular characterization of tetramethyl BODIPY VF dyes* ***17****,* ***18****, and* ***19****.*

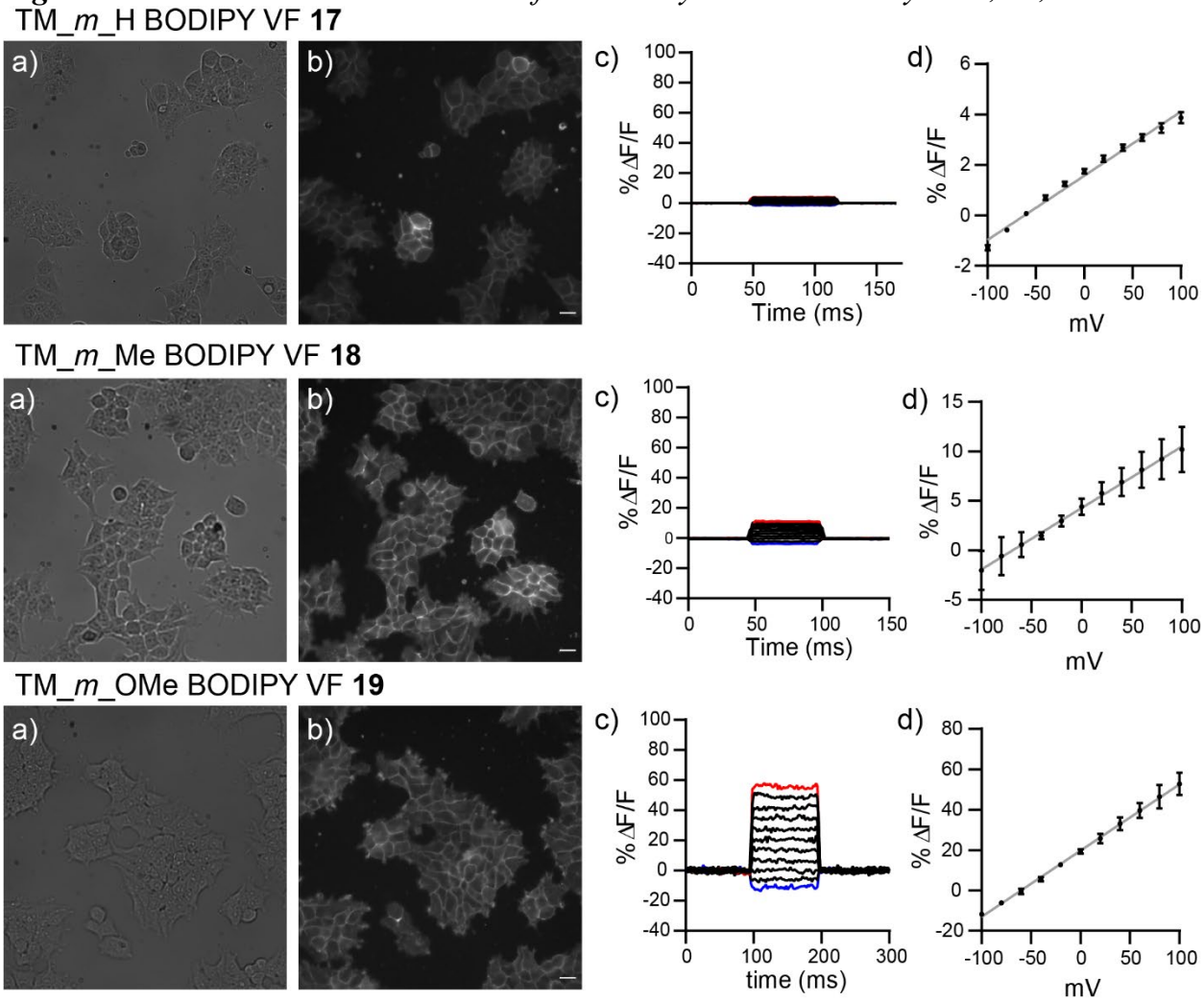

Figure 2.5b. Cellular characterization of H-substituted BODIPY VF dyes **17**, **18**, and **19**. HEK293T cells stained with 1 µM BODIPY VF are visualized under **a)** transmitted light and **b)** widefield fluorescence microscopy. Fluorescence images are adjusted to allow membrane staining to be seen. Scale bars are 20 µm. **c)** Plot of fractional change in fluorescence (ΔF/F) vs. time for hyper- and depolarizing steps (±100 mV in 20 mV increments) from a holding potential of -60 mV in a single HEK cell under whole-cell voltage-clamp mode. All plots are scaled from -40 to 100% ΔF/F to facilitate comparison of voltage sensitivity. **d)** Plot of fractional change in fluorescence (ΔF/F) vs. final membrane potential. Data represent the mean ΔF/F, ± S.E.M., for a minimum of n = 3 separate cells. Grey line is the line of best fit.

Figure 2.5c *cellular characterization of cyano-substituted BODIPY VF dye* ***22****.*

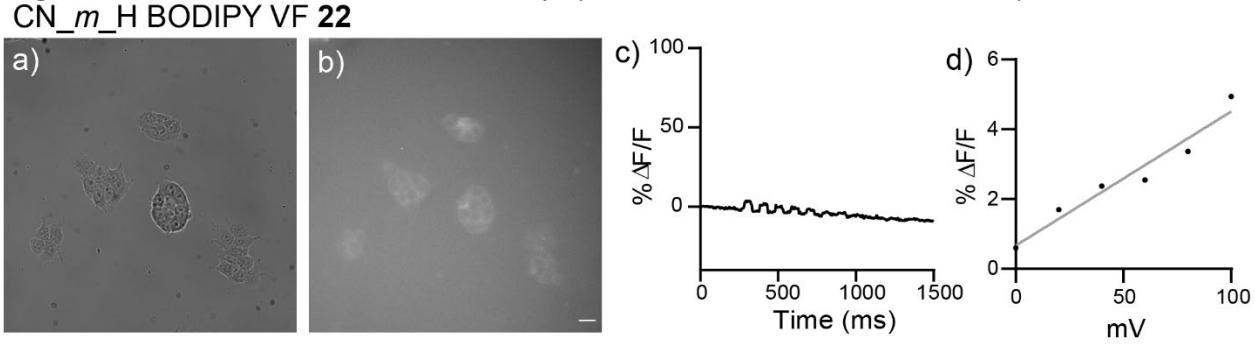

Figure S6. Cellular characterization of cyano-substituted BODIPY VF dye **22**. HEK293T cells stained with 1 μM **22** are visualized under **a)** transmitted light and **b)** widefield fluorescence microscopy. Fluorescence images are adjusted to allow membrane staining to be seen. Scale bars are 20 μm. **c)** Plot of fractional change in fluorescence (ΔF/F) vs. time for hyper- and depolarizing steps (±100 mV in 20 mV increments) from a holding potential of -60 mV in a single HEK cell under whole-cell voltage-clamp mode. BODIPY VoltageFluors with < 5% ΔF/F are shown as unconcatenated, non-bleach corrected traces. All plots are scaled from -40 to 100% ΔF/F to facilitate comparison of voltage sensitivity. **d)** Plot of fractional change in fluorescence (ΔF/F) vs. final membrane potential. Grey line is the line of best fit.

Figure 2.5d *Cellular characterization of carboxy-substituted BODIPY VF dyes* ***28****,* ***29****,* ***30***

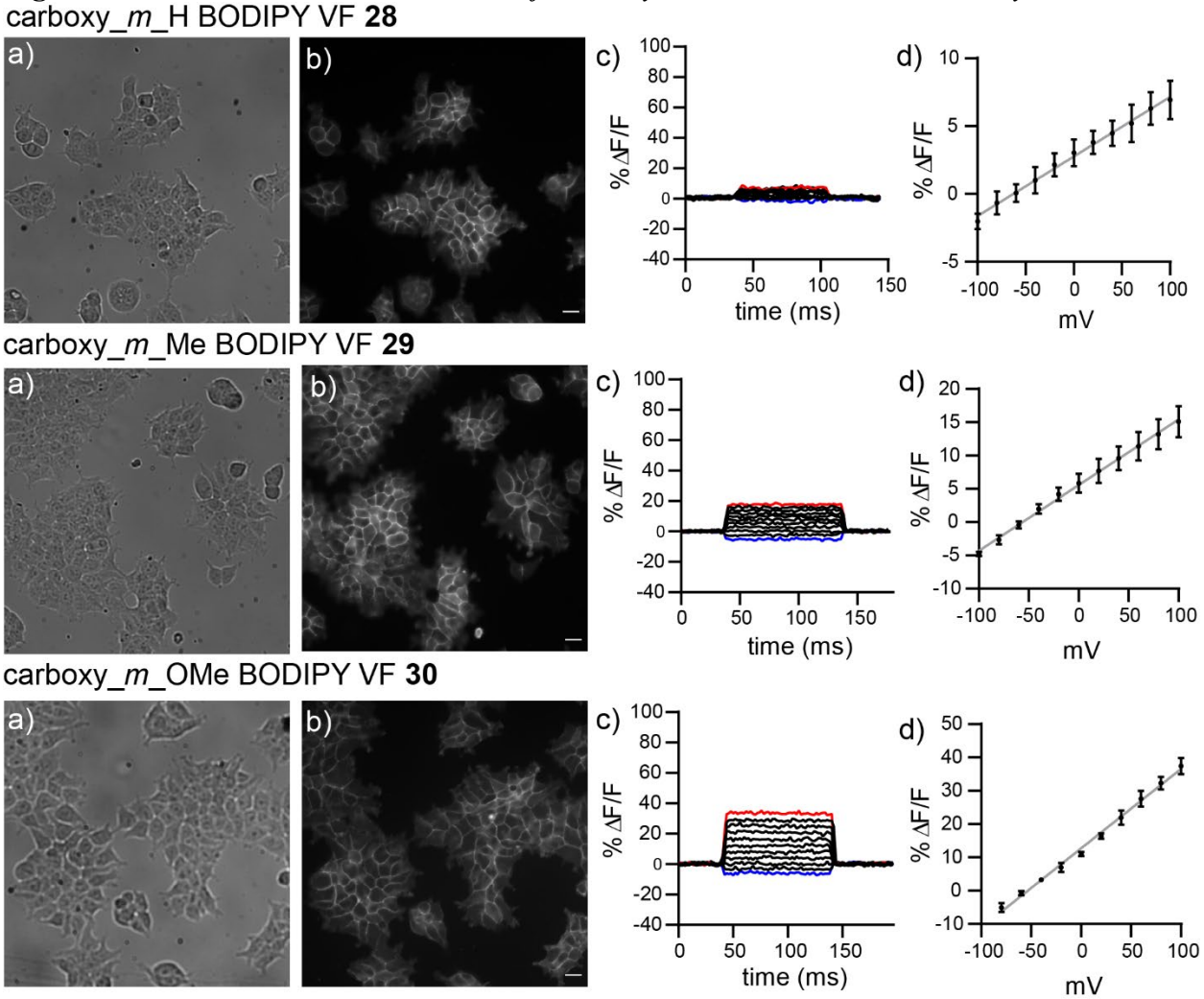

Figure 2.5d. Cellular characterization of carboxy-substituted BODIPY VF dyes **28**, **29**, and **30**. HEK293T cells stained with 1 μM BODIPY VF are visualized under **a)** transmitted light and **b)** widefield fluorescence microscopy. Fluorescence images are adjusted to allow membrane staining to be seen. Scale bars are 20 μm. **c)** Plot of fractional change in fluorescence (ΔF/F) vs. time for hyper- and depolarizing steps (±100 mV in 20 mV increments) from a holding potential of -60 mV in a single HEK cell under whole-cell voltage-clamp mode. All plots are scaled from -40 to 100% ΔF/F to facilitate comparison of voltage sensitivity. **d)** Plot of fractional change in fluorescence (ΔF/F) vs. final membrane potential. Data represent the mean ΔF/F, ± S.E.M., for a minimum of n = 3 separate cells. Grey line is the line of best fit.

Figure 2.5e *Cellular characterization of amide-substituted BODIPY VF dyes* ***35*** *and* ***36****.*

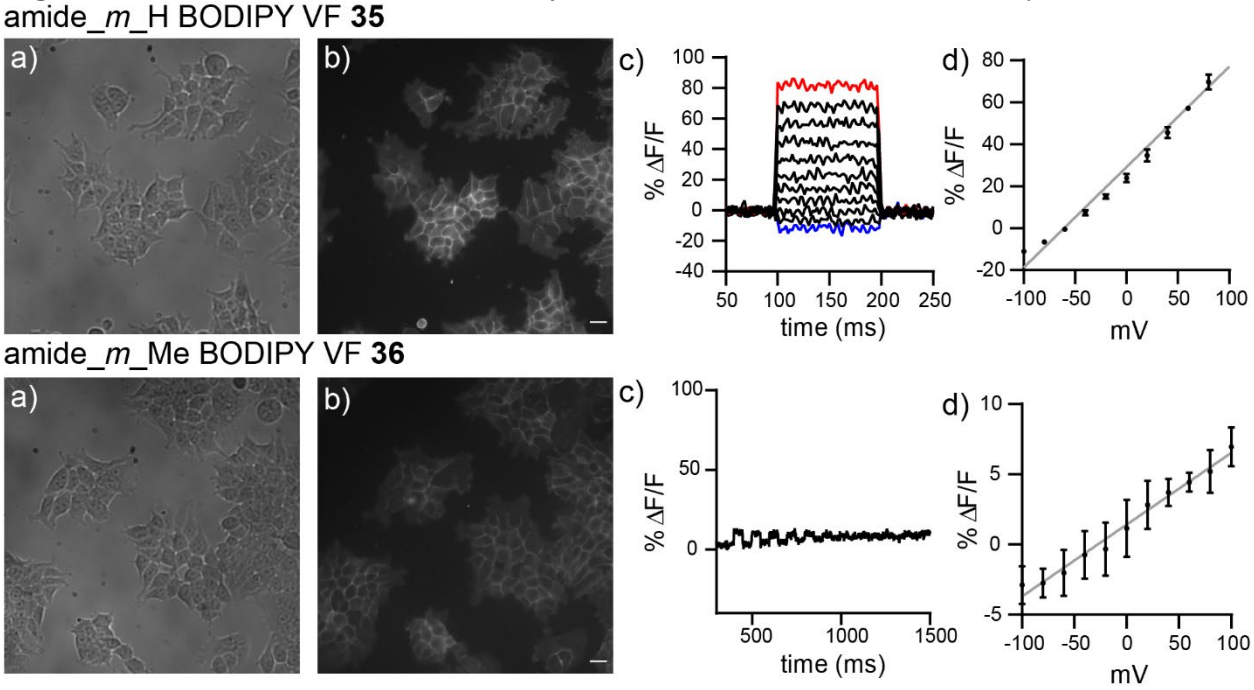

Figure 2.5e. Cellular characterization of amide-substituted BODIPY VF dyes **35** and **36**. HEK293T cells stained with 1 µM BODIPY VF are visualized under **a)** transmitted light and **b)** widefield fluorescence microscopy. Fluorescence images are adjusted to allow membrane staining to be seen. Scale bars are 20 µm. **c)** Plot of fractional change in fluorescence (ΔF/F) vs. time for hyper- and depolarizing steps (±100 mV in 20 mV increments) from a holding potential of -60 mV in a single HEK cell under whole-cell voltage-clamp mode. BODIPY VoltageFluors with < 5% ΔF/F are shown as unconcatenated, non-bleach corrected traces. All plots are scaled from -40 to 100% ΔF/F to facilitate comparison of voltage sensitivity. **d)** Plot of fractional change in fluorescence (ΔF/F) vs. final membrane potential. Data represent the mean ΔF/F, ± S.E.M., for a minimum of n = 3 separate cells. Grey line is the line of best fit.

Figure 2.6 *Voltage imaging in mammalian neurons with carboxymOMe BODIPY VF* ***30****.*

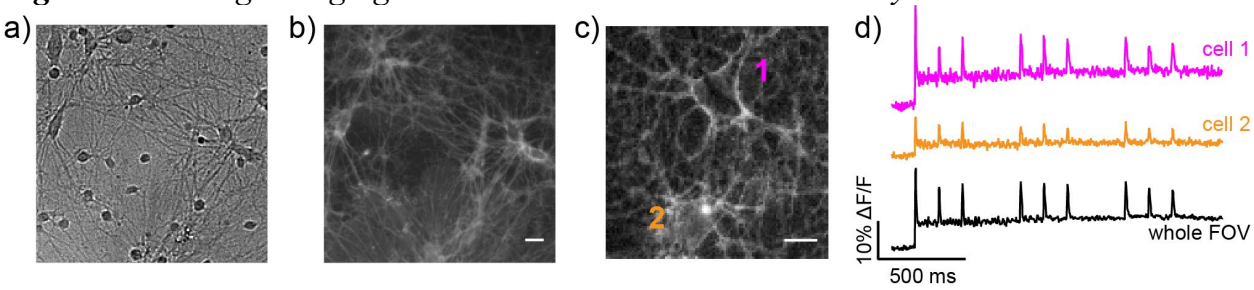

Figure 2.6 Voltage imaging in mammalian neurons with carboxy*m*OMe BODIPY VF **30**. **a)** Transmitted light and **b)** widefield epifluorescence image of cultured rat hippocampal neurons stained with 500 nM carboxy*m*OMe BODIPY VF **30**. Scale bar is 20 µm. **c)** Widefield epifluorescence image of neurons stained with 500 nM carboxy*m*OMe BODIPY VF **30** and imaged at 500 Hz. Image is a single frame from this high-speed acquisition. Scale bar is 20 µm. **d)** Plot of fractional change in fluorescence (ΔF/F) for the cells identified in panel (c) or for the entire field of view (FOV).

Figure 2.7 *Functional imaging in hiPSC-CMs with BODIPY VoltageFluors.*

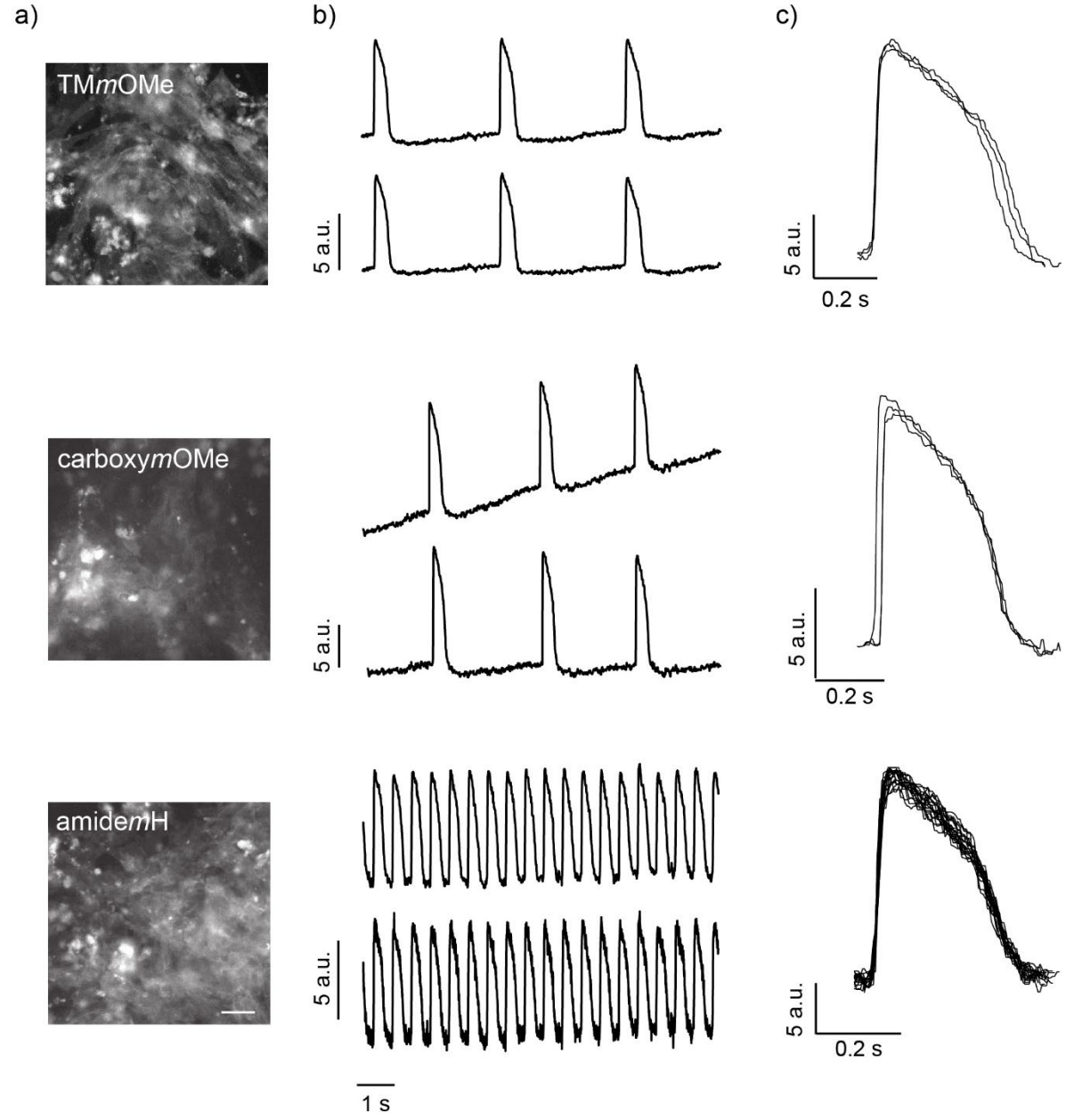

Figure 2.7. Functional imaging in human induced pluripotent stem cell-derived cardiomyocytes (hiPSC-CMs) with TM*m*OMe **19**, carboxy*m*OMe **30**, and amide*m*H **35** BODIPY VoltageFluors. **a)** Widefield, epifluorescence micrograph of hiPSC-CMs stained with 500 nM of each BODIPY VoltageFluor. Scale bar is 50 μm. **b)** Trace of mean pixel intensity (arbitrary fluorescence units, a.u.) from full region of interest (ROI) plotted vs time during 10 second acquisition. Top traces are raw values after median filter, bottom traces are corrected for photobleach. Teal LED powers used were 15% for TM*m*OMe, 15% for carboxy*m*OMe, and 5% for amide*m*H. **c)** Averaged action potential traces from 10 second recordings, not normalized.

Figure 2.8 *Voltage imaging in hiPSC-CMs with TMmOMe BODIPY VF* ***19****.*

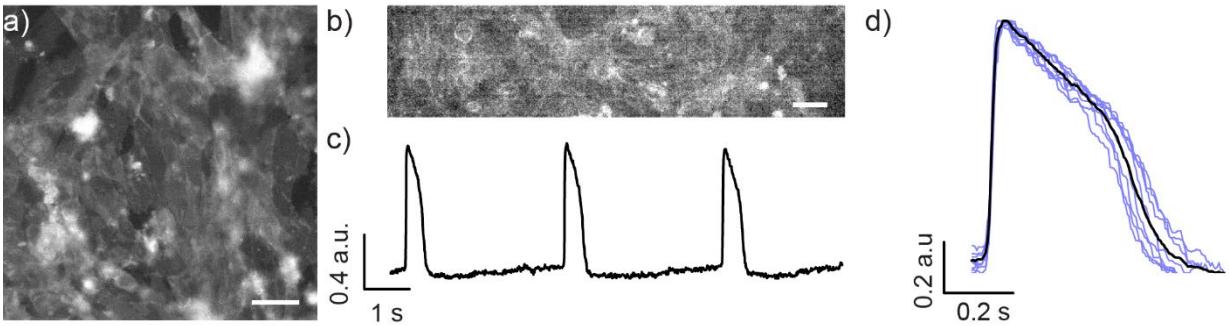

Figure 2.8. Voltage imaging in human induced pluripotent stem cell-derived cardiomyocytes (hiPSC-CMs) with TM*m*OMe BODIPY VF **19**. **a)** Widefield, epifluorescence micrograph of hiPSC-CMs stained with 500 nM TM*m*OMe BODIPY VF **19**. Scale bar is 50 µm. **b)** Single frame of a movie collected at 500 Hz for functional imaging of hiPSC-CM spontaneous action potentials. Scale bar is 50 µm. **c)** Trace of mean pixel intensity (arbitrary fluorescence units, a.u.) from full region of interest (ROI) in panel (b) plotted vs time during 10 second acquisition, corrected for photobleach. **d)** Averaged action potential trace (black) from three 10 second recordings from 3 separate ROIs over individual AP events from each recording (blue).

Figure 2.9 *Comparison of BODIPY and fluorescein VoltageFluors in cardiomyocytes.*

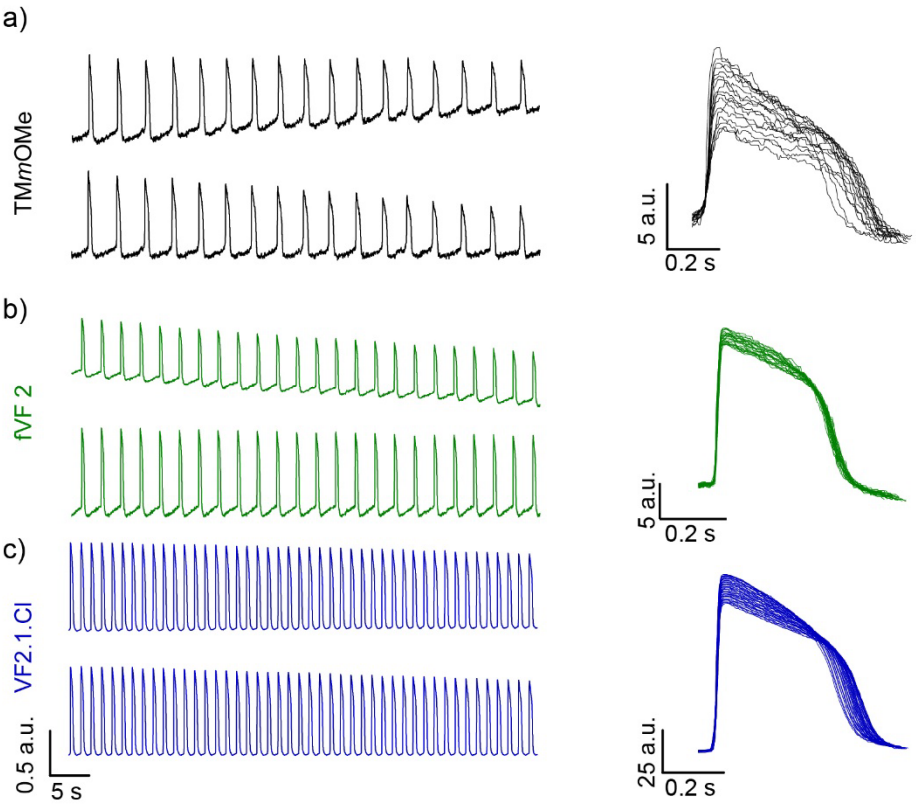

Figure 2.8. Voltage imaging in human induced pluripotent stem cell-derived cardiomyocytes (hiPSC-CMs) with **a)** TM*m*OMe BODIPY VF **19**, **b)** fvf 2,[53] and **c)** VF2.1Cl, all at 500 nM dye and 15% teal LED power.[31] Shown are traces of mean pixel intensity (arbitrary fluorescence units, a.u.) from full regions of interest (ROIs) plotted vs time during 60 second acquisition. Top traces are raw values after median filter, bottom traces are

corrected for photobleach. Final frames are averaged action potential traces from the 60 second recordings, not normalized.

Figure 2.10 *Computation analysis of sulfonated BODIPY energy levels*

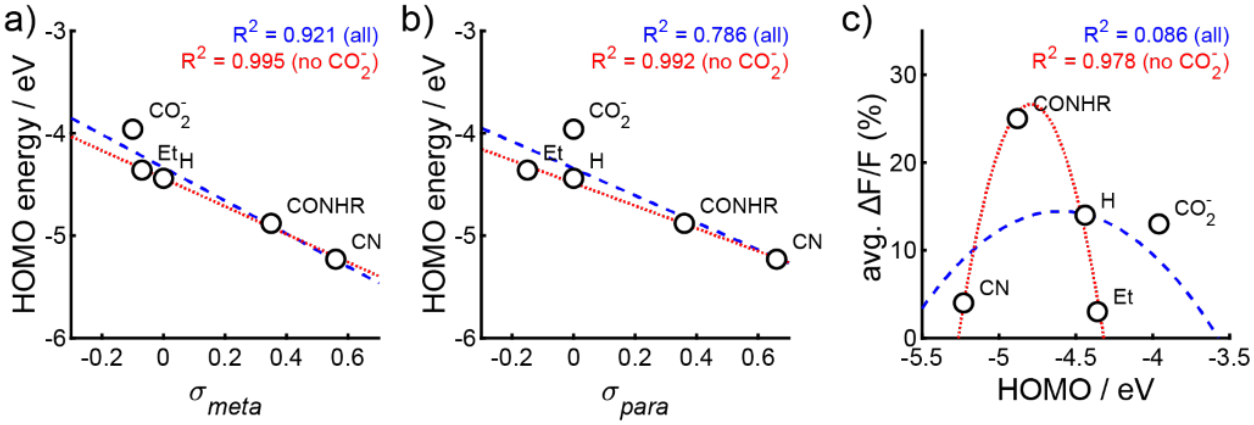

Figure 2.10. Plots of calculated HOMO energy vs. **a)** σ_{meta} or **b)** σ_{para}. HOMO calculations performed with WB97XD functional[64] and def2svp basis set[65] in an inert environment. Blue dashed lines indicate line of best fit including all data points. Red dotted lines depict the line of best fit, excluding σ parameters for carboxylates ($-CO_2^-$). R-squared parameters for each fit are indicated at the top of the plot. Values for σ_{meta} or σ_{para} are taken from Hansch, et al.[66] **c)** Plot of average voltage sensitivity (in units of ΔF/F per 100 mV) for 2,6-substitutions on BODIPY vs. the calculated HOMO level of that BODIPY. Blue dashed line indicates binomial fit including all data. Red dotted line excludes the calculated HOMO level for carboxylate-containing BODIPYs ($-CO_2^-$).

Figure 2.11 *Internalization of amidemH* ***35*** *under constant illumination*

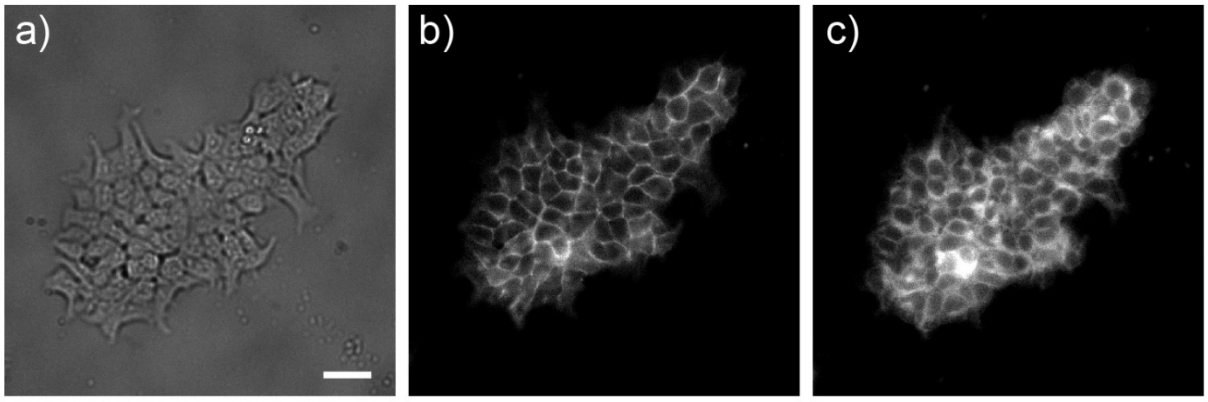

Figure 2.10. Internalization of amide*m*H **35** under constant illumination. HEK293T cells were loaded with 1 µM amide*m*H. **a)** Transmitted light and **b)** epifluorescence image of amide*m*H staining at the start of illumination. **c)** Epifluorescence image of the same group of cells after 2 minutes of constant illumination. Scale bar is 20 µm.

Experimental

Methods

Chemical synthesis and characterization

Chemical reagents and anhydrous solvents were purchased from commercial suppliers and used without further purification. Compounds **1**, **4**, **5**, **9**, **14**, **20**, and **23** were prepared according to literature procedures.[32,33,54,55,67] 2,4-dimethylpyrrole-3-carboxylic acid was purchased from CombiBlocks. All reactions were carried out in flame-dried flasks sealed with septa and conducted under an inert nitrogen atmosphere. Thin layer chromatography (TLC, Silicycle, F254, 250 μm) and preparative thin layer chromatography (pTLC, Silicycle, F254, 1000 μm) were performed on glass-backed plates pre-coated with silica gel and were visualized by fluorescence quenching under UV light. Flash column chromatography was performed on Silicycle Silica Flash F60 (230-400 Mesh) using a forced flow of air at 0.5–1.0 bar.

NMR spectra were measured on a Bruker AVQ-400, AVB-400, AV-500, AV-600, or AV-700 MHz instrument, indicated for each compound. CoC-NMR is supported in part by NIH S10-OD024998. NMR spectra measured on Bruker AVII-900 MHz, 225 MHz, equipped with a TCI cryoprobe accessory, were performed by Dr. Jeffrey Pelton (QB3). Funds for the QB3 900 MHz NMR spectrometer were provided by the NIH through grant GM68933. Chemical shifts are expressed in parts per million (ppm) and are referenced to either *d*$_6$-DMSO, 2.5 ppm, $CDCl_3$, 7.26 ppm, acetone-*d*$_6$, 2.05 ppm, or MeOD, 3.31 ppm. Coupling constants are reported in Hertz (Hz). Splitting patterns are indicated as follows: s, singlet; d, doublet; t, triplet; sep, septet; dd, doublet of doublets; ddd, doublet of doublet of doublets; dt, doublet of triplets; td; triplet of doublets; m, multiplet.

High-resolution mass spectra (HR-ESI-MS) were obtained by Dr. Rita Nichiporuk (QB3 Mass Spectrometry Facility at University of California, Berkeley). High performance liquid chromatography (HPLC) and low resolution ESI Mass Spectrometry were performed on an Agilent Infinity 1200 analytical instrument coupled to an Advion CMS-L ESI mass spectrometer. The column used for the analytical HPLC was Phenomenex Luna 5 μm C18(2) (4.6 mm I.D. × 75 mm) with a flow rate of 1.0 mL/min. The mobile phases were MQ-H_2O with 0.05% trifluoroacetic acid (eluent A) and HPLC grade acetonitrile with 0.05% trifluoroacetic acid (eluent B). Signals were monitored at 254, 400, and 500 nm over 13 min with a gradient of 10-100% eluent B, unless otherwise noted. Ultra-high performance liquid chromatography (UHPLC) for purification of final compounds was performed using a Waters Acquity Autopurificaiton system equipped with a Waters XBridge BEH 5 μm C18 column (19 mm I.D. x 250 mm) with a flow rate of 30.0 mL/min, made available by the Catalysis Facility of Lawrence Berkeley National Laboratory (Berkeley, CA). The mobile phases were MQ-H_2O with 0.05% formic acid (eluent A) and HPLC grade acetonitrile with 0.05% formic acid (eluent B). Signals were monitored at 400 and 500 nm over 20 min with a gradient of 10-100% eluent B, unless otherwise noted.

Spectroscopic studies

Stock solutions of BODIPY fluorophores and VoltageFluors were prepared in DMSO (500 μM–2 mM) and diluted with PBS (10 mM KH_2PO_4, 30 mM $Na_2HPO_4{\cdot}7H_2O$, 1.55 M NaCl, pH 7.4) or filtered absolute ethanol. UV-Vis absorbance and fluorescence spectra were recorded using a Shimadzu 2501 Spectrophotometer and a Quantamaster 4L-format scanning spectrofluorimeter (Photon Technologies International). The fluorimeter is equipped with an LPS-220B 75-W xenon

lamp and power supply, a 1010B lamp housing with integrated igniter, switchable 814 photon-counting/analog photomultiplier detection unit, and MD5020 motor driver. Samples were measured in 1-cm path length quartz cuvettes (Starna Cells).

Relative quantum yields (Φ_{Fl}) were calculated by comparison to fluorescein (Φ_{Fl} = 0.93 in 0.1 M NaOH) and rhodamine 123 (Φ_{Fl} = 0.90 in ethanol) as references.[68,69] Briefly, stock solutions of standards were prepared in DMSO (0.25-1.25 mM) and diluted with appropriate solvent (1:1000 dilution). Absorption and emission (excitation = 470 nm) were taken at 5 concentrations. The absorption value at the excitation wavelength (470 nm) was plotted against the integration of the area of fluorescence curve (475-700 nm). The slope of the linear best fit of the data was used to calculate the relative Φ_{Fl} by the equation $\Phi_{Fl(X)} = \Phi_{Fl(R)}(S_R/S_X)(\eta_X/\eta_R)^2$, where S_R and S_X are the slopes of the reference compound and unknown, respectively, and η is the refractive index of the solution. This method was validated by cross-referencing the reported Φ_{Fl} values of fluorescein and rhodamine 123 to the calculated Φ_{Fl} using the one standard as a reference for the other and vice versa. Calculated Φ_{Fl} within 10% of the reported value for both standards ensured that Φ_{Fl} calculated for BODIPY fluorophores and VoltageFluors was reliable within 10% error.

Cell culture

All animal procedures were approved by the UC Berkeley Animal Care and Use Committees and conformed to the NIH Guide for the Care and Use and Laboratory Animals and the Public Health Policy.

Human embryonic kidney (HEK) 293T cells were acquired from the UC Berkeley Cell Culture Facility. Cells were passaged and plated onto 12 mm glass coverslips coated with Poly-D-Lysine (PDL; 1 mg/mL; Sigma-Aldrich) to a confluency of ~15% and 50% for electrophysiology and imaging, respectively. HEK293T cells were plated and maintained in Dulbecco's modified eagle medium (DMEM) supplemented with 4.5 g/L D-glucose, 10% fetal bovine serum (FBS), and 1% Glutamax.

Hippocampi were dissected from embryonic day 18 Sprague Dawley rats (Charles River Laboratory) in cold sterile HBSS (zero Ca^{2+}, zero Mg^{2+}). All dissection products were supplied by Invitrogen, unless otherwise stated. Hippocampal tissue was treated with trypsin (2.5%) for 15 min at 37 °C. The tissue was triturated using fire polished Pasteur pipettes, in minimum essential media (MEM) supplemented with 5% fetal bovine serum (FBS; Thermo Scientific), 2% B-27, 2% 1M D-glucose (Fisher Scientific) and 1% glutamax. The dissociated cells were plated onto 12 mm diameter coverslips (Fisher Scientific) pre-treated with PDL (as above) at a density of 30-40,000 cells per coverslip in MEM supplemented media (as above). Neurons were maintained at 37 °C in a humidified incubator with 5 % CO_2. At 1 day in vitro (DIV) half of the MEM supplemented media was removed and replaced with Neurobasal media containing 2% B-27 supplement and 1% glutamax. Evoked activity experiments were performed on 12-15 DIV neurons. Unless stated otherwise, for loading of HEK cells and hippocampal neurons, BODIPY VoltageFluors were diluted in DMSO to 1 mM, and then diluted 1:1000 in HBSS and imaging experiments were performed in HBSS.

Differentiation of hiPSC into cardiomyocytes and culture: hiPSCs were cultured on Matrigel (1:100 dilution; Corning)-coated 6 well-plates in E8 medium. When the cell confluency reached 80–90%, which is referred to as day 0, the medium was switched to RPMI 1640 medium (Life Technologies) containing B27 minus insulin supplement (Life Technologies) and 10 μM CHIR99021 GSK3 inhibitor (Peprotech). At day 1, the medium was changed to RPMI 1640

medium containing B27 minus insulin supplement only. At day 2, medium was replaced to RPMI 1640 medium containing B27 supplement without insulin, and 5 μM IWP4 (Peprotech) for 2 days without medium change. On day 4, medium was replaced to RPMI 1640 medium containing B27 minus insulin supplement for 2 days without medium change. On day 6 and 7, medium was replaced to a serum-free medium - RPMI 1640 containing B27 with insulin supplement. After day 7, the medium was changed every other day. Confluent contracting sheets of beating cells appear between days 7 to 15 and are ready for dissociation after this time. Confluent sheets were dissociated with 0.25% trypsin-EDTA (8-30 minutes, depending on density and quality of tissue) and plated onto Matrigel (1:100)-coated Ibidi ® 24 well μ-plates (cat no. 82406) in RPMI 1640 medium containing B27 supplement (containing insulin). Medium was changed every 3 days until imaging. For loading hiPSC cardiomyocytes, VoltageFluors dyes (BODIPY, VF2.1.Cl, or fVF 2) were diluted in DMSO to 500 μM, and then diluted 1:1000 in RPMI 1640 with B27 supplement minus Phenol Red. Imaging experiments were performed in RPMI 1640 with B27 supplement minus Phenol Red.

Epifluorescence microscopy

For HEK293T cells, epifluorescence imaging was performed on an AxioExaminer Z-1 (Zeiss) equipped with a Spectra-X Light engine LED light (Lumencor), controlled with Slidebook (v6, Intelligent Imaging Innovations). Images were acquired with either a W-Plan-Apo 20x/1.0 water objective (Zeiss). Images were focused onto an OrcaFlash4.0 sCMOS camera (sCMOS; Hamamatsu) or an eVolve 128 EMCCD camera (EMCCD; photometrix). For rat hippocampal neurons, μManager (V1.4, open-source, Open Imaging) was used to control the microscope.[70] For BODIPY-VF images, the excitation light was delivered from a LED at 510/25 nm and emission was collected with a triple emission filter (473/22, 543/19, 648/98 nm) after passing through a triple dichroic mirror (475/30, 540/25, 642/96 nm). More detailed imaging information for each experimental application is expanded below.

Membrane staining and photostability in HEK293T cells

HEK293T cells were incubated with a HBSS solution (Gibco) containing BODIPY VoltageFluors (1 μM) at 37°C for 20 min prior to transfer to fresh HBSS (no dye) for imaging. Microscopic images were acquired with a W-Plan-Apo 20x/1.0 water objective (Zeiss) and OrcaFlash4.0 sCMOS camera (Hamamatsu). For image intensity measurements, regions of interest were drawn around cells and the mean fluorescence was calculated in ImageJ (FIJI, NIH).[71] Background fluorescence was subtracted by measuring the fluorescence from regions of interest containing no cells.

For photostability experiments, HEK293T cells were incubated separately with VF2.1.Cl (1 μM), fvf 2 (1 μM), Et*m*H (1 μM), TM*m*OMe (1 μM), carboxy*m*OMe (1 μM), or amide*m*H (1 μM) in HBSS at 37°C for 20 min. Data were acquired with a W-Plan-Apo 20x/1.0 water objective (Zeiss) and OrcaFlash4.0 sCMOS camera (Hamamatsu). Images were taken every 5 seconds for 6 minutes with constant illumination of teal LED (2.48 mW/mm^2; 25 ms exposure time). The obtained fluorescence curves (background subtracted) were normalized with the fluorescence intensity at t = 0 and averaged (three rafts of cells of each dye).

Voltage sensitivity in HEK293T cells

Analysis of voltage sensitivity in HEK cells was performed using ImageJ (FIJI).[71] Briefly, a region of interest (ROI) was selected automatically based on fluorescence intensity and applied as a mask to all image frames. Fluorescence intensity values were calculated at known baseline and voltage step epochs. For analysis of voltage responses in neurons, regions of interest encompassing cell bodies (all of approximately the same size) were drawn in ImageJ and the mean fluorescence intensity for each frame extracted. ΔF/F values were calculated by first subtracting a mean background value from all raw fluorescence frames, to give a background subtracted trace (bkgsub). A baseline fluorescence value (Fbase) is calculated from the median of all the frames and subtracted from each timepoint of the bkgsub trace to yield a ΔF trace. The ΔF was then divided by Fbase to give ΔF/F traces. No averaging has been applied to any voltage traces.

Electrophysiology

For electrophysiological experiments, pipettes were pulled from borosilicate glass (Sutter Instruments, BF150-86-10), with a resistance of 5–8 MΩ, and were filled with an internal solution; (in mM) 125 potassium gluconate, 1 EGTA, 10 HEPES, 5 NaCl, 10 KCl, 2 ATP disodium salt, 0.3 GTP trisodium salt (pH 7.25, 275 mOsm).

Recordings were obtained with an Axopatch 200B amplifier (Molecular Devices) at room temperature. The signals were digitized with Digidata 1332A, sampled at 50 kHz and recorded with pCLAMP 10 software (Molecular Devices) on a PC. Fast capacitance was compensated in the on-cell configuration. For all electrophysiology experiments, recordings were only pursued if series resistance in voltage clamp was less than 30 MΩ. For whole-cell, voltage clamp recordings in HEK 293T cells, cells were held at -60 mV and 100 ms hyper- and de-polarizing steps were applied from -100 to +100 mV in 20 mV increments.

Extracellular field stimulation was delivered by a SD9 Grass Stimulator connected to a recording chamber containing two platinum electrodes (Warner), with triggering provided through the same Digidata 1332A digitizer and pCLAMP 9 software (Molecular Devices) that ran the electrophysiology. Action potentials were triggered by 1 ms 60 V field potentials delivered at 5 Hz. To prevent recurrent activity, the HBBS bath solution was supplemented with synaptic blockers; 10 μM 2,3-Dioxo-6-nitro-1,2,3,4- tetrahydrobenzo[f]quinoxaline-7-sulfonamide (NBQX; Santa Cruz Biotechnology) and 25 μM D(-)-2-Amino-5-phosphonopentanoic acid (D(-)-APV; Sigma-Aldrich). For both evoked action potentials and spontaneous activity, images were binned 4x4 to allow sampling rates of 0.5 kHz and 2500 frames (5 s) were acquired for each recording.

Synthesis of BODIPY dyes

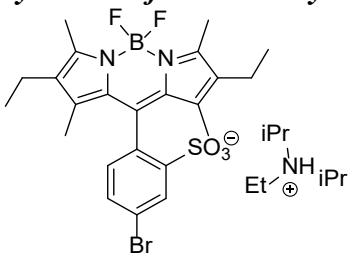

1,3,5,7-tetramethyl-2,6-diethyl-*p*-bromo BODIPY (3). *Para*-bromo sulfonated aldehyde **1** (256 mg, 0.97 mmol, 1 eq) was added to a flame-dried 25 mL round-bottom flask. Flask was evacuated

and backfilled with N_2 3x, then DMF (5 mL), 3-ethyl-2,4-dimethyl-*1H*-pyrrole (287 µL, 2.12 mmol, 2.2 eq) and TFA (2 drops) were added via syringe, and reaction stirred under nitrogen atmosphere overnight. DDQ (219 mg, 0.97 mmol, 1 eq) was then added, stirred for 5 min, then concentrated under reduced pressure. An optional silica plug (3-10% MeOH in DCM gradient) yielded the dipyrromethene as a pink, green iridescent solid, which was taken onto the next step directly.

The dipyrromethene was dissolved in DCM (20 mL), DIPEA (1.91 mL, 11 mmol, 11 eq) and $BF_3{\cdot}Et_2O$ (2 mL, 15.5 mmol, 16 eq) were added via syringe and the solution became green fluorescent. After 10 min, reaction was quenched by addition of water, and organics were washed with 0.25N HCl (3 x 30 mL), brine (40 mL), dried over Na_2SO_4, and concentrated under reduced pressure. Flash chromatography on silica gel (3 → 7% MeOH in DCM, gradient) yielded the BODIPY **3** as a pink, green iridescent solid (252 mg, 49%).

^{1}H NMR (400 MHz, MeOD) δ 8.24 (d, *J* = 2.06 Hz, 1H), 7.76 (dd, *J* = 2.06, 8.20 Hz, 1H), 7.17 (d, *J* = 8.20 Hz, 1H), 3.68 (sep, *J* = 6.64 Hz, 1H, $NEt(iPr)_2H^+$ salt), 3.18 (q, *J* = 7.41 Hz, 2H, $NEt(iPr)_2H^+$ salt), 2.45 (s, 6H), 2.33 (q, *J* = 7.52 Hz, 4H), 1.42 (s, 6H), 1.33 – 1.28 (m, 12H, $NEt(iPr)_2H^+$ salt), 0.98 (t, *J* = 7.51 Hz, 6H). **^{13}C NMR** (400 MHz, MeOD) δ 154.1, 147.2, 140.3, 140.1, 135.2, 133.64, 133.59, 133.3, 133.0, 132.5, 123.9, 55.8 ($NEt(iPr)_2H^+$ salt), 43.8 ($NEt(iPr)_2H^+$ salt), 18.0, 15.2, 13.1, 12.7, 12.1 ppm. **ESI-HR(-)**, calculated for $C_{23}H_{25}BBrF_2N_2O_3S^-$: 537.0836, found: 537.0825.

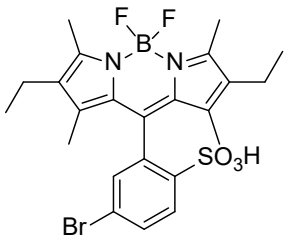

1,3,5,7-tetramethyl-2,6-diethyl-m-bromo BODIPY (11). *Meta*-bromo sulfonated aldehyde **9** (160 mg, 0.60 mmol, 1 eq) was added to a flame-dried 25 mL round-bottom flask. Flask was evacuated and backfilled with N_2 3x, then DMF (5 mL), 3-ethyl-2,4-dimethyl-*1H*-pyrrole (179 µL, 2.12 mmol, 2.2 eq) and TFA (2 drops) were added via syringe, and reaction stirred under nitrogen atmosphere overnight. DDQ (137 mg, 0.60 mmol, 1 eq) was then added, stirred for 5 min, then concentrated under reduced pressure. An optional silica plug (3-10% MeOH in DCM gradient) yielded the dipyrromethene as a pink, green iridescent solid, which was taken onto the next step directly.

The dipyrromethene was dissolved in DCM (20 mL), DIPEA (1.2 mL, 6.9 mmol, 10.4 eq) and $BF_3{\cdot}Et_2O$ (1.19 mL, 9.7 mmol, 16 eq) were added via syringe, and the solution became green fluorescent. After 10 min, reaction was quenched by addition of water, and organics were washed with 0.25N HCl (3 x 10 mL), brine (20 mL), dried over Na_2SO_4, and concentrated under reduced pressure. Flash chromatography on silica gel (3% MeOH in DCM) yielded the BODIPY **11** as a pink, green iridescent solid (126 mg, 33%).

^{1}H NMR (500 MHz, DMSO-*d*$_6$) δ 8.47 (d, *J* = 8.42 Hz, 1H), 8.16 (dd, *J* = 2.08, 8.48 Hz, 1H), 7.85 (d, *J* = 2.10 Hz, 1H), 2.91 (s, 6H), 2.76 (q, *J* = 7.56 Hz, 4H), 1.88 (s, 6H), 1.42 (t, *J* = 7.54 Hz, 6H). **^{13}C NMR** (900 MHz, DMSO-*d*$_6$) δ 162.8, 155.7, 149.7, 149.2, 145.6, 142.3, 142.2, 142.0, 141.64, 141.55, 133.5, 27.2, 24.8, 22.3, 21.5 **ESI-HR(-)**, calculated for $C_{23}H_{25}BBrF_2N_2O_3S^-$: 537.0836, found: 537.0837.

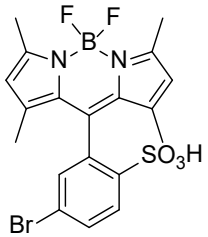

1,3,5,7-tetramethyl-m-bromo BODIPY (12). *Meta*-bromo sulfonated aldehyde **9** (504.9 mg, 1.9 mmol, 1 eq) was added to a flame-dried 25 mL round-bottom flask. Flask was evacuated and backfilled with N_2 3x, then DMF (5 mL), 2,4-dimethyl-*1H*-pyrrole (432 µL, 4.2 mmol, 2.2 eq) and TFA (3 drops) were added via syringe, and reaction stirred under nitrogen atmosphere overnight. DDQ (432 mg, 1.9 mmol, 1 eq) was then added, stirred for 5 min, then concentrated under reduced pressure. An optional silica plug (2-14% MeOH in DCM gradient) yielded the dipyrromethene as a pink, green iridescent solid, which was taken onto the next step directly.

The dipyrromethene was dissolved in DCM (40 mL), DIPEA (3.6 mL, 21 mmol, 11 eq) and $BF_3{\cdot}Et_2O$ (3.8 mL, 30 mmol, 16 eq) were added via syringe and the solution became green fluorescent. After 10 min, reaction was quenched by addition of 10 mL iPrOH. Organics were washed with 0.25N HCl (2 x 20 mL), brine (20 mL), dried over Na_2SO_4, and concentrated under reduced pressure. Flash chromatography on silica gel (1 → 7% MeOH in DCM, gradient) yielded the BODIPY **12** as a pink, green iridescent solid (350 mg, 38%).

^{1}H NMR (400 MHz, MeOD) δ 8.47 (d, *J* = 8.44 Hz, 1H), 8.16 (dd, *J* = 2.08, 8.47 Hz, 1H), 7.87 (d, *J* = 7.87 Hz, 1H), 6.44 (s, 2H), 2.91 (s, 6H), 1.96 (s, 6H). **^{13}C NMR** (900 MHz, DMSO-*d*$_6$) δ 164.5, 155.8, 153.9, 151.2, 144.8, 142.3, 142.1, 141.9, 141.6, 133.4, 131.0, 24.24, 24.21. **ESI-HR(-)**, calculated for $C_{19}H_{17}BBrF_2N_2O_3S^-$: 481.0210, found: 481.0211.

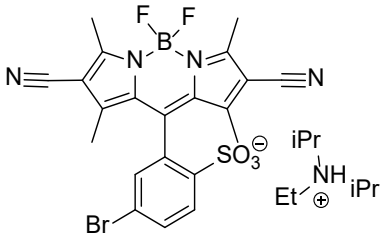

1,3,5,7-tetramethyl-2,6-cyano-m-bromo BODIPY (21). *Meta*-bromo sulfonated aldehyde **9** (256 mg, 0.22 mmol, 1 eq) and 2,4-dimethyl-*1H*-pyrrole-3-carbonitrile (**20**) (58.3 mg, 0.49 mmol, 2.2 mmol) were added to an oven-dried 25 mL round-bottom flask. Flask was evacuated and backfilled with N_2 three times, then dissolved in DMF (680 µL) and DCM (1.01 mL). TFA (100 µL) was added via syringe and reaction stirred under inert N_2 atmosphere overnight. DDQ was then added (50.1 mg, 0.22 mmol, 1 eq), stirred for 5 min, then solution was concentrated under reduced pressure. The dipyrromethene was dissolved in DCM (5 mL), then DIPEA (423 µL, 2.4

mmol, 11 eq) and $BF_3{\cdot}Et_2O$ (436 µL, 3.5 mmol, 16 eq) were added and reaction stirred for 1.5 hrs. Reaction was quenched by addition of water, and organics were washed with water (3 x 30 mL), dried over Na_2SO_4, and concentrated under reduced pressure. Flash chromatography on silica gel (1 → 7% MeOH in DCM, gradient) yielded the BODIPY **21** as a pink, green iridescent solid (33.8 mg, 29%).

^{1}H NMR (400 MHz, Methanol-*d4*) δ 8.04 (d, *J* = 8.5 Hz, 1H), 7.89 (dd, *J* = 8.5, 2.0 Hz, 1H), 7.61 (d, *J* = 2.0 Hz, 1H), 3.71 (p, *J* = 6.6 Hz, 1H, $NEt(iPr)_2H^+$ salt), 3.20 (q, *J* = 7.4 Hz, 2H, $NEt(iPr)_2H^+$ salt), 2.66 (s, 6H), 1.70 (s, 6H), 1.40 – 1.25 (m, 15H, $NEt(iPr)_2H^+$ salt). **^{13}C NMR** (400 MHz, Methanol-*d4*) δ 160.2, 150.9, 146.8, 144.3, 134.9, 133.4, 133.3, 132.5, 132.2, 126.5, 114.7, 106.9, 56.0 ($NEt(iPr)_2H^+$ salt), 55.0 ($NEt(iPr)_2H^+$ salt), 43.9, 14.2, 13.9, 13.3 ppm. **ESI-HR(-)**, calculated for $C_{21}H_{15}BBrF_2N_4O_3S^-$: 531.0115, found: 531.0110.

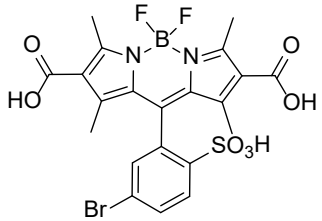

1,3,5,7-tetramethyl-2,6-carboxy-m-bromo BODIPY (32). *Meta*-bromo sulfonated aldehyde **9** (357 mg, 1.4 mmol, 1 eq) and 2,4-dimethylpyrrole-3-carboxylic acid **31** (412 mg, 3.0 mmol, 2.2 eq) were added to a flame-dried 25 mL round-bottom flask. Flask was evacuated and backfilled with N_2 3x, then DMF (10 mL) and TFA (100 µL) were added via syringe and reaction stirred under nitrogen atmosphere overnight. DDQ (306 mg, 1.4 mmol, 1 eq) was added and solution stirred for 5 min then was concentrated under reduced pressure. An optional silica plug (15% MeOH + 1% AcOH in DCM) yielded the dipyrromethene as a pink, green iridescent solid, which was taken onto the next step directly.

DCM (50 mL) was added to 250 mL round-bottom flask containing the dipyrromethene and the solution was sonicated to suspend the material. DIPEA (2.6 mL, 15 mmol, 11 eq) and $BF_3{\cdot}Et_2O$ (2.7 mL, 22 mmol, 16 eq) were added via syringe and the solution became green fluorescent. After 10 min, reaction was quenched by addition of 10 mL iPrOH and solution was concentrated under reduced pressure. Flash chromatography on silica gel (10 → 20% MeOH in DCM + 1% AcOH, gradient) yielded the BODIPY **32** as a pink, green iridescent solid (380 mg, 49%). This material was >90% pure by analytical HPLC and was used without further purification in the next synthetic step. For NMR and spectroscopic characterization, **32** was purified by reverse phase preparative HPLC (10-100% MeCN in water, 0.05% formic acid additive).

^{1}H NMR (400 MHz, Methanol-d4) δ 8.01 (d, *J* = 8.5 Hz, 1H), 7.82 (dd, *J* = 8.5, 2.1 Hz, 1H), 7.52 (d, *J* = 2.0 Hz, 1H), 2.75 (s, 6H), 1.80 (s, 6H). **^{13}C (900 MHz, Methanol-d4)** δ 170.3, 158.9, 145.8, 144.5, 143.6, 135.6, 133.6, 133.2, 132.9, 132.0, 125.9, 14.8, 13.6 ppm. **ESI-HR(-)**, calculated for $C_{21}H_{17}BBrF_2N_2O_7S^-$: 569.0006, found: 569.0008.

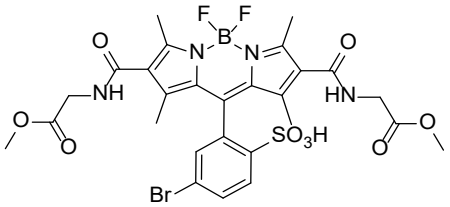

1,3,5,7-tetramethyl-2,6-amide-m-bromo BODIPY (34). 1,3,5,7-tetramethyl-2,6-dicarboxy BODIPY **32** (23 mg, 0.04 mmol), glycine methyl ester (11.3 mg, 0.09 mmol, 2.25 eq), and HATU (34.4 mg, 0.09 mmol, 2.25 eq) were dissolved in DMF (0.5 mL), then DIPEA (70 µL, 0.4 mmol, 10 eq) was added and reaction stirred at rt for 3.5 hrs. Reaction was concentrated to near-dryness under reduced pressure, then 10 mL DCM was added and solution was washed with water (2 x 5 mL), dried over Na_2SO_4, and concentrated under reduced pressure. Preparative TLC (15% MeOH in DCM) yielded amide BODIPY **34** as an orange, green iridescent solid (24 mg, 82%). This material was >95% pure by analytical HPLC and was used without further purification in the next synthetic step. For NMR and spectroscopic characterization, a small amount was further purified by reverse phase preparative HPLC (10-100% MeCN in water, 0.05% formic acid additive).

^{1}H NMR (700 MHz, Methanol-*d*$_4$) δ 8.02 (d, J = 8.5 Hz, 1H), 7.83 (dd, J = 8.5, 2.1 Hz, 1H), 7.54 (d, J = 2.1 Hz, 1H), 4.12 – 3.99 (m, 4H), 3.73 (s, 6H), 2.61 (s, 6H), 1.63 (s, 6H). **^{13}C NMR** (600 MHz, Methanol-*d*$_4$) δ 171.6, 168.1, 155.9, 143.9, 142.9, 133.9, 133.0, 132.7, 132.1, 129.5, 126.1, 52.6, 42.0, 13.5, 13.1 ppm. **LR-MS (ESI+)** calculated for $C_{27}H_{29}BF_2BrN_4O_9S^+$: 713.09, found 713.4. **Analytical HPLC retention time:** 5.02 min (10-100% MeCN in water, 0.05% TFA additive).

Synthesis of BODIPY VoltageFluors

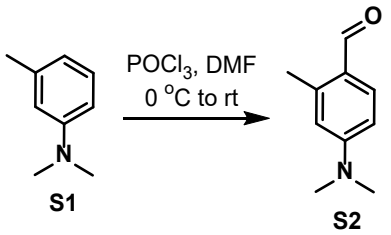

4-(dimethylamino)-2-methylbenzaldehyde (S2). A flame-dried round-bottom flask was charged with *N,N*-dimethyl-*m*-toluidene **S1** (4 g, 29.6 mmol, 1 eq) and evacuated/backfilled with N_2 3x. DMF (45 mL) was added and solution was cooled to 0 °C in an ice-water bath. $POCl_3$ (4.98 mL, 53.6 mmol, 1.8 eq) was added dropwise via syringe and reaction stirred at rt 18 hr. Reaction was poured into ice water (500 mL) and adjusted to pH 9 with 1M NaOH. The resulting precipitate was filtered, washed with water (50 mL), then dried *in vacuo*, yielding **S2** as a white solid (3.19 g, 66%).

^{1}H NMR (400 MHz, Chloroform-*d*) δ 9.98 (s, 1H), 7.67 (d, *J* = 8.7 Hz, 1H), 6.57 (dd, *J* = 8.7, 2.6 Hz, 1H), 6.43 (d, *J* = 2.6 Hz, 1H), 3.07 (s, 6H), 2.63 (s, 3H). **^{13}C NMR** (400 MHz, $CDCl_3$) δ 190.37, 153.52, 142.77, 134.60, 123.34, 113.42, 108.83, 39.96, 20.38. **ESI-HR(+)**, calculated for $C_{10}H_{14}O_1N_1^+$: 164.1070, found: 164.1068.

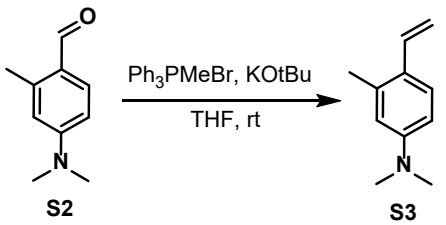

S2 S3

***N,N*,3-trimethyl-4-vinylaniline (S3).** A flame-dried round-bottom flask was charged with Ph_3PMeBr (11.17 g, 31 mmol, 1.6 eq) and evacuated/backfilled 3x with N_2. Anhydrous THF (18 mL) and KOtBu (3.5 g, 31 mmol, 1.6 eq) were added and stirred for 15 min. Aldehyde **S2** was added slowly via a funnel, which was rinsed with THF (8 mL). After 2.5 hrs, solvent was removed under reduced pressure, hexanes were added, filtered through a pad of alumina, and concentrated. Resulting residue was purified further with an alumina column (3 → 5% EtOAc in hexanes, gradient), yielding styrene **S3** as a light yellow oil (2.9 g, 92%).

^{1}H NMR (400 MHz, Chloroform-*d*) δ 7.43 (dd, *J* = 8.7, 1.7 Hz, 1H), 6.89 (ddd, *J* = 17.4, 11.0, 1.9 Hz, 1H), 6.60 (dt, *J* = 8.6, 2.1 Hz, 1H), 6.52 (t, *J* = 2.1 Hz, 1H), 5.50 (dq, *J* = 17.4, 1.4 Hz, 1H), 5.10 (dq, *J* = 10.9, 1.4 Hz, 1H), 2.96 (d, *J* = 1.4 Hz, 6H), 2.35 (d, *J* = 1.8 Hz, 3H). **^{13}C NMR** (400 MHz, Chloroform-*d*) δ 150.31, 137.99, 134.48, 126.23, 125.54, 114.07, 111.07, 110.69, 40.65, 20.38. **ESI-HR(+)**, calculated for $C_{11}H_{16}N_1^+$: 162.1277, found: 162.1275.

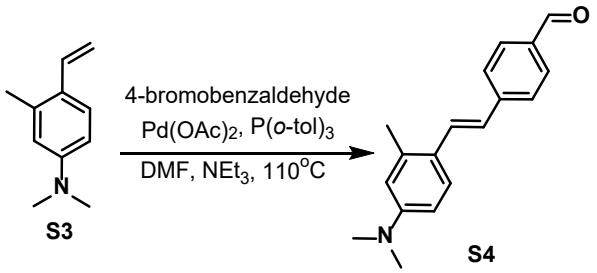

S3 S4

(E)-4-(4-(dimethylamino)-2-methylstyryl)benzaldehyde (S4). A flame-dried Schlenk flask was charged with **S3** (2.9 g, 18 mmol, 1 eq), 4-bromobenzaldehyde (3.3 g, 18 mmol, 1 eq), $Pd(OAc)_2$ (40.4 mg, 0.18 mmol, 1 mol%), and P(*o*-tol)$_3$ (109 mg, 0.36 mmol, 2 mol%). Flask was evacuated and backfilled with N_2 3x, DMF (20 mL) and NEt_3 (8 mL) were added, and reaction stirred at 110 °C 18 hr. Reaction was concentrated under reduced pressure, then residue was dissolved in EtOAc (200 mL) and washed with water (2 x 225 mL) and brine (200 mL). Organics were dried with Na_2SO_4 and concentrated under reduced pressure. Flash chromatography (5 → 20% EtOAc in hexanes, gradient) yielded **S4** as an orange solid (1.55 g, 32%).

^{1}H NMR (400 MHz, Chloroform-*d*) δ 9.97 (s, 1H), 7.87 – 7.80 (m, 2H), 7.61 (d, *J* = 8.1 Hz, 2H), 7.57 (d, *J* = 8.7 Hz, 1H), 7.47 (d, *J* = 16.1 Hz, 1H), 6.90 (d, *J* = 16.1 Hz, 1H), 6.61 (dd, *J* = 8.7, 2.8 Hz, 1H), 6.53 (d, *J* = 2.6 Hz, 1H), 3.00 (s, 6H), 2.45 (s, 3H). **^{13}C NMR** (400 MHz, $CDCl_3$) δ 191.8, 150.7, 145.0, 137.7, 134.7, 130.4, 130.1, 129.7, 126.7, 126.5, 124.1, 123.9, 114.0, 110.6, 40.5, 20.6 ppm. **ESI-HR(+)**, calculated for $C_{18}H_{20}O_1N_1^+$: 266.1539, found: 266.1526.

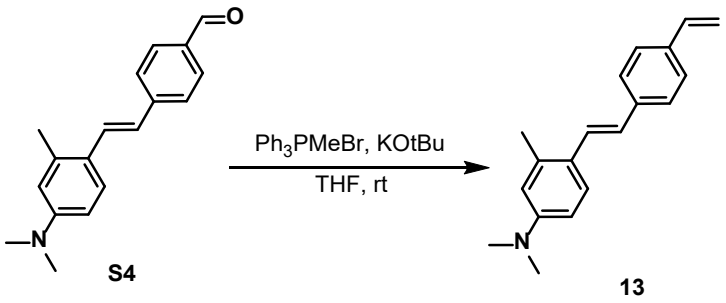

***(E)-N,N*,3-trimethyl-4-(4-vinylstyryl)aniline (13).** A flame-dried round-bottom flask was charged with Ph_3PMeBr (474 mg, 1.3 mmol, 1.6 eq) and evacuated/backfilled 3x with N_2. Anhydrous THF (1.8 mL) and KOtBu (149 mg, 1.3 mmol, 1.6 eq) were added and stirred for 15 min. Aldehyde **S4** was dissolved in THF (1 mL + 1mL rinse) and pipetted into reaction flask. After 20 hrs, solvent was removed under reduced pressure, hexanes were added, filtered through a pad of celite, and concentrated. Flash chromatography on silica (3 → 5% EtOAc in hexanes gradient), yielded **13** as a yellow solid (141 mg, 65%).

^{1}H NMR (400 MHz, Chloroform-*d*) δ 7.65 (d, *J* = 8.7 Hz, 1H), 7.57 (d, *J* = 8.2 Hz, 2H), 7.50 (d, *J* = 8.2 Hz, 2H), 7.42 (d, *J* = 16.1 Hz, 1H), 6.97 (d, *J* = 16.1 Hz, 1H), 6.83 (dd, *J* = 17.6, 10.9 Hz, 1H), 6.72 (dd, *J* = 8.7, 2.7 Hz, 1H), 6.65 (d, *J* = 2.7 Hz, 1H), 5.87 (dd, *J* = 17.6, 0.9 Hz, 1H), 5.34 (dd, *J* = 10.8, 1.0 Hz, 1H), 3.07 (s, 6H), 2.54 (s, 3H). **^{13}C NMR** (400 MHz, $CDCl_3$) δ 150.15, 138.22, 136.92, 136.71, 136.09, 126.59, 126.47, 126.32, 126.30, 125.44, 124.82, 114.08, 113.18, 110.73, 40.51, 20.58. **ESI-HR(+)**, calculated for $C_{19}H_{22}N_1^+$: 264.1747, found: 264.1742.

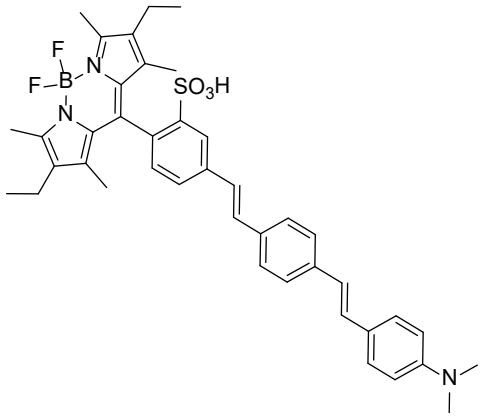

Ethyl BODIPY *p*-normal wire (6). To a flame-dried 10 mL Schlenk flask were added 1,3,5,7-tetramethyl-2,6-diethyl-*p*-bromo BODIPY **3** (87.5 mg, 0.16 mmol, 1 eq), molecular wire **4** (44.5 mg, 0.18 mmol, 1.1 eq), $Pd(OAc)_2$ (3.2 mg, 0.015 mmol, 9 mol%), and P(*o*-tol)$_3$ (8.9 mg, 0.029 mmol, 18 mol%). The flask was evacuated and backfilled with N_2 3x before addition of DMF (1.1 mL) and NEt_3 (60 µL). The Schlenk flask was sealed shut and heated to 70 °C overnight. The DMF was removed *in vacuo* and the residue dissolved in DCM (10 mL). Washed with water (3 x 10 mL), dried over Na_2SO_4, and concentrated under reduced pressure. Flash chromatography on silica gel (4% MeOH in DCM) yielded Et*p*H **6** as a reddish orange solid (105.7 mg, 92%).

^{1}H NMR (400 MHz, Chloroform-*d*) δ 9.83 (s, 1H), 8.42 (d, *J* = 1.8 Hz, 1H), 7.63 (dd, *J* = 8.0, 1.8 Hz, 1H), 7.54 – 7.46 (m, 4H), 7.43 (d, *J* = 8.4 Hz, 2H), 7.29 (d, *J* = 16.7 Hz, 2H), 7.22 – 7.13 (m,

2H), 7.09 (d, J = 16.2 Hz, 1H), 6.92 (d, J = 16.2 Hz, 1H), 6.73 (d, J = 8.2 Hz, 2H), 2.99 (s, 6H), 2.86 (qd, J = 7.2, 4.3 Hz, 6H, Et_3HN^+ salt), 2.49 (s, 6H), 2.32 – 2.25 (m, 4H), 1.46 (s, 6H), 1.08 (t, J = 7.3 Hz, 9H, Et_3HN^+ salt), 0.95 (t, J = 7.4 Hz, 6H). **^{13}C NMR** (400 MHz, Chloroform-*d*) δ 152.4, 143.8, 140.5, 140.1, 138.6, 138.2, 135.5, 132.3, 131.4, 130.4, 129.8, 129.1, 128.4, 127.8, 127.4, 127.2, 126.6, 126.5, 124.1, 112.6, 46.2, 40.6, 29.9, 17.2, 14.9, 12.5, 11.7, 8.32 ppm. **ESI-HR(-)**, calculated for $C_{41}H_{43}BF_2N_3O_3S^-$: 706.3092, found: 706.3074. **Analytical HPLC retention time:** 8.39 min. Estimated purity >99%.

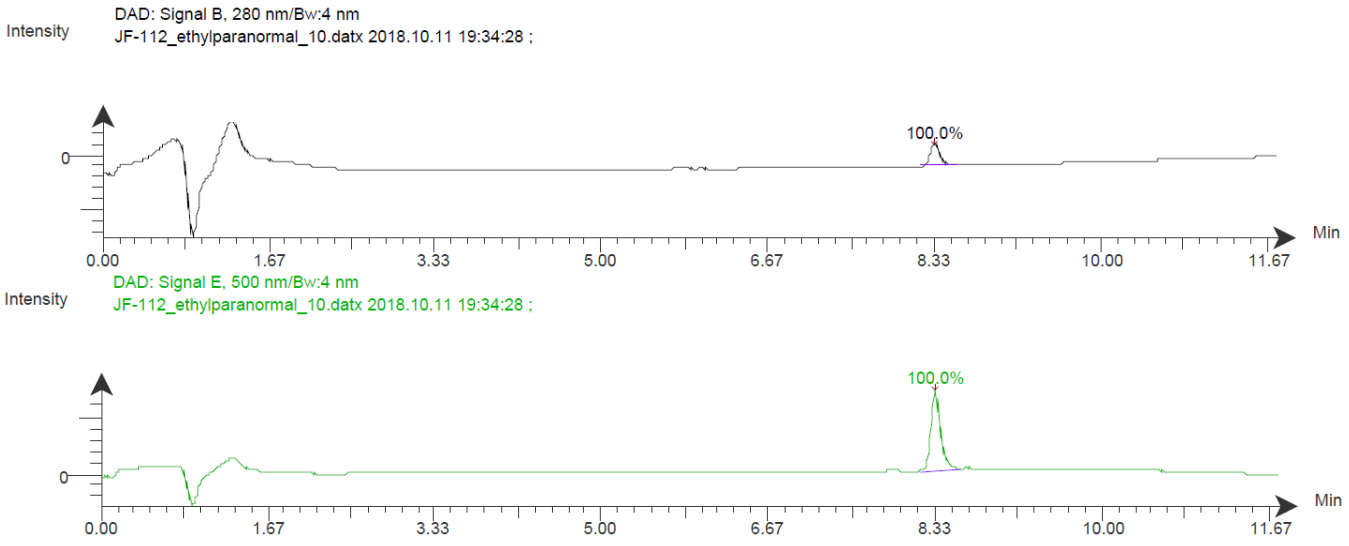

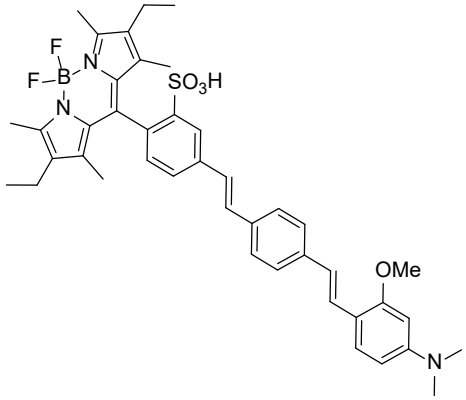

Ethyl BODIPY *p*-methoxy wire (7) To a flame-dried 10 mL Schlenk flask were added 1,3,5,7-tetramethyl-2,6-diethyl-*p*-bromo BODIPY **3** (44.4 mg, 0.08 mmol, 1 eq), methoxy molecular wire **5** (22.6 mg, 0.09 mmol, 1.1 eq), $Pd(OAc)_2$ (1.7 mg, 0.007 mmol, 9 mol%), and P(*o*-tol)$_3$ (4.5 mg, 0.015 mmol, 18 mol%). The flask was evacuated and backfilled with N_2 3x before addition of DMF (0.6 mL) and NEt_3 (300 µL). The Schlenk flask was sealed shut and heated to 70 °C overnight. The DMF was removed *in vacuo* and the residue dissolved in DCM (10 mL). Washed with water (3 x 10 mL), dried over Na_2SO_4, and concentrated under reduced pressure. Flash chromatography on silica gel (4% MeOH in DCM) yielded Et*p*OMe **7** as a reddish orange solid (17.1 mg, 25%).

^{1}H NMR (400 MHz, Chloroform-*d*) δ 8.39 (s, 1H), 7.63 (dd, *J* = 7.9, 1.7 Hz, 1H), 7.55 – 7.40 (m, 6H), 7.26 (apps, 1H), 7.19 – 7.09 (m, 2H), 6.95 (d, *J* = 16.4 Hz, 1H), 6.36 (dd, *J* = 8.7, 2.4 Hz, 1H), 6.23 (d, *J* = 2.4 Hz, 1H), 3.90 (s, 3H), 3.00 (s, 6H), 2.91 – 2.80 (m, 5H, Et_3HN^+ salt), 2.48 (s, 6H), 2.27 (q, *J* = 7.6 Hz, 4H), 1.45 (s, 6H), 1.08 (t, *J* = 7.3 Hz, 7H, Et_3HN^+ salt), 0.95 (t, *J* = 7.5 Hz, 6H). **^{13}C NMR** (600 MHz, Chloroform-*d*) δ 158.2, 152.4, 151.5, 143.5, 140.2, 139.8, 138.8, 138.5, 135.0, 132.2, 131.3, 131.2, 130.4, 129.7, 128.2, 127.3, 127.2, 127.0, 126.4, 126.2, 124.3, 123.9, 115.2, 105.2, 95.6, 77.2, 76.8, 55.4, 46.0, 40.5, 17.0, 14.7, 12.3, 11.6, 8.2 ppm. **ESI-HR(-)**, calculated for $C_{42}H_{45}BF_2N_3O_4S^-$: 736.3197, found: 736.3183. **Analytical HPLC retention time:** 8.63 min. Estimated purity 94%.

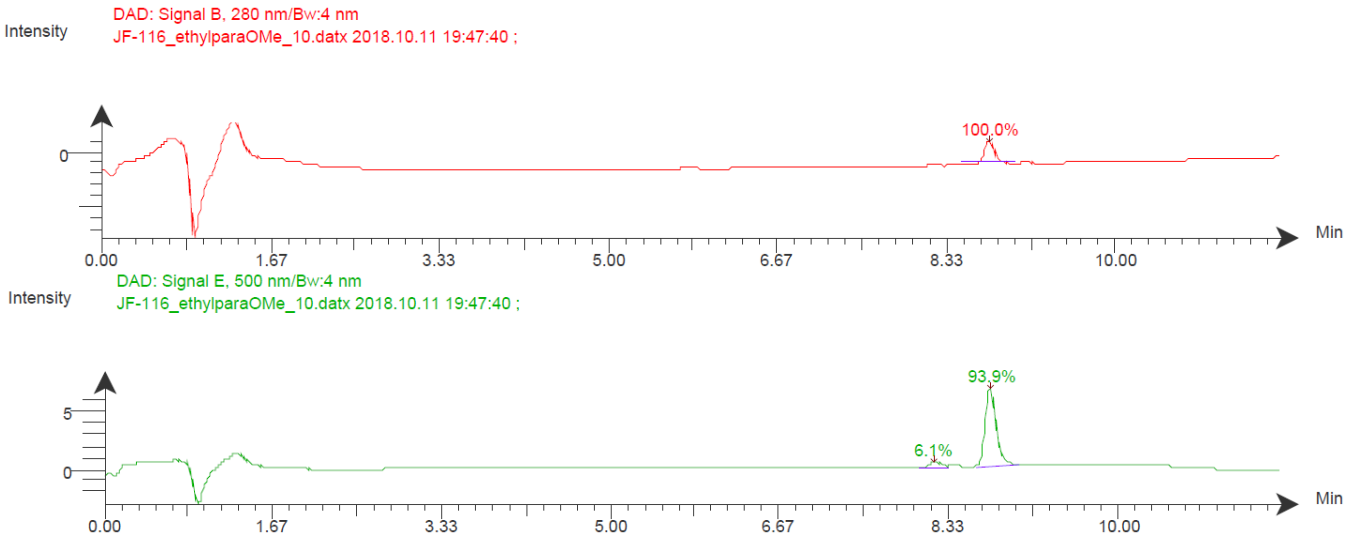

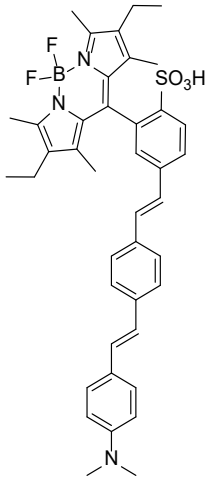

Ethyl BODIPY *m*-normal wire (15) To a flame-dried 10 mL Schlenk flask were added 1,3,5,7-tetramethyl-2,6-diethyl-*m*-bromo BODIPY **12** (51.6 mg, 0.09 mmol, 1 eq), molecular wire **4** (26.2 mg, 0.10 mmol, 1.1 eq), $Pd(OAc)_2$ (1.9 mg, 0.009 mmol, 9 mol%), and P(*o*-tol)$_3$ (5.2 mg, 0.017 mmol, 18 mol%). The flask was evacuated and backfilled with N_2 3x before addition of DMF (660 µL) and NEt_3 (330 µL). The Schlenk flask was sealed shut and heated to 70 °C overnight. The DMF was removed *in vacuo* and the residue dissolved in DCM (10 mL). Washed with water (3 x

10 mL), dried over Na_2SO_4, and concentrated under reduced pressure. Flash chromatography on silica gel (4% MeOH in DCM) yielded Et*m*H **15** as a reddish orange solid (17.3 mg, 26%).

^{1}H NMR (500 MHz, Methanol-d_4) δ 8.06 (d, J = 8.3 Hz, 1H), 7.77 (dd, J = 8.4, 1.9 Hz, 1H), 7.52 (d, J = 8.4 Hz, 2H), 7.47 (d, J = 8.4 Hz, 3H), 7.44 – 7.39 (m, 4H), 7.29 (d, J = 16.4 Hz, 1H), 7.19 (d, J = 16.4 Hz, 1H), 7.09 (d, J = 16.2 Hz, 1H), 6.93 (d, J = 16.3 Hz, 1H), 6.76 (d, J = 8.8 Hz, 3H), 2.96 (s, 8H), 2.47 (s, 6H), 2.34 (q, J = 7.5 Hz, 4H), 1.46 (s, 6H), 0.99 (t, J = 7.6 Hz, 6H). **^{13}C NMR** (700 MHz, Methanol-d_4) δ 153.5, 151.7, 143.6, 141.9, 141.6, 140.1, 139.7, 136.7, 134.9, 133.3, 132.6, 132.1, 130.5, 130.2, 128.7, 128.7, 128.3, 127.4, 127.3, 126.9, 124.9, 113.9, 40.8, 17.9, 15.1, 12.6, 11.93. **ESI-HR(-)**, calculated for $C_{41}H_{43}BF_2N_3O_3S^-$: 706.3092, found: 706.3077. **Analytical HPLC retention time:** 7.59 min. Estimated purity >99%.

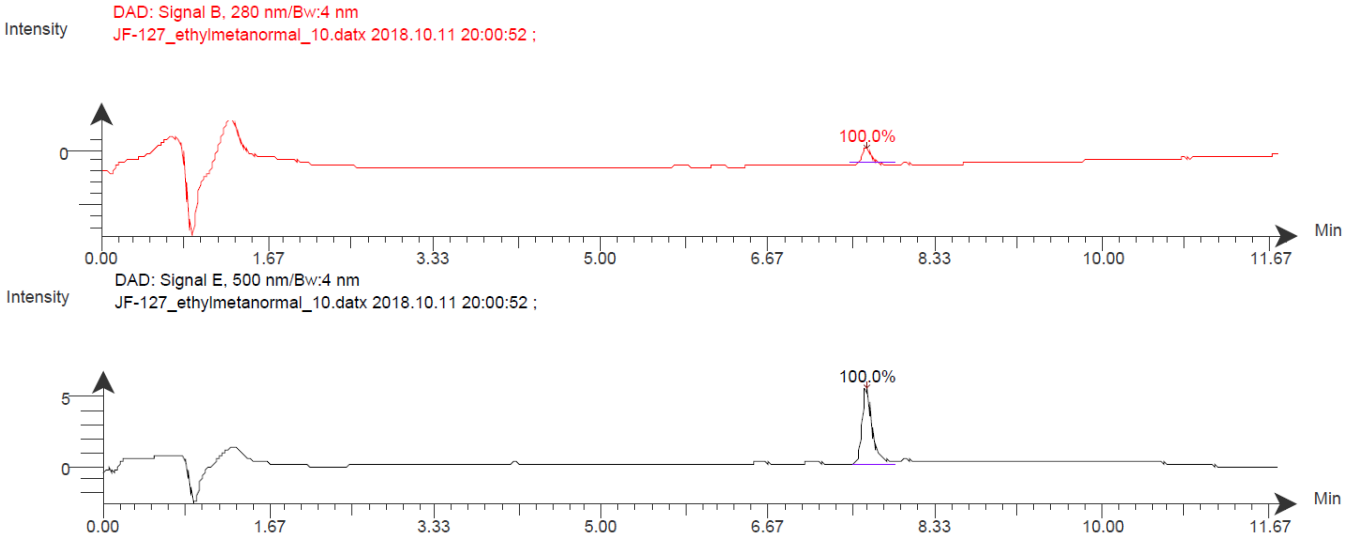

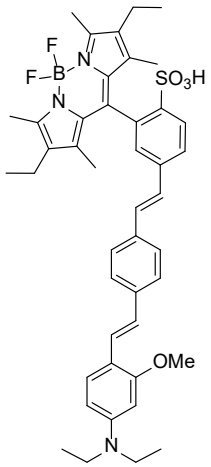

Ethyl BODIPY *m*-methoxy wire (16). To a flame-dried 10 mL Schlenk flask were added 1,3,5,7-tetramethyl-2,6-diethyl-m-bromo BODIPY **11** (49.3 mg, 0.09 mmol, 1 eq), methoxy molecular wire **14** (30.9 mg, 0.10 mmol, 1.1 eq), $Pd(OAc)_2$ (1.8 mg, 0.008 mmol, 9 mol%), and P(*o*-tol)$_3$ (5.0 mg, 0.016 mmol, 18 mol%). The flask was evacuated and backfilled with N_2 3x before addition of

DMF (660 µL) and NEt_3 (330 µL). The Schlenk flask was sealed shut and heated to 70 °C overnight. The DMF was removed *in vacuo* and the residue dissolved in DCM (10 mL). Washed with water (3 x 10 mL), dried over Na_2SO_4, and concentrated under reduced pressure. Flash chromatography on silica gel (0 → 5% MeOH in DCM, gradient) yielded Et*m*OMe **16** as a reddish orange solid (20.0 mg, 29%).

^{1}H NMR (400 MHz, Methanol-d4) δ 8.06 (d, *J* = 8.3 Hz, 1H), 7.75 (dd, *J* = 8.3, 1.8 Hz, 1H), 7.47 (d, *J* = 8.2 Hz, 2H), 7.44 – 7.34 (m, 6H), 7.26 (d, *J* = 16.4 Hz, 1H), 7.14 (d, *J* = 16.4 Hz, 1H), 6.89 (d, *J* = 16.4 Hz, 1H), 6.33 (d, *J* = 9.1 Hz, 1H), 6.26 (d, *J* = 2.4 Hz, 1H), 3.86 (s, 3H), 3.40 (q, *J* = 7.1 Hz, 4H), 3.07 (q, *J* = 7.3 Hz, 4H), 2.65 (s, 10H), 2.47 (s, 6H), 2.33 (q, *J* = 7.5 Hz, 4H), 1.45 (s, 6H), 1.18 (dt, *J* = 8.6, 7.1 Hz, 12H), 0.98 (t, *J* = 7.5 Hz, 6H). **^{13}C NMR** (400 MHz, MeOD) δ 159.88, 153.62, 150.1, 143.21, 142.05, 141.56, 140.52, 140.25, 136.19, 134.78, 133.36, 132.59, 132.25, 130.43, 128.62, 128.49, 128.27, 127.46, 127.12, 126.56, 125.18, 124.35, 115.6, 106.17, 96.36, 55.87, 47.76, 45.70, 40.43 (DMSO), 17.87, 15.11, 13.00, 12.59, 11.95, 9.09 ppm. **ESI-HR(-)**, calculated for $C_{44}H_{49}BF_2N_3O_4S^-$: 764.3510, found: 764.3492. **Analytical HPLC retention time:** 6.95 min. Estimated purity >99%.

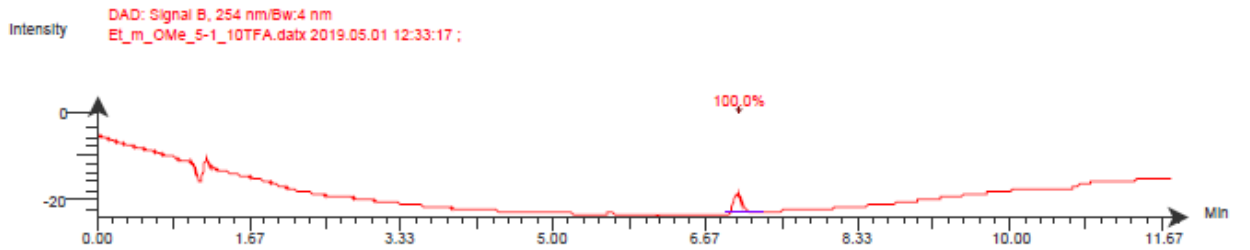

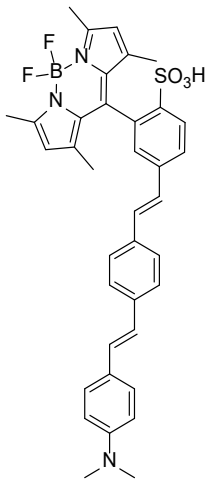

Tetramethyl BODIPY *m*-normal wire (17). To a flame-dried 10 mL Schlenk flask were added 1,3,5,7-tetramethyl-*m*-bromo BODIPY **12** (35.6 mg, 0.07 mmol, 1 eq), molecular wire **4** (18.1 mg, 0.07 mmol, 1.1 eq), $Pd(OAc)_2$ (0.15 mg, 0.0006 mmol, 9 mol%), and P(*o*-tol)$_3$ (0.4 mg, 0.0013 mmol, 18 mol%). The flask was evacuated and backfilled with N_2 3x before addition of DMF (440 µL) and NEt_3 (220 µL). The Schlenk flask was sealed shut and heated to 70 °C overnight. The DMF was removed *in vacuo* and the residue dissolved in DCM (10 mL). Washed with water (3 x 10 mL), dried over Na_2SO_4, and concentrated under reduced pressure. Flash chromatography on silica gel (0% to 4% MeOH in DCM) yielded TM*m*H **17** as an orange solid (23.1 mg, 56%).

^{1}H NMR (900 MHz, Methanol-d_4) δ 8.06 (d, J = 8.2 Hz, 1H), 7.77 (dd, J = 8.3, 1.9 Hz, 1H), 7.55 – 7.52 (m, 2H), 7.48 (dd, J = 9.3, 2.9 Hz, 2H), 7.43 – 7.39 (m, 3H), 7.30 (d, J = 16.3 Hz, 1H), 7.20 (d, J = 16.3 Hz, 1H), 7.09 (dd, J = 16.2, 2.9 Hz, 1H), 6.93 (d, J = 16.2 Hz, 1H), 6.77 – 6.73 (m, 2H), 5.99 (s, 2H), 2.96 (d, J = 1.6 Hz, 7H), 2.48 (s, 6H), 1.55 (s, 6H). **^{13}C NMR** (900 MHz, Methanol-d_4) 155.5, 151.9, 144.9, 143.4, 142.9, 142.0, 139.7, 136.6, 134.2, 133.3, 132.2, 130.5, 130.3, 128.7, 128.4, 128.3, 127.3, 126.8, 124.8, 121.6, 113.8, 40.8, 14.8, 14.6 ppm. **ESI-HR(-)**, calculated for $C_{37}H_{35}BF_2N_3O_3S^-$: 650.2466, found: 650.2457. **Analytical HPLC retention time:** 6.65 min. Estimated purity >99%.

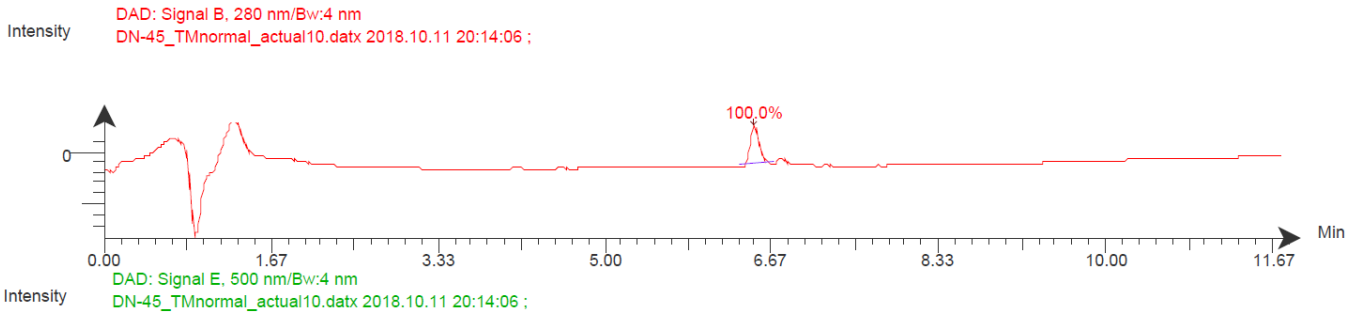

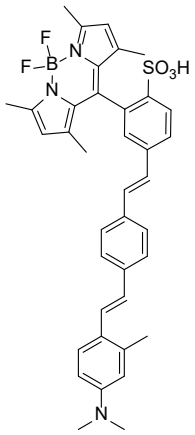

Tetramethyl BODIPY *m*-methyl wire (18). To a flame-dried 10 mL Schlenk flask were added 1,3,5,7-tetramethyl-*m*-bromo BODIPY **12** (50.4 mg, 0.10 mmol, 1 eq), methyl molecular wire **13** (30.2 mg, 0.11 mmol, 1.1 eq), $Pd(OAc)_2$ (1.2 mg, 0.005 mmol, 9 mol%), and P(*o*-tol)$_3$ (3.2 mg, 0.01 mmol, 18 mol%). The flask was evacuated and backfilled with N_2 3x before addition of DMF (700 µL) and NEt_3 (350 µL). The Schlenk flask was sealed shut and heated to 70 °C overnight. The DMF was removed *in vacuo* and the residue dissolved in DCM (10 mL). Washed with water (3 x 10 mL), dried over Na_2SO_4, and concentrated under reduced pressure. Flash chromatography on silica gel (1 → 4% MeOH in DCM, gradient) yielded TM*m*Me **18** as an orange solid (24 mg, 35%).

^{1}H NMR (700 MHz, DMSO-d_6) δ 7.88 (d, J = 8.2 Hz, 1H), 7.70 (d, J = 9.0 Hz, 1H), 7.58 – 7.51 (m, 5H), 7.39 – 7.31 (m, 3H), 7.26 (d, J = 16.4 Hz, 1H), 6.90 (d, J = 16.2 Hz, 1H), 6.59 (d, J = 8.6 Hz, 1H), 6.54 (d, J = 2.7 Hz, 1H), 6.04 (s, 2H), 3.32 (s, 6H), 2.92 (s, 7H), 2.43 (s, 6H), 2.37 (s, 3H), 1.45 (s, 6H). **^{13}C NMR** (900 MHz, DMSO-d_6) δ 152.8, 149.9, 144.9, 143.0, 138.5, 137.8, 136.5, 135.2, 131.5, 129.5, 128.9, 126.9, 126.5, 126.3, 126.2, 126.1, 125.9, 124.4, 123.7, 120.2, 113.7, 110.4, 53.4, 48.6, 39.9, 20.1, 18.0, 16.70, 14.1, 13.9 ppm. **ESI-HR(-)**, calculated for $C_{38}H_{37}BF_2N_3O_3S^-$: 664.2622, found: 664.2612. **Analytical HPLC retention time:** 6.50 min. Estimated purity 95%.

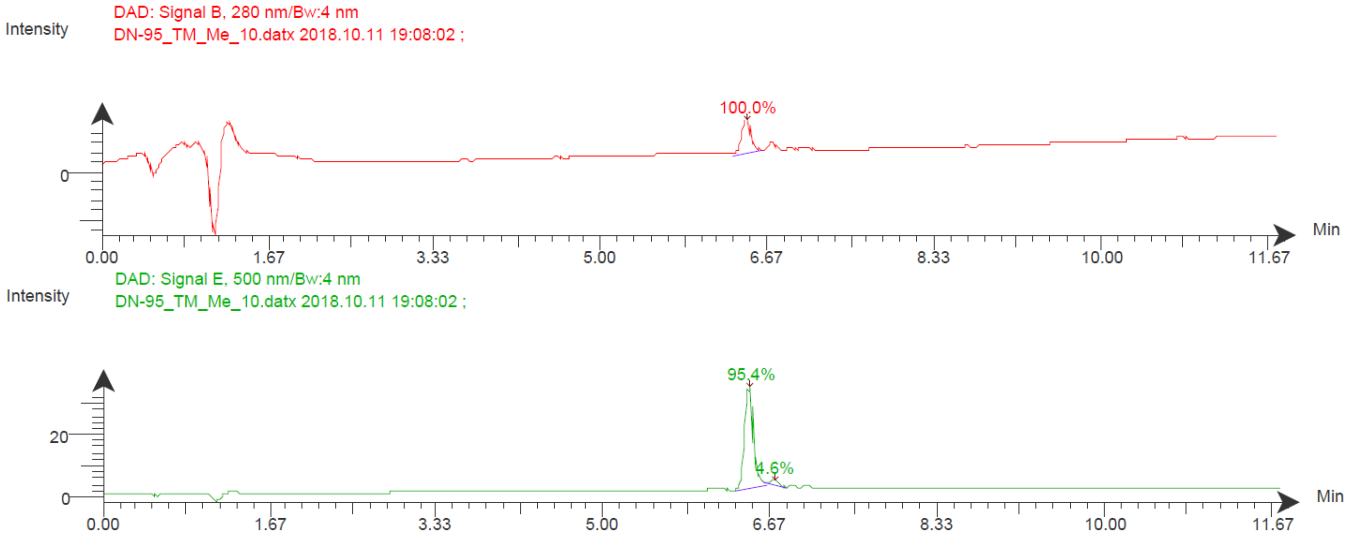

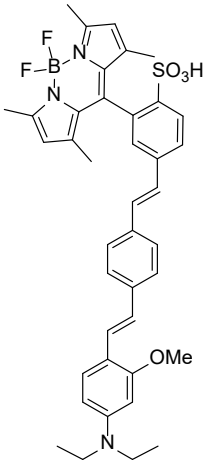

Tetramethyl BODIPY *m*-methoxy wire (19). To a flame-dried 10 mL Schlenk flask were added 1,3,5,7-tetramethyl-*m*-bromo BODIPY **12** (51.1 mg, 0.09 mmol, 1 eq), methoxy molecular wire **14** (30.2 mg, 0.10 mmol, 1.1 eq), $Pd(OAc)_2$ (1.1 mg, 0.005 mmol, 9 mol%), and P(*o*-tol)$_3$ (2.9 mg, 0.01 mmol, 18 mol%). The flask was evacuated and backfilled with N_2 3x before addition of DMF (630 µL) and NEt_3 (310 µL). The Schlenk flask was sealed shut and heated to 100 °C overnight. The DMF was removed *in vacuo* and the residue dissolved in DCM (10 mL). Washed with water (3 x 10 mL), dried over Na_2SO_4, and concentrated under reduced pressure. Flash chromatography on silica gel (0% to 4% MeOH in DCM) yielded TM*m*OMe **19** as an orange solid (30.5 mg, 62%).

^{1}H NMR (300 MHz, Methanol-d_4) δ 8.06 (d, J = 8.3 Hz, 1H), 7.75 (dd, *J* = 8.4, 1.9 Hz, 1H), 7.48 (d, *J* = 8.2 Hz, 2H), 7.45 – 7.33 (m, 5H), 7.26 (d, *J* = 16.4 Hz, 1H), 7.14 (d, *J* = 16.3 Hz, 1H), 6.89 (d, *J* = 16.5 Hz, 1H), 6.32 (dd, *J* = 8.7, 2.4 Hz, 1H), 6.24 (d, *J* = 2.3 Hz, 1H), 5.99 (s, 2H), 3.86 (s, 3H), 3.40 (q, *J* = 7.0 Hz, 4H), 2.48 (s, 6H), 1.53 (s, 6H), 1.18 (t, *J* = 7.0 Hz, 6H). **^{13}C NMR** (400 MHz, Methanol-d_4) δ 159.9, 155.5, 150.2, 144.9, 143.2, 142.9, 142.0, 140.6, 136.2, 134.1, 133.3, 132.3, 130.4, 128.3, 127.5, 127.1, 126.5, 125.2, 124.2, 121.6, 106.0, 96.2, 55.9, 45.6, 14.63, 14.56, 13.0 ppm. **ESI-HR(-)**, calculated for $C_{40}H_{41}BF_2N_3O_4S^-$: 708.2884, found: 708.2873. **Analytical HPLC retention time:** 6.16 min. Estimated purity 96%.

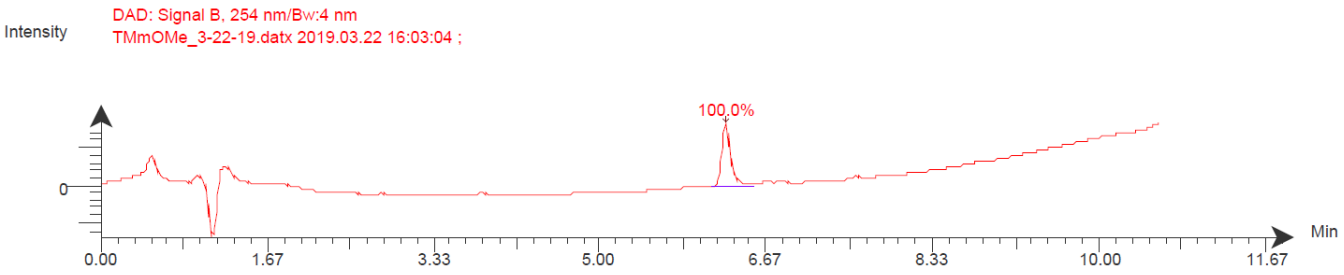

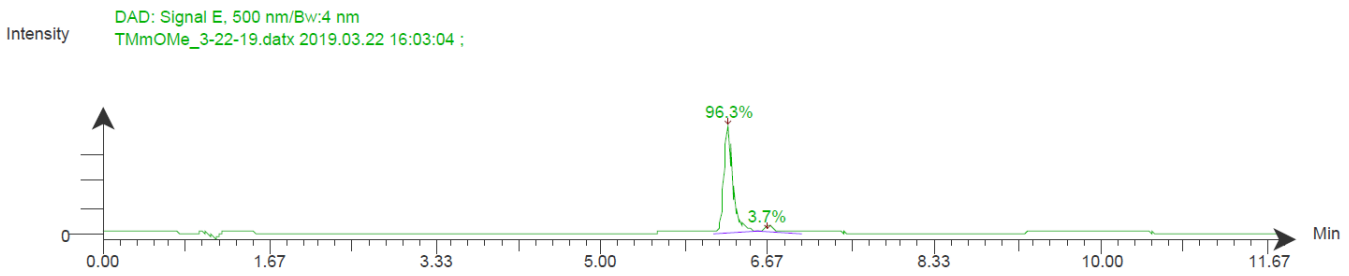

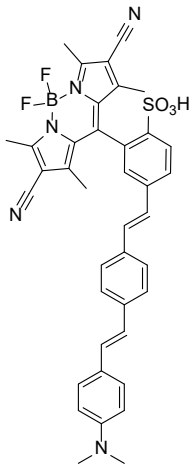

2,6-cyano BODIPY *m*-normal wire (22). To a flame-dried 4 mL dram vial were added 1,3,5,7-tetramethyl-2,6-cyano-*m*-bromo BODIPY **21** (29.2 mg, 0.05 mmol, 1 eq), molecular wire **4** (15.0 mg, 0.06 mmol, 1.1 eq) and $Pd(dba)_2$ (12.5 mg, 0.014 mmol, 25 mol%). The vial was evacuated and backfilled with N_2 3x before addition of 1M $P(tBu)_3$ in toluene (27 µL, 0.03 mmol, 50 mol%) and DMF (1.1 mL). The vial was sealed shut and heated to 70 °C overnight. The DMF was removed *in vacuo* and the residue dissolved in DCM (7 mL) and IPA (3 mL). Washed with water (3 x 10 mL), sat. aq. sodium bicarbonate (10 mL), dried over Na_2SO_4, and concentrated under reduced pressure. Flash chromatography on silica gel (10% MeOH in DCM) yielded cyano*m*H **6** as a yellowish solid (2.1 mg, 6%).

^{1}H NMR (400 MHz, Methanol-d_4) δ 8.11 (d, J = 8.3 Hz, 1H), 7.93 – 7.86 (m, 1H), 7.55 (d, J = 8.2 Hz, 2H), 7.52 – 7.45 (m, 3H), 7.45 – 7.32 (m, 3H), 7.23 (d, J = 16.4 Hz, 1H), 7.11 (d, J = 16.2 Hz, 1H), 6.93 (d, J = 16.3 Hz, 1H), 6.76 (d, J = 8.6 Hz, 2H), 2.97 (s, 6H), 2.67 (s, 6H), 1.74 (s, 6H). **^{13}C NMR** (400 MHz, Methanol-d_4) δ 159.6, 151.9, 151.0, 143.0, 142.8, 140.0, 136.5, 133.0, 131.8, 130.8, 130.4, 128.8, 128.7, 128.4, 127.3, 127.0, 126.3, 124.7, 114.7, 113.8, 49.6, 49.4, 49.2, 48.8, 48.6, 48.4, 40.7, 14.0, 13.7 ppm. **ESI-HR(-)**, calculated for $C_{39}H_{33}BF_2N_5O_3S^-$: 700.2371, found: 700.2356. **Analytical HPLC retention time:** 6.94 min. Estimated purity >99%.

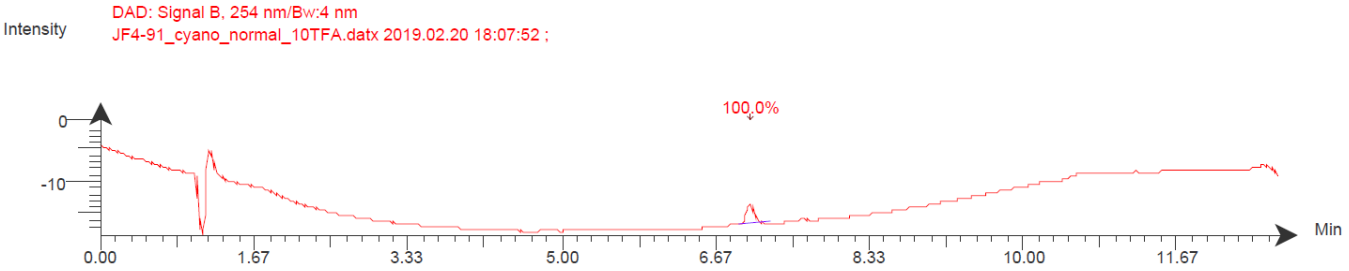

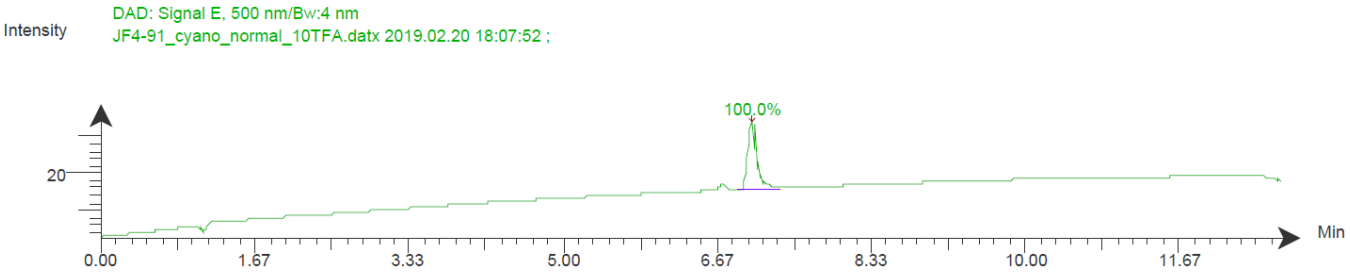

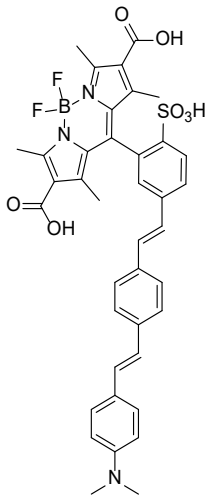

2,6-carboxy BODIPY *m*-normal wire (28). To a flame-dried 4 mL dram vial were added 1,3,5,7-tetramethyl-2,6-carboxy-*m*-bromo BODIPY **32** (42.6 mg, 0.07 mmol, 1 eq), molecular wire **4** (20.5 mg, 0.08 mmol, 1.1 eq) and $Pd_2(dba)_2$ (13.7 mg, 0.014 mmol, 20 mol%). The vial was evacuated and backfilled with N_2 3x before addition of 1M $P(tBu)_3$ in toluene (30 µL, 0.03 mmol, 50 mol%) and DMF (1.5 mL). The vial was sealed shut and heated to 70 °C overnight. The DMF was removed *in vacuo*. Preparatory thin layer chromatography (12% MeOH + 1% AcOH in DCM) yielded carboxy*m*H **28** as a yellow-orange solid (3.1 mg, 6%). This material was 93% pure by analytical HPLC. For NMR and spectroscopic characterization, a small amount was further purified by reverse phase preparative HPLC (10-100% MeCN in water, 0.05% formic acid additive).

^{1}H NMR (900 MHz, DMSO-d_6) δ 7.88 (d, J = 8.1 Hz, 1H), 7.74 (dd, J = 8.4, 1.8 Hz, 1H), 7.57 – 7.50 (m, 4H), 7.46 – 7.41 (m, 3H), 7.39 (d, J = 16.4 Hz, 1H), 7.27 (d, J = 16.4 Hz, 1H), 7.16 (d, J = 16.3 Hz, 1H), 6.96 (d, J = 16.3 Hz, 1H), 6.72 (d, J = 8.5 Hz, 2H), 2.93 (s, 7H), 2.71 (s, 6H), 1.73 (s, 6H). **ESI-HR(-)**, calculated for $C_{39}H_{35}BF_2N_3O_7S^-$: 738.2262, found: 738.2241.
Analytical HPLC retention time: 5.24 min. Estimated purity >99%.

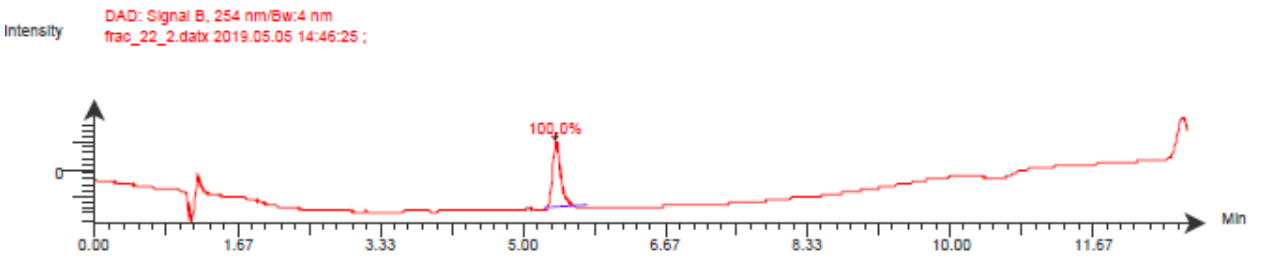

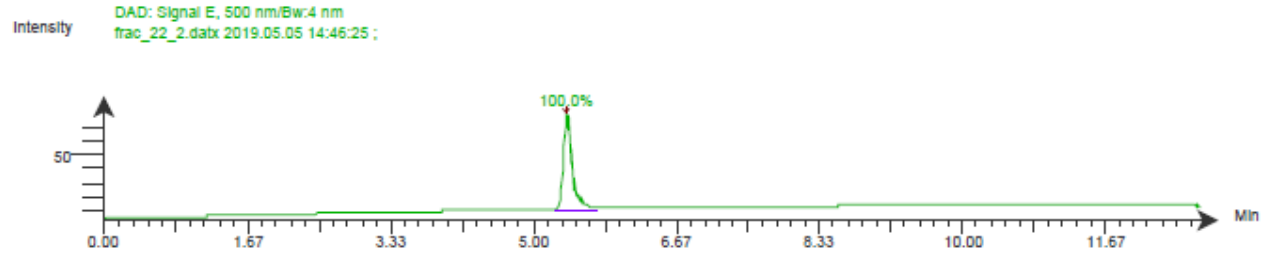

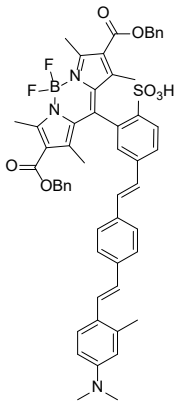

OBn methyl wire (26). To a flame-dried 10 mL Schlenk flask were added OBn BODIPY **24** (107 mg, 0.1 mmol, 1 eq), methyl molecular wire **13** (41.3 mg, 0.16 mmol, 1.1 eq), $Pd(OAc)_2$ (2.9 mg, 0.013 mmol, 9 mol%), and P(*o*-tol)$_3$ (7.8 mg, 0.026 mmol, 18 mol%). The flask was evacuated and backfilled with N_2 3x before addition of DMF (2 mL) and NEt_3 (1 mL). The Schlenk flask was sealed shut and heated to 100 °C overnight. The DMF was removed *in vacuo* and the residue dissolved in DCM (10 mL). Washed with water (3 x 10 mL), dried over Na_2SO_4, and concentrated under reduced pressure. Flash chromatography on silica gel (3 → 7% MeOH in DCM, gradient) yielded OBn*m*Me **26** as an orange solid (39.3 mg, 30%).

^{1}H NMR (900 MHz, Methanol-d_4) δ 7.98 (d, J = 8.2 Hz, 1H), 7.59 (dd, J = 8.3, 1.8 Hz, 1H), 7.41 (d, J = 8.7 Hz, 1H), 7.34 (s, 4H), 7.30 (d, J = 7.1 Hz, 4H), 7.27 (td, J = 8.9, 8.1, 2.4 Hz, 6H), 7.25 – 7.21 (m, 2H), 7.16 (d, J = 1.7 Hz, 1H), 7.10 (d, J = 16.2 Hz, 1H), 6.99 (d, J = 16.2 Hz, 1H), 6.75 (d, J = 16.0 Hz, 1H), 6.54 (dd, J = 8.8, 2.6 Hz, 1H), 6.49 (d, J = 2.6 Hz, 1H), 5.16 (s, 4H), 2.86 (s, 6H), 2.74 (s, 7H), 2.32 (s, 3H), 1.69 (s, 6H). **^{13}C NMR** (900 MHz, Methanol-d_4) δ 165.6, 159.8, 151.6, 149.2, 147.3, 142.9, 142.2, 140.0, 138.0, 137.5, 136.2, 133.3, 133.3, 132.6, 130.7, 129.6, 129.3, 129.2, 128.3, 128.1, 127.7, 127.7, 127.4, 127.2, 126.5, 126.1, 126.0, 122.6, 118.2, 115.3, 112.0, 67.1, 49.9, 40.8, 30.8, 30.8, 30.7, 20.7, 15.42, 15.41, 15.39, 14.5, 14.2 ppm. **ESI-HR(-)**, calculated for $C_{54}H_{49}BF_2N_3O_7S^-$: 932.3358, found: 932.3369. **Analytical HPLC retention time:** 8.91 min.

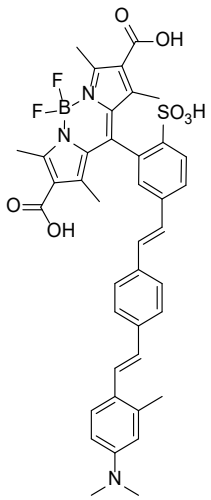

2,6-carboxy BODIPY *m*-methyl wire (29). To a flame-dried 10 mL Schlenk flask was added $Pd(OAc)_2$ (1.4 mg, 0.019 mmol, 9 mol%). The flask was evacuated and backfilled with N_2 3x before addition of DCM (230 µL), Et_3SiH (26 µL, 0.161 mmol, 2.4 eq), NEt_3 (3 µL, 0.019, 28 mol%). The mixture was stirred for 15 minutes at rt, then **26** (62.6 mg, 0.067 mmol, 1 eq) was dissolved in DCM and transferred to the reaction via syringe (200µL + 200µL rinse). The Schlenk flask was sealed shut and stirred at rt 4 h. The reaction mixture was quenched with sat. aq. NH_4Cl (2 mL), extracted with DCM (3 x 10 mL), dried over Na_2SO_4, and concentrated under reduced pressure. Preparatory thin layer chromatography (15% MeOH + 1% AcOH in DCM) yielded carboxy*m*Me **29** as a yellow-orange solid (8.8 mg, 31%).

^{1}H NMR (600 MHz, Methanol-d_4) δ 8.07 (d, J = 8.2 Hz, 1H), 7.81 (dd, J = 8.0, 1.6 Hz, 1H), 7.75 (dd, J = 7.8, 5.0 Hz, 1H), 7.57 – 7.43 (m, 6H), 7.35 (d, J = 16.2 Hz, 1H), 7.32 (d, J = 16.4 Hz, 1H), 7.21 (d, J = 8.3 Hz, 1H), 6.87 (d, J = 16.1 Hz, 1H), 6.64 (dd, J = 8.7, 2.8 Hz, 1H), 6.57 (d, J = 2.7 Hz, 1H), 2.94 (s, 6H), 2.74 (s, 7H), 2.39 (s, 3H), 1.80 (s, 6H). **ESI-HR(-)**, calculated for $C_{40}H_{37}BF_2N_3O_7S^-$: 752.2419, found: 752.2411. **Analytical HPLC retention time:** 5.28 min. Estimated purity >99%.

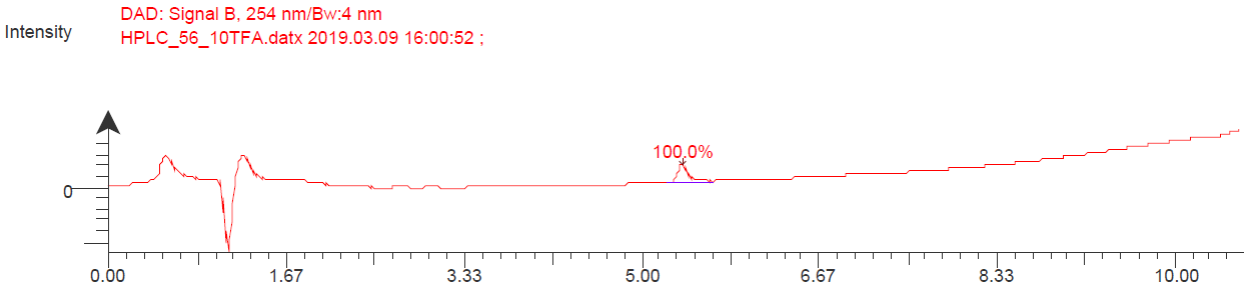

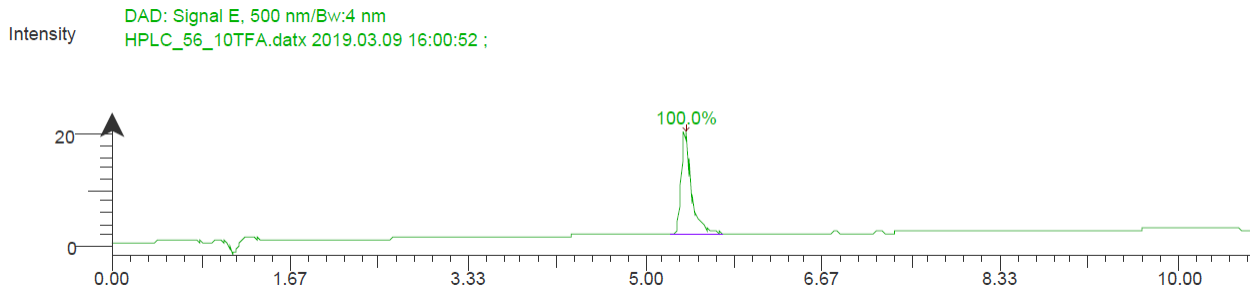

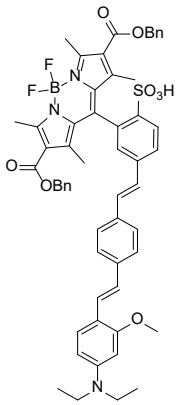

OBn methoxy wire (27). To a flame-dried 25 mL Schlenk flask were added OBn BODIPY **24** (608 mg, 0.81 mmol, 1 eq), methoxy molecular wire **14** (274 mg, 0.89 mmol, 1.1 eq), $Pd(OAc)_2$ (5.5 mg, 0.024 mmol, 3 mol%), and P(*o*-tol)$_3$ (14.8 mg, 0.049 mmol, 6 mol%). The flask was evacuated and backfilled with N_2 3x before addition of DMF (10.8 mL) and NEt_3 (5.4 mL). The Schlenk flask was sealed shut and heated to 100 °C overnight. The DMF was removed *in vacuo* and the residue dissolved in DCM (10 mL). Washed with water (3 x 10 mL), dried over Na_2SO_4, and concentrated under reduced pressure. Flash chromatography on silica gel (4 → 10% MeOH in DCM, gradient) yielded OBn*m*OMe **27** as an orange solid (336.8 mg, 43%).

^{1}H NMR (400 MHz, Acetone-d_6) δ 8.06 (d, J = 8.3 Hz, 1H), 7.75 (d, J = 8.0 Hz, 1H), 7.56 (d, J = 8.1 Hz, 2H), 7.30 (s, 17H), 7.27 (d, J = 7.9 Hz, 1H), 6.97 (d, J = 16.4 Hz, 1H), 6.33 (dd, J = 8.7, 2.5 Hz, 1H), 6.29 (d, J = 2.4 Hz, 1H), 5.27 (s, 4H), 3.88 (s, 3H), 3.44 (q, J = 7.0 Hz, 4H), 2.77 (s, 7H), 1.86 (s, 7H), 1.17 (t, J = 7.0 Hz, 6H). **ESI-HR(-)**, calculated for $C_{56}H_{53}BF_2N_3O_8S^-$: 976.3620, found: 976.3606. **Analytical HPLC retention time:** 8.27 min.

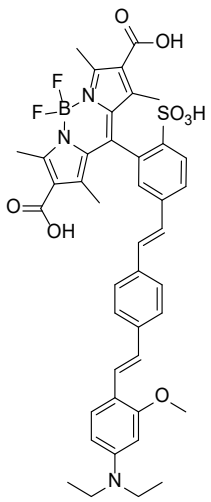

2,6-carboxy BODIPY *m*-methoxy wire (30). To a flame-dried 20 mL scintillation vial was added $Pd(OAc)_2$ (10.4 mg, 0.027 mmol). The vial was evacuated and backfilled with N_2 3x before addition of Et_3SiH (250 µL, 0.9 mmol), NEt_3 (20 µL, 0.086), and DCM (2.9 mL). This 5x stock solution was stirred at rt for 15 min. To another flame-dried 20 mL scintillation vial equipped with a stir bar was added **27** (67.2 mg, 0.07 mmol, 1 eq). The vial was evacuated and backfilled with N_2 3x before addition of the stock solution (640 µL). The vial was sealed and stirred at rt 18 h. The reaction mixture was quenched with sat. aq. NH_4Cl (3 mL), extracted with 3:1 DCM:IPA (3 x 10 mL), dried over Na_2SO_4, and concentrated under reduced pressure. Flash chromatography on silica gel (5 → 15% MeOH + 1% AcOH in DCM, gradient) yielded carboxy*m*OMe **30** as a yellow-orange solid (7.5 mg, 14%).

^{1}H NMR (500 MHz, DMSO-d_6) δ 7.86 (d, J = 8.2 Hz, 1H), 7.73 – 7.66 (m, 1H), 7.54 (d, J = 8.1 Hz, 2H), 7.43 (t, J = 8.4 Hz, 3H), 7.38 – 7.27 (m, 3H), 7.24 (d, J = 16.5 Hz, 1H), 6.92 (d, J = 16.4 Hz, 1H), 6.28 (dd, J = 8.9, 2.3 Hz, 1H), 6.20 (d, J = 2.3 Hz, 1H), 3.83 (s, 3H), 2.69 (s, 6H), 1.72 (s, 6H), 1.10 (d, J = 7.0 Hz, 6H). **ESI-HR(-)**, calculated for $C_{42}H_{41}BF_2N_3O_8S^-$: 796.2681, found: 796.2669. **Analytical HPLC retention time:** 5.19 min. Estimated purity >99%.

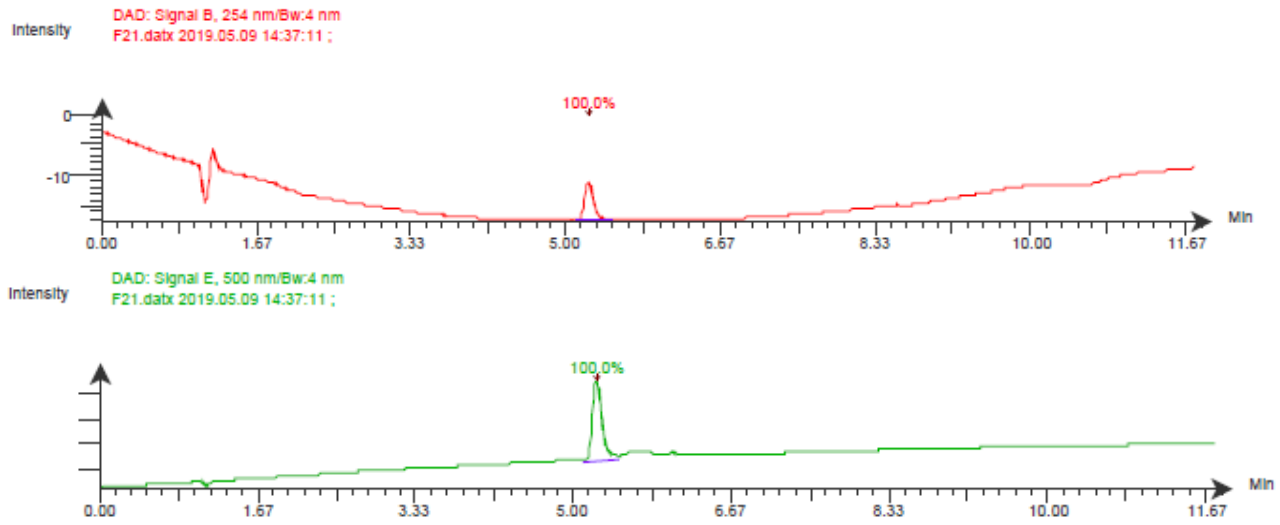

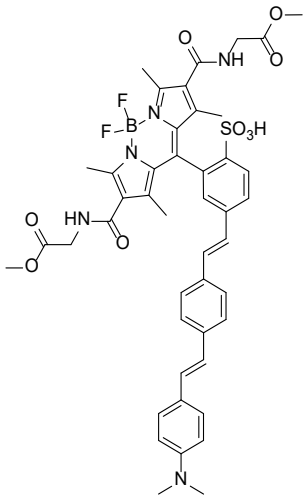

2,6-amide BODIPY *m*-normal wire (35). To a flame-dried 4 mL dram vial were added amide BODIPY **34** (15.6 mg, 0.02 mmol, 1 eq), molecular wire **4** (6.5 mg, 0.03 mmol, 1.1 eq), $Pd(OAc)_2$ (1.2 mg, 0.005 mmol, 25 mol%), and P(*o*-tol)$_3$ (3.3 mg, 0.011 mmol, 50 mol%). The vial was evacuated and backfilled with N_2 3x before addition of DMF (350 µL) and NEt_3 (150 µL). The dram vial was sealed shut and heated to 100 °C 18 h. Solution was concentrated *in vacuo* and the residue dissolved in DCM (10 mL). Washed with sat. aq. NH_4Cl (10 mL), water (3 x 10 mL), dried over Na_2SO_4, and concentrated under reduced pressure. Flash chromatography on silica gel (10% MeOH in DCM) yielded amide*m*H **35** as a yellow-orange solid (4.1 mg, 21%).

^{1}H NMR (500 MHz, DMSO-d_6) δ 7.88 (d, J = 8.2 Hz, 1H), 7.74 (d, J = 8.5 Hz, 1H), 7.58 – 7.50 (m, 4H), 7.43 (d, J = 8.8 Hz, 2H), 7.36 (s, 2H), 7.28 (d, J = 16.5 Hz, 1H), 7.16 (d, J = 16.3 Hz, 1H), 6.96 (d, J = 16.4 Hz, 1H), 6.72 (d, J = 8.8 Hz, 2H), 3.99 – 3.86 (m, 4H), 3.62 (s, 6H), 2.93 (s, 6H), 2.55 (s, 6H), 1.55 (s, 6H). **ESI-HR(-)**, calculated for $C_{40}H_{41}BF_2N_3O_4S^-$: 880.3005, found: 880.2984. **Analytical HPLC retention time:** 5.47 min. Estimated purity >99%.

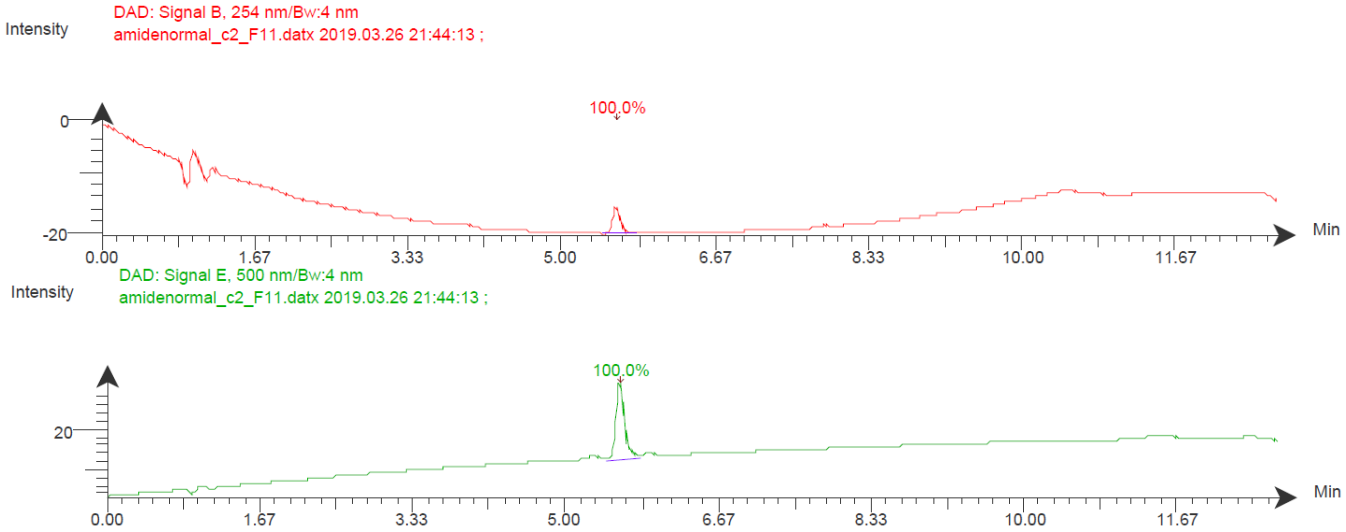

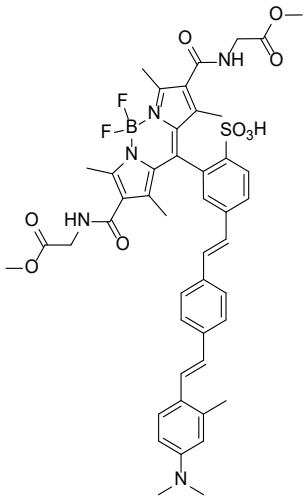

2,6-amide BODIPY *m*-methyl wire (36). To a flame-dried 4 mL dram vial were added amide BODIPY **34** (21.0 mg, 0.03 mmol, 1 eq), methyl molecular wire **13** (9.3 mg, 0.04 mmol, 1.1 eq), $Pd(OAc)_2$ (1.7 mg, 0.007 mmol, 25 mol%), and P(*o*-tol)$_3$ (4.5 mg, 0.015 mmol, 50 mol%). The vial was evacuated and backfilled with N_2 3x before addition of DMF (400 µL) and NEt_3 (300 µL). The dram vial was sealed shut and heated to 100 °C overnight. The solution was concentrated *in vacuo* and the residue dissolved in DCM (10 mL). Washed with water (10 mL), and the water layer was extracted with DCM (3 x 10 mL). The organics were combined, washed with brine (1 x 10 mL), dried over Na_2SO_4, and concentrated under reduced pressure. Flash chromatography on silica gel (15 → 20% MeOH in DCM) yielded amide*m*Me **6** as a yellow-orange solid (8.7 mg, 34%).

^{1}H NMR (400 MHz, Methanol-d_4) δ 8.10 (d, J = 8.3 Hz, 1H), 7.84 (dd, J = 8.4, 1.9 Hz, 1H), 7.59 – 7.46 (m, 6H), 7.35 (dd, J = 16.3, 8.3 Hz, 2H), 7.23 (d, J = 16.4 Hz, 1H), 6.88 (d, J = 16.1 Hz, 1H), 6.64 (dd, J = 8.8, 2.7 Hz, 1H), 6.58 (d, J = 2.6 Hz, 1H), 4.05 (d, J = 2.5 Hz, 4H), 3.72 (s, 6H), 2.95 (s, 6H), 2.62 (s, 6H), 2.40 (s, 3H), 1.68 (s, 6H). **^{13}C NMR** (700 MHz, Methanol-d_4) δ 171.73, 168.41, 155.64, 151.91, 146.24, 143.29, 142.58, 140.22, 138.07, 136.78, 133.51, 133.15, 132.70, 129.35, 129.33, 128.49, 127.91, 127.82, 127.54, 127.26, 126.78, 126.34, 49.68, 42.17, 40.91, 13.61, 13.31, 13.29. **ESI-HR(-)**, calculated for $C_{46}H_{47}BF_2N_5O_9S^-$: 894.3161, found: 894.3149. **Analytical HPLC retention time:** 5.24 min. Estimated purity >99%.

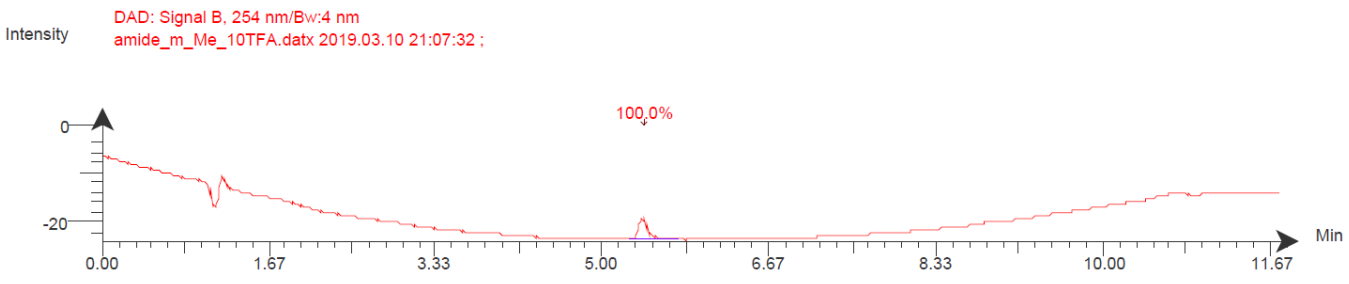

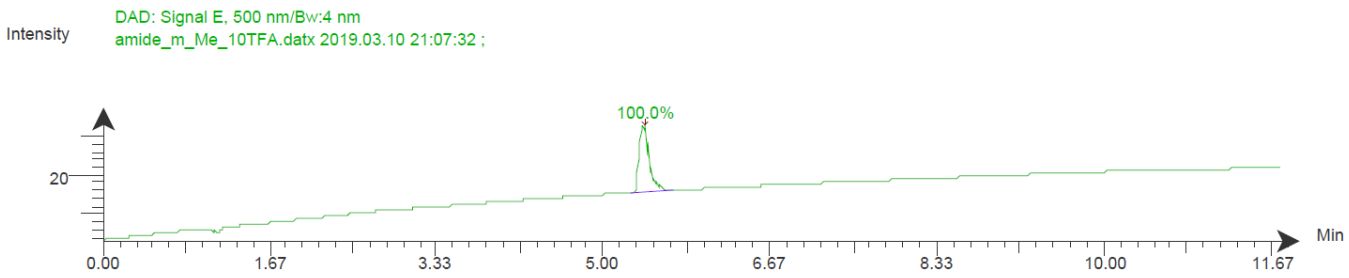
Intensity
DAD: Signal E, 500 nm/Bw:4 nm
amide_m_Me_10TFA.datx 2019.03.10 21:07:32 ;
100.0%
20
0.00
1.67
3.33
5.00
6.67
8.33
10.00
11.67
Min

Compound NMR Spectra

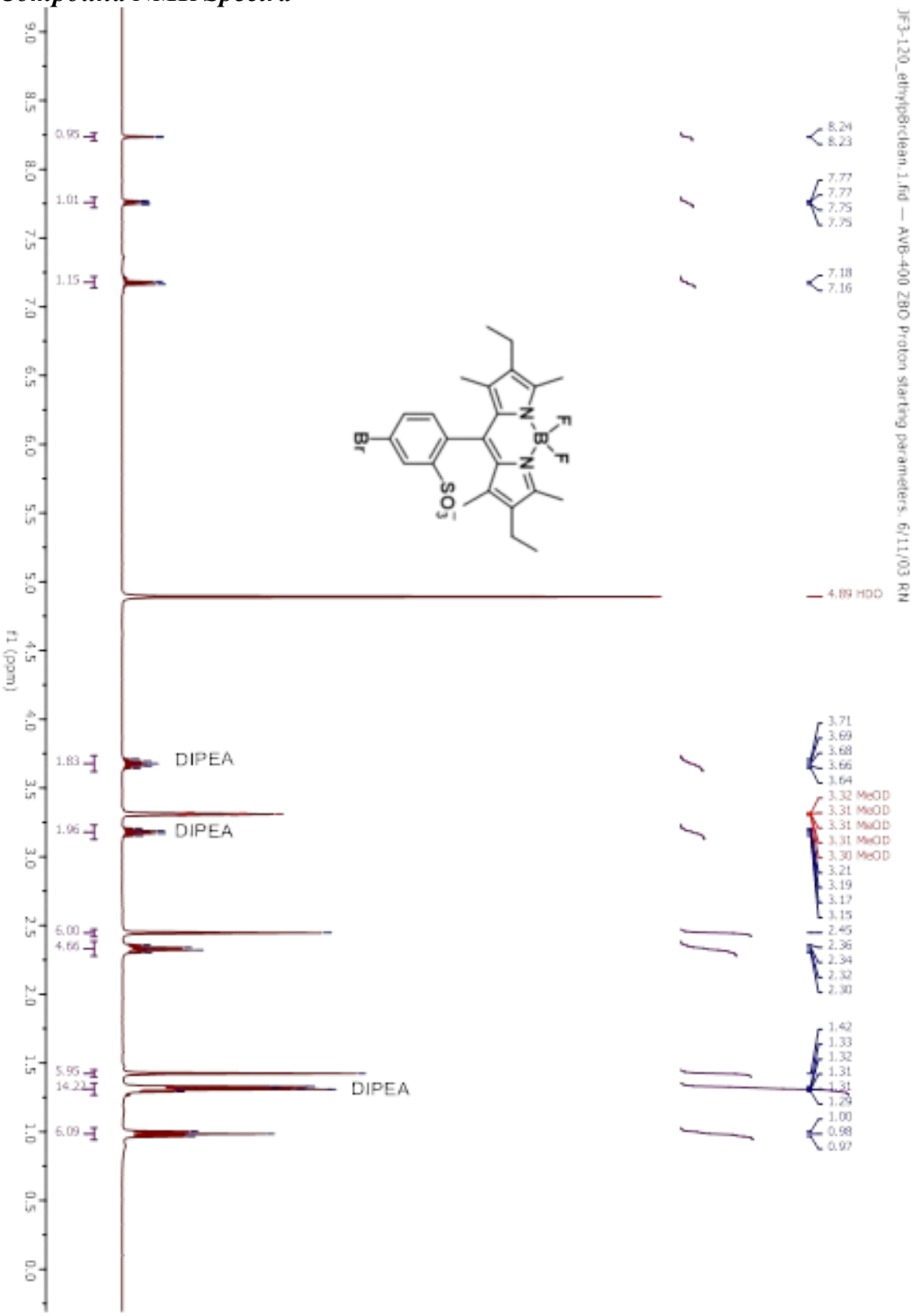

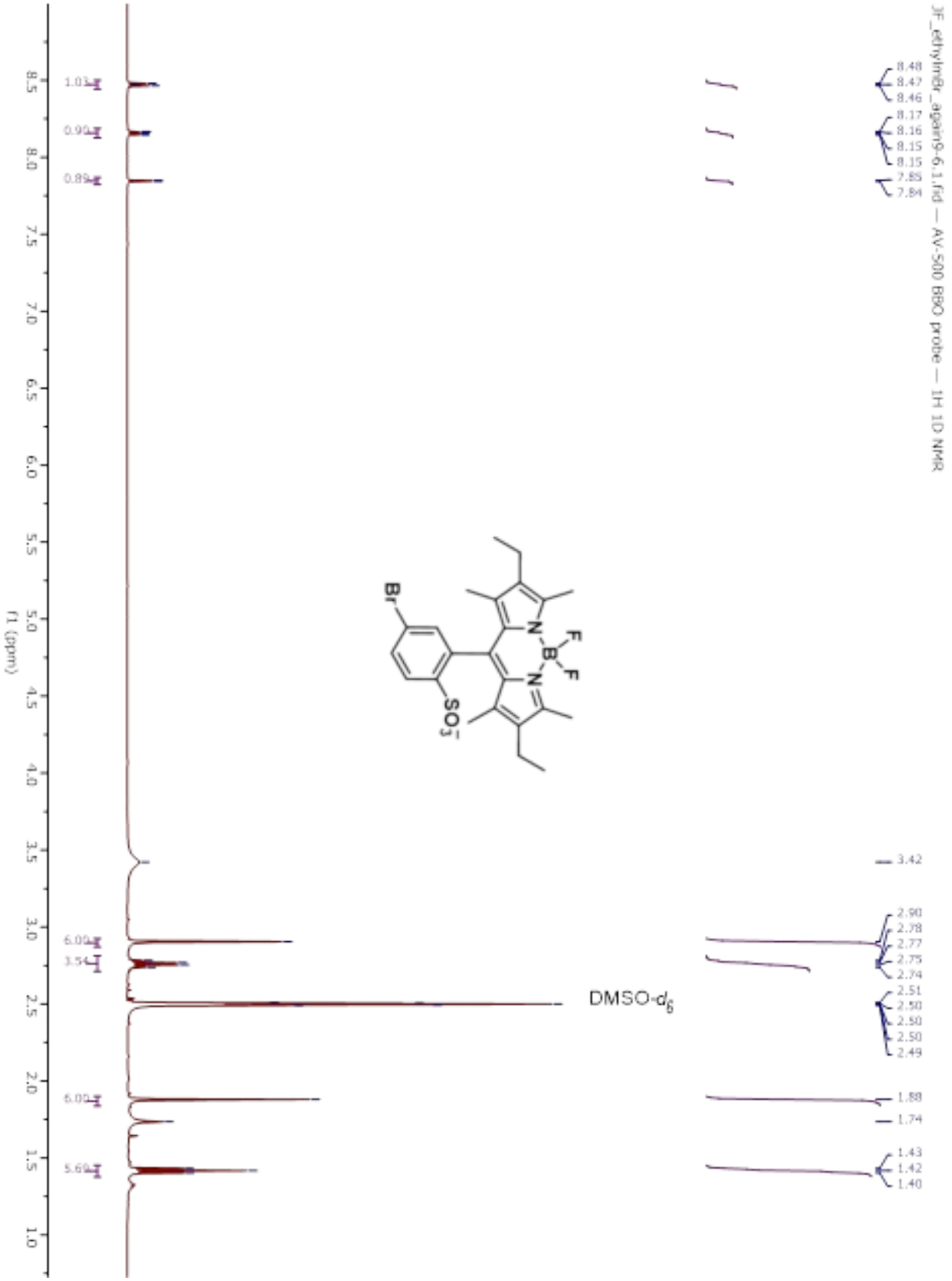
JF_ethylmBr_again9-6.1.fid — AV-500 BBO probe — 1H 1D NMR
8.48
8.47
8.46
8.17
8.16
8.15
8.15
7.85
7.84
3.42
2.90
2.78
2.77
2.75
2.74
2.51
2.50
2.50
2.50
2.49
1.88
1.74
1.43
1.42
1.40
DMSO-d_6
1.01
0.90
0.89
6.09
3.54
6.00
5.69
f1 (ppm)
Br
F
F
B
N
N
SO3−

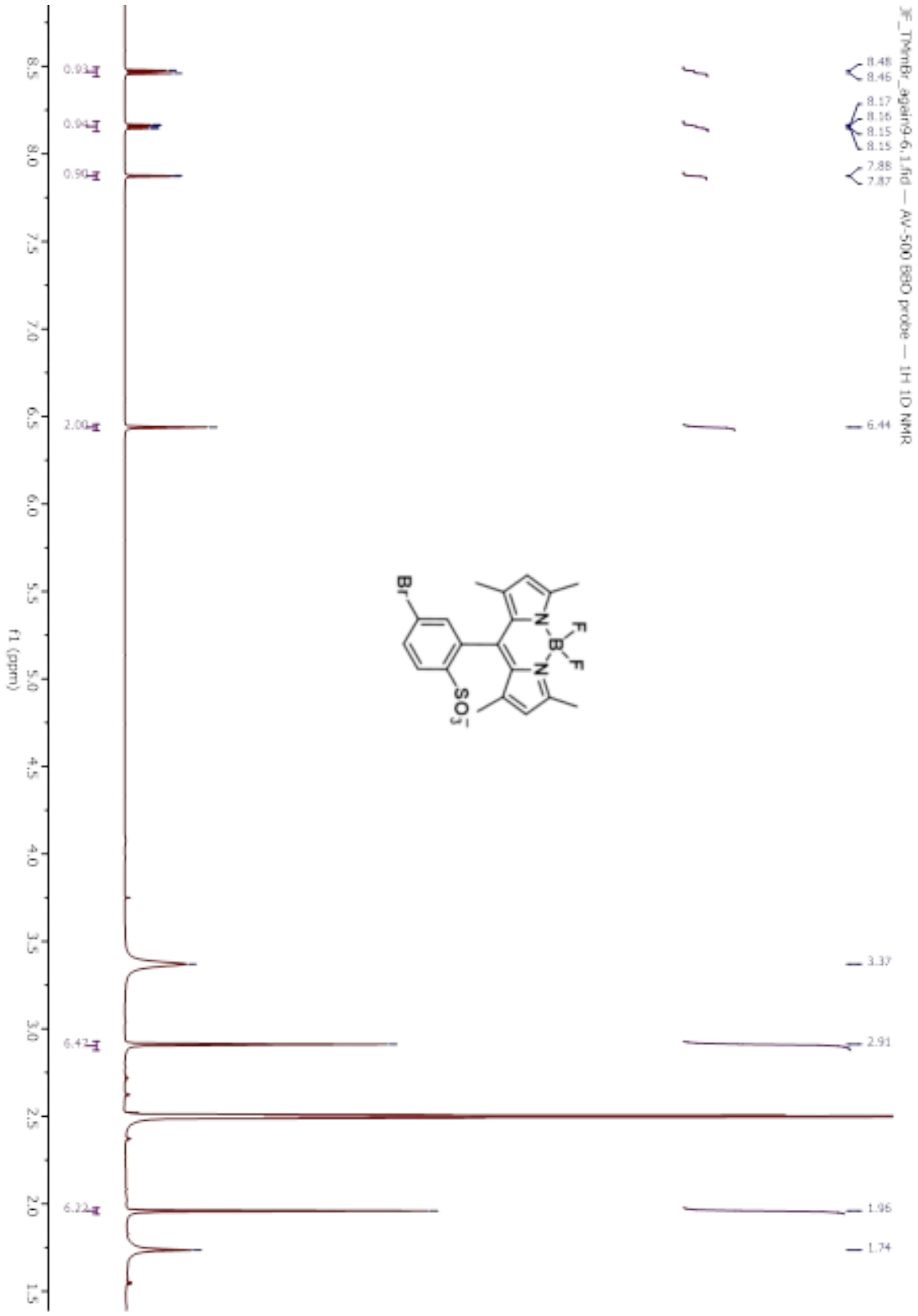
JF_TMmBr_again9-6.1.fid — AV-500 BBO probe — 1H 1D NMR
8.48
8.46
8.17
8.16
8.15
8.15
7.88
7.87
6.44
3.37
2.91
1.96
1.74
0.93
0.94
0.90
2.00
6.47
6.22
f1 (ppm)
Br
N
B
F
F
SO3−

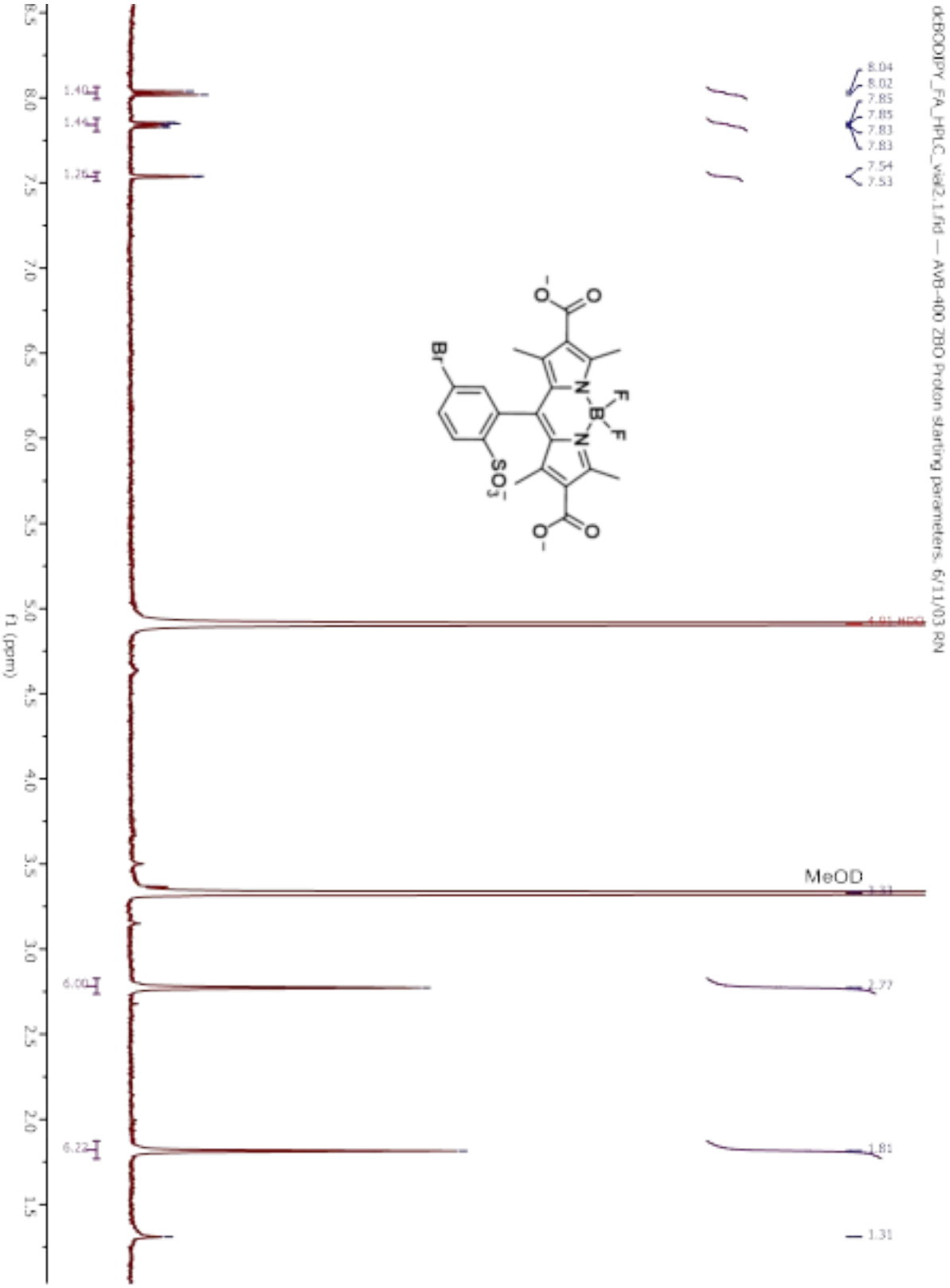
dcBODIPY_FA_HPLC_vial2.1.fid — AVB-400 ZBO Proton starting parameters. 6/11/03 RN
8.04
8.02
7.85
7.85
7.83
7.83
7.54
7.53
MeOD
1.40
1.46
1.26
6.00
6.22
2.77
1.81
1.31
f1 (ppm)

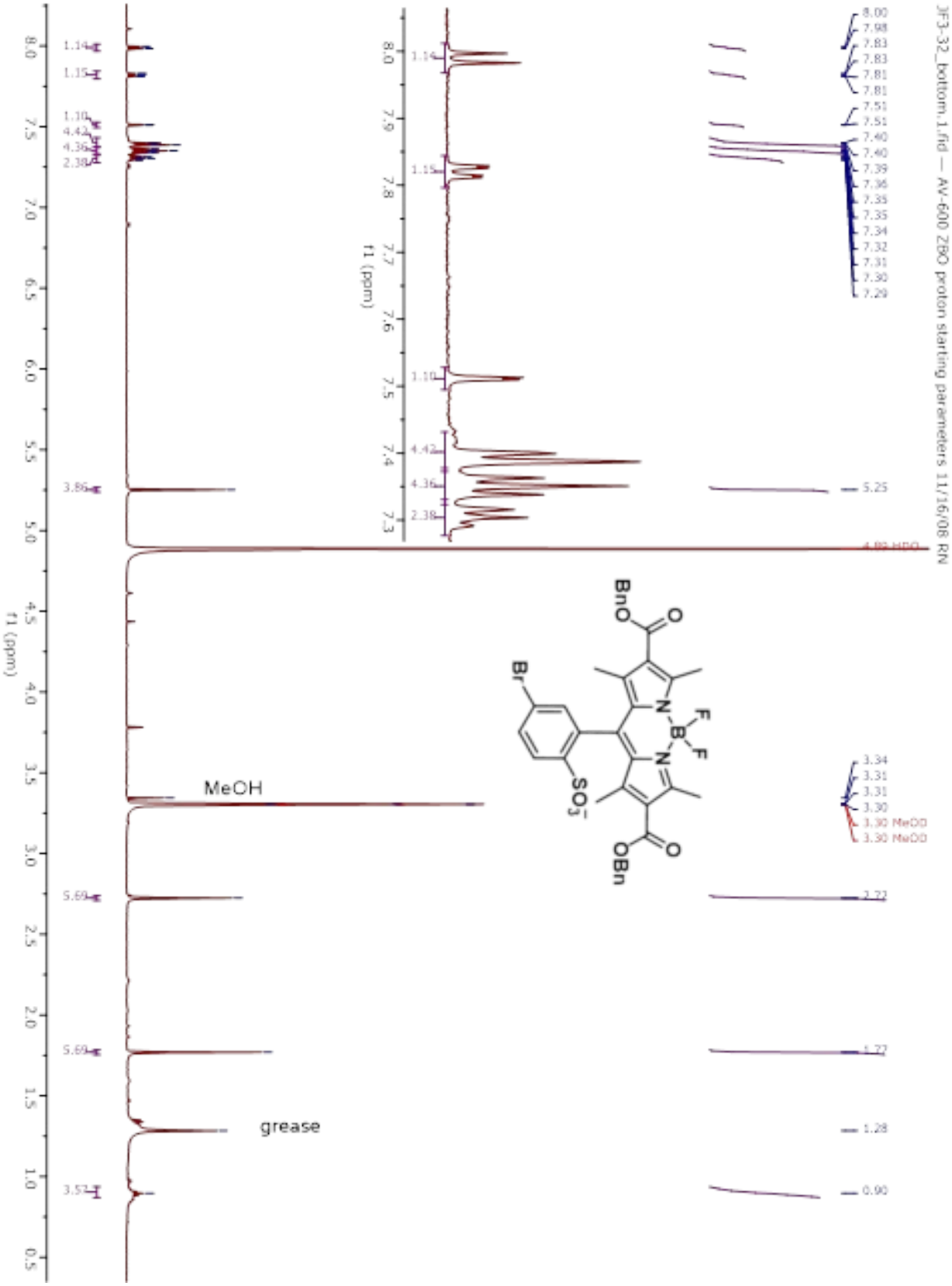
JF3-32_bottom.1.fid — AV-600 ZBO proton starting parameters 11/16/06 RN
f1 (ppm)
MeOH
grease
BnO
O
Br
F
B
N
SO3−
OBn
8.00
7.98
7.83
7.83
7.81
7.81
7.51
7.51
7.40
7.40
7.39
7.36
7.35
7.35
7.34
7.32
7.31
7.30
7.29
5.25
3.34
3.31
3.31
3.30
3.30 MeOD
3.30 MeOD
2.22
1.27
1.28
0.90

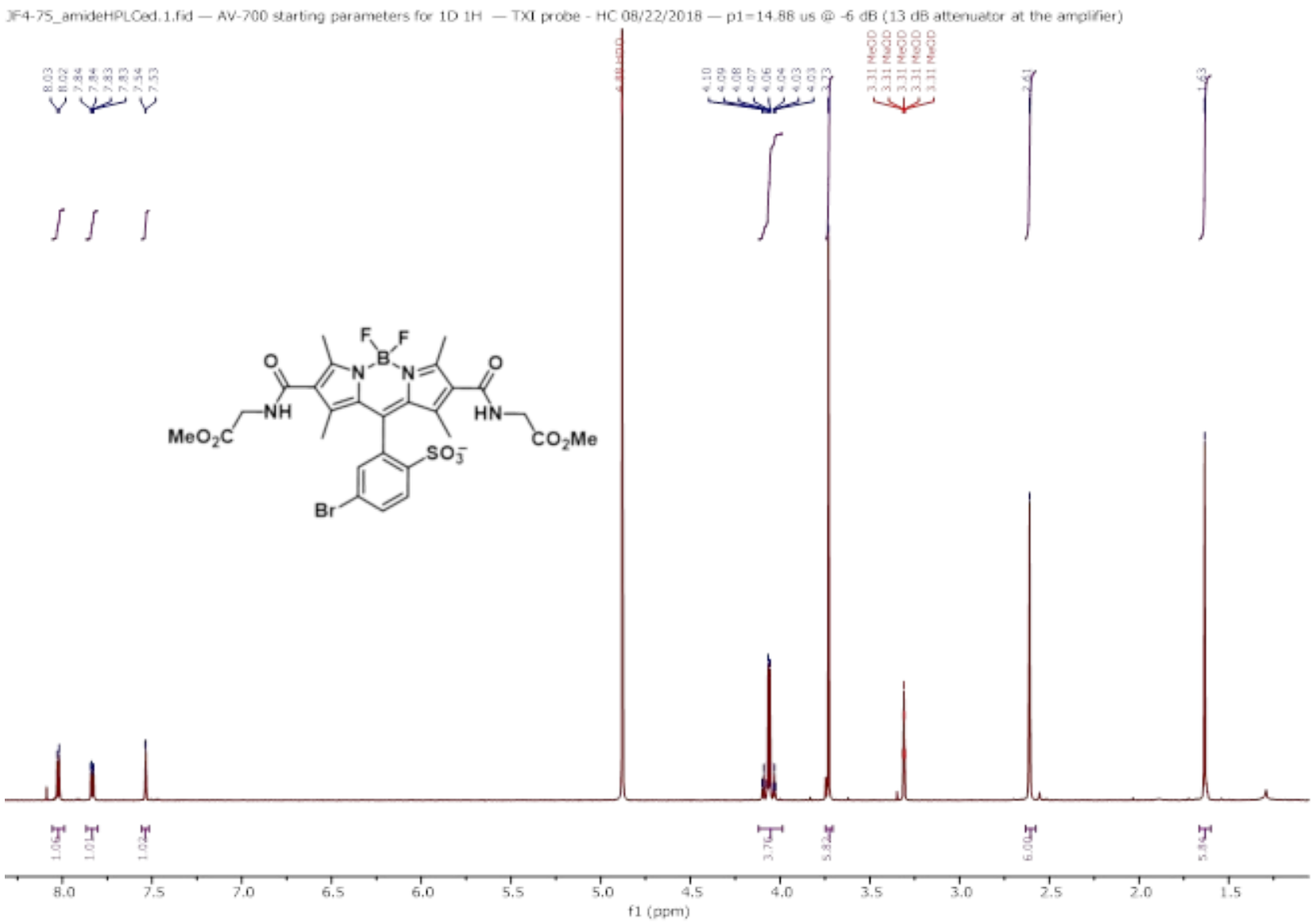
JF4-75_amideHPLCed.1.fid — AV-700 starting parameters for 1D 1H — TXI probe - HC 08/22/2018 — p1=14.88 us @ -6 dB (13 dB attenuator at the amplifier)
8.03
8.02
7.84
7.84
7.83
7.83
7.54
7.53
4.88 HDO
4.10
4.09
4.08
4.07
4.06
4.04
4.03
4.03
3.73
3.31 MeOD
3.31 MeOD
3.31 MeOD
3.31 MeOD
3.31 MeOD
2.41
1.63
F
F
B
N
N
O
O
NH
HN
MeO2C
CO2Me
SO3−
Br
1.06
1.01
1.02
3.76
5.82
6.00
5.86
8.0
7.5
7.0
6.5
6.0
5.5
5.0
4.5
4.0
3.5
3.0
2.5
2.0
1.5
f1 (ppm)

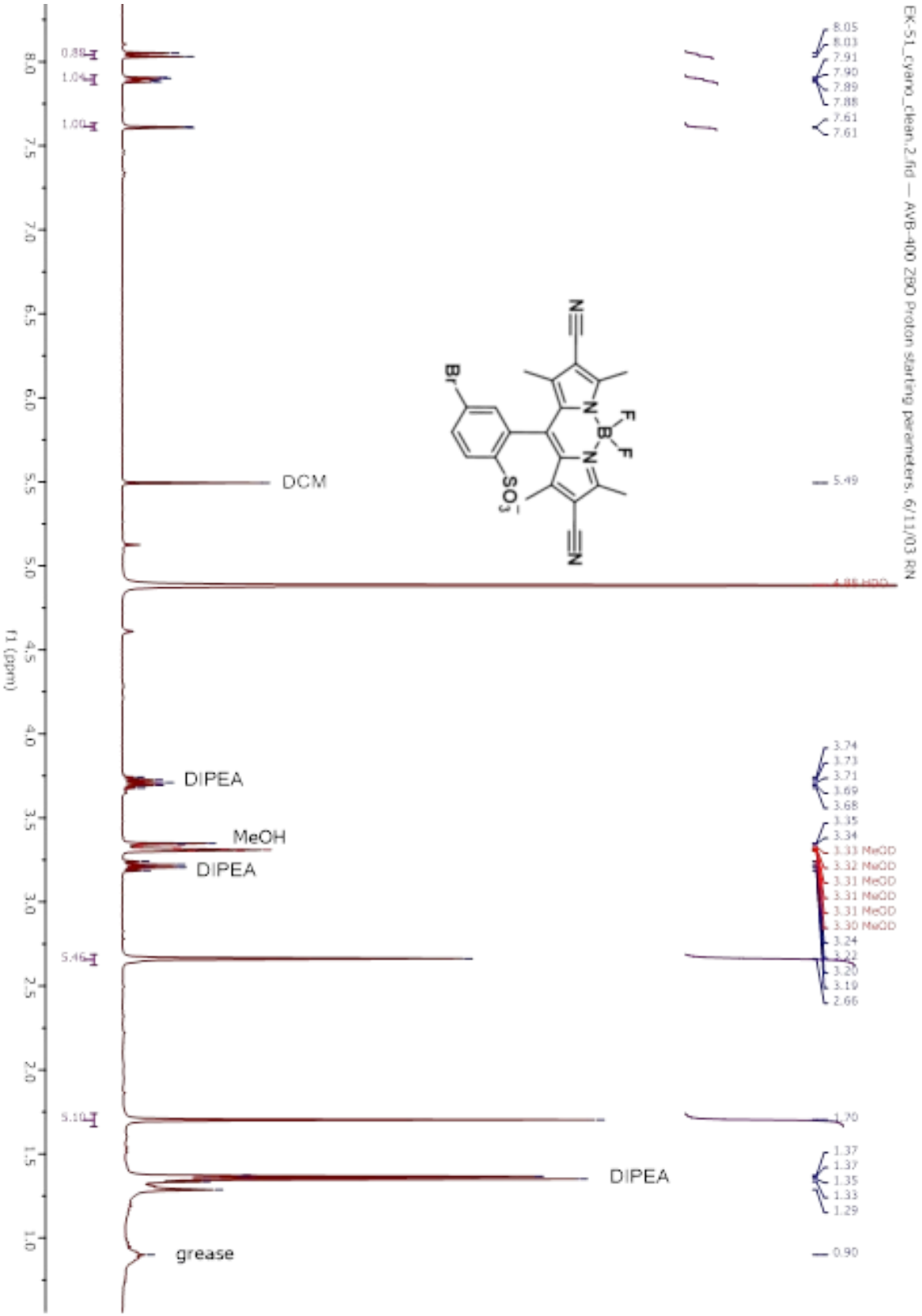
EK-51_cyano_clean.2.fid — AVB-400 ZBO Proton starting parameters, 6/11/03 RN
f1 (ppm)
DCM
DIPEA
MeOH
DIPEA
DIPEA
grease
Br
F
B
F
N
N
SO3−
CN
CN

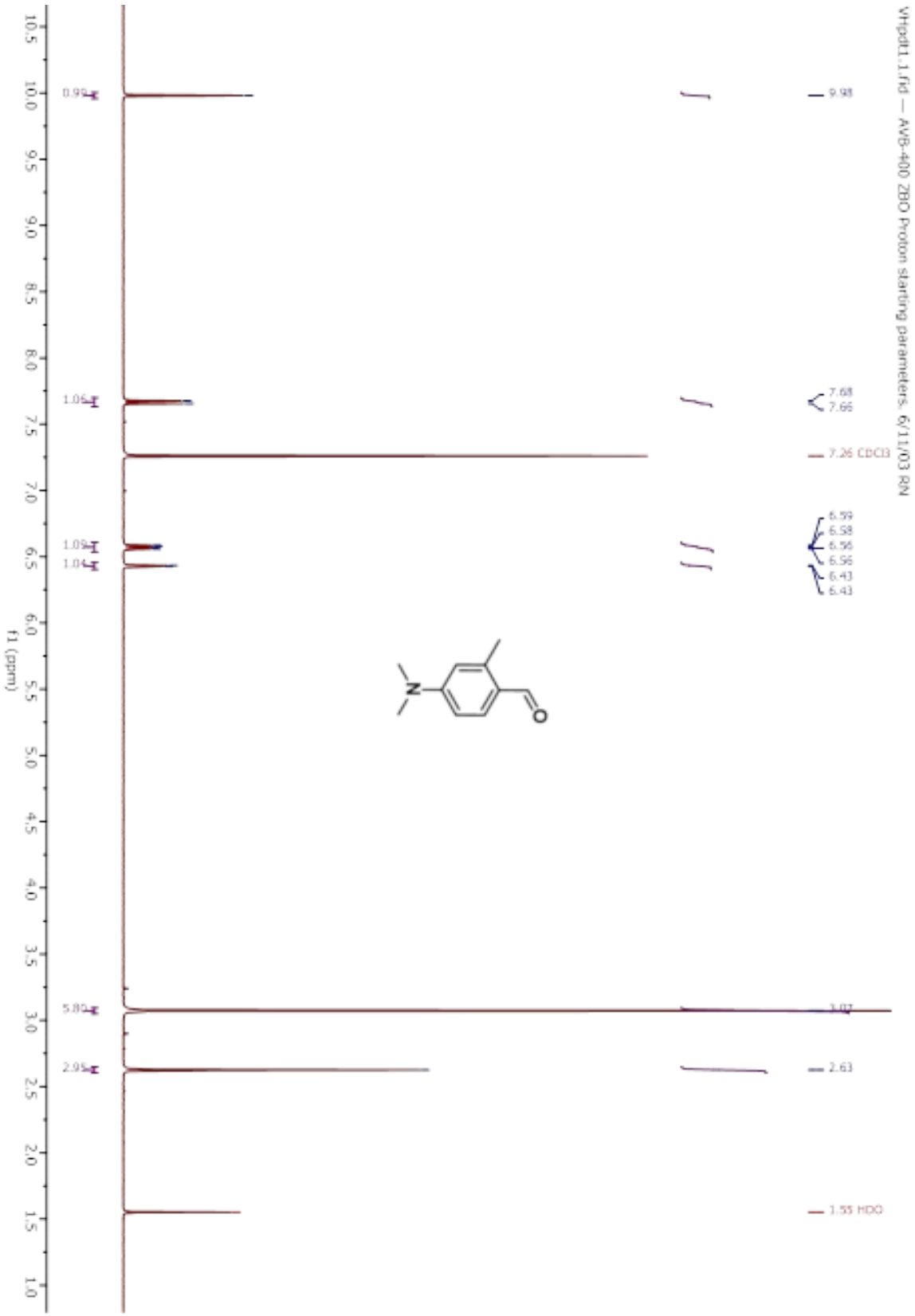
VHpdt1_1.fid — AVB-400 ZBO Proton starting parameters. 6/11/03 RN
9.98
7.68
7.66
7.26 CDCl3
6.59
6.58
6.56
6.56
6.43
6.43
3.07
2.63
1.55 H2O
0.99
1.06
1.09
1.04
5.80
2.95
f1 (ppm)

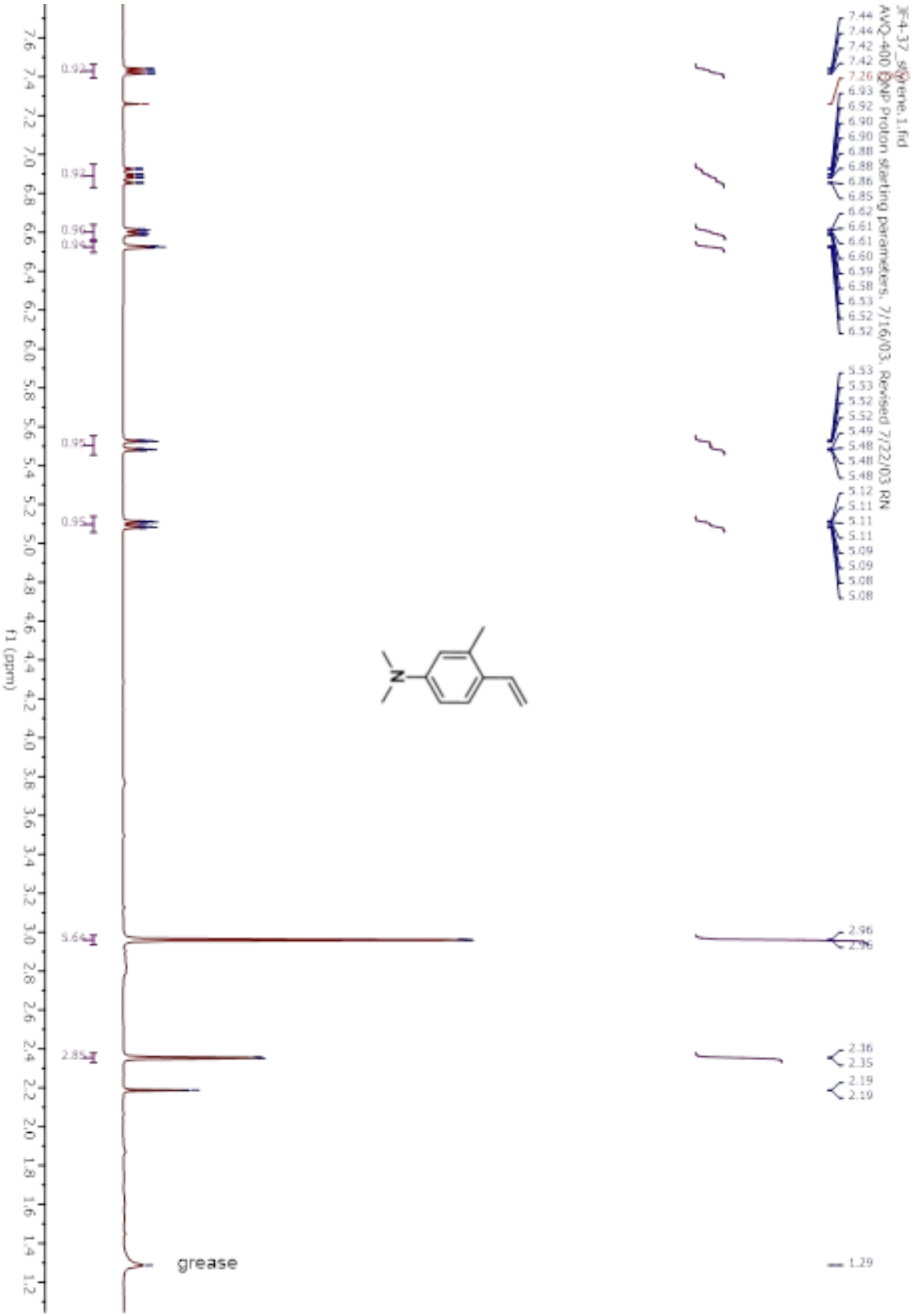
JF4-37_styrene_1.fid
AVQ-400 BNP Proton starting parameters, 7/16/03, Revised 7/22/03 RN
7.44
7.44
7.42
7.42
7.26
6.93
6.92
6.90
6.90
6.88
6.88
6.86
6.85
6.62
6.61
6.61
6.60
6.59
6.58
6.53
6.52
6.52
5.53
5.53
5.52
5.52
5.49
5.48
5.48
5.48
5.12
5.11
5.11
5.11
5.09
5.09
5.08
5.08
2.96
2.96
2.36
2.35
2.19
2.19
1.29
0.92
0.92
0.96
0.94
0.95
0.95
5.64
2.85
grease
f1 (ppm)

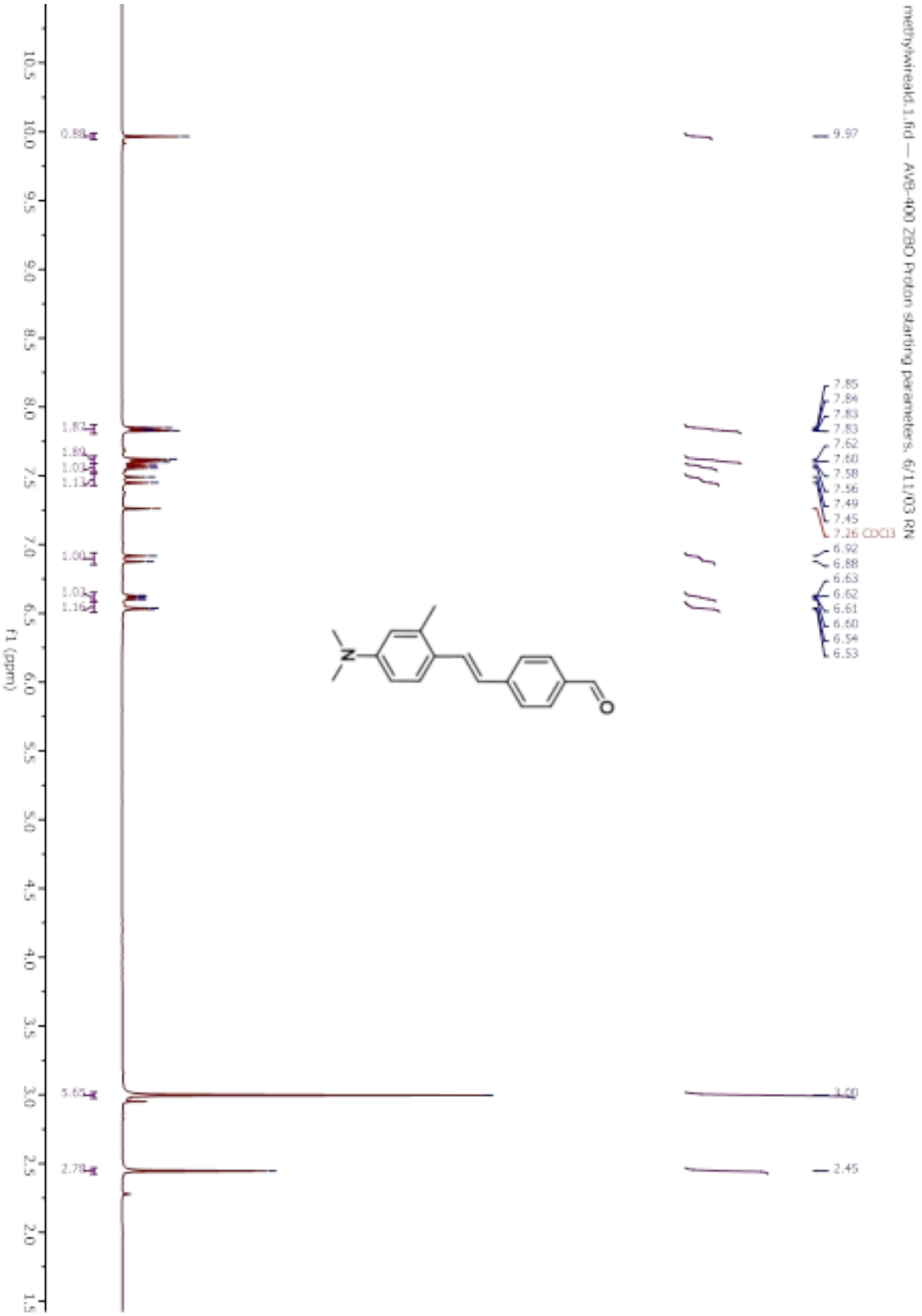
methylvinealdi.1.fid — AVB-400 ZBO Proton starting parameters, 6/11/03 RN
9.97
7.85
7.84
7.83
7.83
7.62
7.60
7.58
7.56
7.49
7.45
7.26 CDCl3
6.92
6.88
6.63
6.62
6.61
6.60
6.54
6.53
3.00
2.45
f1 (ppm)

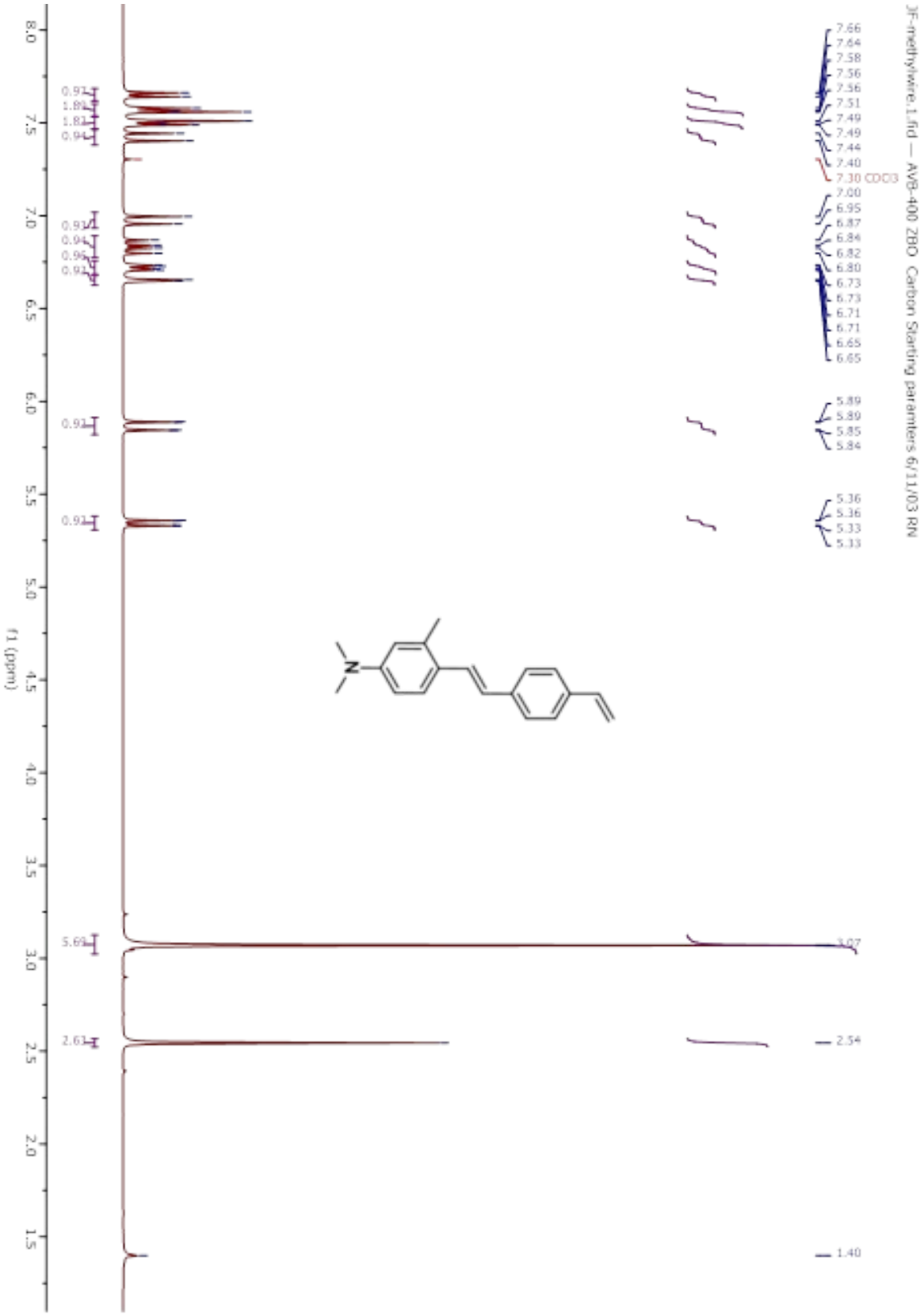
JF-methylwire.1.fid — AVB-400 ZBO Carbon Starting parameters 6/11/03 RN
7.66
7.64
7.58
7.56
7.56
7.51
7.49
7.49
7.44
7.40
7.30 CDCl3
7.00
6.95
6.87
6.84
6.82
6.80
6.73
6.73
6.71
6.71
6.65
6.65
5.89
5.89
5.85
5.84
5.36
5.36
5.33
5.33
3.07
2.54
1.40
f1 (ppm)

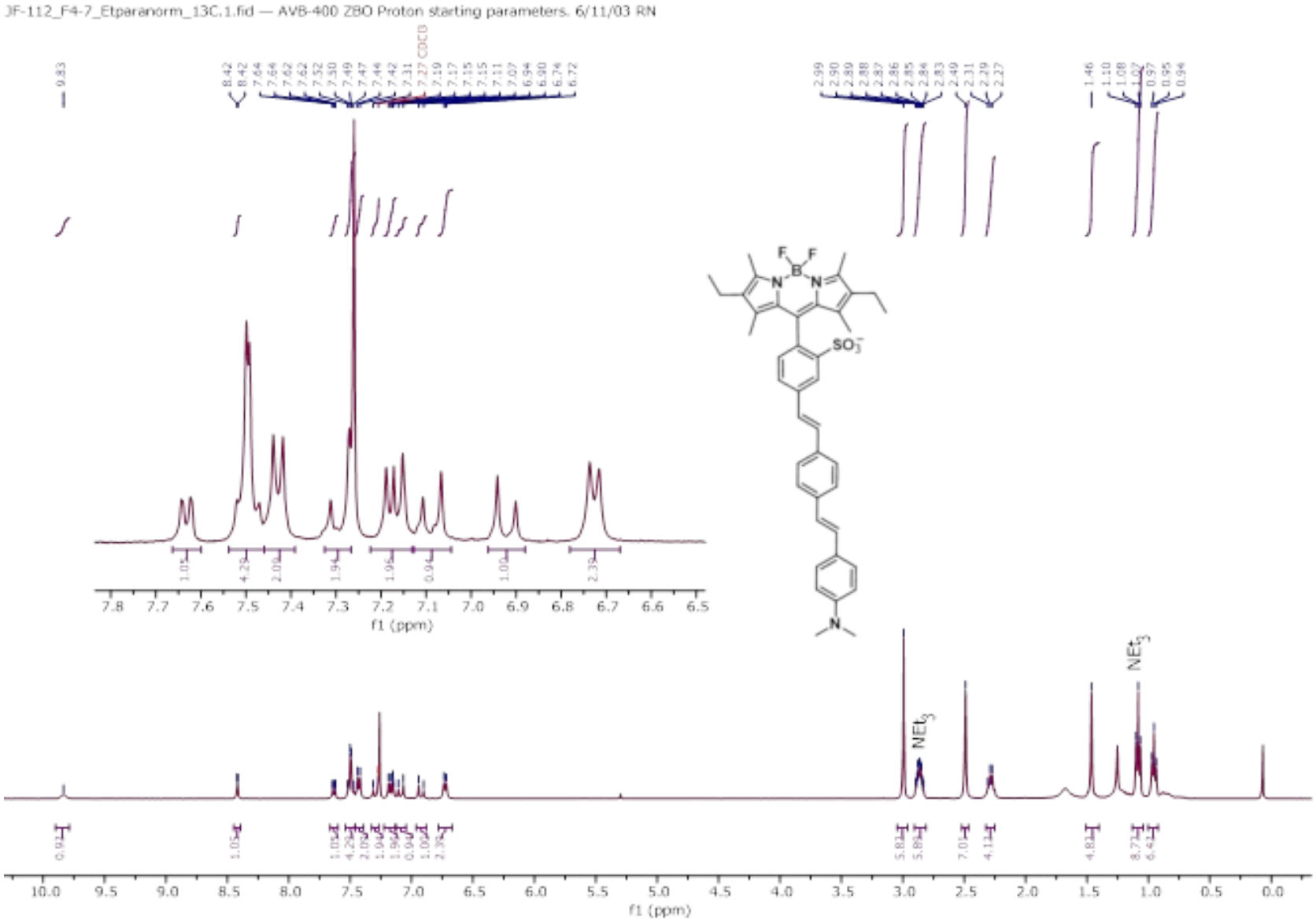
JF-112_F4-7_Etparanorm_13C.1.fid — AVB-400 ZBO Proton starting parameters. 6/11/03 RN
CDCl3
NEt3
NEt3
f1 (ppm)
f1 (ppm)

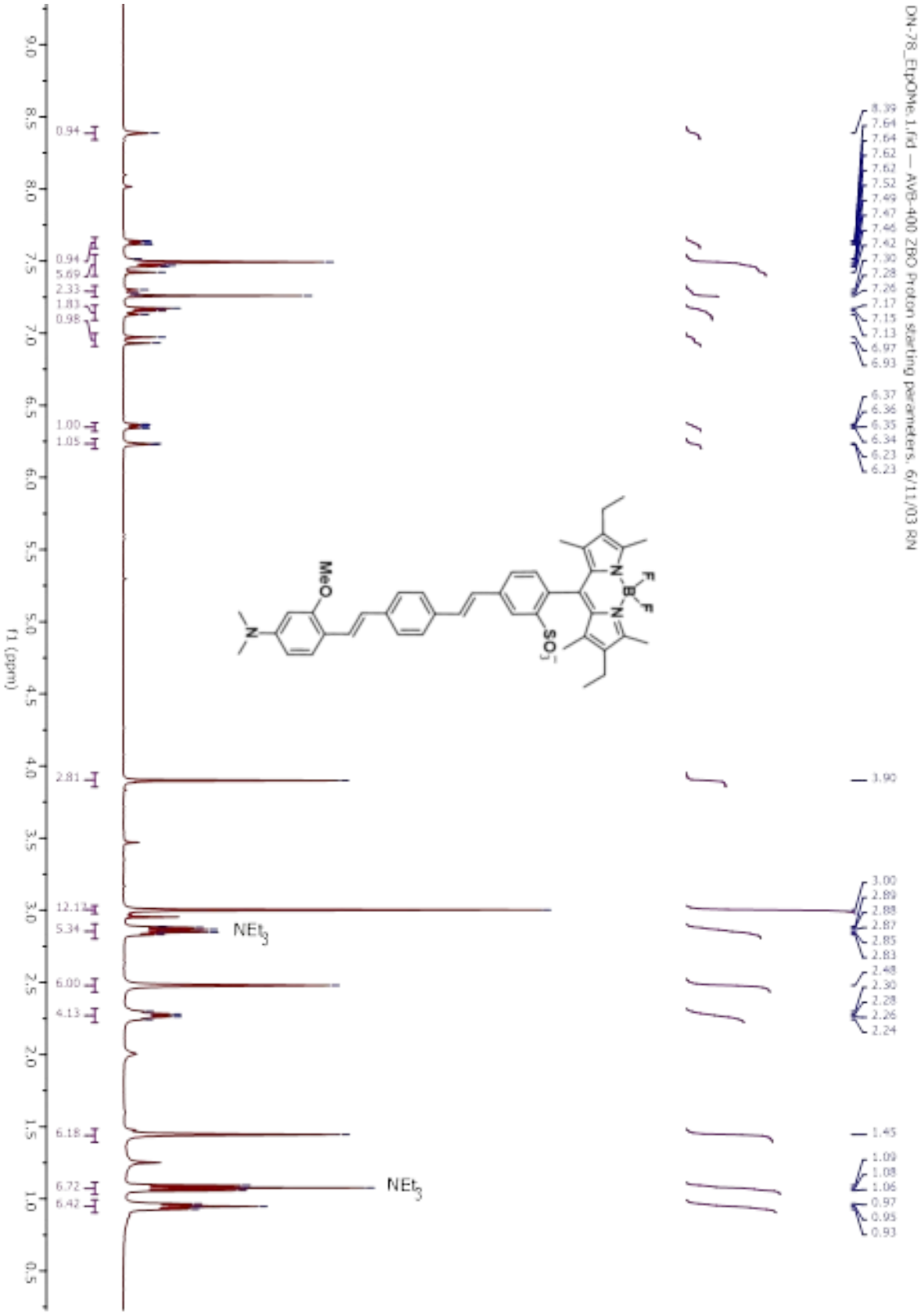
DN-78_EtpOMe.1.fid — AV8-400 ZBO Proton starting parameters. 6/11/03 RN
f1 (ppm)
NEt3
NEt3
MeO
SO3-
F
F
B
N
N

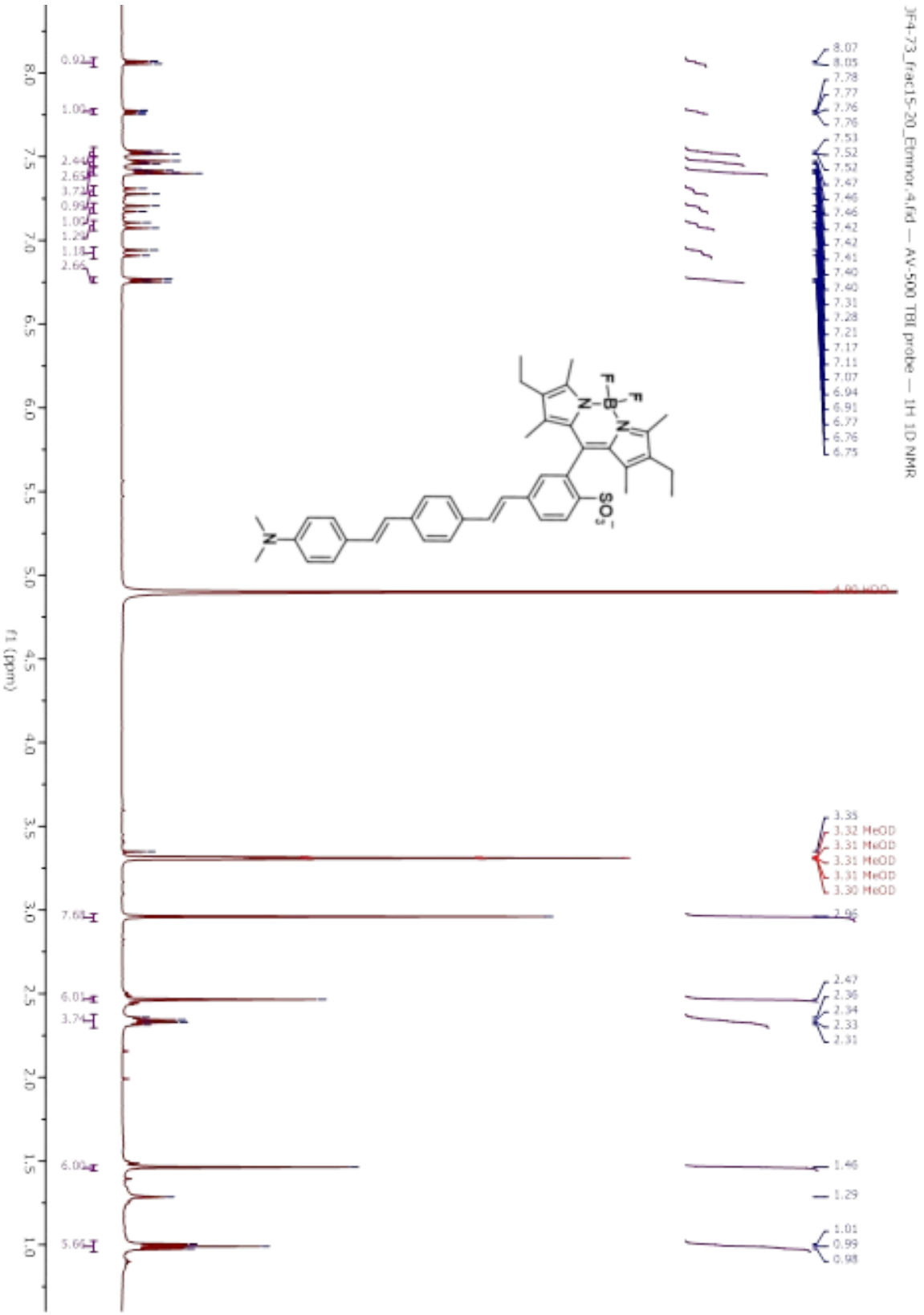
JF4-73_frac15-20_Etmnor.4.fid — AV-500 TBI probe — 1H 1D NMR
f1 (ppm)
8.07
8.05
7.78
7.77
7.76
7.76
7.53
7.52
7.52
7.47
7.46
7.46
7.42
7.42
7.41
7.40
7.40
7.31
7.28
7.21
7.17
7.11
7.07
6.94
6.91
6.77
6.76
6.75
4.80 HOD
3.35
3.32 MeOD
3.31 MeOD
3.31 MeOD
3.31 MeOD
3.30 MeOD
2.95
2.47
2.36
2.34
2.33
2.31
1.46
1.29
1.01
0.99
0.98

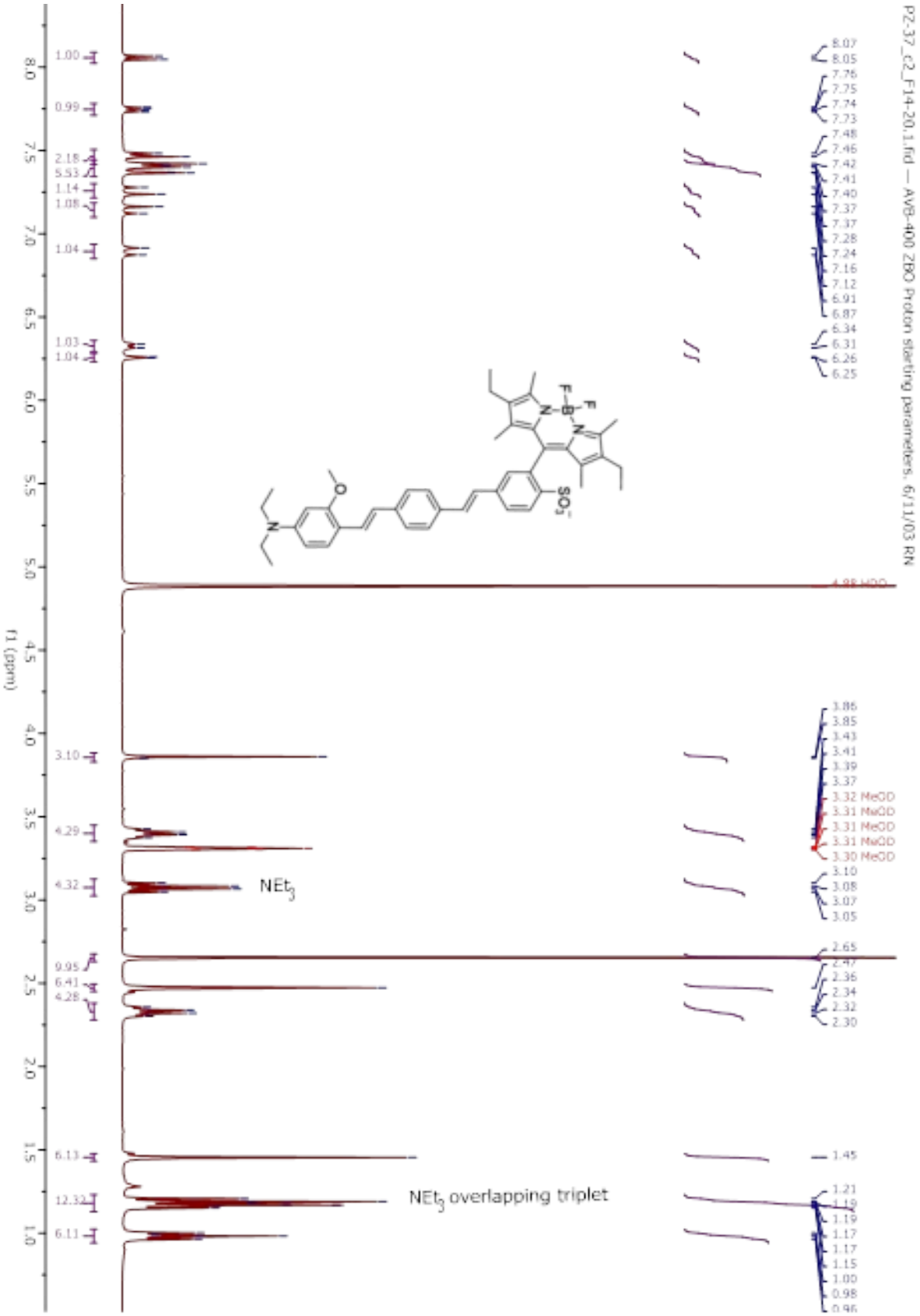
PZ-37_c2_F14-20.1.fid — AVB-400 ZBO Proton starting parameters. 6/11/03 RN
f1 (ppm)
NEt3
NEt3 overlapping triplet
MeOD

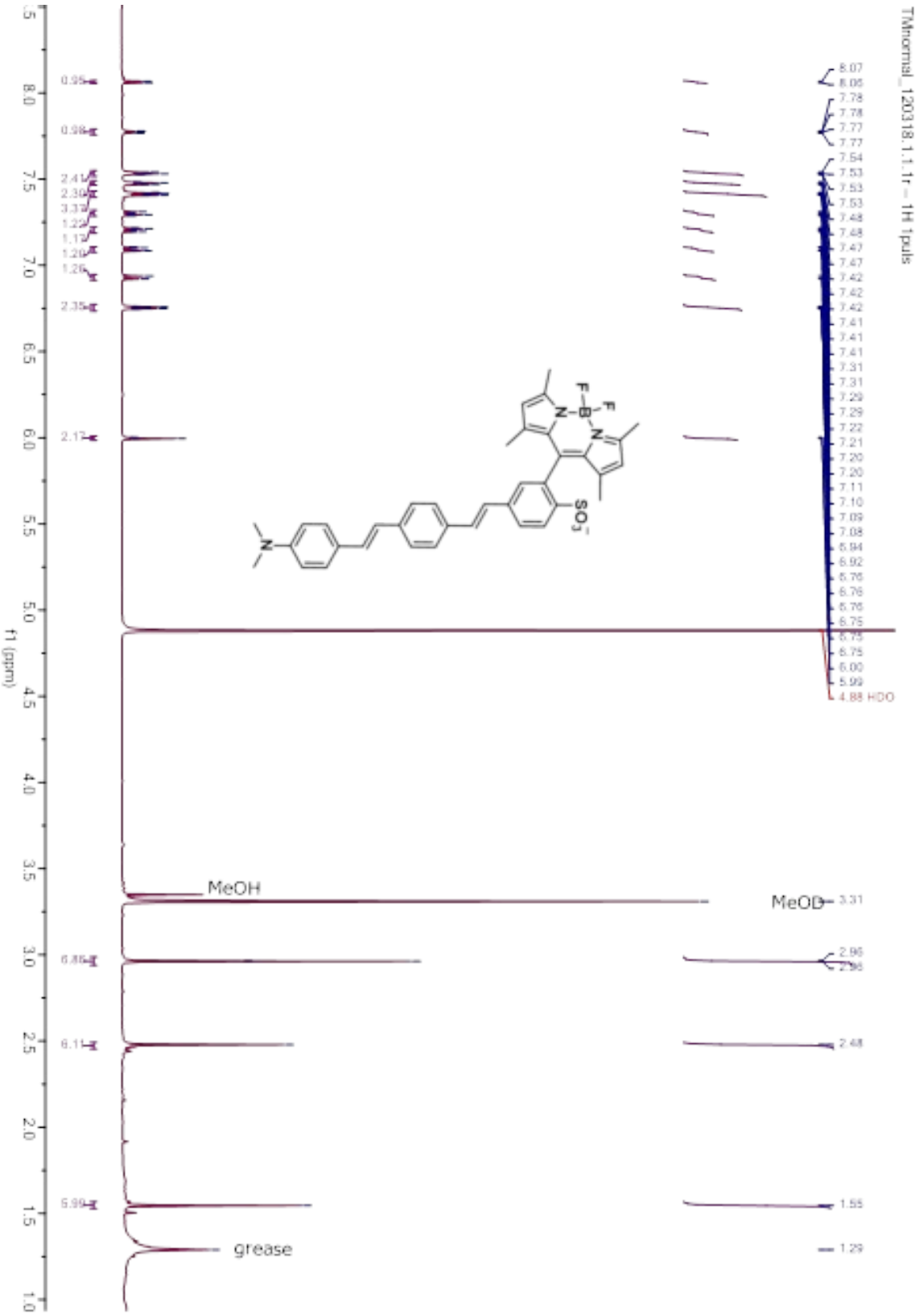
TMnormal_120318.1.1.1r – 1H 1puls
f1 (ppm)
MeOH
MeOD
grease
4.88 HDO

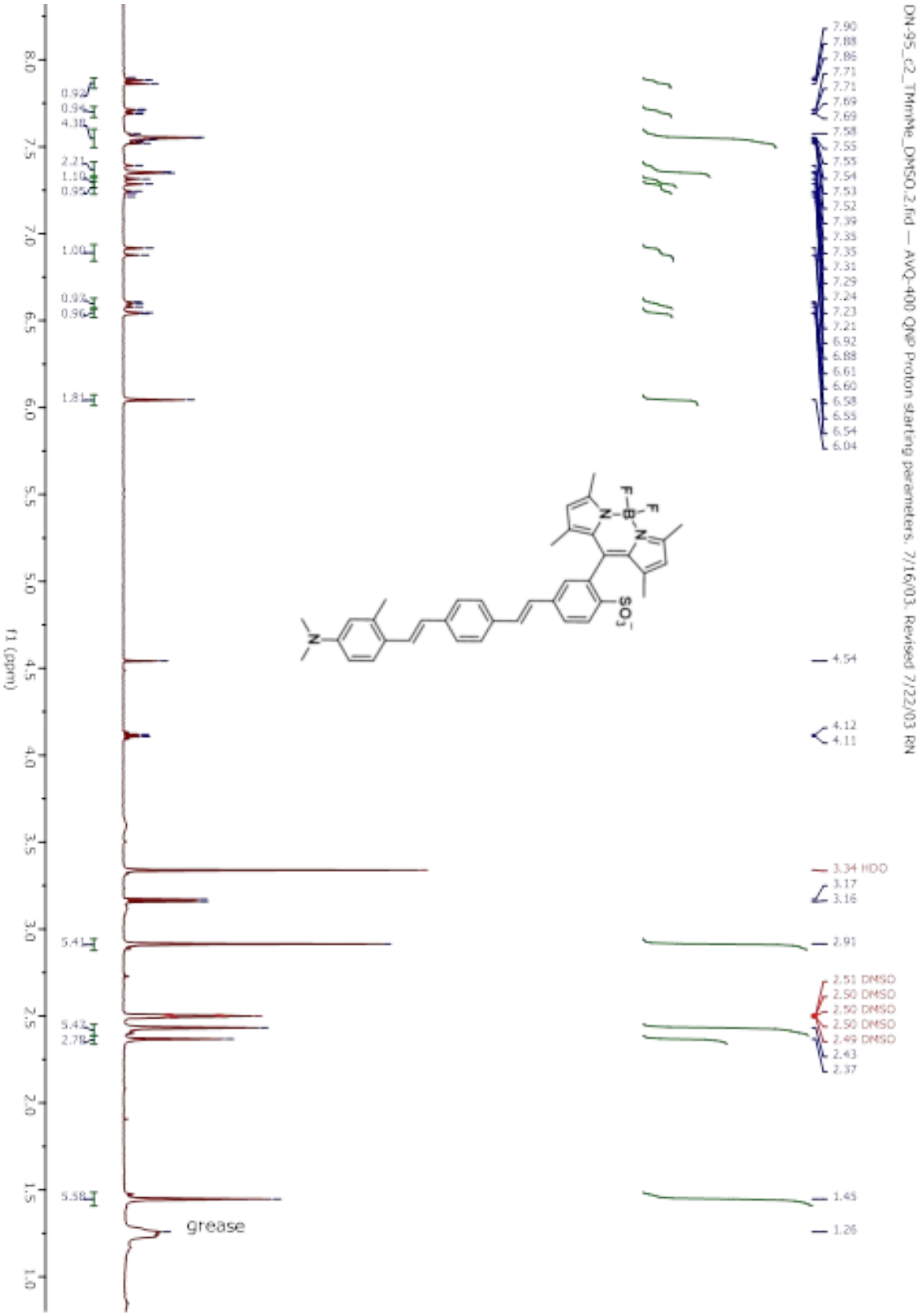
DN-95_c2_TMnMe_DMSO.2.fid — AVQ-400 QNP Proton starting parameters: 7/16/03. Revised 7/22/03 RN
f1 (ppm)
grease
3.34 HDO
2.51 DMSO
2.50 DMSO
2.50 DMSO
2.50 DMSO
2.49 DMSO

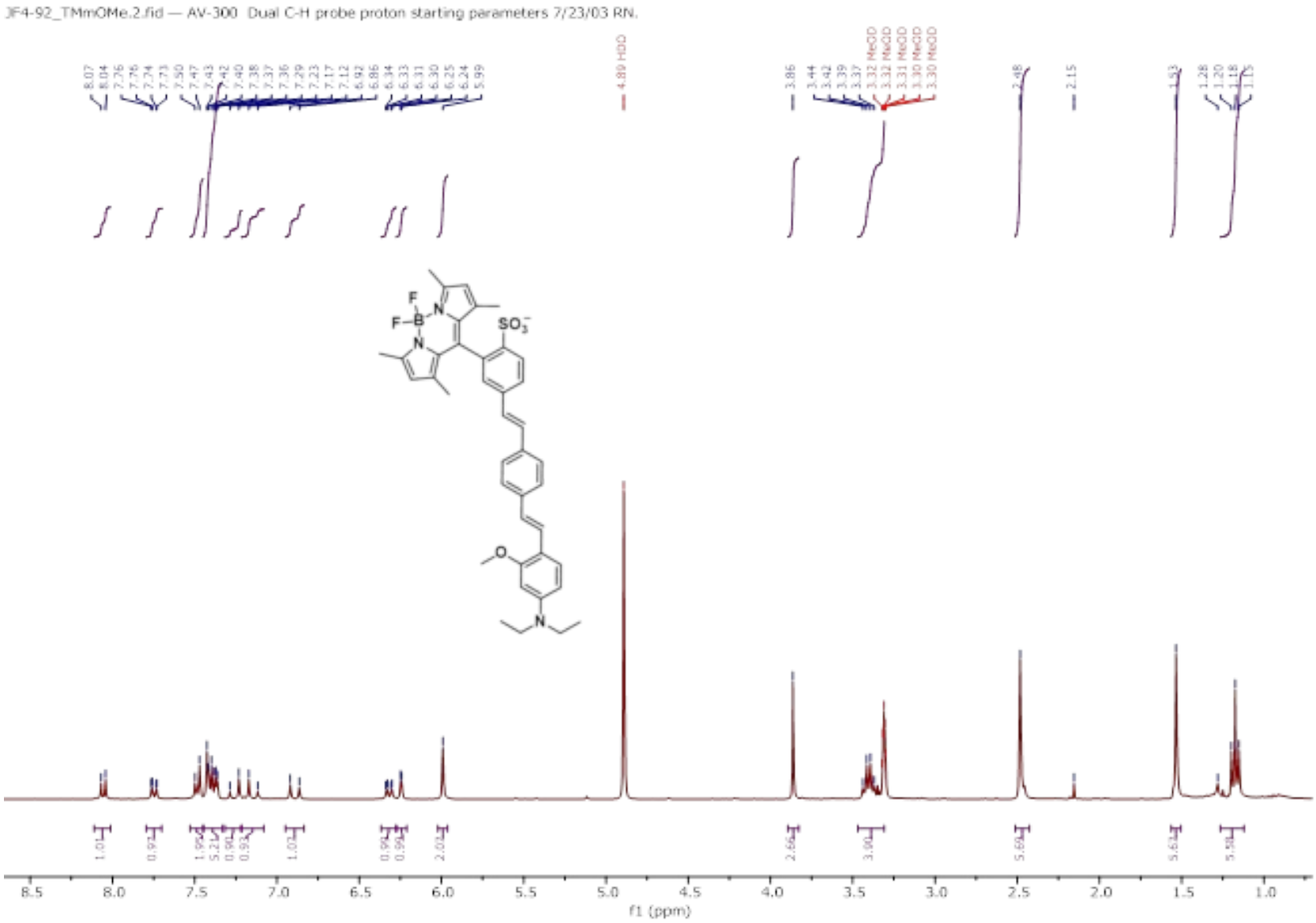
JF4-92_TMmOMe.2.fid — AV-300 Dual C-H probe proton starting parameters 7/23/03 RN.
8.07
8.04
7.76
7.76
7.74
7.73
7.50
7.47
7.43
7.42
7.40
7.38
7.37
7.36
7.29
7.23
7.17
7.12
6.92
6.86
6.34
6.33
6.31
6.30
6.25
6.24
5.99
4.89 HDO
3.86
3.44
3.42
3.39
3.37
3.32 MeOD
3.32 MeOD
3.31 MeOD
3.30 MeOD
3.30 MeOD
2.48
2.15
1.53
1.28
1.20
1.18
1.15
F
F–B
N
N
SO3−
O
N
1.01
0.97
1.95
5.21
0.94
0.93
1.02
0.95
0.95
2.01
2.66
3.90
5.69
5.63
5.58
8.5
8.0
7.5
7.0
6.5
6.0
5.5
5.0
4.5
4.0
3.5
3.0
2.5
2.0
1.5
1.0
f1 (ppm)

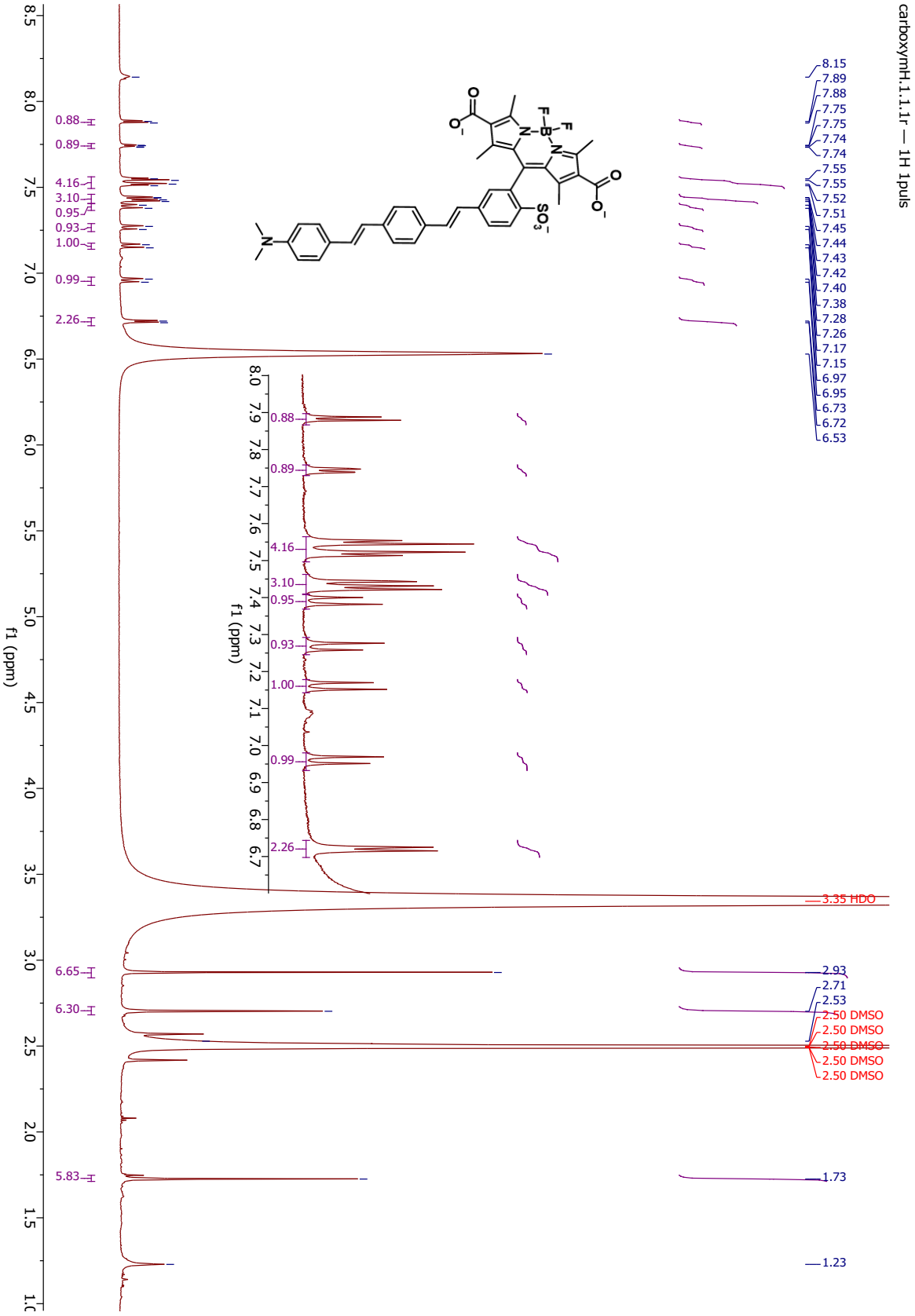
carboxymH.1.1.1r — 1H 1puls
f1 (ppm)
0.88
0.89
4.16
3.10
0.95
0.93
1.00
0.99
2.26
6.65
6.30
5.83
8.15
7.89
7.88
7.75
7.75
7.74
7.74
7.55
7.55
7.52
7.51
7.45
7.44
7.43
7.42
7.40
7.38
7.28
7.26
7.17
7.15
6.97
6.95
6.73
6.72
6.53
3.35 HDO
2.93
2.71
2.53
2.50 DMSO
2.50 DMSO
2.50 DMSO
2.50 DMSO
2.50 DMSO
1.73
1.23

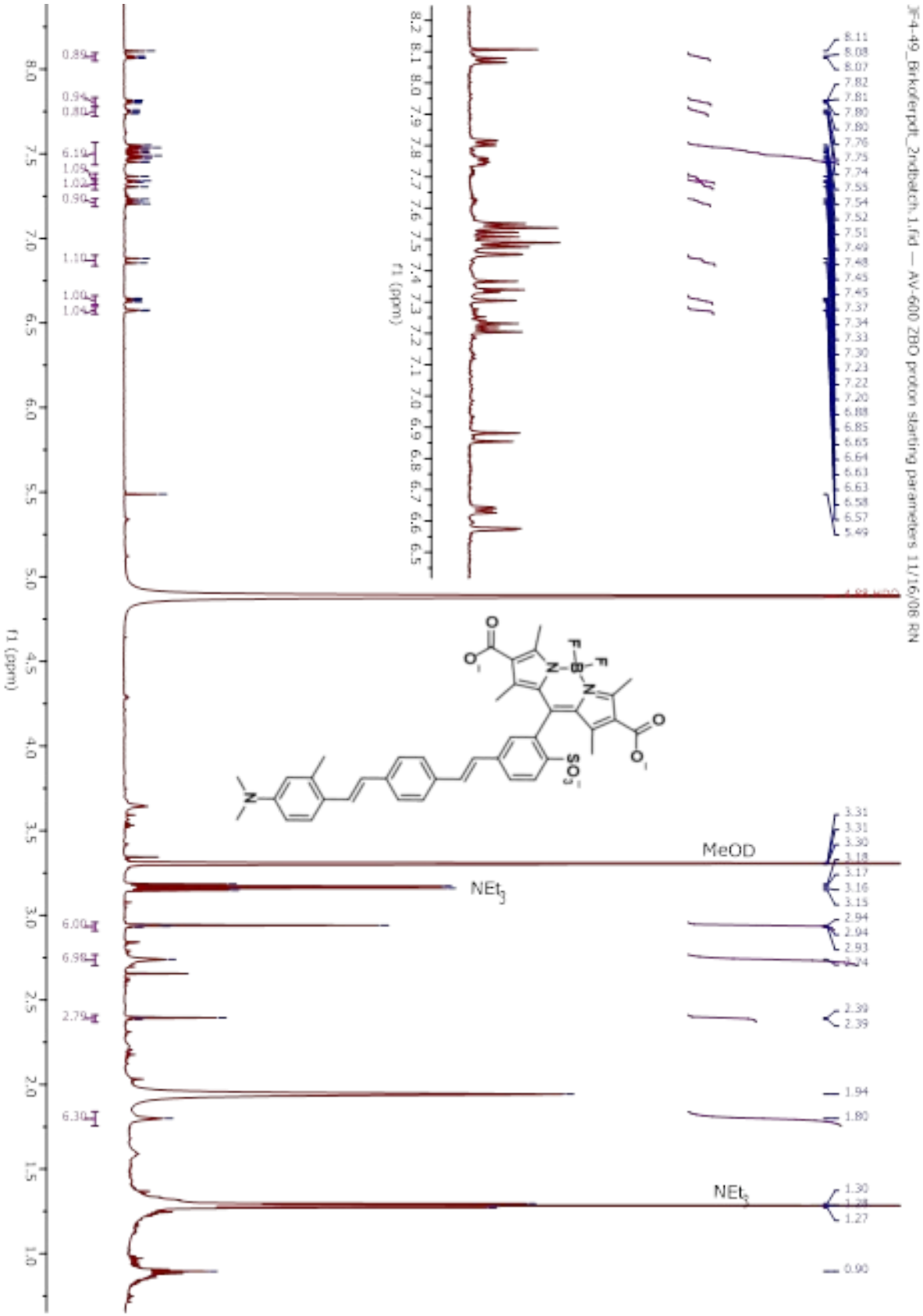
JF4-49_Berkoferpdt_2ndbatch.1.fid — AV-600 ZBO proton starting parameters 11/16/06 RN
f1 (ppm)
MeOD
NEt3
NEt3

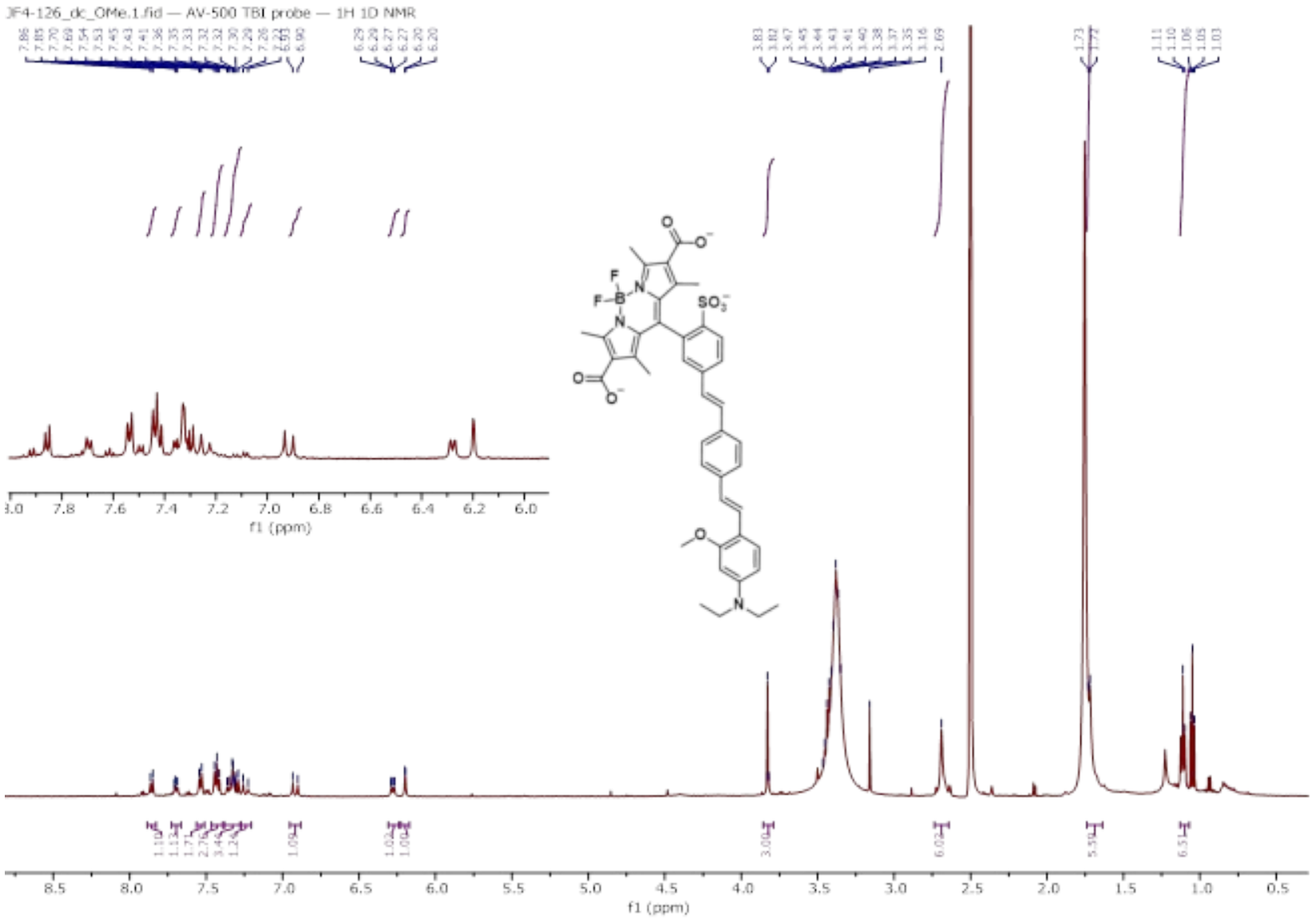
JF4-126_dc_OMe.1.fid — AV-500 TBI probe — 1H 1D NMR
f1 (ppm)

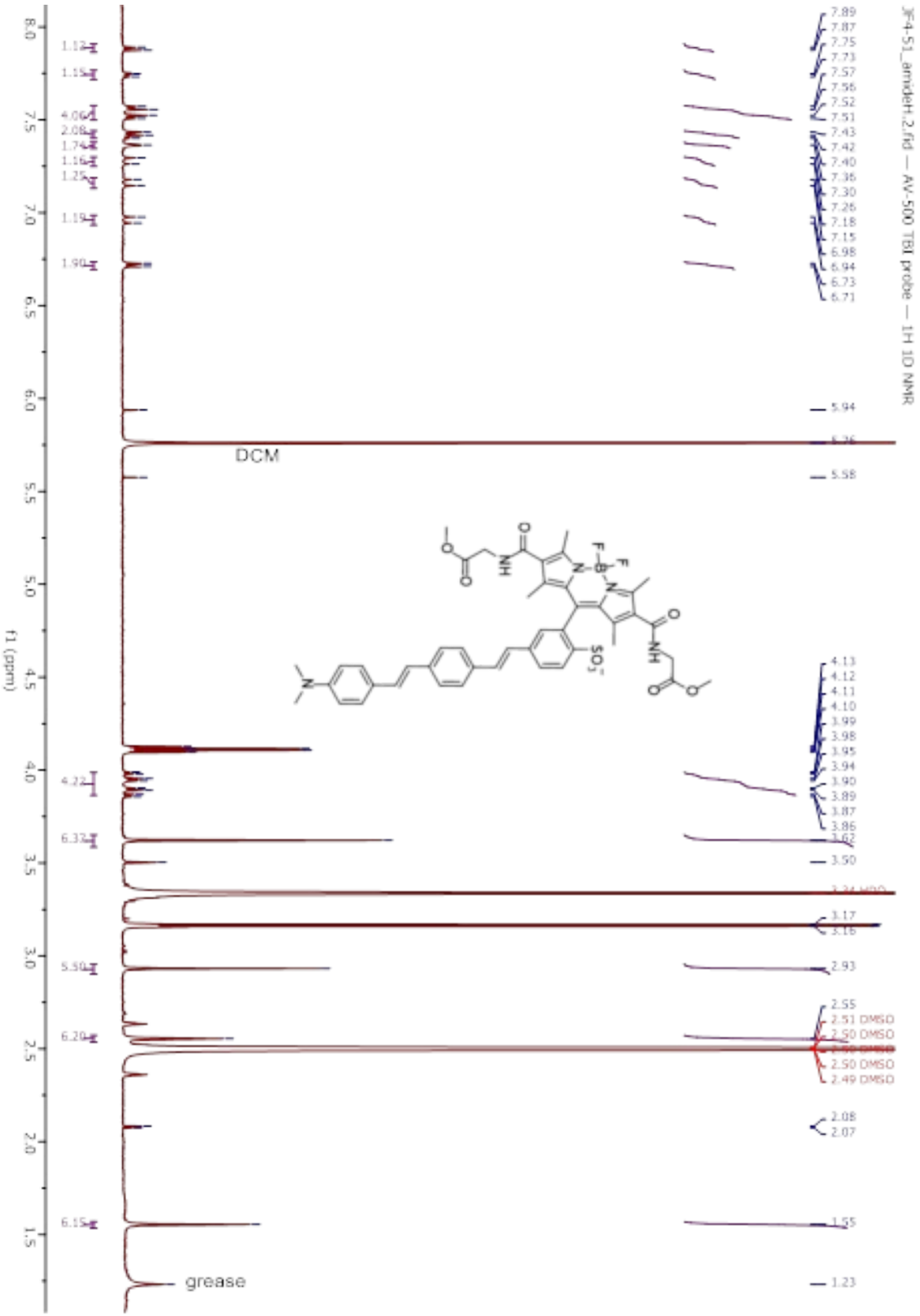
JF4-51_amideH.2.fid — AV-500 TBI probe — 1H 1D NMR
f1 (ppm)
DCM
grease
DMSO

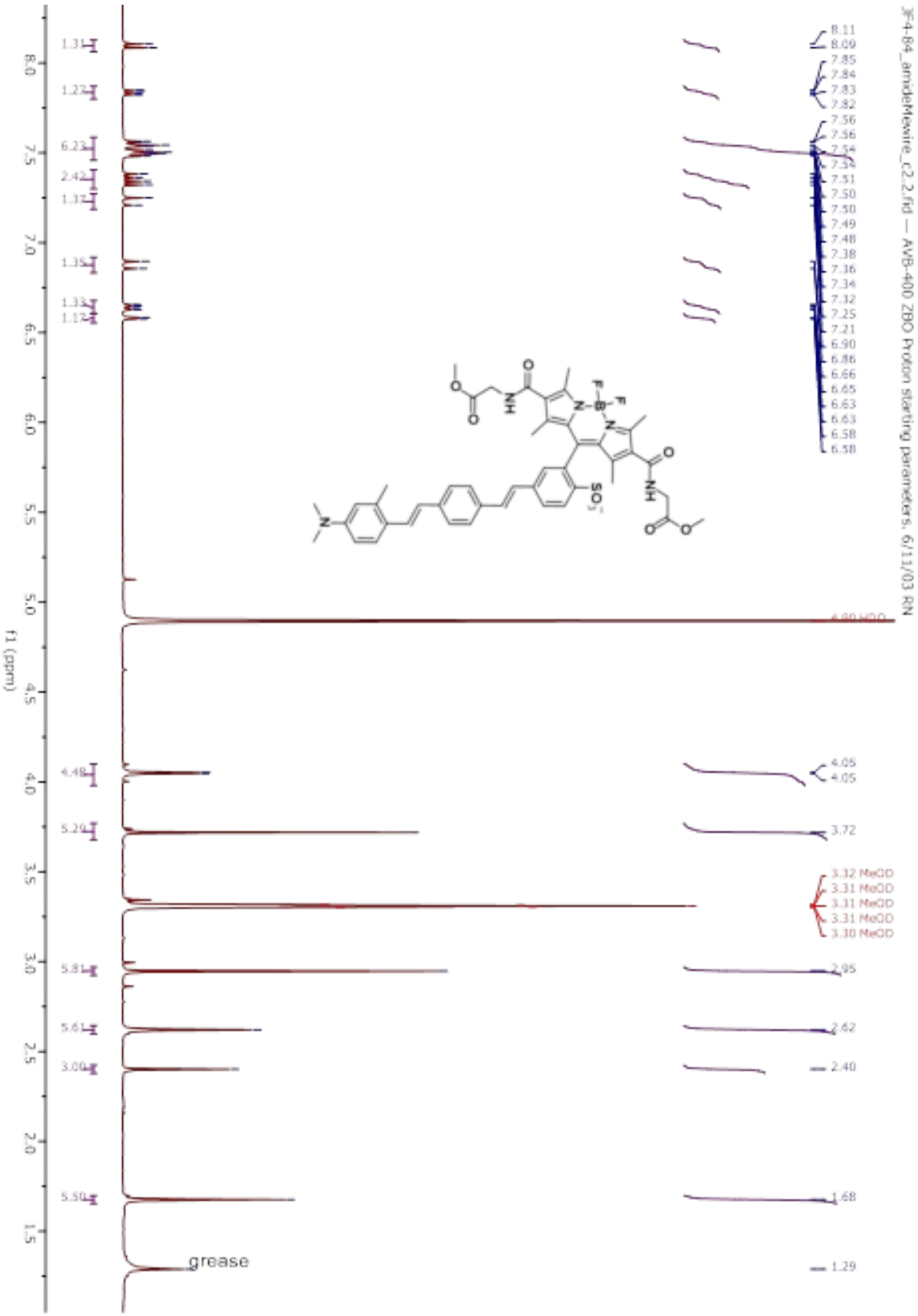
JF4-84_amideMexire_c2.2.fid — AVB-400 ZBO Proton starting parameters 6/11/03 RN
f1 (ppm)
grease

References

(1) Perkin, W. H. Producing a New Coloring Matter for Dyeing with a Lilac or Purple Color Stuffs of Silk, Cotton, Wool, or Other Materials. *British Patent* **1856**, *No. 1984*.

(2) Cliffe, W. H. In the Footsteps of Perkin. *J. Soc. Dye. Colour.* **1956**, *72* (12), 563–566.

(3) Welham, R. D. The Early History of the Synthetic Dye Industry II - The Industrial History (1856-1900). *J. Soc. Dye. Colour.* **1963**, *79* (4), 146–152.

(4) Baeyer, A. Ueber Eine Neue Klasse von Farbstoffen. *Berichte der Dtsch. Chem. Gesellschaft* **1871**, *4* (2), 555–558.

(5) Ceresole, M. Verfahren Zur Darstellung von Farbstoffen Aus Der Gruppe Des Meta-Amidophenolphtaleins. *German Patent* **1887**, *No. 44002*.

(6) Sandmeyer, T. Red Dye. *US Patent* **1896**, *No. US573299A*.

(7) Tsien, R. Y. Building and Breeding Molecules to Spy on Cells and Tumors. *FEBS Lett.* **2005**, *579* (4), 927–932.

(8) Lavis, L. D.; Raines, R. T. Bright Building Blocks for Chemical Biology. *ACS Chem. Biol* **2014**, *9*, 855–866.

(9) Lavis, L. D. Teaching Old Dyes New Tricks: Biological Probes Built from Fluoresceins and Rhodamines. *Annu. Rev. Biochem.* **2017**, *86* (1), 825–843.

(10) Loudet, A.; Burgess, K. BODIPY Dyes and Their Derivatives: Syntheses and Spectroscopic Properties. *Chem. Rev.* **2007**, *107*, 4891–4932.

(11) Treibs, A.; Kreuzer, F. -H. Difluorboryl-Komplexe von Di- Und Tripyrrylmethenen. *Justus Liebigs Ann. Chem.* **1968**, *718* (1), 208–223.

(12) Ziessel, R.; Ulrich, G.; Harriman, A. The Chemistry of Bodipy: A New El Dorado for Fluorescence Tools. *New J. Chem.* **2007**, *31*, 496–501.

(13) Ulrich, G.; Ziessel, R.; Harriman, A. The Chemistry of Fluorescent Bodipy Dyes: Versatility Unsurpassed. *Angew. Chemie - Int. Ed.* **2008**, *47* (7), 1184–1201.

(14) Boens, N.; Leen, V.; Dehaen, W. Fluorescent Indicators Based on BODIPY. *Chem. Soc. Rev.* **2012**, *41*, 1130–1172.

(15) Kowada, T.; Maeda, H.; Kikuchi, K. BODIPY-Based Probes for the Fluorescence Imaging of Biomolecules in Living Cells. *Chem. Soc. Rev* **2015**, *44*, 4953–4972.

(16) Darst, M. R. T. K. P.; Lee, K. D.; Martin, C. W.; J, P. Electrogenerated Chemiluminescence and Proton-Dependent Switching of Fluorescence: Functionalized Difluoroboradiaza-s-Indacenes. *Angew. Chem. Int. Ed.* **1997**, *12*, 1333–1335.

(17) Urano, Y.; Asanuma, D.; Hama, Y.; Koyama, Y.; Barrett, T.; Kamiya, M.; Nagano, T.; Watanabe, T.; Hasegawa, A.; Choyke, P. L.; et al. Selective Molecular Imaging of Viable Cancer Cells with pH-Activatable Fluorescence Probes. *Nat. Med.* **2009**, *15* (1), 104–109.

(18) Kollmannsberger, M.; Rurack, K.; Resch-Genger, U.; Rettig, W.; Org Daub, J. Design of an Efficient Charge-Transfer Processing Molecular System Containing a Weak Electron Donor: Spectroscopic and Redox Properties and Cation-Induced Fluorescence Enhancement. *Chem. Phys. Lett.* **2000**, *329*, 363–369.

(19) Baruah, M.; Qin, W.; Vallée, R. A. L.; Beljonne, D.; Rohand, T.; Dehaen, W.; Boens, N. A Highly Potassium-Selective Ratiometric Fluorescent Indicator Based on BODIPY Azacrown Ether Excitable with Visible Light. *Org. Lett.* **2005**, *7* (20), 4377–4380.

(20) Müller, B. J.; Borisov, S. M.; Klimant, I. Red- to NIR-Emitting, BODIPY-Based, K+-Selective Fluoroionophores and Sensing Materials. *Adv. Funct. Mater.* **2016**, *26* (42), 7697–7707.

(21) Lin, Q.; Buccella, D. Highly Selective, Red Emitting BODIPY-Based Fluorescent Indicators for Intracellular Mg^{2+} Imaging. *J. Mater. Chem. B* **2018**, *6*, 7247.

(22) Basarić, N.; Baruah, M.; Qin, W.; Metten, B.; Smet, M.; Dehaen, W.; Boens, N. Synthesis and

Spectroscopic Characterisation of BODIPY Based Fluorescent Off-on Indicators with Low Affinity for Calcium. *Org. Biomol. Chem.* **2005**, *3* (15), 2755–2761.
(23) Kamiya, M.; Johnsson, K. Localizable and Highly Sensitive Calcium Indicator Based on a BODIPY Fluorophore. *Anal. Chem.* **2010**, *82* (15), 6472–6479.
(24) Zeng, L.; Miller, E. W.; Pralle, A.; Isacoff, E. Y.; Chang, C. J. A Selective Turn-On Fluorescent Sensor for Imaging Copper in Living Cells. *J. Am. Chem. Soc.* **2005**, *128* (1), 10–11.
(25) Wu, Y.; Peng, X.; Guo, B.; Fan, J.; Zhang, Z.; Wang, J.; Cui, A.; Gao, Y. Boron Dipyrromethene Fluorophore Based Fluorescence Sensor for the Selective Imaging of Zn(II) in Living Cells. *Org. Biomol. Chem.* **2005**, *3* (8), 1387–1392.
(26) Dodani, S. C.; He, Q.; Chang, C. J. A Turn-On Fluorescent Sensor for Detecting Nickel in Living Cells Synthesis of Nickelsensor-1 (NS1). *J. Am. Chem. Soc.* **2009**, *131*, 18020–18021.
(27) Kim, T. Il; Park, S.; Choi, Y.; Kim, Y. A BODIPY-Based Probe for the Selective Detection of Hypochlorous Acid in Living Cells. *Chem. - An Asian J.* **2011**, *6* (6), 1358–1361.
(28) Gabe, Y.; Urano, Y.; Kikuchi, K.; Kojima, H.; Nagano, T. Highly Sensitive Fluorescence Probes for Nitric Oxide Based on Boron Dipyrromethene Chromophore-Rational Design of Potentially Useful Bioimaging Fluorescence Probe. *J. Am. Chem. Soc.* **2004**, *126* (10), 3357–3367.
(29) Belzile, M.-N.; Godin, R.; Andrés, A.; Durantini, M.; Cosa, G. Monitoring Chemical and Biological Electron Transfer Reactions with a Fluorogenic Vitamin K Analogue Probe. **2016**.
(30) Yang, Z.; He, Y.; Lee, J.-H.; Park, N.; Suh, M.; Chae, W.-S.; Cao, J.; Peng, X.; Jung, H.; Kang, C.; et al. A Self-Calibrating Bipartite Viscosity Sensor for Mitochondria. **2013**.
(31) Miller, E. W.; Lin, J. Y.; Frady, E. P.; Steinbach, P. a; Kristan, W. B.; Tsien, R. Y. Optically Monitoring Voltage in Neurons by Photo-Induced Electron Transfer through Molecular Wires. *Proc. Natl. Acad. Sci. U. S. A.* **2012**, *109* (6), 2114–2119.
(32) Woodford, C. R.; Frady, E. P.; Smith, R. S.; Morey, B.; Canzi, G.; Palida, S. F.; Araneda, R. C.; Kristan, W. B.; Kubiak, C. P.; Miller, E. W.; et al. Improved PeT Molecules for Optically Sensing Voltage in Neurons. *J. Am. Chem. Soc.* **2015**, *137* (5), 1817–1824.
(33) Deal, P. E.; Kulkarni, R. U.; Al-Abdullatif, S. H.; Miller, E. W. Isomerically Pure Tetramethylrhodamine Voltage Reporters. *J. Am. Chem. Soc* **2016**, *138*, 9085–9088.
(34) Kulkarni, R. U.; Yin, H.; Pourmandi, N.; James, F.; Adil, M. M.; Schaffer, D. V.; Wang, Y.; Miller, E. W. A Rationally Designed, General Strategy for Membrane Orientation of Photoinduced Electron Transfer-Based Voltage-Sensitive Dyes. *ACS Chem. Biol.* **2017**, *12* (2), 407–413.
(35) Niu, S. L.; Ulrich, G.; Ziessel, R.; Kiss, A.; Renard, P.-Y.; Romieu, A. Water-Soluble BODIPY Derivatives. *Org. Lett.* **2009**, *11* (10), 2049–2052.
(36) Brizet, B.; Bernhard, C.; Volkova, Y.; Rousselin, Y.; Harvey, P. D.; Goze, C.; Denat, F. Boron Functionalization of BODIPY by Various Alcohols and Phenols. *Org. Biomol. Chem* **2013**, *11*, 7729–7737.
(37) Courtis, A. M.; Santos, S. a; Guan, Y.; Hendricks, J. A.; Ghosh, B.; Szantai-Kis, D. M.; Reis, S. a; Shah, J. V; Mazitschek, R. Monoalkoxy BODIPYs--a Fluorophore Class for Bioimaging. *Bioconjug. Chem.* **2014**, *25* (6), 1043–1051.
(38) Li, L.; Han, J.; Nguyen, B.; Burgess, K. Syntheses and Spectral Properties of Functionalized, Water-Soluble BODIPY Derivatives. *J. Org. Chem.* **2008**, *73* (5), 1963–1970.
(39) Komatsu, T.; Urano, Y.; Fujikawa, Y.; Kobayashi, T.; Kojima, H.; Terai, T.; Hanaoka, K.; Nagano, T. Development of 2,6-Carboxy-Substituted Boron Dipyrromethene (BODIPY) as a Novel Scaffold of Ratiometric Fluorescent Probes for Live Cell Imaging. *Chem. Commun. (Camb).* **2009**, No. 45, 7015–7017.
(40) Lincoln, R.; Greene, L. E.; Krumova, K.; Ding, Z.; Cosa, G. Electronic Excited State Redox Properties for BODIPY Dyes Predicted from Hammett Constants: Estimating the Driving Force of Photoinduced Electron Transfer. *J. Phys. Chem. A* **2014**, *118* (45), 10622–10630.
(41) Wagner, R. W.; Lindsey, J. S. Boron-Dipyrromethene Dyes for Incorporation in Synthetic Multi-Pigment Light-Harvesting Arrays. *Pure Appl. Chem.* **1996**, *68* (7), 1373–1380.

(42) D'souza, F.; Smith, P. M.; Zandler, M. E.; Mccarty, A. L.; Itou, M.; Araki, Y.; Ito, O. Energy Transfer Followed by Electron Transfer in a Supramolecular Triad Composed of Boron Dipyrrin, Zinc Porphyrin, and Fullerene: A Model for the Photosynthetic Antenna-Reaction Center Complex. *J. Am. Chem. Soc.* **2004**, *126* (25), 7898–7907.
(43) Lou, Z.; Hou, Y.; Chen, K.; Zhao, J.; Ji, S.; Zhong, F.; Dede, Y.; Dick, B. Different Quenching Effect of Intramolecular Rotation on the Singlet and Triplet Excited States of Bodipy. *J. Phys. Chem. C* **2018**, *122*, 185–193.
(44) Bricks, J. L.; Kovalchuk, A.; Trieflinger, C.; Nofz, M.; Bü, M.; Tolmachev, A. I.; Rg Daub, J.; Rurack, K. On the Development of Sensor Molecules That Display Fe^{III}-Amplified Fluorescence. *J. Am. Chem. Soc.* **2005**, *127*, 13522–13529.
(45) Courtis, A. M.; Santos, S. a.; Guan, Y.; Hendricks, J. A.; Ghosh, B.; Szantai-Kis, D. M.; Reis, S. a.; Shah, J. V.; Mazitschek, R. Monoalkoxy BODIPYs-A Fluorophore Class for Bioimaging. *Bioconjug. Chem.* **2014**, *25* (6), 1043–1051.
(46) Komatsu, T.; Oushiki, D.; Takeda, A.; Miyamura, M.; Ueno, T.; Terai, T.; Hanaoka, K.; Urano, Y.; Mineno, T.; Nagano, T. Rational Design of Boron Dipyrromethene (BODIPY)-Based Photobleaching-Resistant Fluorophores Applicable to a Protein Dynamics Study. *Chem. Commun.* **2011**, *47* (36), 10055.
(47) Rumyantsev, E. V; Alyoshin, S. N.; Marfin, Y. S. Kinetic Study of Bodipy Resistance to Acids and Alkalis: Stability Ranges in Aqueous and Non-Aqueous Solutions. *Inorganica Chim. Acta* **2013**, *408*, 181–185.
(48) Birkofer, L.; Bierwirth, E.; Ritter, A. Decarbobenzoxylierungen Mit Triäthylsilan. *Chem. Ber.* **1961**, *94* (3), 821–824.
(49) Coleman, R. S.; Shah, J. A. Chemoselective Cleavage of Benzyl Ethers, Esters, and Carbamates in the Presence of Other Easily Reducible Groups. *Synthesis* **1999**, 1399–1400.
(50) Dewar, M. J. S. Colour and Constitution. Part I. Basic Dyes. *J. Chem. Soc.* **1950**, *Sep*, 2329–2334.
(51) Hung, J.; Liang, W.; Luo, J.; Shi, Z.; K-Y Jen, A.; Li, X. Rational Design Using Dewar's Rules for Enhancing the First Hyperpolarizability of Nonlinear Optical Chromophores. *J. Phys. Chem. C* **2010**, *114*, 22284–22288.
(52) Olsen, S. A Quantitative Quantum Chemical Model of the Dewar-Knott Color Rule for Cationic Diarylmethanes. *Chem. Phys. Lett.* **2012**, *532*, 106–109.
(53) Boggess, S. C.; Gandhi, S. S.; Siemons, B. A.; Huebsch, N.; Healy, K. E.; Miller, E. W. New Molecular Scaffolds for Fluorescent Voltage Indicators. *ACS Chem. Biol* **2019**, *14*, 390–396.
(54) Komatsu, T.; Oushiki, D.; Takeda, A.; Miyamura, M.; Ueno, T.; Terai, T.; Hanaoka, K.; Urano, Y.; Mineno, T.; Nagano, T. Rational Design of Boron Dipyrromethene (BODIPY)-Based Photobleaching-Resistant Fluorophores Applicable to a Protein Dynamics Study. *Chem. Commun.* **2011**, *47* (36), 10055.
(55) Kulkarni, R. U.; Vandenberghe, M.; Thunemann, M.; James, F.; Andreassen, O. A.; Djurovic, S.; Devor, A.; Miller, E. W. In Vivo Two-Photon Voltage Imaging with Sulfonated Rhodamine Dyes. *ACS Cent. Sci.* **2018**, *4*, 1371–1378.
(56) Grenier, V.; Daws, B. R.; Liu, P.; Miller, E. W. Spying on Neuronal Membrane Potential with Genetically Targetable Voltage Indicators. *J. Am. Chem. Soc.* **2019**, *141*, 1349–1358.
(57) Liu, P.; Grenier, V.; Hong, W.; Muller, V. R.; Miller, E. W. Fluorogenic Targeting of Voltage-Sensitive Dyes to Neurons. *J. Am. Chem. Soc.* **2017**, *139*, 17334–17340.
(58) Bai, D.; Benniston, A. C.; Clift, S.; Baisch, U.; Steyn, J.; Everitt, N.; Andras, P. Low Molecular Weight Neutral Boron Dipyrromethene (Bodipy) Dyads for Fluorescence-Based Neural Imaging. *J. Mol. Struct.* **2014**, *1065–1066*, 10–15.
(59) Sirbu, D.; Butcher, J. B.; Waddell, P. G.; Andras, P.; Benniston, A. C. Locally Excited State–Charge Transfer State Coupled Dyes as Optically Responsive Neuron Firing Probes. *Chem. - A Eur. J.* **2017**, *23* (58), 14639–14649.
(60) Zheng, Q.; Jockusch, S.; Zhou, Z.; Blanchard, S. C. The Contribution of Reactive Oxygen Species

to the Photobleaching of Organic Fluorophores. *Photochem. Photobiol.* **2014**, *90* (2), 448–454.
(61) Zheng, Q.; Jockusch, S.; Rodríguez-Calero, G. G.; Zhou, Z.; Zhao, H.; Altman, R. B.; Abruña, H. D.; Blanchard, S. C. Intra-Molecular Triplet Energy Transfer Is a General Approach to Improve Organic Fluorophore Photostability. *Photochem. Photobiol. Sci.* **2016**, *15*, 196–203.
(62) Zheng, Q.; Juette, M. F.; Jockusch, S.; Wasserman, M. R.; Zhou, Z.; Altman, R. B.; Blanchard, S. C. Ultra-Stable Organic Fluorophores for Single-Molecule Research. *Chem. Soc. Rev* **2014**, *43*, 1044–1056.
(63) Huang, Y. L.; Walker, A. S.; Miller, E. W. A Photostable Silicon Rhodamine Platform for Optical Voltage Sensing. *J. Am. Chem. Soc.* **2015**, *137* (33), 10767–10776.
(64) Chai, J.-D.; Head-Gordon, M. Long-Range Corrected Hybrid Density Functionals with Damped Atom-Atom Dispersion Correctionsw. *Phys. Chem. Chem. Phys.* **2008**, *10*, 6615–6620.
(65) Weigend, F.; Ahlrichs, R. Balanced Basis Sets of Split Valence, Triple Zeta Valence and Quadruple Zeta Valence Quality for H to Rn: Design and Assessment of Accuracy. *Phys. Chem. Chem. Phys.* **2005**, *7*, 3297–3305.
(66) Hansch, C.; Leo, A.; Taft, R. W. A Survey of Hammett Substituent Constants and Resonance and Field Parameters. *Chem. Rev.* **1991**, *91*, 165–195.
(67) Ueno, T.; Urano, Y.; Kojima, H.; Nagano, T. Mechanism-Based Molecular Design of Highly Selective Fluorescence Probes for Nitrative Stress. *J. Am. Chem. Soc.* **2006**, *128*, 10640–10641.
(68) Weber, G.; Teale, F. W. J. Determination of the Absolute Quantum Yield of Fluorescent Solutions. *Trans. Faraday. Soc.* **1957**, *53*, 646–655.
(69) Kubin, R. F.; Fletcher, A. N. Fluorescence Quantum Yields of Some Rhodamine Dyes. *Journal of Luminescence* **1982**, *27*, 455–462.
(70) Edelstein, A. D.; Tsuchida, M. A.; Amodaj, N.; Pinkard, H.; Vale, R. D.; Stuurman, N. Advanced Methods of Microscope Control Using μManager Software. *J. Biol. Methods* **2014**, *1* (2), 10.
(71) Schindelin, J.; Arganda-Carreras, I.; Frise, E.; Kaynig, V.; Longair, M.; Pietzsch, T.; Preibisch, S.; Rueden, C.; Saalfeld, S.; Schmid, B.; et al. Fiji: An Open-Source Platform for Biological-Image Analysis. *Nat. Methods* **2012**, *9* (7), 676–682.

Appendix A: Improving hydrophilicity of *ortho*-sulfonated BODIPY dyes: monoalkoxy and disulfonated BODIPY VoltageFluors

Portions of this work were performed in collaboration with the following persons:
Synthesis with Patrick Zhang
Imaging with Dr. Rishikesh Kulkarni

Introduction

Initial 2,6-ethyl BODIPY voltage-sensitive dyes (Et*p*H and Et*p*OMe, **Chapter 2**) localized to the cell membrane in HEK293T cells, but the membrane staining was dim even after loading with Pluronic F-127 (pluronic) and they had no measurable voltage sensitivity. We hypothesized increasing the hydrophilicity of the relatively greasy 2,6-ethyl BODIPY dye head might increase the amount of dye delivered to the membrane or improve membrane orientation, therefore improving voltage sensitivity.

The first strategy we used was to apply previously reported methodology to displace one of the BODIPY fluorines with an alcohol, yielding monoalkoxy BODIPYs.[1] The formation of monoalkoxy BODIPYs relies on Lewis acid TMSOTf to activate the difluoro BODIPY, abstracting one fluorine and forming a borenium intermediate stabilized by the triflate counteranion (**Scheme A1**).[2,3] This methodology allows for alcohols with both hydroxy and amino terminal groups to be added, as well as alcohols functionalized with tetrazines. Tetrazines can quench the BODIPY fluorophore, and bioorthogonal reaction with strained cyclopropene or trans-cyclooctene moieties can facilitate fluorogenic targeting of the BODIPY fluorophore.[4–7]

The second strategy we wanted to test was adding a second *ortho*-sulfonate to the *meso*-phenyl BODIPY ring. This modification improves both the membrane orientation and increase the voltage sensitivity by ~19% in our fluorescein-based VoltageFluors.[8] This approach would be simple to evaluate because the synthesis is similar to mono-sulfonated BODIPY VoltageFluors.

Results & Discussion

Synthesis of monoalkoxy, ortho-sulfonated BODIPY dyes

The first monoalkoxy reaction we tried was using glycolic acid as the alcohol nucleophile, because the carboxylate would be a useful handle for attaching targeting moieties in addition to increasing the water solubility.[9] This was an ambitious nucleophile to attempt, because the original methodology did not report any free carboxylates or sulfonates.[1] We did not observe either of the possible diastereomers from this reaction, possibly due to glycolic acid's poor solubility in DCM/$CHCl_3$ (**Scheme A2**). We decided to take a step back and try a reported nucleophile for this reaction and decided on ethylene glycol because of its lower polarity and terminal alcohol functional handle. The monoalkoxy reaction with ethylene glycol yielded both mono- and di-ethylene glycol products (**Scheme A3**). The NMR of the mono-ethylene glycol **3.6** appeared to contain primarily one diastereomer, though determining which diastereomer would only be possible through obtaining a crystal structure. The NMR of the di-ethylene glycol product **3.7** clearly showed 4 methylene triplets between 3 and 3.7 ppm, corresponding to the two inequivalent ethylene glycol moieties—one syn to the sulfonate group, one anti.

We next tried the monoalkoxy reaction with ethyl glycolate, hoping protecting the carboxylic acid as the ester would improve the reaction. Ethyl glycolate was prepared and distilled (**Scheme A4**), and the following monoalkoxy reaction (**Scheme A5a**) was much more successful than the glycolic acid attempted previously. The NMR of product **3.9** is not entirely convincing—the ethyl group of the ethyl glycolate is present, but the methylene singlet is not seen in the expected range of 3-4 ppm (the singlet at 2.99 ppm is the aniline methyl groups at the bottom of the molecular wire). High-resolution electrospray ionization mass spectrometry (HRMS-ESI) did confirm the presence of the product, with a strong $[M-H]^-$ ionization, and ^{19}F NMR also supported product formation. Instead of two inequivalent fluorine multiplets at ~144 ppm as seen in the starting material, we see a single fluorine multiplet (split by boron) at -151.2 to -151.4 ppm.

Lithium hydroxide saponification of the ethyl ester of **3.9** was attempted to yield the carboxylate handle, but resulted in decomposition to non-fluorescent by-products. Interestingly, when we repeated the monoalkoxy reaction with ethyl glycolate, we isolated not **3.9** but cyclized product **3.10** (**Scheme A5b**), supported by HRMS-ESI, the absence of fluorines in ^{19}F NMR, and the disappearance of the ethyl group of the ethyl glycolate moiety in ^{1}H NMR.

Cellular characterization/discussion of monoalkoxy BODIPY probes

Mono-ethylene glycol Et*p*H **3.6** was the only monoalkoxy probe characterized in HEK293T cells. Membrane localization and brightness was significantly improved for **3.6** compared to its Et*p*H precursor, and while Et*p*H displayed no voltage sensitivity, we did see slight fluctuations in fluorescence intensity of **3.6** corresponding to depolarizing steps after injecting current into single HEK cells under whole-cell voltage-clamp mode (**Figure A1**).

There were a few reasons we did not actively pursue monoalkoxy BODIPYs beyond the 2,6-ethyl VoltageFluor series. The first was difficulty of purification and characterization. Monoalkoxy BODIPY compounds were more acid sensitive than their 4,4-difluoro BODIPY precursors. They showed some decomposition on silica, and the alternative alumina columns for purification were very slow and long. Monoalkoxy BODIPY compounds could not be analyzed by commonly used LC-MS eluents—in eluent with either 0.05% TFA or FA, the only masses observed were $[M–boron+H]^+$, which meant that starting material and product were indistinguishable by LC-MS since the functionalization was on boron. All mass data had to be obtained by submitting samples to the HRMS-ESI, which was expensive and time-consuming compared to LC-MS. Finally, the reaction was difficult to reproduce in our hands (such as the formation of **3.9** and **3.10** under identical reaction conditions), and the formation of multiple diastereomers for mono-substituted BODIPYs also complicated purification.

Synthesis of disulfonated BODIPY dyes/VoltageFluors

Disulfonated BODIPYs and VoltageFluors were prepared very similarly to BODIPY VoltageFluors with a single ortho-sulfonate (**Chapter 2**). Disulfonated aldehyde building block **3.11** was prepared through an S_NAr reaction of the difluoro precursor with sodium sulfite.[8] The BODIPY condensation in DMF solvent proceeded readily (**Scheme A6**), but was lower yielding due to a combination of the disulfonated aldehyde being more sterically hindered and the difficulty of purifying the disulfonated BODIPY products (**3.12** & **3.13**). Heck couplings between disulfonated BODIPYs **3.12** & **3.13** and molecular wires **4** & **14** were also lower than analogous monosulfonated Heck couplings, with average isolated yields of 12-16%. 2,6-ethyl disulf BODIPY **3.12** displayed a λ_{abs} of 542 nm, λ_{em} of 557 nm, and ϕ_{fl} of 0.97.

Cellular characterization of disulf VoltageFluors

2,6-ethyl disulfonated VoltageFluors Et_ds_H **3.14** and Et_ds_OMe **3.15** showed excellent membrane localization and did not require Pluronic F-127 as a co-solvent for loading like their 2,6-ethyl mono-sulfonated analogues (**Figure A2 a & c**). Both 2,6-ethyl probes photobleached rapidly in a quadratic fashion. Et_ds_H displayed no voltage sensitivity and Et_ds_OMe was modestly voltage sensitive—estimated at 3% $\Delta F/F$ after bleach correction. The tetramethyl disulf probes TM_ds_H and TM_ds_OMe also brightly stained HEK293T cell membranes (**Figure A2 e & g**) and were more voltage sensitive than related 2,6-ethyl probes, following a similar trend to

the *meta* probes discussed in Chapter 2. TM_ds_H has a 1.5% ΔF/F and TM_ds_OMe has an 8.2% ΔF/F, but with noticeably worse signal-to-noise and brightness (**Figure A2 f**, **h**).

Conclusions & Future Directions

Both monoalkoxy substitution on boron and addition of a second sulfonate on the meso-pendant ring were found to be beneficial for the hydrophilicity of BODIPY VoltageFluors. The main reason these approaches were not continued past the 2,6-ethyl and tetramethyl series was synthetic tractability. The monoalkoxy substitution on boron has the potential to form two diastereomers of the resulting probe (i.e. **Scheme A2**), complicating purification and characterization. These compounds also showed inferior stability to silica and acidic LC-MS eluent additives compared to their 4,4-difluoro precursors. Additionally, later derivatives of the meta BODIPY VoltageFluors such as TM*m*OMe **19**, Carboxy*m*OMe **30**, and Amide*m*H **35** (**Chapter 2**) were sufficiently hydrophilic that they did not require pluronic for loading, eliminating the need for the monoalkoxy solubilizing moiety. This methodology might be worth trying to improve the cellular brightness of TM*m*OMe, because that probe's brightness was its biggest liability, or to make fluorogenic versions of BODIPY VoltageFluors by appending a tetrazine-containing group to the boron.[1]

The disulfonated BODIPYs and VoltageFluors had significantly more difficult purifications and lower isolated yields than their mono-sulfonated relatives (**Chapter 2**). While the second sulfonate benefitted membrane localization in HEK293T cells, disulfonated probes were less voltage sensitive than mono-sulfonated probes with the molecular wire in the *meta* position relative to the fluorophore. Et*m*H **15** and Et*m*OMe **16** have voltage sensitivities of 1.8 and 5.4% ΔF/F (**Chapter 2**) compared to 0 and 3% ΔF/F for Et_ds_H **3.14** and Et_ds_OMe **3.15** (**Table A1**). For the tetramethyl series, TM*m*H **17** and TM*m*OMe **19** have 2.5 and 33% ΔF/F, whereas analogous disulfonated VoltageFluors TM_ds_H and TM_ds_OMe have voltage sensitivities of 1.5 and 8.2% ΔF/F (**Table A1**). The increased voltage sensitivity for the *meta* isomers led us to continue with only that scaffold for the cyano, carboxy, and amide derivatives, though the disulfonated BODIPY VoltageFluors scaffold has potential with the right fluorophore/wire pairing. Disulfonated BODIPY fluorophores such as **3.12** and **3.13** (**Scheme A6**) could also be investigated for biological imaging applications outside of voltage imaging because of their excellent water-solubility and ϕ_{fl}.

Figures & Schemes

Scheme A1 *Proposed formation of monoalkoxy BODIPYs*[1]

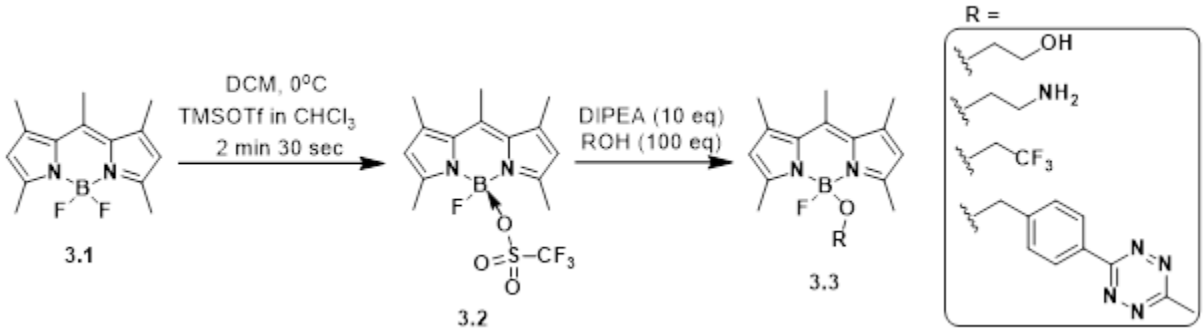

Scheme A2 *Attempted monoalkoxy reaction with glycolic acid*

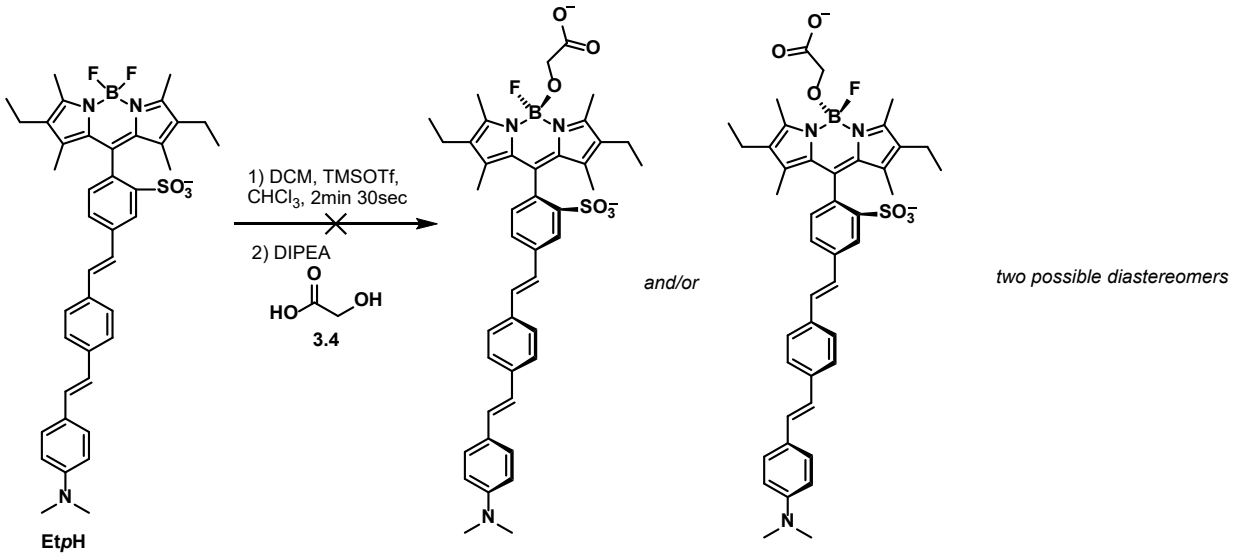

Scheme A3 *Mono- and di-alkoxy EtpH with ethylene glycol*

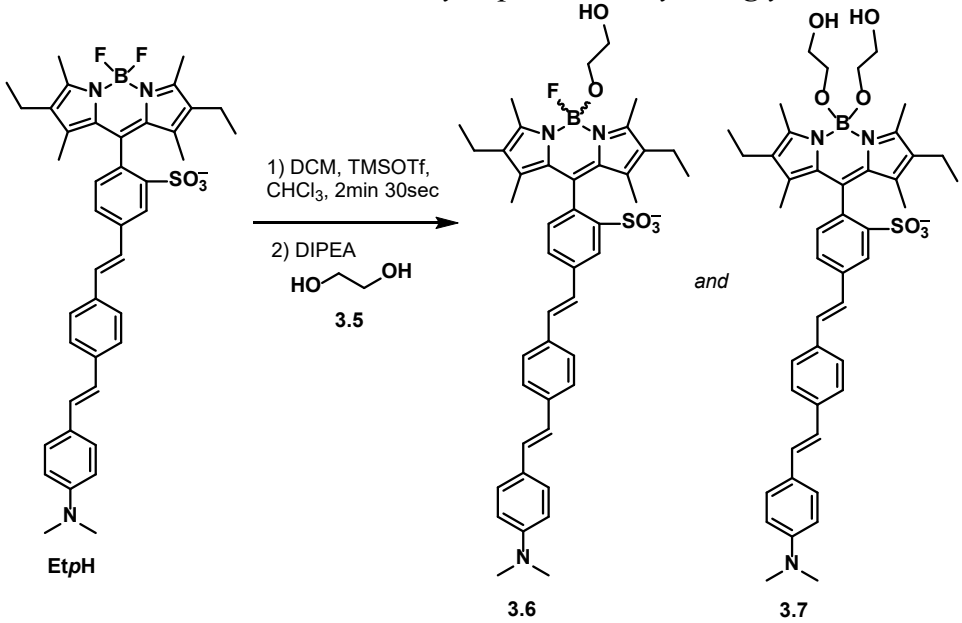

Scheme A4 *Synthesis of ethyl glycolate*[10,11]

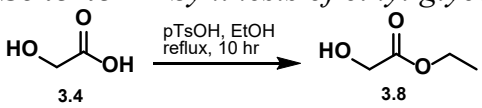

Scheme A5 *Monoalkoxy reactions with ethyl glycolate*

a)

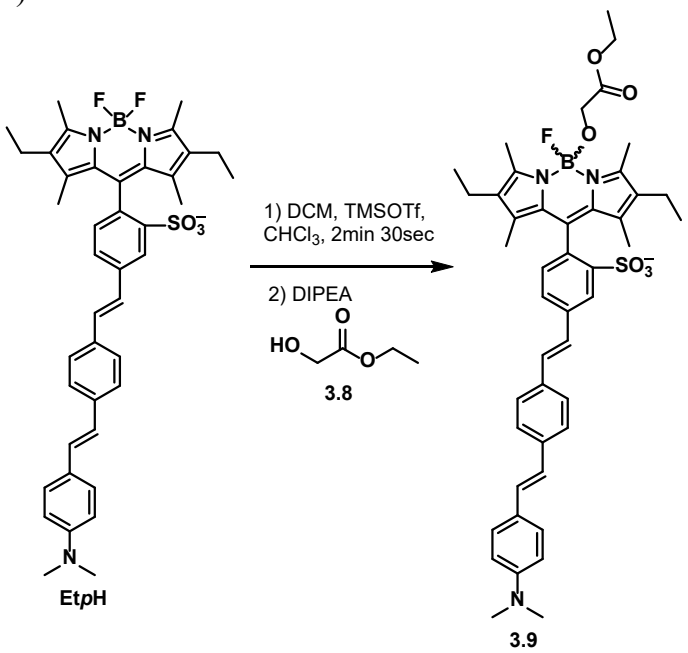

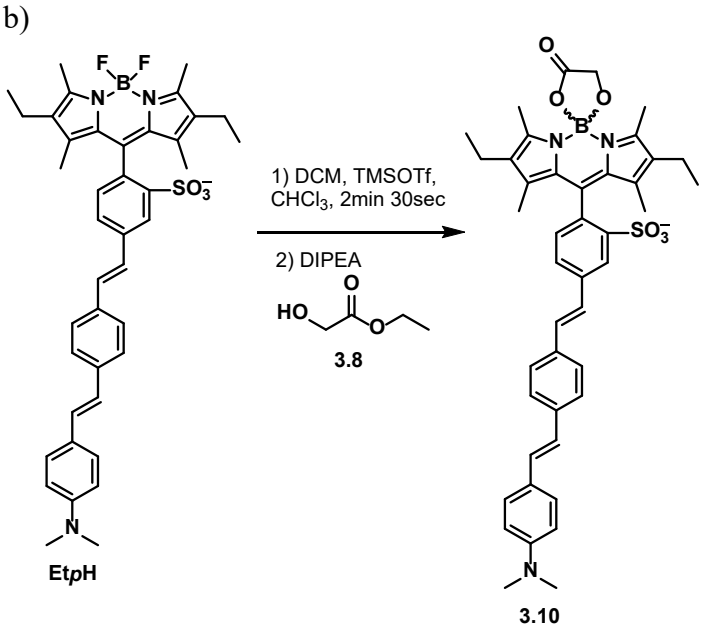

Figure A1 *Membrane staining and voltage sensitivity for ethylene glycol EtpH* ***3.6***

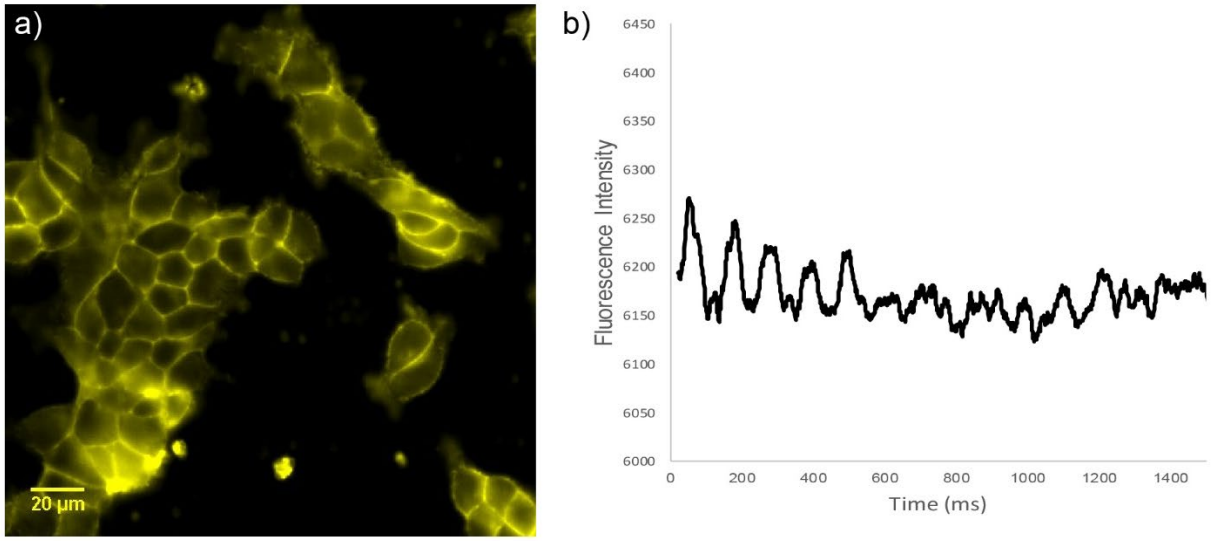

Figure A1 a) Membrane staining of 2 µM ethylene glycol Et*p*H **3.6** and **b)** Moving average of epifluorescence microscopy showing voltage steps (±100 mV in 20 mV increments) from a holding potential of -60 mV in a single HEK cell under whole-cell voltage-clamp mode.

Scheme A6 *Synthesis of disulfonated BODIPYs & VoltageFluors*

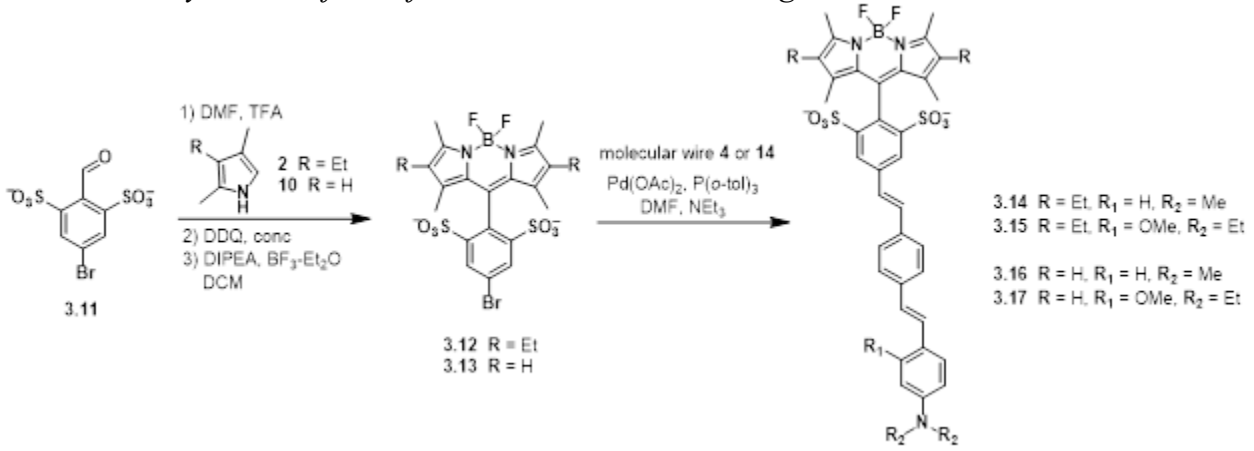

Table A1 *Spectroscopic/Cellular Characterization of disulfonated BODIPY VoltageFluors*

Name (compound #)	*λmax abs (nm)*[a]	*λmax em (nm)*[a]	*% ΔF/F per 100 mV*[b]
Et_ds_H	540	555	0
Et_ds_OMe	539	555	3 ± 0.8
TM_ds_H	515	532	1.5 ± 0.3
TM_ds_OMe	514	530	8.2 ± 1.1

[a]Determined in water with 1% SDS. [b]Determined in HEK293T cells (n = 3 cells).

Figure A2 *Representative membrane staining and voltage sensitivity of disulf probes*

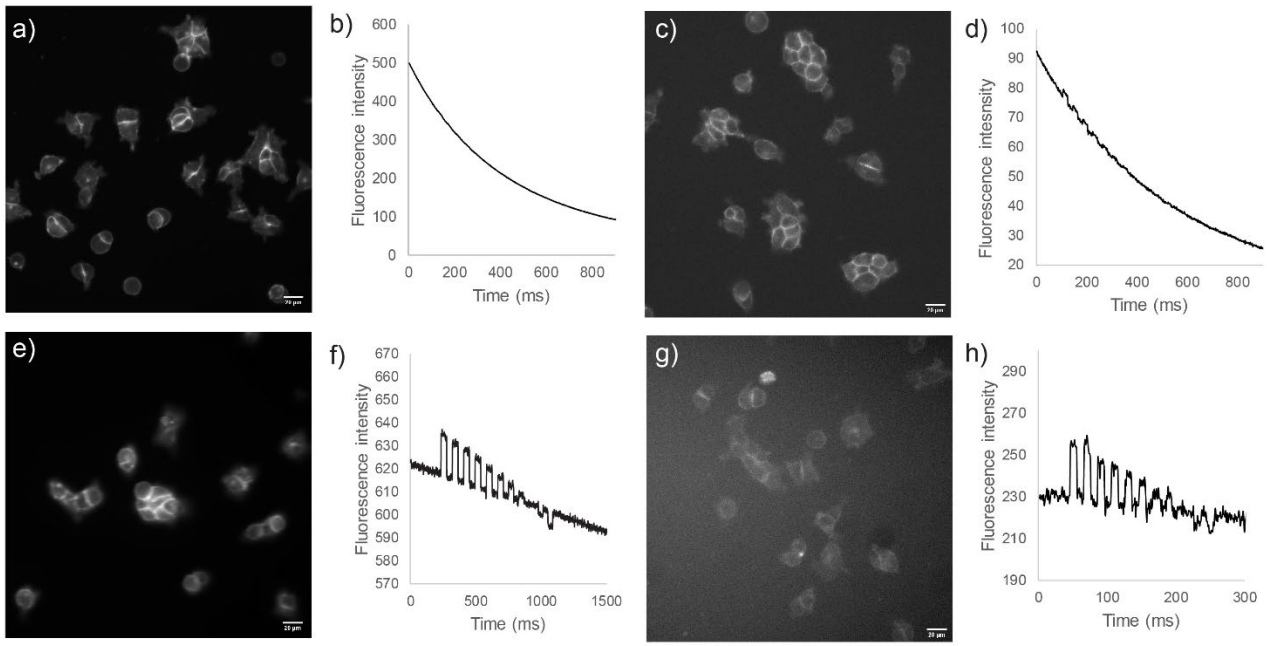

Figure A2. Widefield fluorescence micrograph of HEK293T cells stained with 200 nM **a)** Et_ds_H **3.14**, **c)** Et_ds_OMe **3.15**, **e)** TM_ds_H **3.16**, **g)** TM_ds_OMe **3.17**. Scale bar is 20 µm. Plot of fluorescence intensity vs. time for hyper- and de-polarizing steps (±100 mV in 20 mV increments) from a holding potential of –60 mV in a single HEK cell under whole-cell voltage clamp mode for **b)** Et_ds_H **3.14**, **d)** Et_ds_OMe **3.15**, **f)** TM_ds_H **3.16**, **h)** TM_ds_OMe **3.17**.

Experimental

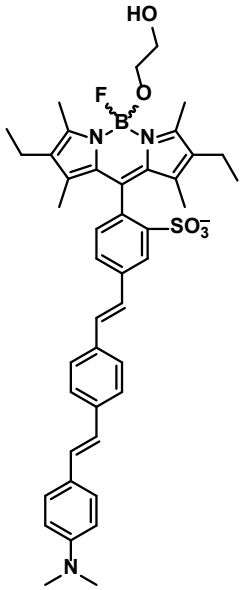

Mono-ethyleneglycol Et*p*H (3.6) In a flame-dried round-bottom flask, Et*p*H **6** (50 mg, 0.07 mmol, 1 equiv) was dissolved in DCM for a final concentration of 1.9 mM. The solution was chilled at 0 °C on an ice−water bath and, under stirring, TMSOTf (5 equiv) was added as a 10% (v/v) stock solution in $CHCl_3$ (640 µL). The reaction proceeded for 2 min and 30 s. Then, a premixed solution of ethylene glycol (395 µL, 7.1 mmol, 100 equiv) and DIPEA (123 µL, 0.71 mmol,10 equiv) was rapidly injected into the reaction. The mixture was then partitioned between 1:1 DCM:H_2O. The organics were washed with H_2O + 10% brine (3 x 20 mL), dried over Na_2SO_4, gravity filtered, and solvents removed *in vacuo*. Flash chromatography (5 →10% MeOH in DCM, gradient) yielded **3.6** as an orange solid (10.95 mg, 21%).

^{1}H NMR (400 MHz, MeOD) δ 8.30 (m, 1H), 8.13 (m, 1H), 7.81 (d, *J* = 8.1 Hz, 1H), 7.60 (d, *J* = 8.4 Hz, 2H), 7.54 (d, *J* = 8.4 Hz, 2H), 7.45 (d, *J* = 8.8 Hz, 2H), 7.36 (d, *J* = 16.4 Hz, 1H), 7.32 (d, *J* = 16.4 Hz, 1H), 7.22 (d, *J* = 7.6 Hz, 1H), 7.14 (d, *J* = 16.0 Hz, 1H), 6.98 (d, *J* = 16.0 Hz, 1H), 6.79 (d, *J* = 8.4 Hz, 2H), 3.45 (appt, *J* = 6.1, 6.4 Hz, 2H), 3.07 (appt, *J* = 6.1, 6.4 Hz, 2H), 2.99 (s, 6H), 2.51 (s, 6H), 2.36 (q, *J* = 7.2 Hz, 4H) 1.50 (s, 6H), 1.01 (m, 6H). **HRMS (ESI$^-$)** calculated for $C_{43}H_{48}BFN_3O_5S^-$ $[M-H]^-$ 748.3397, found 748.3377.

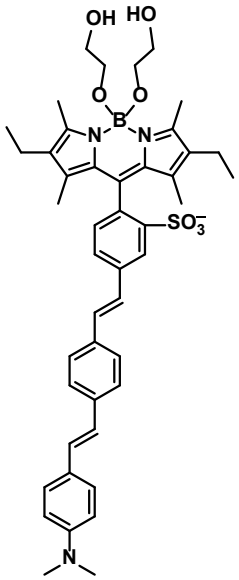

Di-ethyleneglycol Et*p*H (3.7) In a flame-dried round-bottom flask, Et*p*H **6** (50 mg, 0.07 mmol, 1 equiv) was dissolved in DCM for a final concentration of 1.9 mM. The solution was chilled at 0 °C on an ice−water bath and, under stirring, TMSOTf (5 equiv) was added as a 10% (v/v) stock solution in $CHCl_3$ (640 µL). The reaction proceeded for 2 min and 30 s. Then, a premixed solution of ethylene glycol (395 µL, 7.1 mmol, 100 equiv) and DIPEA (123 µL, 0.71 mmol,10 equiv) was rapidly injected into the reaction. The mixture was then partitioned between 1:1 DCM:H_2O. The organics were washed with H_2O + 10% brine (3 x 20 mL), dried over Na_2SO_4, gravity filtered, and solvents removed *in vacuo*. Flash chromatography (5 → 10% MeOH in DCM, gradient, then 100% MeOH flush) yielded **3.7** as an orange solid (10.64 mg, 19%).

^{1}H NMR (400 MHz, Methanol-d_4) δ 8.30 (d, J = 1.6 Hz, 1H), 7.81 (d, J = 8.3 Hz, 1H), 7.60 (d, J = 8.2 Hz, 2H), 7.54 (d, J = 8.2 Hz, 2H), 7.45 (d, J = 8.6 Hz, 2H), 7.37 (d, J = 16.4 Hz, 1H), 7.30 (d, J = 16.2 Hz, 1H), 7.23 (d, J = 7.9 Hz, 1H), 7.14 (d, J = 16.4 Hz, 1H), 6.98 (d, J = 16.2 Hz, 1H), 6.79 (d, J = 8.6 Hz, 2H), 3.52 (t, J = 5.7 Hz, 2H), 3.44 (t, J = 5.8 Hz, 2H), 3.27 (t, J = 5.6 Hz, 2H), 3.11 (t, J = 5.7 Hz, 2H), 2.99 (s, 6H), 2.54 (s, 6H), 2.39 – 2.32 (m, 4H), 1.48 (s, 6H), 1.00 (t, J = 7.5 Hz, 9H). **HRMS (ESI$^-$)** calculated for $C_{45}H_{53}BN_3O_7S^-$ $[M-H]^-$ 790.3703, found 790.3690.

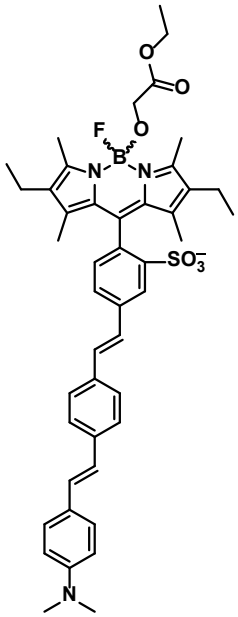

Ethyl glycolate Et*p*H (3.9) In a flame-dried round-bottom flask, Et*p*H **6** (36 mg, 0.051 mmol, 1 equiv) was dissolved in DCM for a final concentration of 1.9 mM. The solution was chilled at 0 °C on an ice−water bath and, under stirring, TMSOTf (5 equiv) was added as a 10% (v/v) stock solution in $CHCl_3$ (460 µL). The reaction proceeded for 2 min and 30 s. Then, a premixed solution of ethyl glycolate (482 µL, 5.1 mmol, 100 equiv) and DIPEA (89 µL, 0.51 mmol, 10 equiv) was rapidly injected into the reaction. The mixture was then partitioned between 1:1 DCM:H_2O. The organics were washed with H_2O + 10% brine (3 x 20 mL), dried over Na_2SO_4, gravity filtered, and solvents removed *in vacuo*. Flash chromatography (3 → 20% MeOH in DCM, gradient) yielded **3.7** as an orange-pink solid (28.3 mg, 37%).

^{1}H NMR (300 MHz, Chloroform-*d*) δ 7.62 (d, *J* = 7.9 Hz, 1H), 7.49 (d, *J* = 2.6 Hz, 6H), 7.43 (d, *J* = 8.7 Hz, 2H), 7.18 (d, *J* = 7.9 Hz, 2H), 7.09 (d, *J* = 16.4 Hz, 1H), 6.92 (d, *J* = 16.2 Hz, 1H), 6.73 (d, *J* = 8.9 Hz, 2H), 2.99 (s, 6H), 2.93 (d, *J* = 7.3 Hz, 5H), 2.53 (s, 4H), 2.49 (s, 3H), 2.27 (d, *J* = 7.5 Hz, 5H), 1.47 (s, 4H), 1.44 (s, 4H), 1.25 (s, 10H), 1.14 (s, 4H), 0.96 (s, 3H). **^{19}F NMR** (400 MHz, Chloroform-*d*) δ -151.3 (appq, 1F). **HRMS (ESI$^-$)** calculated for $C_{45}H_{50}BFN_3O_6S^-$ $[M-H]^-$ 790.3503, found 790.3501.

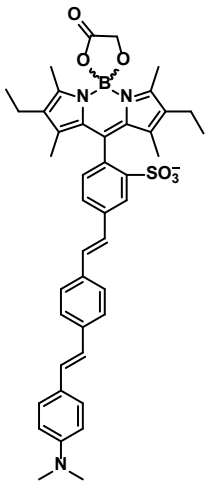

Cyclized glycolate Et*p*H (3.10) In a flame-dried round-bottom flask, Et*p*H **6** (73.5 mg, 0.1 mmol, 1 equiv) was dissolved in DCM for a final concentration of 1.9 mM. The solution was chilled at 0 °C on an ice−water bath and, under stirring, TMSOTf (5 equiv) was added as a 10% (v/v) stock solution in $CHCl_3$ (941 µL). The reaction proceeded for 2 min and 30 s. Then, a premixed solution of ethyl glycolate (984 µL, 10 mmol, 100 equiv) and DIPEA (200 µL, 1 mmol,10 equiv) was rapidly injected into the reaction. The mixture was then partitioned between 1:1 DCM:H_2O. The organics were washed with H_2O + 10% brine (3 x 20 mL), dried over Na_2SO_4, gravity filtered, and solvents removed *in vacuo*. Flash chromatography (3 → 10% MeOH in DCM, gradient) yielded **3.7** as an orange-pink solid (28.3 mg, 37%).

^{1}H NMR (600 MHz, Methanol-d_4) δ 8.26 (d, J = 32.9 Hz, 1H), 7.81 (d, J = 9.7 Hz, 1H), 7.59 (d, J = 8.4 Hz, 2H), 7.52 (d, J = 8.2 Hz, 2H), 7.44 (d, J = 8.7 Hz, 2H), 7.36 (d, J = 16.3 Hz, 1H), 7.31 – 7.23 (m, 2H), 7.13 (d, J = 16.3 Hz, 1H), 6.96 (d, J = 16.3 Hz, 1H), 6.77 (d, J = 8.7 Hz, 2H), 3.35 (s, 4H), 3.34 (s, 1H), 2.97 (s, 5H), 2.38 – 2.30 (m, 5H), 1.50 (s, 2H), 1.47 (s, 1H), 0.98 (s, 1H). **HRMS (ESI$^-$)** calculated for $C_{43}H_{45}BN_3O_6S^-$ $[M-H]^-$ 742.3128, found 742.3109.

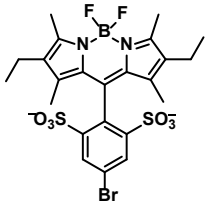

2,6-ethyl disulf BODIPY (3.12) A flame-dried round-bottom flask was charged with 5-bromo-2-formylbenzene-1,3-disulfonic acid **3.11** (304 mg, 0.88 mmol, 1 eq) and 3-ethyl-2,4-dimethyl-*1H*-pyrrole **2** (261 µL, 3.28 mmol, 2.2 eq), then DMF (5 mL) and TFA (1 drop) were added and reaction stirred at rt 18 h. DDQ (200 mg, 0.88 mmol, 1 eq) was added and reaction concentrated *in vacuo*. DCM (35 mL), DIPEA (2.45 mL, 14 mmol, 16 eq), and $BF_3{\cdot}Et_2O$ (1.73 mL, 14 mmol, 16 eq) were added and stirred 10 min. Reaction was quenched with IPA and concentrated. Flash chromatography on silica gel (0 → 5% MeOH in DCM, gradient) yielded **3.12** as a pink solid (130 mg, 24%).

^{1}H NMR (400 MHz, Chloroform-d) δ 8.54 (s, 2H), 2.41 (s, 6H), 2.23 (q, J = 7.4 Hz, 4H), 1.48 (s, 6H), 0.91 (t, J = 7.4 Hz, 6H). **^{19}F NMR** (400 MHz, Chloroform-d) δ -143.5 (appq, 2F).

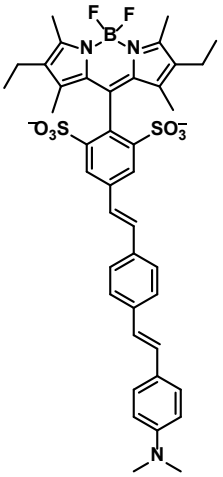

Et_ds_H (3.14) To a flame-dried 10 mL Schlenk flask were added 2,6-ethyl disulf BODIPY **3.12** (16.3 mg, 0.03 mmol, 1 eq), molecular wire **4** (7.29 mg, 0.03 mmol, 1.1 eq), $Pd(OAc)_2$ (0.6 mg, 0.002 mmol, 9 mol%), and P(*o*-tol)$_3$ (1.5 mg, 0.005 mmol, 18 mol%). Flask was evacuated and backfilled with N_2 3x, then DMF (350 µL) and NEt_3 (180 µL) were added via syringe, flask was sealed shut, and heated to 70 °C 19 h. Reaction was concentrated *in vacuo*, and preparative thin layer chromatography (10% MeOH + 0.2% NEt_3) yielded **3.14** as a pink solid (13.8 mg, 66%).

^{1}H NMR (300 MHz, Chloroform-*d*) δ 8.57 (s, 2H), 7.45 (d, *J* = 20.6 Hz, 6H), 7.36 (d, *J* = 16.5 Hz, 1H), 7.18 (d, *J* = 16.0 Hz, 1H), 7.08 (d, *J* = 15.9 Hz, 1H), 6.92 (d, *J* = 16.3 Hz, 1H), 6.72 (d, *J* = 8.7 Hz, 2H), 2.99 (s, 6H), 2.43 (s, 6H), 2.25 (q, *J* = 7.4 Hz, 4H), 1.54 (s, 6H), 0.90 (m, 6H). **^{19}F NMR** (400 MHz, Chloroform-*d*) -143.4 (appq, 2F).

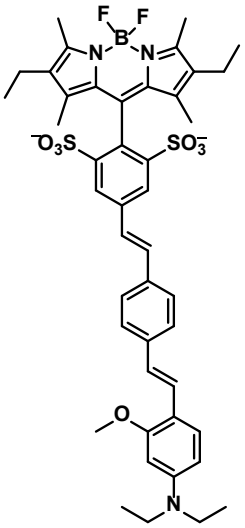

Et_ds_OMe (3.15) To a flame-dried 10 mL Schlenk flask were added 2,6-ethyl disulf BODIPY **3.12** (32.3 mg, 0.05 mmol, 1 eq), methoxy wire **14** (17.7 mg, 0.057 mmol, 1.1 eq), $Pd(OAc)_2$ (1.1 mg, 0.005 mmol, 9 mol%), and P(*o*-tol)$_3$ (2.9 mg, 0.009 mmol, 18 mol%). Flask was evacuated and backfilled with N_2 3x, then DMF (697 µL) and NEt_3 (349 µL) were added, flask was sealed shut, and heated to 70 °C 21 h. Reaction was concentrated *in vacuo*, and flash chromatography

(1% MeOH + 0.5% NEt_3 → 7% MeOH + 0.5% NEt_3, gradient) yielded **3.15** as a pink solid (5.42 mg, 12.3%).

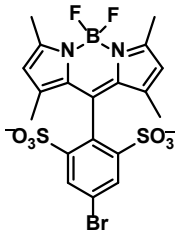

Tetramethyl disulf BODIPY (3.13) A flame-dried round-bottom flask was charged with 5-bromo-2-formylbenzene-1,3-disulfonic acid **3.11** (203.4 mg, 0.59 mmol, 1 eq) and 2,4-dimethylpyrrole (134 µL, 1.3 mmol, 2.2 eq), then DMF (2 mL) and TFA (2 drops) were added, and reaction stirred at rt 2 h. DDQ (339 mg, 1.49 mmol, 1 eq) was added, and reaction concentrated *in vacuo*. DCM (20 mL), DIPEA (1.13 mL, 6.5 mmol, 11 eq), and $BF_3{\cdot}Et_2O$ (1.16 mL, 9.4 mmol, 16 eq) were added and stirred 10 min. Reaction was quenched with IPA (10 mL), washed with water (2 x 30 mL), brine (1 x 30 mL), dried over Na_2SO_4, and concentrated. Flash chromatography (3 → 6% MeOH in DCM + 0.5% NEt_3) followed by PTLC (10% MeOH + 0.5% NEt_3) to yield **3.13** as a pink solid (80.8 mg, 24%).

^{1}H NMR (400 MHz, Methanol-*d*$_4$) δ 8.38 (s, 2H), 5.87 (s, 2H), 2.46 (s, 6H), 1.55 (s, 6H). **^{19}F NMR** (400 MHz, Chloroform-*d*) δ -145.3 (appq, 2F). **Analytical HPLC retention time:** 2.43 min, 543/545 m/z $[M\text{-}F]^+$

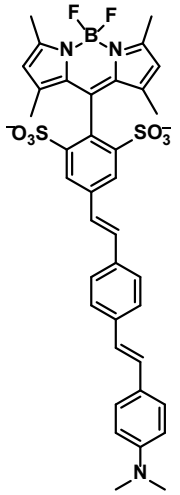

TM_ds_H (3.16) To a flame-dried 25 mL Schlenk flask were added TM disulf BODIPY **3.13** (90 mg, 0.16 mmol, 1 eq), molecular wire **4** (44 mg, 0.18 mmol, 1.1 eq), $Pd(OAc)_2$ (3.2 mg, 0.014 mmol, 9 mol%), and P(*o*-tol)$_3$ (8.8 mg, 0.029 mmol, 18 mol%). Flask was evacuated and backfilled with N_2 3x, then DMF (2 mL) and NEt_3 (1 mL) were added, flask was sealed shut, and heated to 100 °C 21 h. Reaction was concentrated *in vacuo*, and flash chromatography (3% MeOH + 0.1% NEt_3) followed by PTLC (10% MeOH + 0.5% NEt_3) yielded **3.16** as a pink solid (18.7 mg, 16%).

^{1}H NMR (300 MHz, Methanol-d_4) δ 8.46 (s, 2H), 7.64 – 7.49 (m, 4H), 7.44 (d, J = 8.8 Hz, 2H), 7.36 (s, 1H), 7.32 (s, 1H), 7.13 (d, J = 16.3 Hz, 1H), 6.96 (d, J = 16.3 Hz, 1H), 6.77 (d, J = 8.9 Hz, 2H), 5.90 (s, 2H), 2.97 (s, 6H), 2.46 (s, 6H), 1.59 (s, 6H).

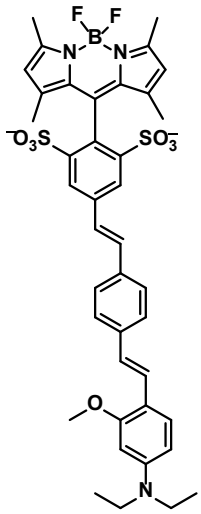

TM_ds_OMe (3.17) To a flame-dried 10 mL Schlenk flask were added TM disulf BODIPY **3.13** (16.5 mg, 0.03 mmol, 1 eq), methoxy wire **14** (8.1 mg, 0.03 mmol, 1.1 eq), $Pd(OAc)_2$ (0.6 mg, 0.003 mmol, 9 mol%), and P(*o*-tol)$_3$ (1.6 mg, 0.005 mmol, 18 mol%). Flask was evacuated and backfilled with N_2 3x, then DMF (392 μL) and NEt_3 (196 μL) were added, flask was sealed shut, and heated to 100 °C 18 h. Reaction was concentrated *in vacuo*, dissolved in 2:1 DCM:IPA (10:5 mL), washed with water (2 x 10 mL), brine (10 mL), dried over Na_2SO_4, and concentrated. PTLC (10% MeOH + 0.5% NEt_3) yielded **3.17** as a pink solid (3.2 mg, 2%).

Analytical HPLC retention time: 4.69 min, 790.6 m/z $[M+H]^+$.

Compound NMR Spectra

JF-132_frac38-46.1.fid — AVB-400 ZBO Proton starting parameters. 6/11/03 RN

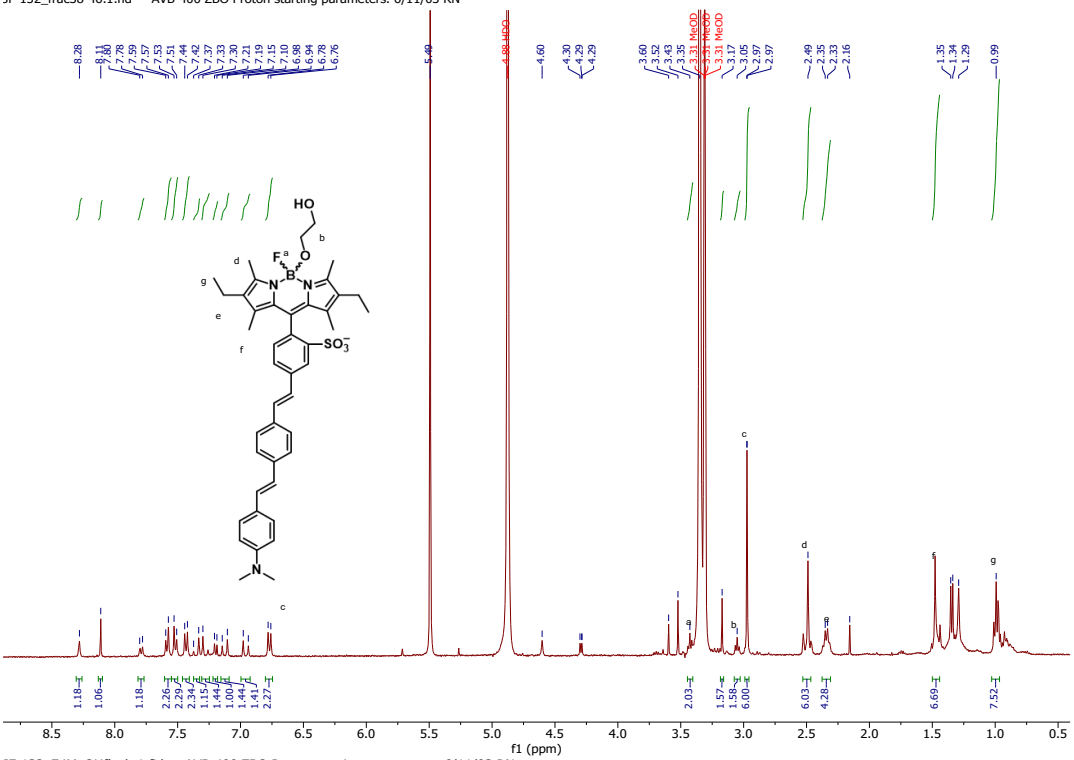

JF-132_E4MeOHflush.1.fid — AVB-400 ZBO Proton starting parameters. 6/11/03 RN

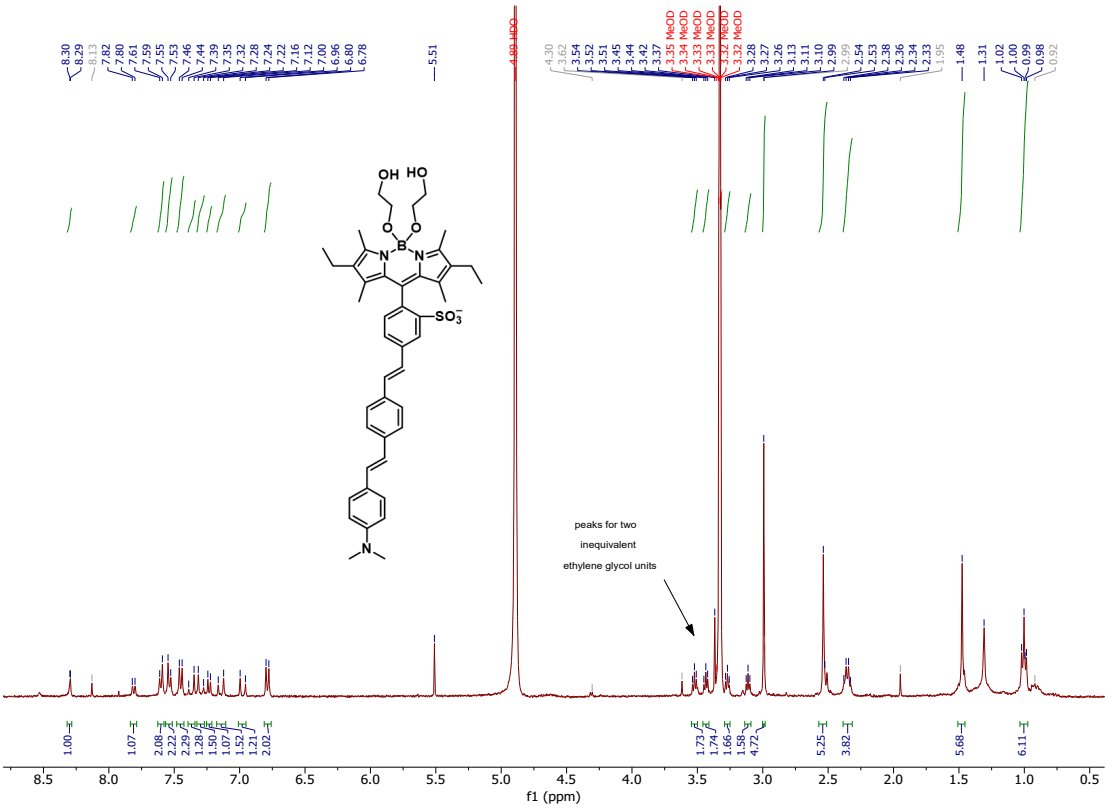

PZ-32_PTLC_toporange.1.fid — AV-300 Dual C-H probe proton starting parameters 7/23/03 RN.

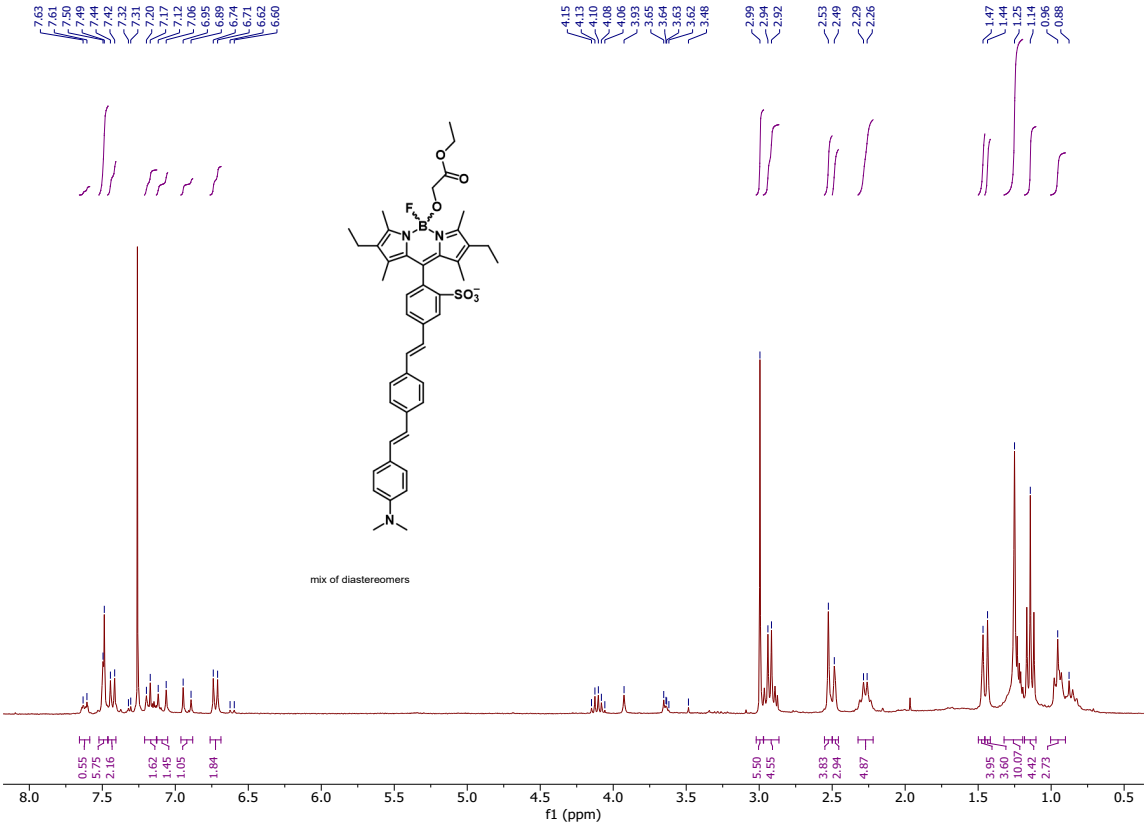

JF-144_frac87-100toppink.1.fid — AV-600 ZBO proton starting parameters 11/16/08 RN

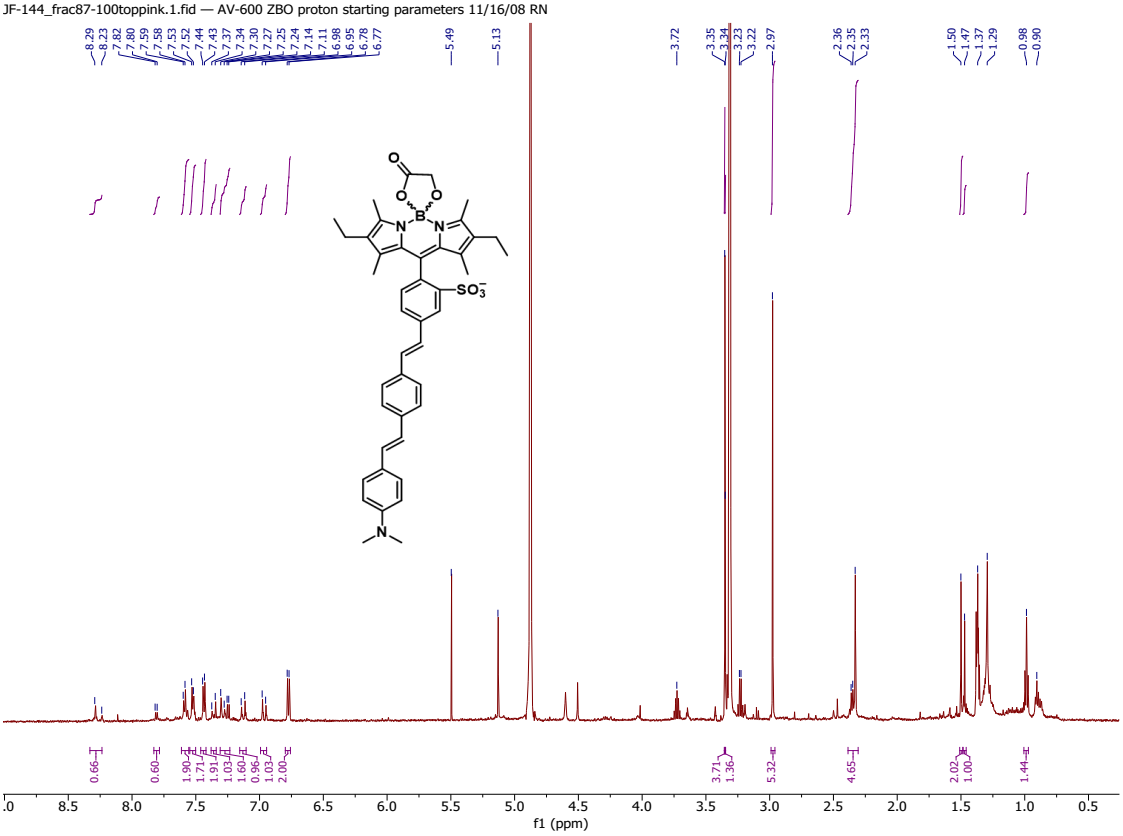

JF-152orgs_frac6-8.1.fid — AVB-400 ZBO Proton starting parameters. 6/11/03 RN

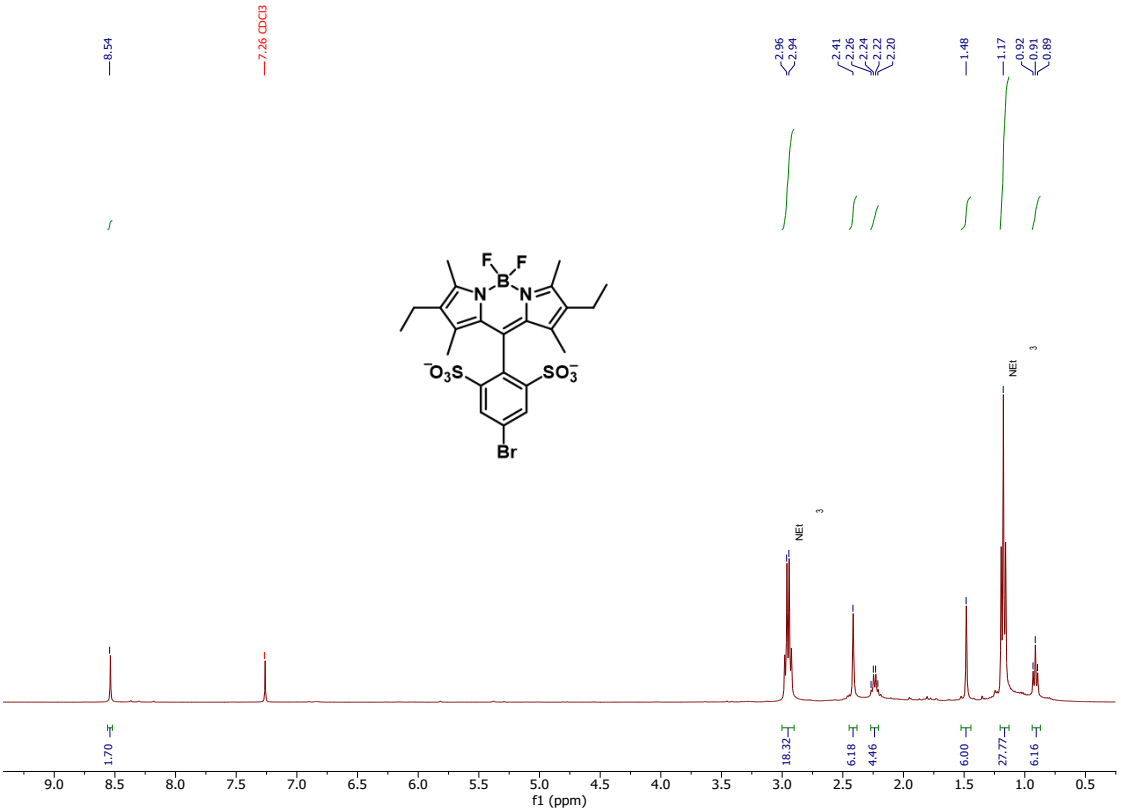

jf2-13_ptlc_poh.1.fid — AV-300 Dual C-H probe proton starting parameters 7/23/03 RN.

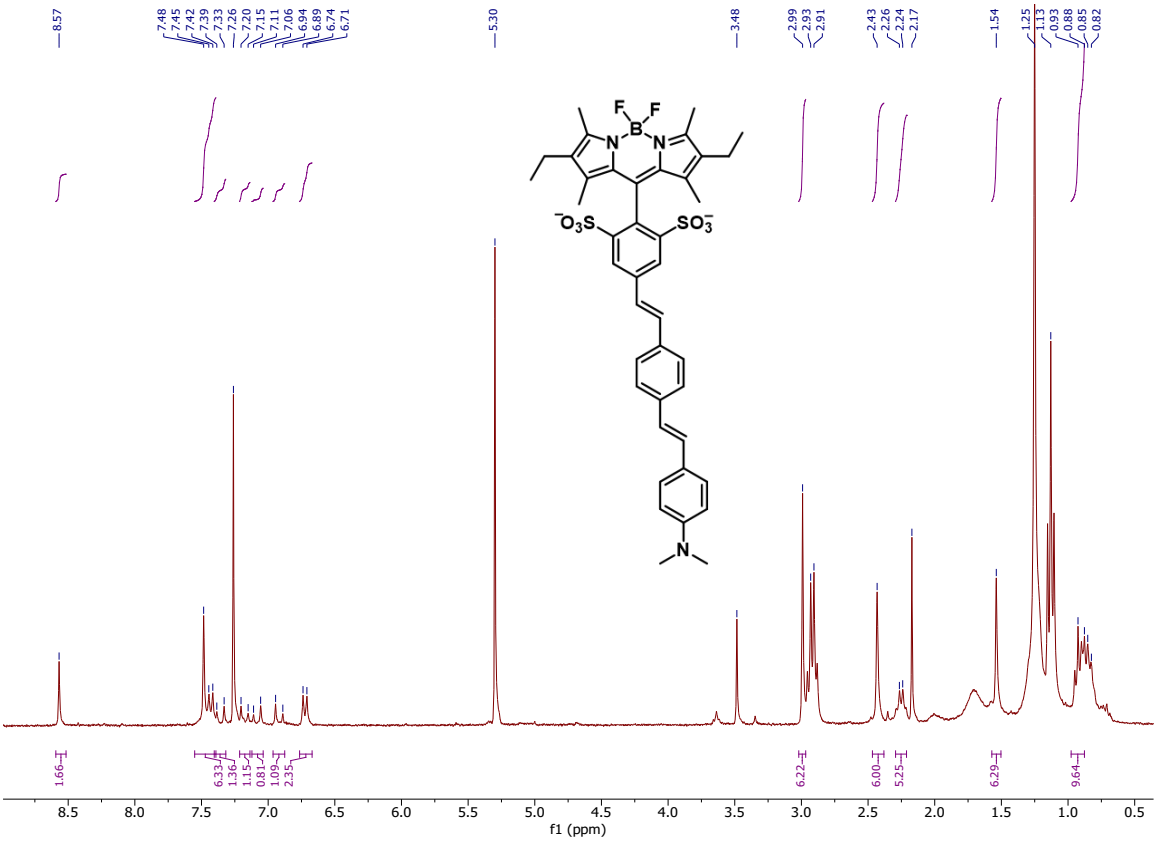

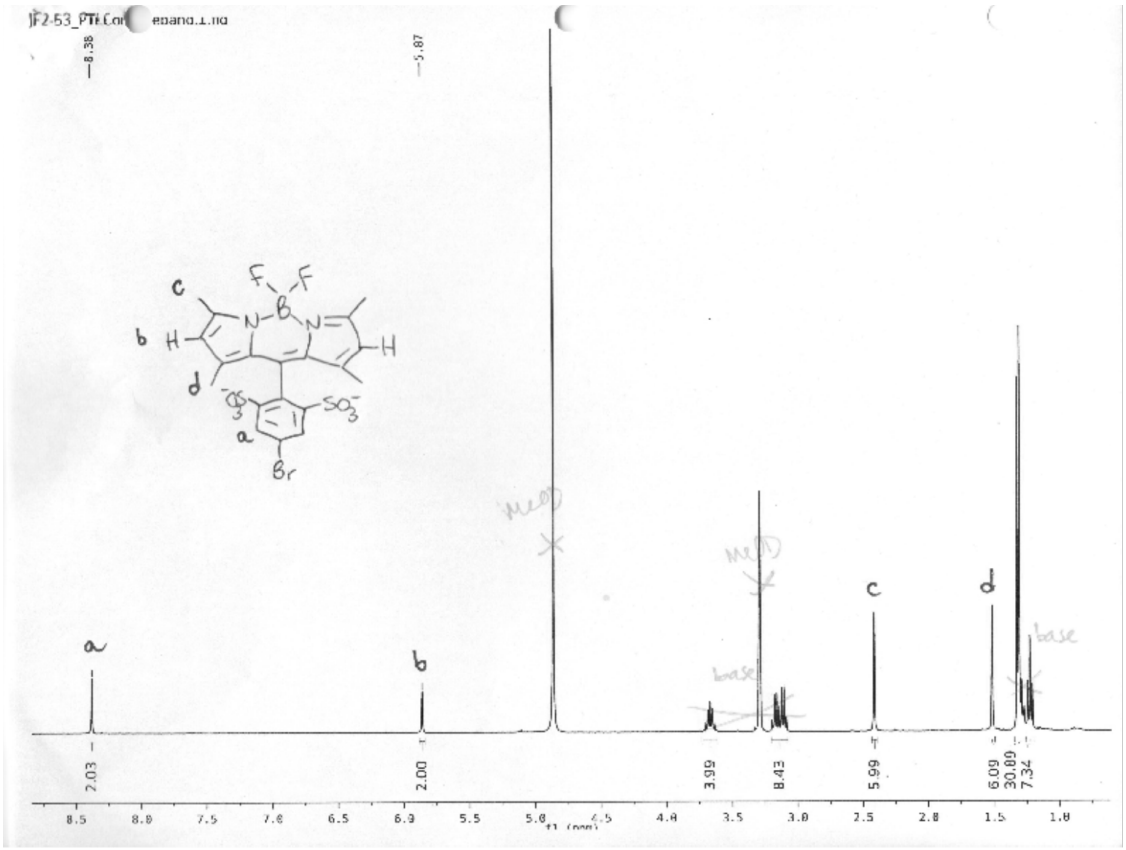
8.38
5.87
c
b
H
F
F
B
N
N
H
d
SO_3^-
^-O_3S
a
Br
a
b
c
d
base
base
2.03
2.00
3.99
8.43
5.99
6.09
30.89
7.34
8.5
8.0
7.5
7.0
6.5
6.0
5.5
5.0
4.5
4.0
3.5
3.0
2.5
2.0
1.5
1.0

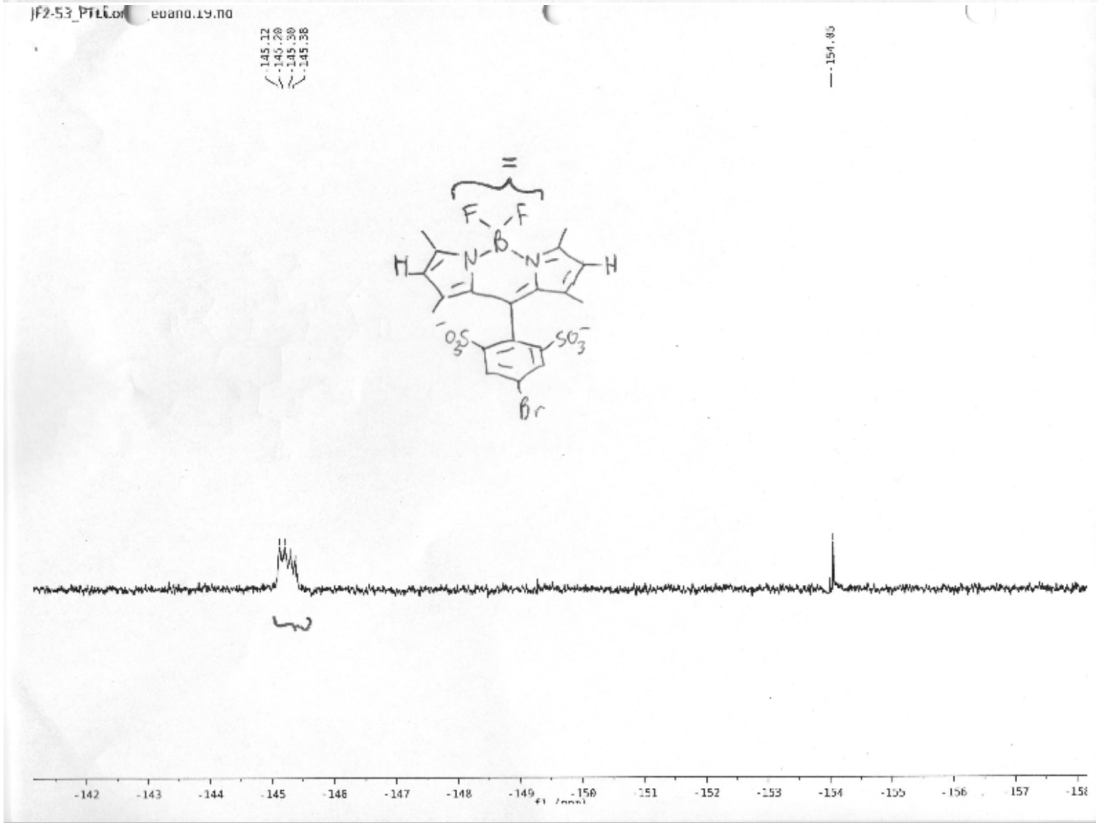
145.12
145.20
145.30
145.38
154.80
H
F
F
B
N
N
H
H
^-O_3S
SO_3^-
Br
-142
-143
-144
-145
-146
-147
-148
-149
-150
-151
-152
-153
-154
-155
-156
-157
-158

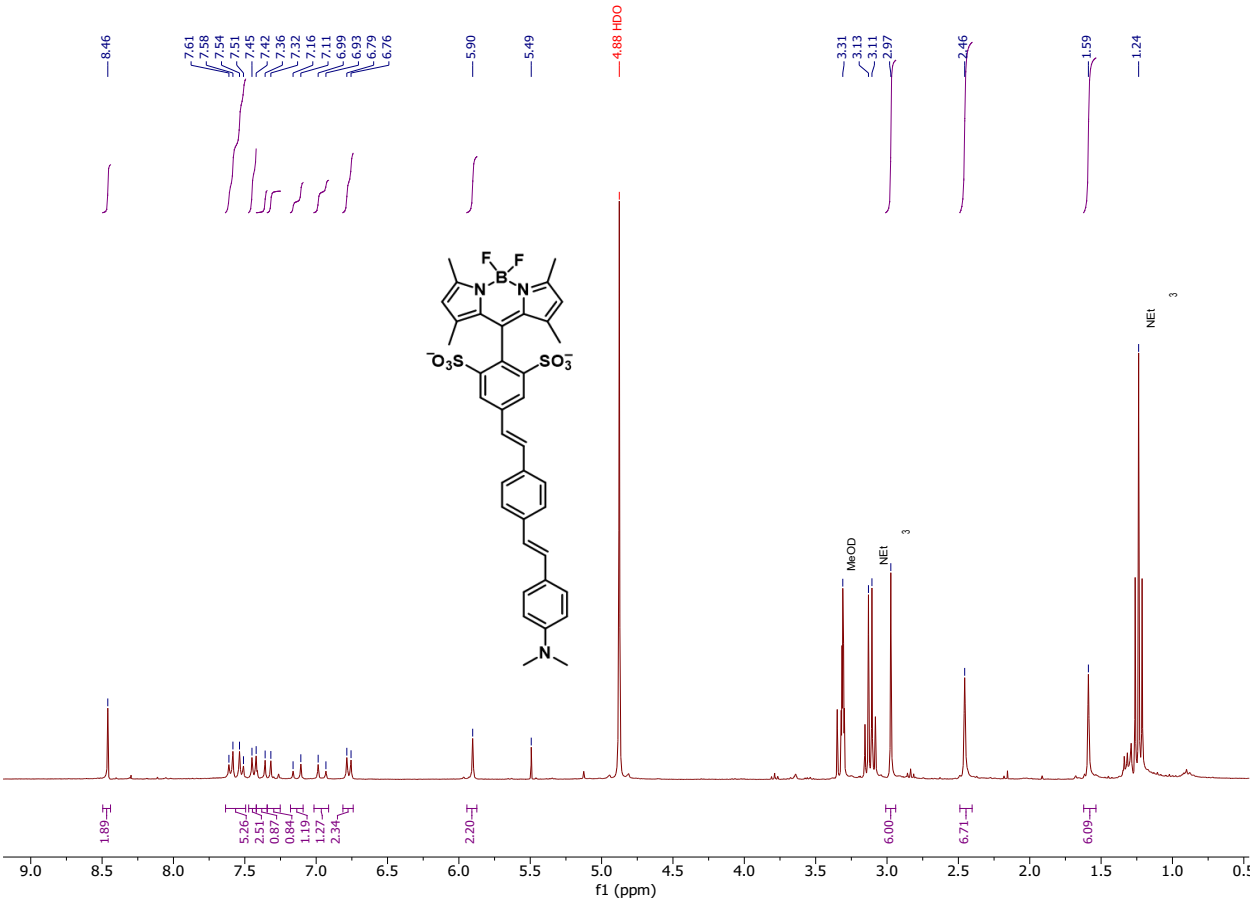
JF2-61_disulfheckPTLC.1.fid — AV-300 Dual C-H probe proton starting parameters 7/23/03 RN.
8.46
7.61
7.58
7.54
7.51
7.45
7.42
7.36
7.32
7.16
7.11
6.99
6.93
6.79
6.76
5.90
5.49
4.88 HDO
3.31
3.13
3.11
2.97
2.46
1.59
1.24
MeOD
NEt
3
1.89
5.26
2.51
0.87
0.84
1.19
1.27
2.34
2.20
6.00
6.71
6.09
f1 (ppm)

References

(1) Courtis, A. M.; Santos, S. a; Guan, Y.; Hendricks, J. A.; Ghosh, B.; Szantai-Kis, D. M.; Reis, S. a; Shah, J. V; Mazitschek, R. Monoalkoxy BODIPYs--a Fluorophore Class for Bioimaging. *Bioconjug. Chem.* **2014**, *25* (6), 1043–1051.

(2) Hudnall, T. W.; Gabbai, F. P. A BODIPY Boronium Cation for the Sensing of Fluoride Ions. *Chem. Commun.* **2008**, *38*, 4596–4597.

(3) Bonnier, C.; Piers, W. E.; Parvez, M.; Sorensen, T. S. Borenium Cations Derived from BODIPY Dyes. *Chem. Commun.* **2008**, *38*, 4593–4595.

(4) Devaraj, N. K.; Weissleder, R. Biomedical Applications of Tetrazine Cycloadditions. *Acc. Chem. Res.* **2011**, *44* (9), 816–827.

(5) Carlson, J. C. T.; Meimetis, L. G.; Hilderbrand, S. A.; Weissleder, R. BODIPY-Tetrazine Derivatives as Superbright Bioorthogonal Turn-on Probes. *Angew. Chemie - Int. Ed.* **2013**, *52* (27), 6917–6920.

(6) Yang, J.; Šečkute, J.; Cole, C. M.; Devaraj, N. K. Live-Cell Imaging of Cyclopropene Tags with Fluorogenic Tetrazine Cycloadditions. *Angew. Chemie - Int. Ed.* **2012**, *51* (30), 7476–7479.

(7) Dumas-Verdes, C.; Miomandre, F.; Lépicier, E.; Galangau, O.; Vu, T. T.; Clavier, G.; Méallet-Renault, R.; Audebert, P. BODIPY-Tetrazine Multichromophoric Derivatives. *European J. Org. Chem.* **2010**, No. 13, 2525–2535.

(8) Kulkarni, R. U.; Yin, H.; Pourmandi, N.; James, F.; Adil, M. M.; Schaffer, D. V.; Wang, Y.; Miller, E. W. A Rationally Designed, General Strategy for Membrane Orientation of Photoinduced Electron Transfer-Based Voltage-Sensitive Dyes. *ACS Chem. Biol.* **2017**, *12* (2), 407–413.

(9) Grenier, V.; Daws, B. R.; Liu, P.; Miller, E. W. Spying on Neuronal Membrane Potential with Genetically Targetable Voltage Indicators. *J. Am. Chem. Soc.* **2019**, *141*, 1349–1358.

(10) Tang, Y.; Cheng, Q.; Zhang, J.; Yang, C.; Wang, S.; Wang, X.; Zhao, Z. Synthesis and Application of Glycolic Esters in Methanol-Gasoline as Bifunctional Additives. *J. Chem. Soc. Pak.* **2014**, *36* (6), 1109–1113.

(11) Iványi, T.; Lázár, I. Synthesis and in Vitro Enzyme Hydrolysis of Trioxadiaza-and Tetraoxadiaza-Crown Ether-Based Complexing Agents with Disposable Ester Pendant Arms. *Synthesis (Stuttg).* **2005**, *20*, 3555–3564.

Appendix B: Chlorination attempts on 1,3,5,7-Tetramethyl *meta*-bromo (TM*m*Br) BODIPY

Portions of this work were performed in collaboration with the following persons:
Synthesis with Divya Natesan

Introduction

One of the synthetic advantages of the BODIPY fluorophore is it retains some of the diverse reactivity of its pyrrole precursor.[1] In the case of 1,3,5,7-tetramethyl (TM) BODIPY, the 2,6-positions can be readily functionalized via electrophilic aromatic substitution reactions or radical reactions. We sought to chlorinate TM*m*Br BODIPY (**Chapter 2, compound 12**) in our search for the voltage sensitivity "sweet spot" between 2,6-ethyl and 2,6-cyano, because Cosa et. al. reported the HOMO level of 2,6-dichloro BODIPY falling in between them (**Figure B1**).[2] As an added bonus, 2,6-chlorination cause a bathochromatic shift in the absorbance and emission properties of the BODIPY.[2] Red-shifted absorbance and emission properties are beneficial for imaging applications because of reduced light scattering and phototoxicity, and increased tissue penetration.[3–5]

Despite the potential benefits of halogenating the BODIPY scaffold, reports of 2,6-fluoro and 2,6-chloro BODIPY in the literature are scarce compared to 2,6-bromo and 2,6-iodo BODIPY derivatives, which are often used as triplet state sensitizers or precursors to functionalization via palladium-catalyzed cross coupling.[6–11] We anticipated the potential for 2,6-chloro BODIPYs to be susceptible to nucleophilic attack via a S_NAr mechanism, but decided to attempt to chlorinate TM*m*Br using two previously reported methods—*N*-chlorosuccinimide (NCS),[2] and a hypervalent iodide chlorinating agent.[12]

Results & Discussion

Routes towards 2,6-dichloro BODIPY VoltageFluor

We first subjected TM*m*Br BODIPY **12** to *N*-chlorosuccinimide conditions (**Scheme B1a**).[2] After 4 hours, thin layer chromatography (TLC) showed a shift from a yellow, green fluorescent spot to a pink, yellow fluorescent spot. Liquid chromatography-mass spectrometry (LC-MS) showed that the reaction was incomplete—it contained a mixture of unmodified starting material and mono-chlorinated material (13.3 min, 497/499/501 m/z). After stirring at room temperature for an additional 18 hours, TLC showed a pink, orange fluorescent spot (**Figure B2**), a good sign that both sides of the BODIPY scaffold had been chlorinated.

Following aqueous work-up and isolation by column chromatography, it was unclear whether the isolated material was the correct product. By NMR, there was no singlet at 6.44 ppm corresponding to the 2,6-hydrogens of the TM*m*Br **12** starting material, suggesting they had indeed been replaced by chlorines. The chemical shift of the 1,7-methyl groups on the BODIPY core appeared at 1.55 ppm, typical for BODIPY derivatives, but the 3,5-methyl groups were more deshielded than expected, at 3.41 ppm (see **Experimental**). Similar 2,6-dichloro BODIPYs in the literature report this singlet at 2.55–2.59 ppm, and the 2,6-dicyano BODIPY **21** we synthesized previously had a chemical shift of 2.66 ppm for this singlet. We would not expect this singlet to differ by more than 1 ppm from reported 2,6-chloro BODIPYs or be more deshielded than the methyl groups of 2,6-cyano BODIPY, so this singlet did not support formation of the correct product. Mass spectrometry data also did not support formation of the desired product—by LC-MS, we found 581.2 m/z, significantly higher than the $[M-F]^+$ ion we expected in ESI^+, 530.95. Since the desired product does not contain any good basic functional groups to facilitate ionization in positive mode, we also submitted it for HRMS-ESI(-), but did not see the $[M-H]^-$ molecular ion of the desired product.

Both the NMR and LC-MS results were reproducible by repeating the reaction under identical conditions. We tried a Heck coupling on the suspected product (**Scheme B1a**), and the

NMR of the isolated Heck product looked like the desired product, but again we were unable to obtain mass confirmation of the product.

As a final effort, we decided to try an alternate chlorination method, using a hypervalent iodide reagent.[12] The chlorinating agent, 1-chloro-1,2-benziodoxol-3-one, was readily synthesized from 2-iodobenzoic acid and matched the literature NMR (**Scheme B1b**). Similar to the chlorination reaction with NCS, we observed a fluorescence shift for the BODIPY from green, to yellow, to orange with subsequent chlorinations. For one of my attempts using these conditions, both the LC-MS (**Figure B3**) and NMR post-work-up (see **Experimental**) seemed to support formation of the product, though both were messy. The 3,5-methyl groups appear at 2.55 ppm, matching reported spectra for similar 2,6-dichloro BODIPYs, and the disappearance of the singlet at 6.44 ppm supports the replacement of the 2,6-hydrogens of the TM*m*Br starting material. Unfortunately, this material decomposed on silica when I attempted to purify it, and subsequent trials with these conditions did not reproduce the promising crude NMR/LC-MS.

Conclusion

Both NCS and 1-chloro-1,2-benziodoxol-3-one seemed to be effective reagents for chlorinating the 2,6-positions of TMmBr **12**, evidenced by the fluorescence shift from green to orange, disappearance of the singlet at 6.44 ppm in the NMR corresponding to the 2,6-hydrogens in TM*m*Br, and in the case of 1-chloro-1,2-benziodoxol-3-one, the presence of a $[M+H]^+$ ion in the LC-MS, though not as a major component (**Figure B3**). We were unable to successfully isolate and fully characterize the 2,6-dichloro, *ortho*-sulfonated BODIPY. It is possible that the electron-poor nature of the fluorophore and chlorine being a good leaving group for S_NAr made the fluorophore susceptible to nucleophilic attack at the 2,6-positions. We suspect that the reason no biological probes are reported with 2,6-dichloro BODIPY or 2,6-difluoro BODIPY fluorophores could be instability under aqueous conditions, and chose to move on to more established scaffolds such as 2,6-carboxy BODIPYs.[13]

Figures & Schemes

Figure B1 *Calculated HOMO levels for BODIPYs with various 2,6-substitution*[2]

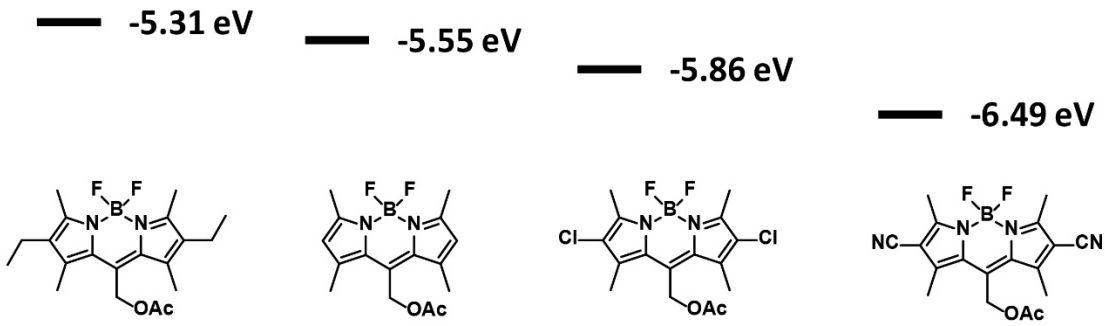

Scheme B1 *Synthetic routes towards 2,6-dichloro VoltageFluors*

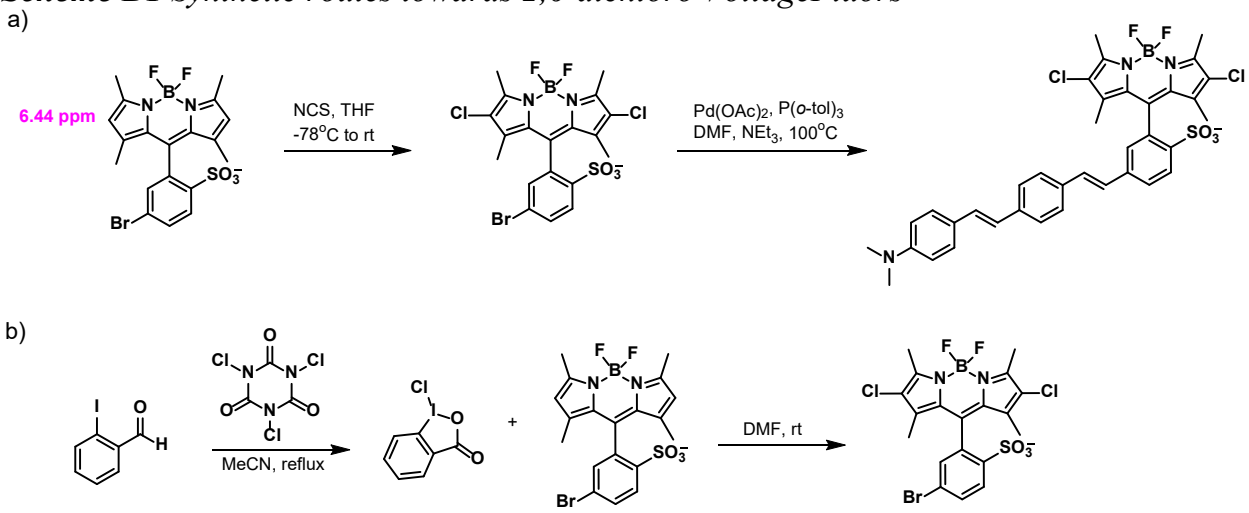

Figure B2 *Thin layer chromatography (TLC) of NCS chlorination reaction*

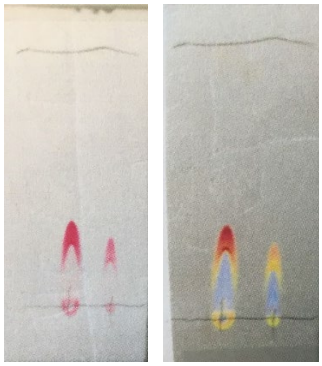

Figure B2. Thin layer chromatography (TLC) of crude reaction of TM*m*Br chlorination with NCS. Left under ambient light, right under long wave illumination. The orange fluorescence suggests the successful addition of the chlorines.

Figure B3 *Possible mass confirmation of di-chlorinated product*

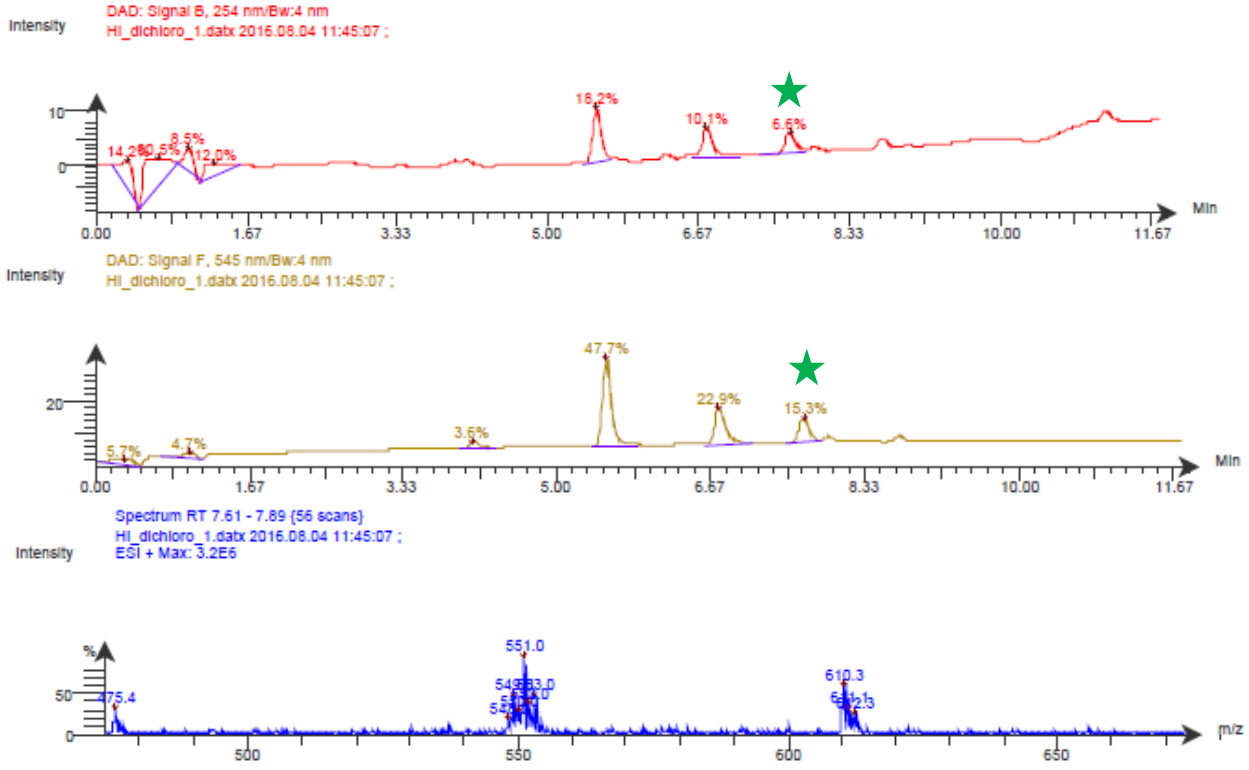

Experimental

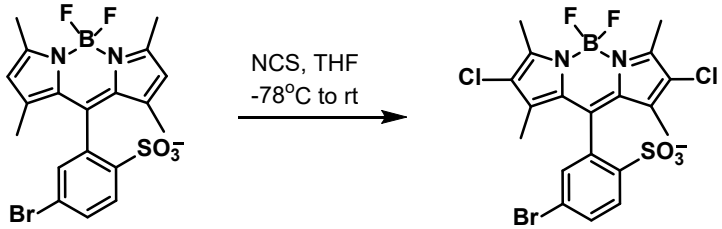

TM*m*Br chlorination with NCS. In a flame-dried round-bottom flask, TMmBr **12** (174.2 mg, 0.36 mmol, 1 equiv) was dissolved in anhydrous THF (6 mL). The solution was chilled to –78 °C in a small dewar containing dry ice and acetone. NCS (96.5 mg, 0.72 mmol, 2 eq) was added in two portions, and reaction slowly warmed to rt. After 24 h, diluted with 20 mL EtOAc, washed with brine (30 mL), dried over Na_2SO_4, gravity filtered, and solvents removed *in vacuo*. Flash chromatography (1 → 7% MeOH in DCM, gradient) yielded the suspected product as a pink solid.

^{1}H NMR (600 MHz, MeOD) δ 8.03 (d, *J* = 8.6 Hz, 1H), 7.85 (dd, *J* = 2.0, 8.4 Hz, 1H), 7.56 (d, *J* = 2.0 Hz, 1H), 3.41 (s, 6H), 1.55 (s, 6H). **LRMS (ESI$^+$)** calculated for $C_{19}H_{16}BBrCl_2FN_2O_3S^+$ [M-F]$^+$ 530.9519, found 581.2. **HRMS (ESI$^-$)** calculated for $C_{19}H_{14}BBrCl_2F_2N_2O_3S^-$ [M-H]$^-$ 547.9352, found 610.9605, 580.9507.

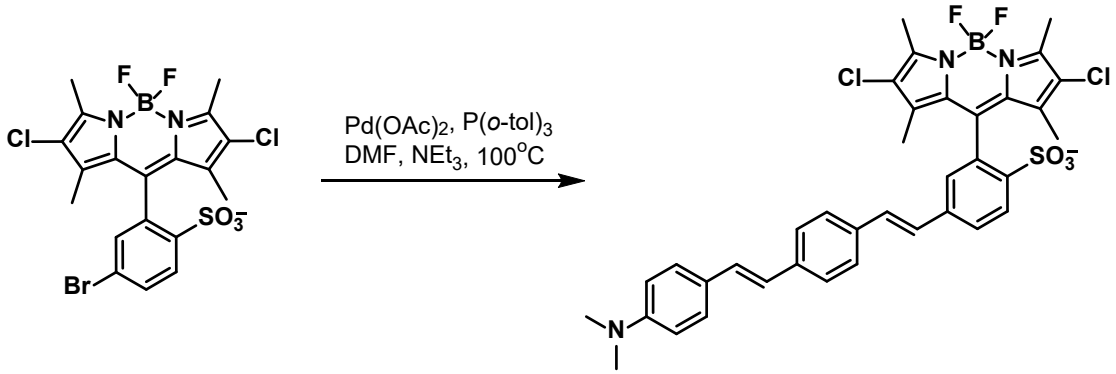

Heck coupling on NCS chlorination product. To a flame-dried 10 mL Schlenk flask were added the suspected 2,6-dichloro ortho-sulfonated BODIPY (118.2 mg, 0.21 mmol, 1 eq), molecular wire **4** (58.8 mg, 0.24 mmol, 1.1 eq), $Pd(OAc)_2$ (4.3 mg, 0.02 mmol, 9 mol%), and P(*o*-tol)$_3$ (11.8 mg, 0.04 mmol, 18 mol%). Flask was evacuated/backfilled 3x with N_2, then DMF (2.9 mL) and NEt_3 (1.4 mL) were added, Schlenk flask was sealed shut, and stirred at 70 °C 17 h. Concentrated reaction *in vacuo*, diluted with DCM (20 mL), washed with water (30 mL) and brine (30 mL), dried over Na_2SO_4, gravity filtered, and solvents removed *in vacuo*. Preparative thin layer chromatography (10% MeOH + 0.5% NEt_3) yielded the suspected product as a coral solid.

^{1}H NMR (400 MHz, Chloroform-*d*) δ 8.21 (d, *J* = 8.2 Hz, 1H), 7.68 (d, *J* = 7.5 Hz, 1H), 7.46 (s, 4H), 7.41 (d, *J* = 8.7 Hz, 2H), 7.32 (d, *J* = 1.9 Hz, 1H), 7.16 (d, *J* = 15.9 Hz, 1H), 7.12 – 7.03 (m, 2H), 6.90 (d, *J* = 16.2 Hz, 1H), 6.71 (d, *J* = 8.7 Hz, 2H), 2.99 (s, 7H), 2.55 (s, 5H), 1.55 (d, *J* = 2.6 Hz, 6H). **LRMS (ESI$^+$)** calculated for $C_{37}H_{35}BCl_2F_2N_3O_3S^+$ [M+H]$^+$ 720.1832, found 571.2 (5.96 min), 761.2, 763.3 (6.59 min).

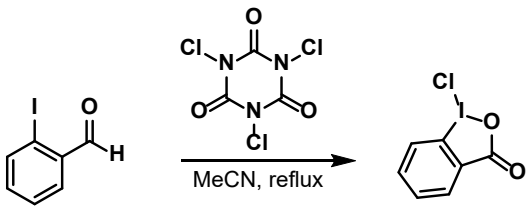

1-chloro-1,2-benziodoxol-3-one. An oven-dried 3-neck round-bottom flask was equipped with a condenser, addition funnel, and one septum. 2-iodobenzoic acid (4.97 g, 20 mmol) was dissolved in MeCN (38 mL) and heated to 75 °C. The addition funnel was charged with a solution of trichloroisocyanuric acid (1.58 g, 6.8 mmol) in MeCN (7.5 mL). Solution was slowly added to the reaction flask over 5 min. Addition funnel was rinsed with 5 mL MeCN once empty and reaction refluxed for another 5 min. Reaction was then filtered over a pad of celite, washed with hot MeCN, and concentrated *in vacuo*. Resulting yellow solid was filtered and washed with cold MeCN. Crystals were dried *in vacuo*, yielding the product as light yellow crystals (4.08 g, 72%).
NMR spectrum matched the reported spectrum.[14]

^{1}H NMR (300 MHz, $CDCl_3$): δ 7.79 (m, 1H), 7.99 (ddd, J = 8.6, 7.2, 1.6 Hz, 1H), 8.23 (ddd, J = 14.0, 8.0, 1.3 Hz, 2H).

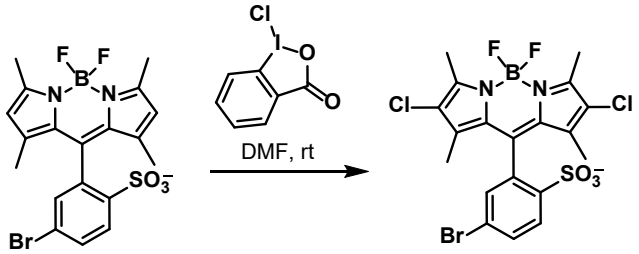

TM*m*Br chlorination with 1-chloro-1,2-benziodoxol-3-one. TM*m*Br **12** (129.1 mg, 0.26 mmol, 1 eq) was dissolved in anhydrous DMF (1.79 mL), then 1-chloro-1,2-benziodoxol-3-one (166.4 mg, 0.59 mmol, 2.2 eq) was added and reaction stirred at rt 18 h. Poured reaction into a separatory funnel with sat. aq. $NaHCO_3$ (20 mL), extracted with EtOAc (3 x 20 mL), dried over Na_2SO_4, gravity filtered, and solvents removed *in vacuo*. Flash chromatography (3 → 7% MeOH in DCM) caused product to decompose. NMR data included is for crude NMR.

^{1}H NMR (300 MHz, Acetone-d_6) δ 8.03 (m, 7H—overlapped with DMF, should be 1H), 7.84 (dd, J = 8.5, 2.1 Hz, 2H), 7.53 (d, J = 2.2 Hz, 2H), 2.55 (s, 6H), 1.54 (d, J = 4.9 Hz, 10H), 1.49 (s, 7H). **LRMS (ESI$^+$)** calculated for $C_{19}H_{16}BBrCl_2F_2N_2O_3S^+$ $[M+H]^+$ 550.95814, found 551.0 (7.52 min).

Compound Spectra

Chlorination with NCS

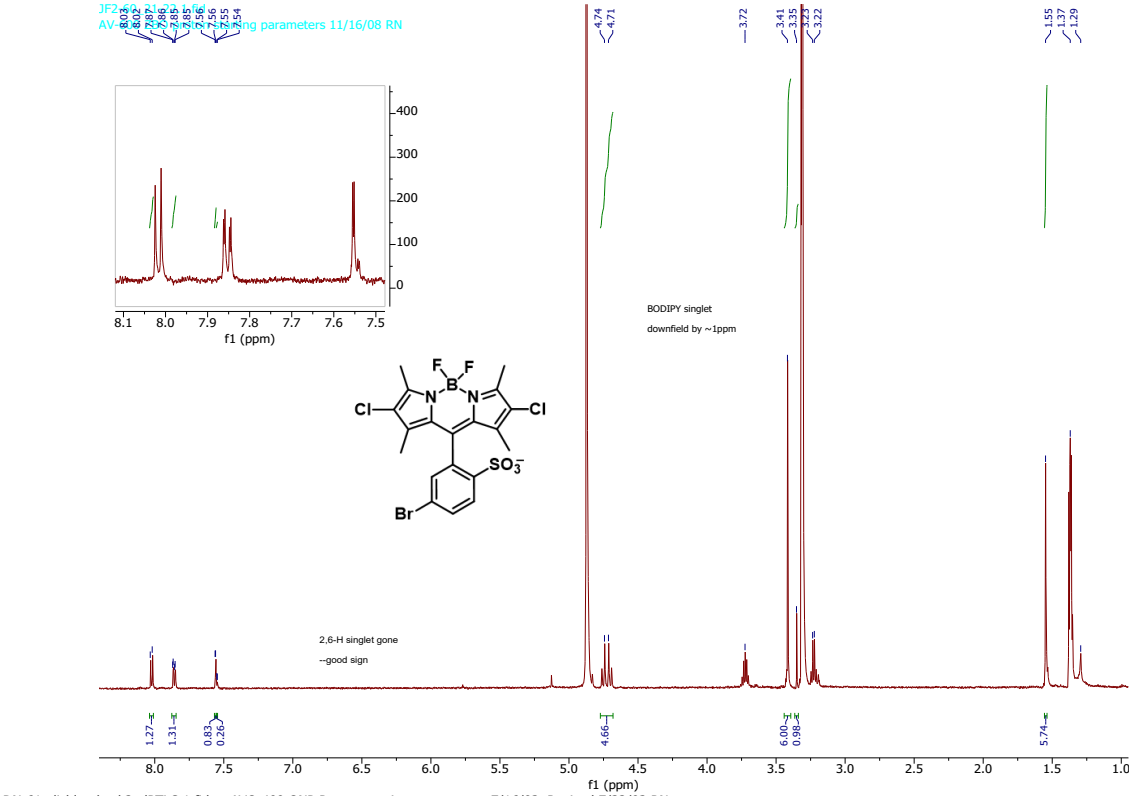

DN-61_dichloroheck2ndPTLC.1.fid — AVQ-400 QNP Proton starting parameters. 7/16/03. Revised 7/22/03 RN

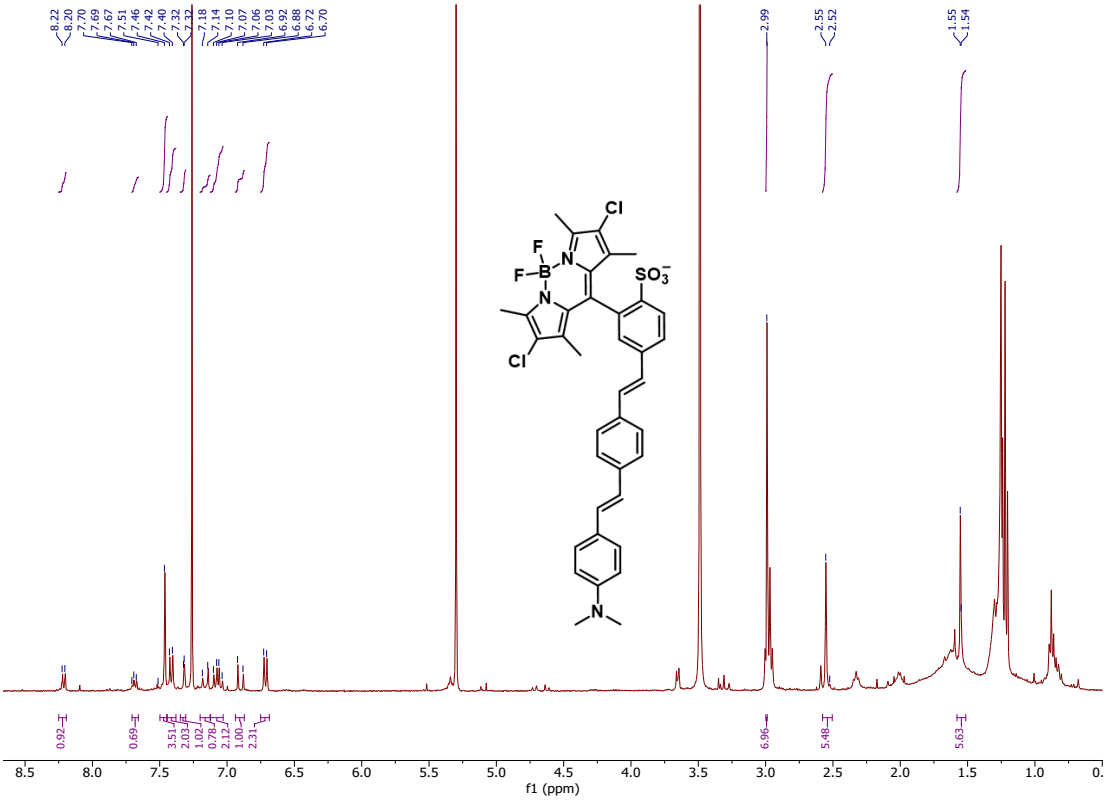

Crude NMR of HI-Cl chlorination

JF-HI-Cl_WU.1.fid — AV-300 Dual C-H probe proton starting parameters 7/23/03 RN.

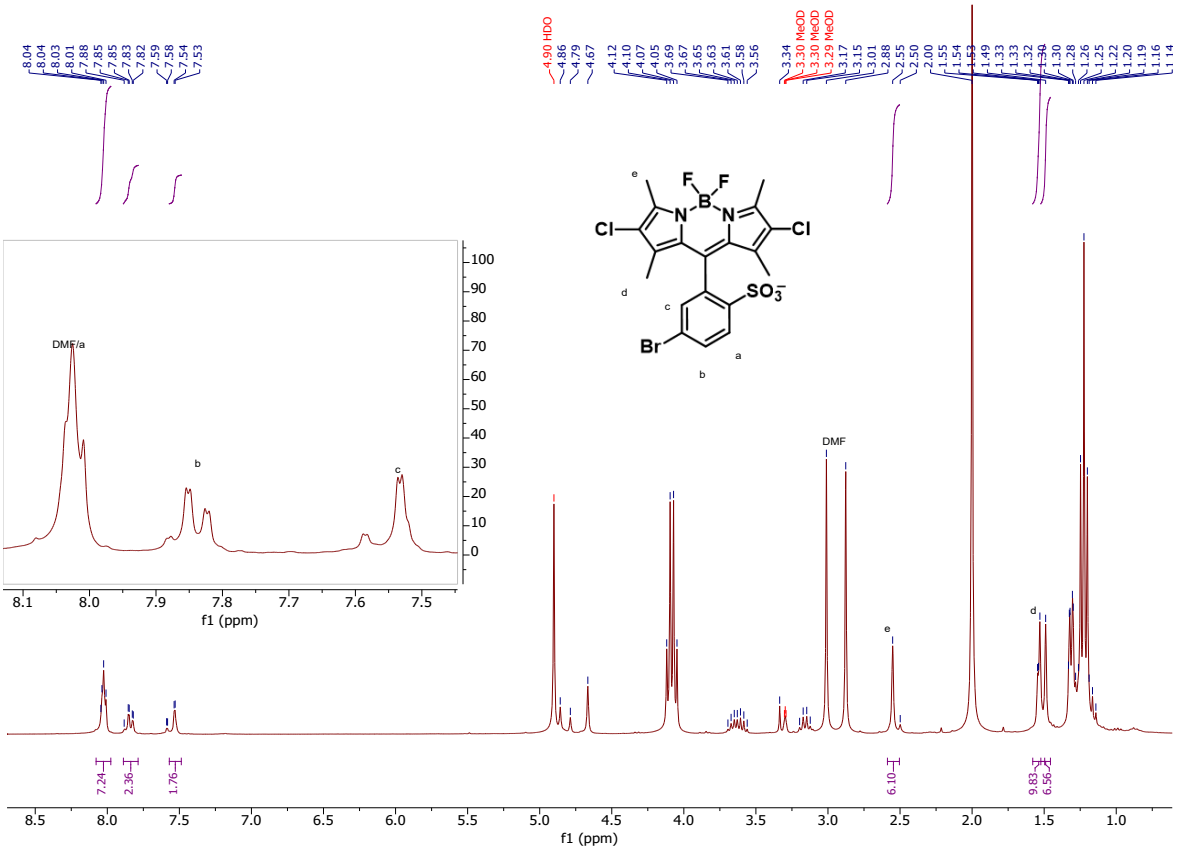

References

(1) Loudet, A.; Burgess, K. BODIPY Dyes and Their Derivatives: Syntheses and Spectroscopic Properties. *Chem. Rev.* **2007**, *107*, 4891–4932.

(2) Lincoln, R.; Greene, L. E.; Krumova, K.; Ding, Z.; Cosa, G. Electronic Excited State Redox Properties for BODIPY Dyes Predicted from Hammett Constants: Estimating the Driving Force of Photoinduced Electron Transfer. *J. Phys. Chem. A* **2014**, *118* (45), 10622–10630.

(3) Kulkarni, R. U.; Vandenberghe, M.; Thunemann, M.; James, F.; Andreassen, O. A.; Djurovic, S.; Devor, A.; Miller, E. W. In Vivo Two-Photon Voltage Imaging with Sulfonated Rhodamine Dyes. *ACS Cent. Sci.* **2018**, *4*, 1371–1378.

(4) Deal, P. E.; Kulkarni, R. U.; Al-Abdullatif, S. H.; Miller, E. W. Isomerically Pure Tetramethylrhodamine Voltage Reporters. *J. Am. Chem. Soc* **2016**, *138*, 9085–9088.

(5) Huang, Y. L.; Walker, A. S.; Miller, E. W. A Photostable Silicon Rhodamine Platform for Optical Voltage Sensing. *J. Am. Chem. Soc.* **2015**, *137* (33), 10767–10776.

(6) Kamkaew, A.; Hui Lim, S.; Hong Boon Lee, bc; Voon Kiew, L.; Yong Chung, L.; Burgess, K. BODIPY Dyes in Photodynamic Therapy. *Chem. Soc. Rev.* **2013**, *42*, 77–88.

(7) Meng, L.-B.; Zhang, W.; Li, D.; Li, Y.; Hu, X.-Y.; Wang, L.; Li, G. PH-Responsive Supramolecular Vesicles Assembled by Water-Soluble Pillar[5]Arene and a BODIPY Photosensitizer for Chemo-Photodynamic Dual Therapy. *Chem. Commun.* **2015**, *51*, 14381–14384.

(8) Awuah, S. G.; Das, S. K.; D'Souza, F.; You, Y. Thieno-Pyrrole-Fused BODIPY Intermediate as a Platform to Multifunctional NIR Agents. *Chem. - An Asian J.* **2013**, *8* (12), 3123–3132.

(9) Awuah, S. G.; You, Y. Boron Dipyrromethene (BODIPY)-Based Photosensitizers for Photodynamic Therapy. *RSC Adv.* **2012**, *2*, 11169–11183.

(10) Yogo, T.; Urano, Y.; Ishitsuka, Y.; Maniwa, F.; Nagano, T. Highly Efficient and Photostable Photosensitizer Based on BODIPY Chromophore. *J. Am. Chem. Soc.* **2005**, *127*, 12162–12163.

(11) Niu, S. L.; Ulrich, G.; Ziessel, R.; Kiss, A.; Renard, P. Y.; Romieu, A. Water-Soluble BODIPY Derivatives. *Org. Lett.* **2009**, *11* (10), 2049–2052.

(12) Wang, M.; Zhang, Y.; Wang, T.; Wang, C.; Xue, D.; Xiao, J. Story of an Age-Old Reagent: An Electrophilic Chlorination of Arenes and Heterocycles by 1-Chloro-1,2-Benziodoxol-3-One. *Org. Lett.* **2016**, *18*, 1976–1979.

(13) Komatsu, T.; Urano, Y.; Fujikawa, Y.; Kobayashi, T.; Kojima, H.; Terai, T.; Hanaoka, K.; Nagano, T. Development of 2,6-Carboxy-Substituted Boron Dipyrromethene (BODIPY) as a Novel Scaffold of Ratiometric Fluorescent Probes for Live Cell Imaging. *Chem. Commun.* **2009**, *45*, 7015–7017.

(14) Matoušek, V.; Pietrasiak, E.; Schwenk, R.; Togni, A. One-Pot Synthesis of Hypervalent Iodine Reagents for Electrophilic Trifluoromethylation. *J. Org. Chem.* **2013**, *78* (13), 6763–6768.

Appendix C: Alternate routes towards BODIPY-based VoltageFluor scaffolds

Portions of this work were performed in collaboration with the following persons:
Synthesis with Divya Natesan and Evan Koretsky

Introduction

2,6-dicarboxy BODIPY VoltageFluors proved difficult to synthesize via traditional Heck couplings (**Chapter 2, Scheme C1**). We decided to pursue Suzuki couplings because we had some success using a *N*-methyliminodiacetic acid (MIDA) boronate molecular wire **1.13** in a Suzuki coupling with a zwitterionic BODIPY (**Chapter 1, Scheme C2a**), and Suzuki couplings are generally reliable and mild.[1,2]

A second strategy I designed is a linear bottom-up route towards the VoltageFluor scaffold (**Scheme C4**). This route is less convergent than a Heck or Suzuki strategy, but allows for formation of the fluorophore last. This is advantageous because the BODIPY fluorophore is acid- and base-sensitive, and we often observe decomposition of the fluorophore during palladium-catalzyed cross coupling reactions due to the combination of base and heat.

Results & Discussion

Suzuki coupling strategy toward BODIPY VoltageFluors

The previous method used to transform molecular wire **4** into a Suzuki partner was olefin metathesis with a vinyl MIDA boronate (**Scheme C2a**). While it worked, the reaction resulted in a mixture of difficult to separate *E/Z* isomers, the product **1.16** had very limited solubility, and we only obtained a 6% yield. We decided to try a recently reported boryl Heck strategy for synthesizing alkenyl boronic esters.[3] This method reported 97-99% isolated yields of the desired *E* isomer for electron rich styrene substrates similar to molecular wire **4** (**Scheme C2b**).

The catalyst for the boryl Heck coupling **5.2** and catecholchloroborane **5.1** were synthesized according to reported methods.[3] Catecholchloroborane was stored and transferred to the reaction flask in a nitrogen-flushed glovebag. Our first attempts at following the literature procedure exactly for the boryl Heck coupling (**Scheme C2b**) were unsuccessful. Molecular wire **4** was not very soluble in α,α,α-trifluorotoluene at the reported concentration of 0.5M, and the substrates reported in the literature were also oils, facilitating the concentrated reaction. We contacted the first author on the methods paper, Dr. William Reid, and he advised that while DCM or DMF solvents did not work for this methodology, a toluene co-solvent of up to 50% could be used without affecting the reaction, and the reaction should still work at a lower concentration. Decreasing the reaction concentration and switching to EtOAc:hexanes column eluent instead of the reported DCM:hexanes eluent for column chromatography purification eventually yielded our desired boronic acid pinacol (Bpin) molecular wire **5.3**.

Both MIDA boronate wire **1.13** and Bpin molecular wire **5.3** have advantages and disadvantages in their synthesis, purification, and bench stability. The synthesis of MIDA boronate **1.13** is simpler because the reagents are all commercially available and the olefin metathesis reaction is very simple to set up,[4] but it formed a ~1:1 mixture of *E*/*Z* isomers. Bpin molecular wire **5.3** required synthesizing the catecholchloroborane **5.1** and catalyst **5.2**, though both could be done on large gram-scales.[3] Setting up the boryl Heck coupling was more complex—the catecholchloroborane was transferred to a flame-dried Schlenk flask in a nitrogen flushed glovebag, then it stirred with the palladium complex and base for 15 min, then molecular wire **4** and additional solvent were added. In terms of purification, both were difficult, as boronate esters have poor solubility in many organic solvents. The purification of Bpin wire **5.3** was slightly easier because the boryl Heck coupling was much more selective for the desired *E*-isomer than the olefin metathesis reaction that formed MIDA boronate **1.13**. MIDA boronate **1.13** had much better bench stability than Bpin wire **5.3**—**1.13** was stable at room temperature under air, but **5.3** was found to

decompose within a month or two via protodeborylation back to molecular wire **4** in a -20 °C freezer. Flushing the scintillation vial with nitrogen then storing Bpin wire **5.3** in a -80 °C freezer slowed the decomposition, but the freeze-thaw cycles each time the wire was used still slowly lead to decomposition.

Once the Bpin wire **5.3** was isolated, we tried a wide variety of Suzuki coupling conditions (**Table C1**), unfortunately without success. We next decided to pursue a "bottom up" route, that would ideally couple molecular wire **4** to sulfonated aldehyde **9**, followed by a BODIPY condensation to yield the desired dicarboxy probes.

"Bottom-up" linear strategy towards BODIPY VoltageFluors

When we performed a Heck coupling between molecular wire **4** and sulfonated aldehyde **9**, we were pleased that it gave much better conversion to product than Heck couplings on 2,6-dicarboxy BODIPY **32**. NMR analysis determined that the isolated product was in fact the undesired geminal product **5.5**, not the trans product **5.4** (**Scheme C4, Figure C1**). This came as a surprise, because all our previous Heck couplings between molecular wire **4** with fluorophores as the aryl bromide yielded the desired trans product.

The electronics of the alkene coupling partner play a large role in the regiochemical outcome of Heck-type cross coupling reactions.[5,6] The migratory insertion step is thought to be irreversible, thus determining the regiochemical outcome, and occurs preferentially at the more electron deficient alkene carbon.[5] In the case of our aniline-based molecular wire **4**, the terminal olefin carbon would have a δ– charge, and the internal olefin carbon has more δ+ charge. Because sulfonated aldehyde **9** is a relatively small cross-coupling partner, electronics dominated over sterics and the migratory insertion step occurred at the internal olefin carbon, leading to the undesired geminal product.

To have the electronics of the Heck coupling work in our favor, I designed a synthetic route that reversed the Heck coupling partners to favor the desired regiochemistry (**Scheme C5**). Aldehyde **9** was converted from an aryl bromide to the styrene coupling partner **5.6** via a Suzuki coupling with potassium vinyltrifluoroborate, The corresponding aryl bromide coupling partner **5.8** was synthesized by forming a Horner-Wadsworth-Emmons reagent from 4-bromobenzyl bromide, and reacting it with 4-(dimethylamino)-benzaldehyde.[7] Our standard Heck coupling conditions of $Pd(OAc)_2$, P(*o*-tol)$_3$, DMF, and NEt_3 resulted in sub-par conversion for these substrates, possibly because electron-rich aryl bromides such as **5.8** have slower rates of oxidative addition compared to electron-poor aryl bromides.

We found an interesting Heck coupling in the literature that formed sulfonated stilbenes using just $Pd(OAc)_2$ as catalyst and triethanolamine as solvent, ligand, and base.[8,9] This methodology worked well for the Heck coupling between **5.6** and **5.8**, consistently giving 60-70% conversion to the desired all-trans product (**Scheme C5**). Purification of Heck product **5.4** was challenging because of the product's very polar, zwitterionic character. The triethanolamine could not be removed via an aqueous work-up because **5.4** was also water-soluble, even at acidic pH. Instead we had to crash out the crude product in a large excess of diethyl ether (1/100 v/v), and then purify the product via a long silica column.

When we subjected **5.4** to a BODIPY condensation in DMF with 2,4-dimethylpyrrole-3-carboxylic acid **31** (**Scheme C5**), we did see some promising orange/pink spots by TLC after treatment with DDQ, both typical colors for the dipyrromethene intermediate before chelating boron. We observed multiple slightly green fluorescent spots after treatment with DIPEA and $BF_3{\cdot}Et_2O$. Because the fluorophore was quenched by the molecular wire, it was difficult to tell

which spot on the TLC was the desired product. Product **28** was not cleanly isolated from our two attempts at this condensation, but it likely could be optimized as a second route to BODIPY VoltageFluors. Once the more convergent Heck coupling route employing benzyl protecting groups on the carboxylates (**Chapter 2**) proved to be higher yielding and much easier to purify than sulfonated aldehyde **5.4**, we redirected our efforts to focus entirely on that route.

Conclusion/Future Work

Neither the Suzuki strategy or bottom-up route ended up being the best route toward BODIPY VoltageFluors, but both yielded potentially useful synthetic intermediates that are generalizable to VoltageFluors with any fluorophore. Both boronate ester molecular wires **1.13** and **5.3** could be useful Suzuki coupling partners for VoltageFluor synthesis. MIDA boronate **1.13** is shorter to synthesize and more bench stable than Bpin wire **5.3**, and if the *E/Z* isomer ratio could be improved in the olefin metathesis reaction, it likely would be the superior Suzuki wire partner. Before I employed the HWE strategy to synthesize aryl bromide **5.8**, I synthesized it via a Wittig strategy that yielded a 1:1 mixture of *E/Z* isomers, and was able to isomerize most of the (*Z*)-isomer to the desired (*E*)-isomer by heating in toluene with trace iodine.[10] This strategy could potentially be applied to MIDA boronate wire **1.16** to increase the amount of *E* product prior to purification.

The bottom-up route yielded a useful aldehyde building block for VoltageFluors, **5.4**. This intermediate could be useful for any fluorophore sensitive to the heat or base associated with Heck or Suzuki couplings. The Heck coupling conditions using triethanolamine as solvent, ligand, and base are also very robust and could be useful for other highly polar Heck coupling substrates.

Figures & Schemes

Scheme C1 *Heck coupling conditions attempted on 2,6-dicarboxy BODIPY* ***32***

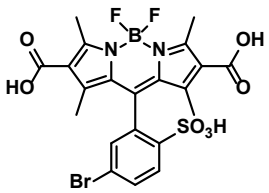

32

Molecular wire
$Pd(OAc)_2$, $P(o\text{-}tol)_3$
DMF, NEt_3
70°C
→ no rxn, starting material still intact

Molecular wire
$Pd(OAc)_2$, $P(o\text{-}tol)_3$
DMF, NEt_3
100°C
→ works for normal wire sometimes, sometimes significant decomp or decarboxylation due to base

Molecular wire
$Pd_2(dba)_3$, $P(tBu)_3$
DMF, Cs_2CO_3
70°C
→ decomp

Molecular wire
$Pd_2(dba)_3$, $P(tBu)_3$
DMF, NEt_3
70°C
→ decomp

Molecular wire
$Pd_2(dba)_3$, $P(tBu)_3$
DMF, no base
100°C
→ often no conversion, up to 20-30% conversion (better for normal and methyl wires than OMe)

Molecular wire
$Pd(OAc)_2$, XPhos
DMF, no base
100C
→ unmodified SM

Molecular wire
$Pd(OAc)_2$, SPhos
DMF, no base
100C
→ unmodified SM

Scheme C2 *Methods of Suzuki wire formation*

a)

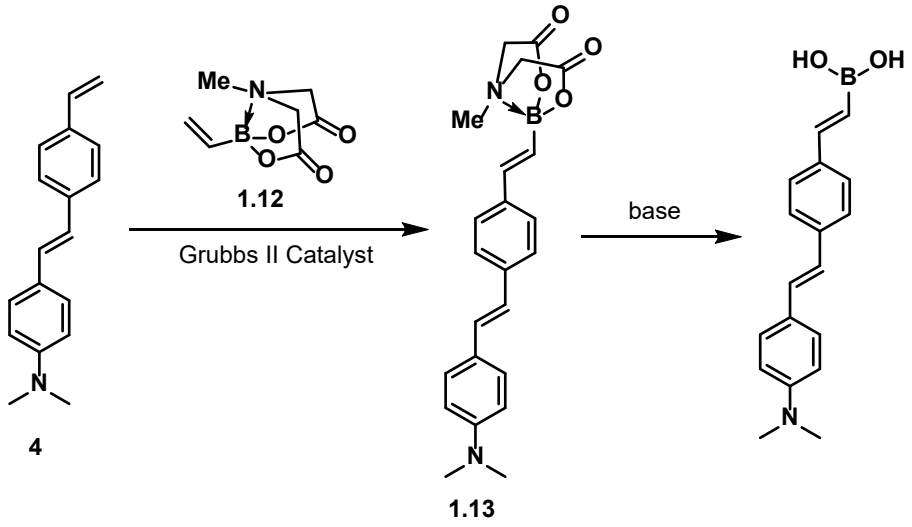

b)

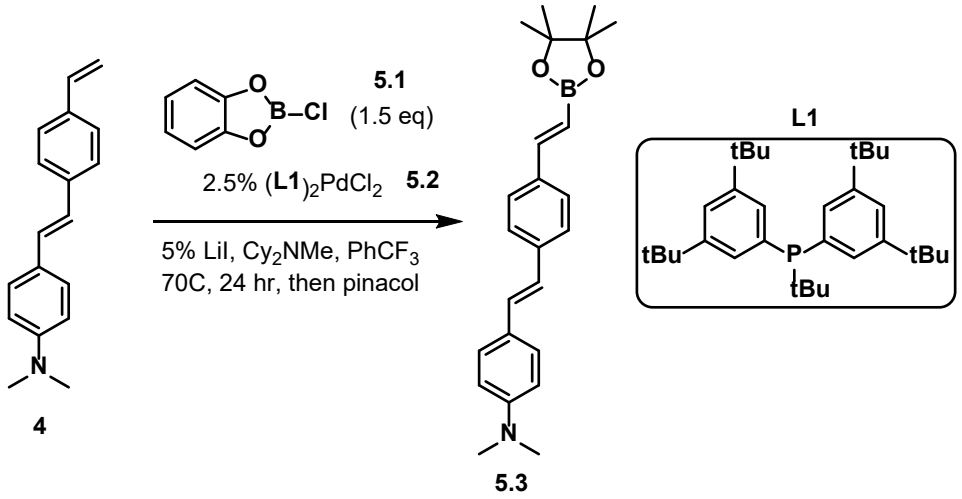

Reported substrates:

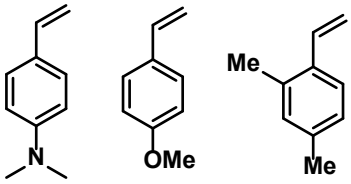

Scheme C3 *Synthesis of Boryl Heck reagents*

a)

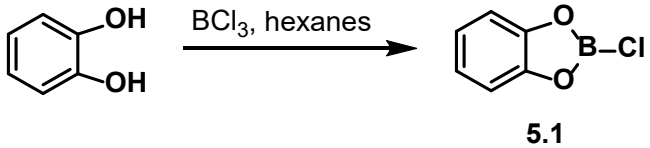

b)

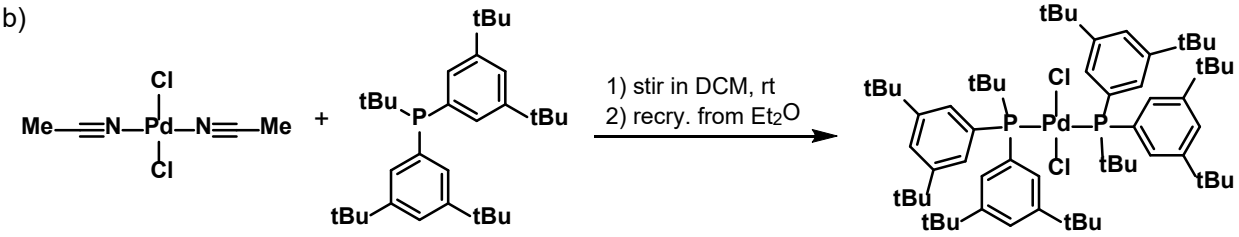

5.2

Table C1 *Suzuki coupling conditions*

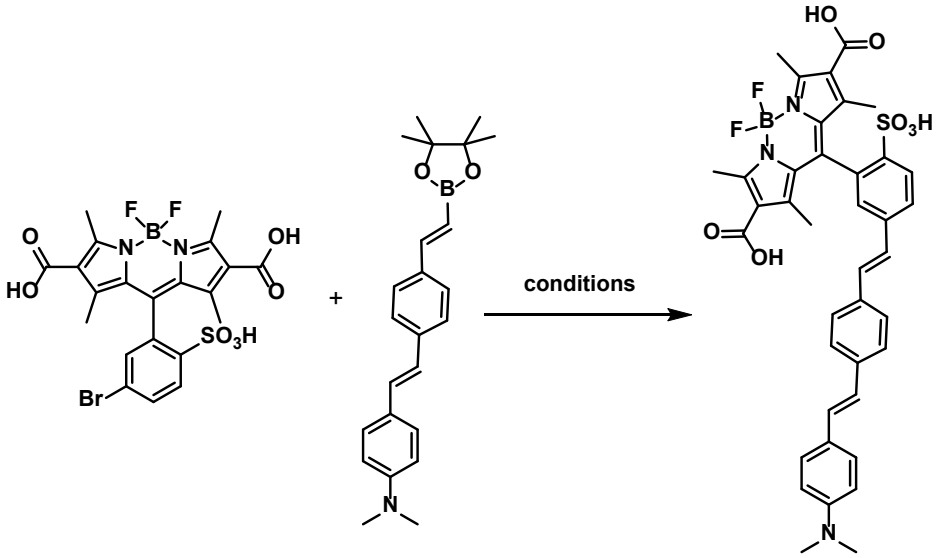

Entry	*Base*	*Catalyst*	*Cat. mol%*	*Ligand*	*Solvent*	*Temp*	*Result*
1	K_2CO_3	$PdCl_2(dppf)\text{-}CH_2Cl_2$	10	N/A	DMF	75	decomp
2	K_2CO_3	$PdCl_2(dppf)\text{-}CH_2Cl_2$	50	N/A	DMF	75	SM + decomp
3	K_3PO_4	$Pd(OAc)_2$	10	SPhos	4:1 dioxane:H_2O	40	SM
4	K_3PO_4	$Pd(OAc)_2$	10	SPhos	4:1 dioxane:H_2O	60	SM
5	K_3PO_4	$Pd(OAc)_2$	10	SPhos	4:1 dioxane:H_2O	100	SM + decomp
6	K_3PO_4	$PdCl_2(dppf)\text{-}CH_2Cl_2$	10	N/A	4:1 dioxane:H_2O	60	SM + decomp
7	K_3PO_4	$Pd(PPh_3)_4$	10	N/A	H_2O	100	SM + decomp

Scheme C4 *Heck coupling between Rishi's aldehyde and molecular wire yields geminal product*

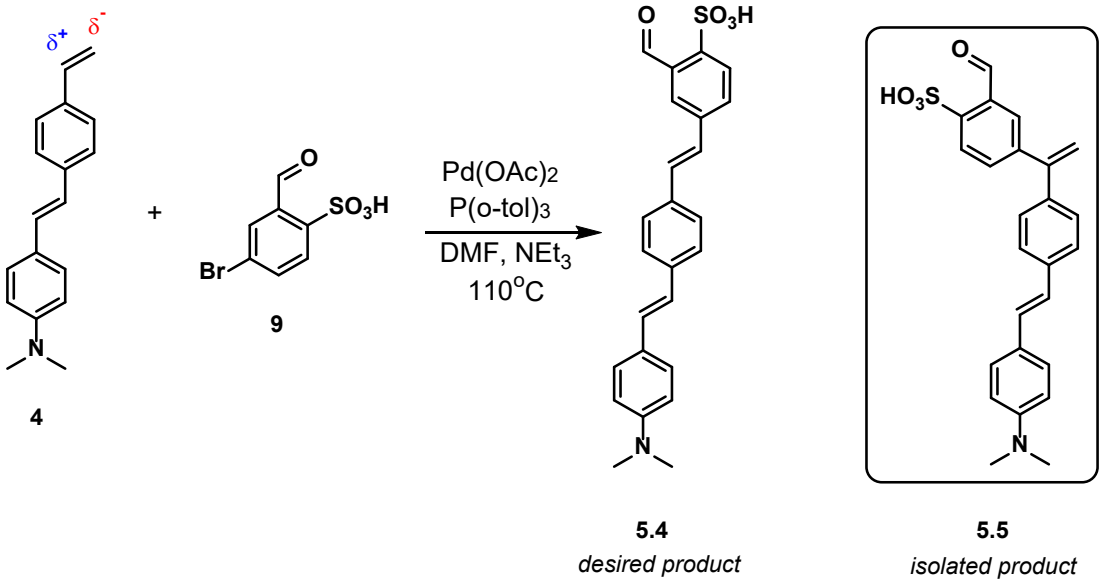

Figure C1 *^{1}H NMR assignment of geminal Heck product*

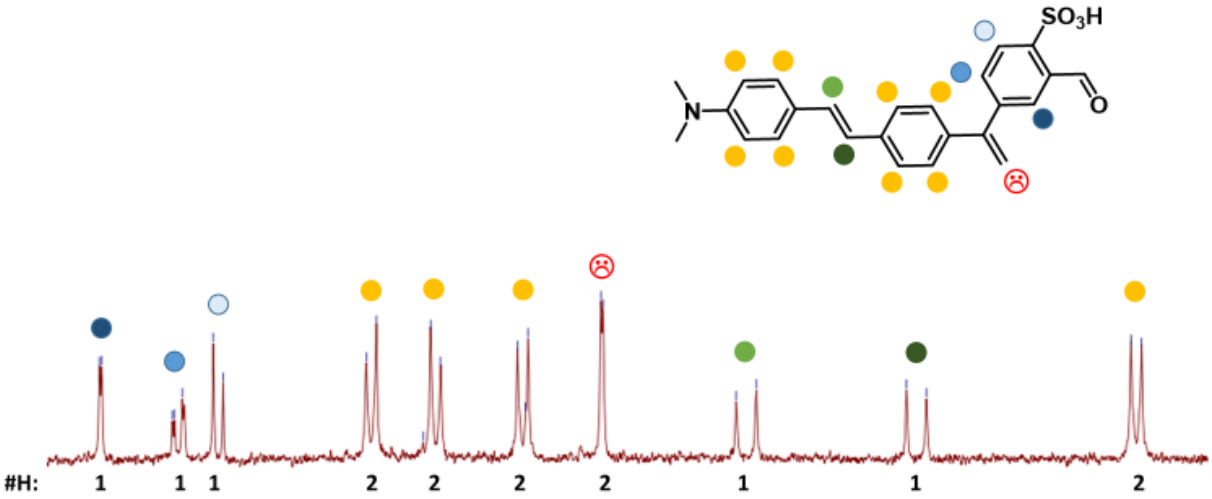

Scheme C5 *Bottom-up strategy to all trans sulf-ald-wire*

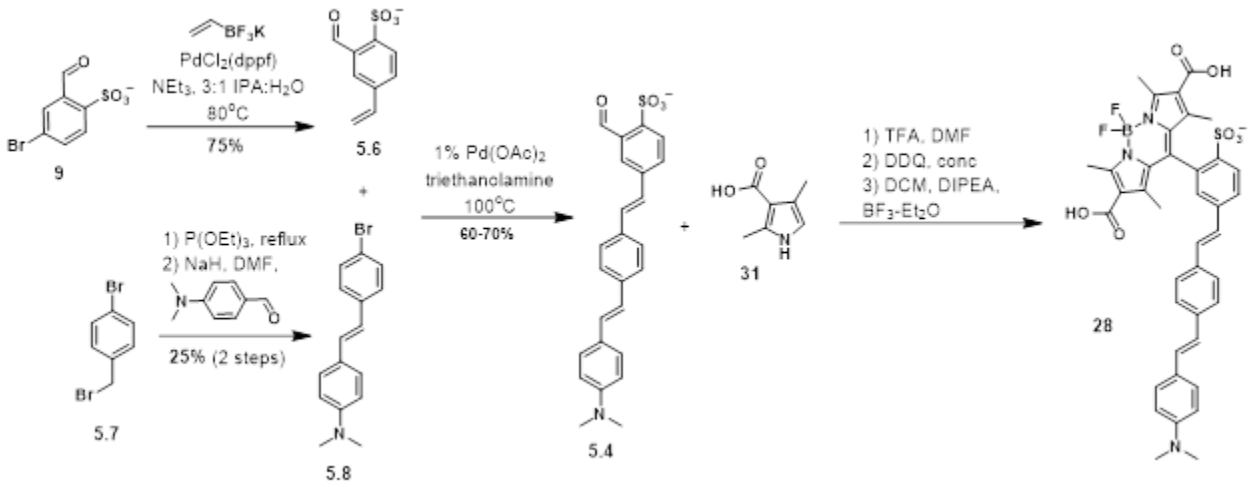

Experimental

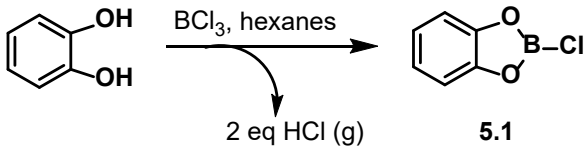

5.1

Catecholchloroborane (5.1). (Modified from Reid, et al. *J. Am. Chem. Soc.* **2016**, *138* (17), 5539–5542) An oven-dried Schlenk flask was charged with catechol (2.6 g, 23.6 mmol, 0.95 equiv), evacuated/backfilled with N_2 3x, then chilled to 0 °C in an ice bath. Anhydrous hexanes (50 mL) were transferred to the flask via cannula, then flask was equipped with an oven-dried addition funnel. 1M BCl_3 in heptane (24.9 mL, 25 mmol, 1 eq) was added to addition funnel, then added slowly dropwise to reaction flask. Reaction was allowed to slowly warm to rt and stir 18 h. Gently concentrated reaction *in vacuo*, with a trap of NaOH pellets in between flask and vacuum pump. **5.1** was isolated as a grey solid (3.7 g, quantitative).

^{1}H NMR (600 MHz, Chloroform-*d*) δ 7.24 (ddq, *J* = 12.8, 7.0, 3.1 Hz, 2H), 7.18 – 7.07 (m, 2H). **^{11}B NMR** (600 MHz, Chloroform-*d*) δ 28.9 ppm.

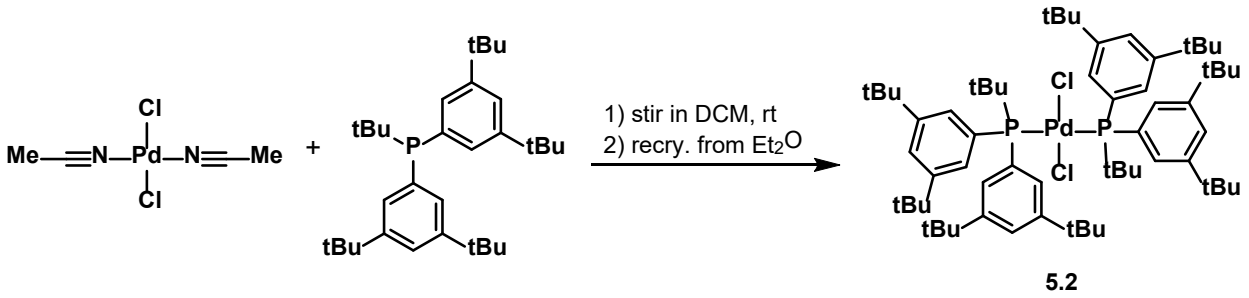

5.2

$(L_1)_2PdCl_2$ (5.2). (Modified from Reid, et al. *J. Am. Chem. Soc.* **2016**, *138* (17), 5539–5542) A flame-dried 25 mL round-bottom flask was charged with bis(3,5-di-tert-butylphenyl)(tert-butyl)phosphine (416 mg, 0.89 mmol, 2 eq), bis(acetonitrile)dichloropalladium (II) (115 mg, 0.45 mmol, 1 eq), dissolved in DCM (9 mL), and stirred at rt 30 min. Concentrated at rt under reduced pressure, added Et_2O to flask (5.6 mL), then placed in freezer 48 h. Mixture was filtered and washed with cold Et_2O (20 mL) to yield **5.2** as a fluffy, light yellow solid (424 mg, 86%).

^{1}H NMR (400 MHz, Chloroform-*d*) δ 8.18 (td, *J* = 5.3, 1.8 Hz, 8H), 7.70 (d, *J* = 1.8 Hz, 4H), 1.86 (t, *J* = 7.3 Hz, 17H), 1.43 (s, 72H). **^{31}P NMR** (400 MHz, Chloroform-*d*) δ 41.96 ppm.

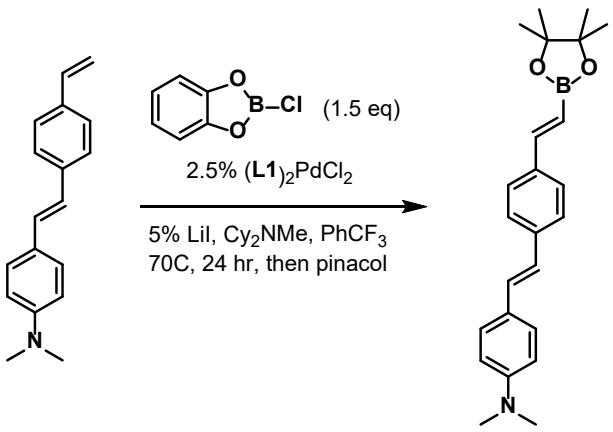

5.3

Bpin molecular wire (5.3). An oven-dried Schlenk flask was charged with catecholchloroborane **5.1** (102 mg, 0.66 mmol, 1.5 eq), $(L_1)_2PdCl_2$ 5.**2** (12.3 mg, 0.01 mmol, 2.5 mol%), and LiI (3.0 mg, 0.02 mmol, 5 mol%). Flask was evacuated/backfilled 3x with N_2, α,α,α-trifluorotoluene (441 µL) was added, then Cy_2NMe (472 µL, 2.2 mmol, 5 eq) and an additional 441 µL of trifluorotoluene were added and reaction stirred at 70 °C for 15 min. Flask was briefly opened and molecular wire **4** (110 mg, 0.44 mmol, 1 eq) was added. Reaction continued to stir at 70 °C for 24 h. Two hours in, an additional 500 µL of trifluorotoluene was added. After the 24 h, the reaction was removed from heat and pinacol (156.4 mg, 1.3 mmol, 3 eq) and trifluorotoluene (500 µL) were added and stirred for 1 h. Filtered solution through celite with DCM, washed filtrate with 1M HCl (3 x 20 mL), dried over Na_2SO_4, and concentrated *in vacuo*. Column chromatography on boric acid impregnated silica (5 → 8% EtOAc in hexanes, gradient) yielded Bpin wire **5.3** as a yellow-green solid (74 mg, 45%).

^{1}H NMR (300 MHz, Chloroform-*d*) δ 7.28 – 7.06 (m, 7H), 6.88 (d, *J* = 16.3 Hz, 1H), 6.70 (d, *J* = 16.2 Hz, 1H), 6.55 – 6.49 (m, 2H), 5.96 (d, *J* = 18.4 Hz, 1H), 2.80 (s, 6H), 1.13 (d, *J* = 2.4 Hz, 12H).

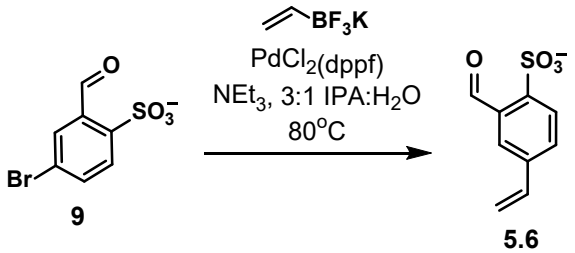

9 **5.6**

2-formyl-4-vinylbenzenesulfonate (5.6). Sulfonated aldehyde **9** (140.8 mg, 0.53 mmol, 1 eq), $PdCl_2$(dppf) (39 mg, 0.05 mmol, 10 mol%), and NEt_3 (222 µL, 1.6 mmol, 3 eq) were dissolved in IPA:H_2O (4:1.3 mL), then freeze-pump-thawed 3x with N_2. Reaction was heated to 80 °C 17 h, then solvents were removed *in vacuo*. Flash chromatography (12% MeOH in DCM) yielded **5.6** as an ivory solid (125.3 mg, 75%).

^{1}H NMR (400 MHz, Methanol-d_4) δ 10.90 (s, 1H), 7.99 – 7.91 (m, 2H), 7.73 (dd, J = 8.1, 2.0 Hz, 1H), 6.82 (dd, J = 17.6, 11.0 Hz, 1H), 5.94 (dd, J = 17.6, 0.7 Hz, 1H), 5.40 (dd, J = 11.0, 0.7 Hz, 1H).

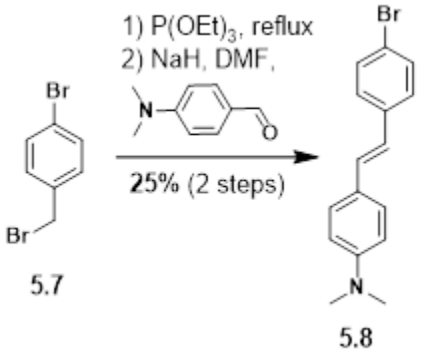

(*E*)-4-(4-bromostyryl)-N,N-dimethylaniline (5.8). 4-bromobenzyl bromide (1.5 g, 6 mmol, 1 eq) was added to a flame-dried round-bottom flask. Flask was equipped with a reflux condenser, evacuated/backfilled with N_2 3x, triethyl phosphate (3.1 mL, 18 mmol, 3 eq) was added via syringe and reaction refluxed at 160 °C for 2 h, then was concentrated *in vacuo*. NaH (576 mg, 24 mmol, 4 eq), 4-(dimethylamino)-benzaldehyde (895 mg, 6 mmol, 1 eq), and DMF (9 mL) were added, and reaction stirred at rt 18 h. Reaction was quenched with EtOH (20 mL) and water (50 mL), filtered over a Hirsch funnel, precipitate dissolved in DCM and washed with water (3 x 50 mL), then dried over Na_2SO_4 and concentrated *in vacuo*. Column chromatography (3 → 25% EtOAc in hexanes) yielded **5.8** as a white solid (455 mg, 25% over two steps).

^{1}H NMR (300 MHz, DMSO-d_6) δ 7.60 – 7.39 (m, 6H), 7.20 (d, J = 16.6 Hz, 1H), 7.03 – 6.91 (m, 1H), 6.75 (d, J = 8.4 Hz, 2H), 2.96 (s, 6H).

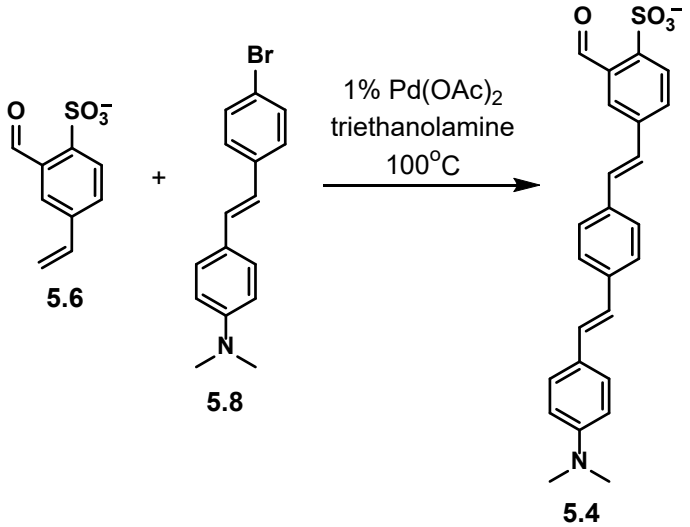

4-((*E*)-4-((*E*)-4-(dimethylamino)styryl)styryl)-2-formylbenzenesulfonate (5.4). A flame-dried 4 mL dram vial was charged with 2-formyl-4-vinylbenzenesulfonate **5.6** (98 mg, 0.46 mmol, 1.1 eq), aryl bromide **5.8** (127 mg, 0.42 mmol, 1 eq), and $Pd(OAc)_2$ (1 mg, 0.004 mmol, 1 mol%). Vial was evacuated/backfilled with N_2 3x, then triethanolamine (1.7 mL) was added, vial cap was sealed

shut with electrical tape, and reaction stirred at 100 °C 21 h. Reaction was diluted with MeOH (2 mL) and pipetted into Et_2O (400 mL). Resulting yellow precipitate was purified via column chromatography (10 → 15% MeOH in DCM) yielding **5.4** as a yellow solid (12.9 mg, 7%) alongside mixed fractions that were later purified by a second column.

^{1}H NMR (500 MHz, DMF-d_7) δ 11.36 (s, 1H), 8.17 (d, J = 8.0 Hz, 1H), 8.07 (dd, J = 8.0, 1.9 Hz, 1H), 7.90 (d, J = 8.1 Hz, 2H), 7.80 (d, J = 8.2 Hz, 2H), 7.76 – 7.67 (m, 3H), 7.67 – 7.56 (m, 2H), 7.46 (d, J = 16.3 Hz, 1H), 7.27 (d, J = 16.3 Hz, 1H), 6.98 (d, J = 8.6 Hz, 2H), 3.18 (s, 6H).

Compound Spectra

JF3-74_catBClcrude.1.fid — AV-600 ZBO proton starting parameters 11/16/08 RN

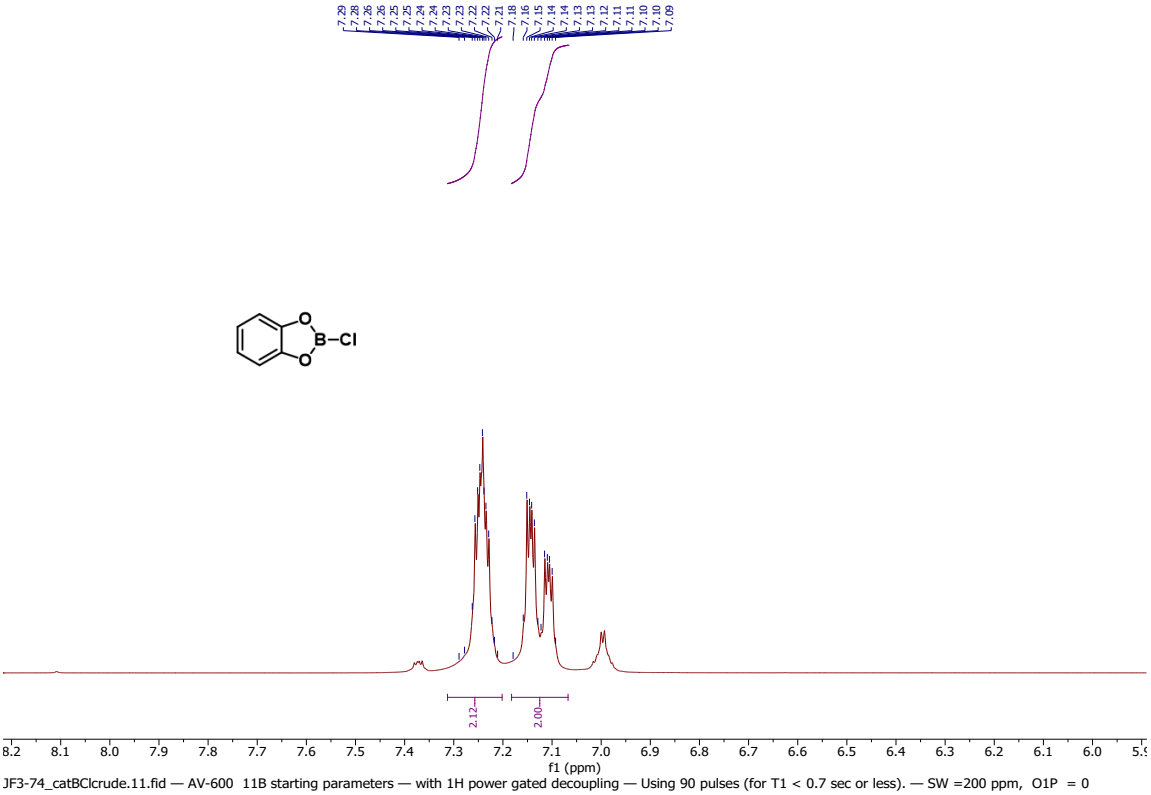

JF3-74_catBClcrude.11.fid — AV-600 11B starting parameters — with 1H power gated decoupling — Using 90 pulses (for T1 < 0.7 sec or less). — SW =200 ppm, O1P = 0

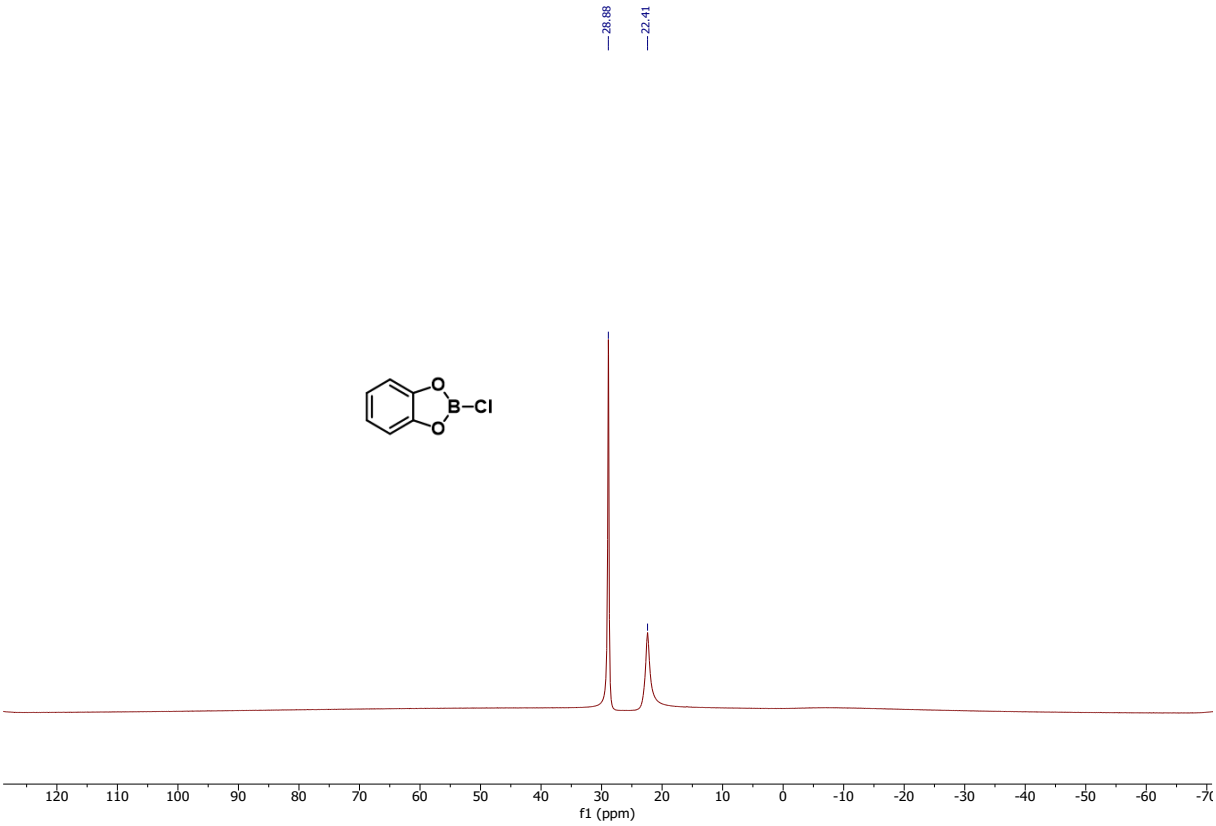

DN-134_conc.1.fid — AVQ-400 QNP Proton starting parameters. 7/16/03. Revised 7/22/03 RN

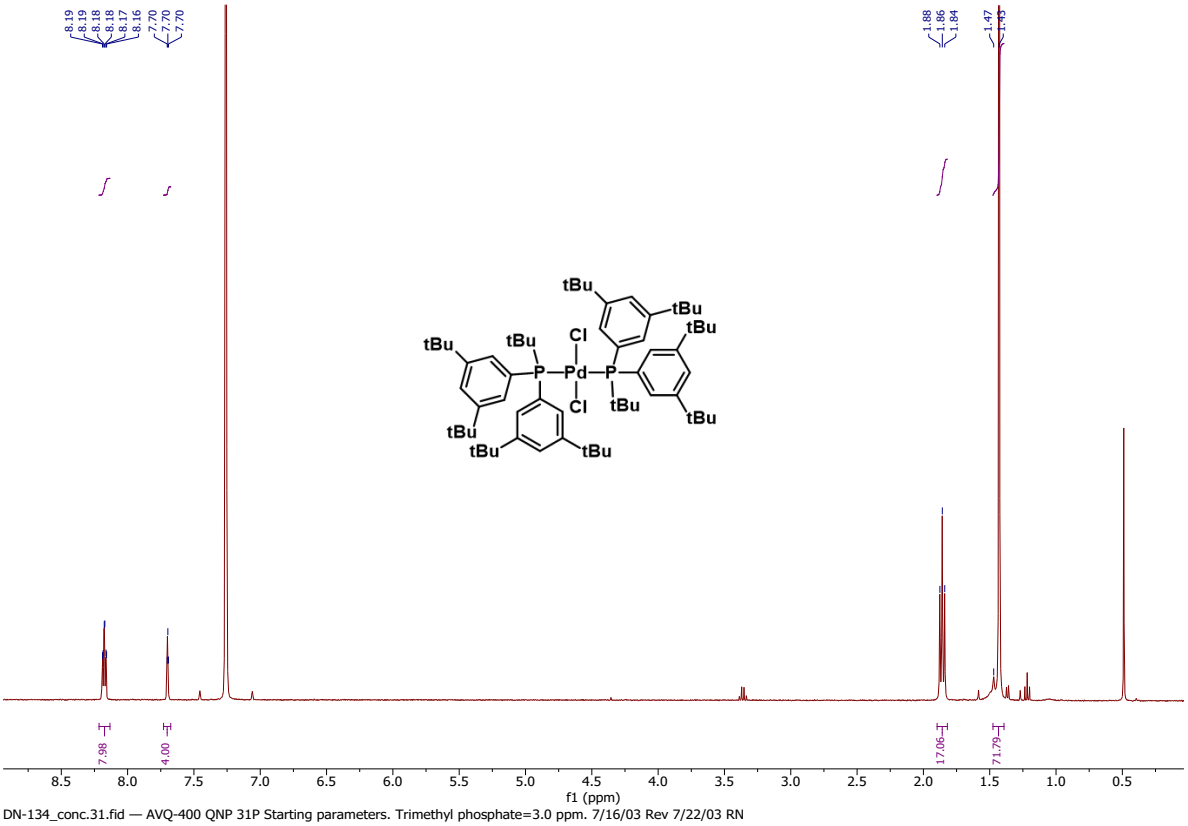

DN-134_conc.31.fid — AVQ-400 QNP 31P Starting parameters. Trimethyl phosphate=3.0 ppm. 7/16/03 Rev 7/22/03 RN

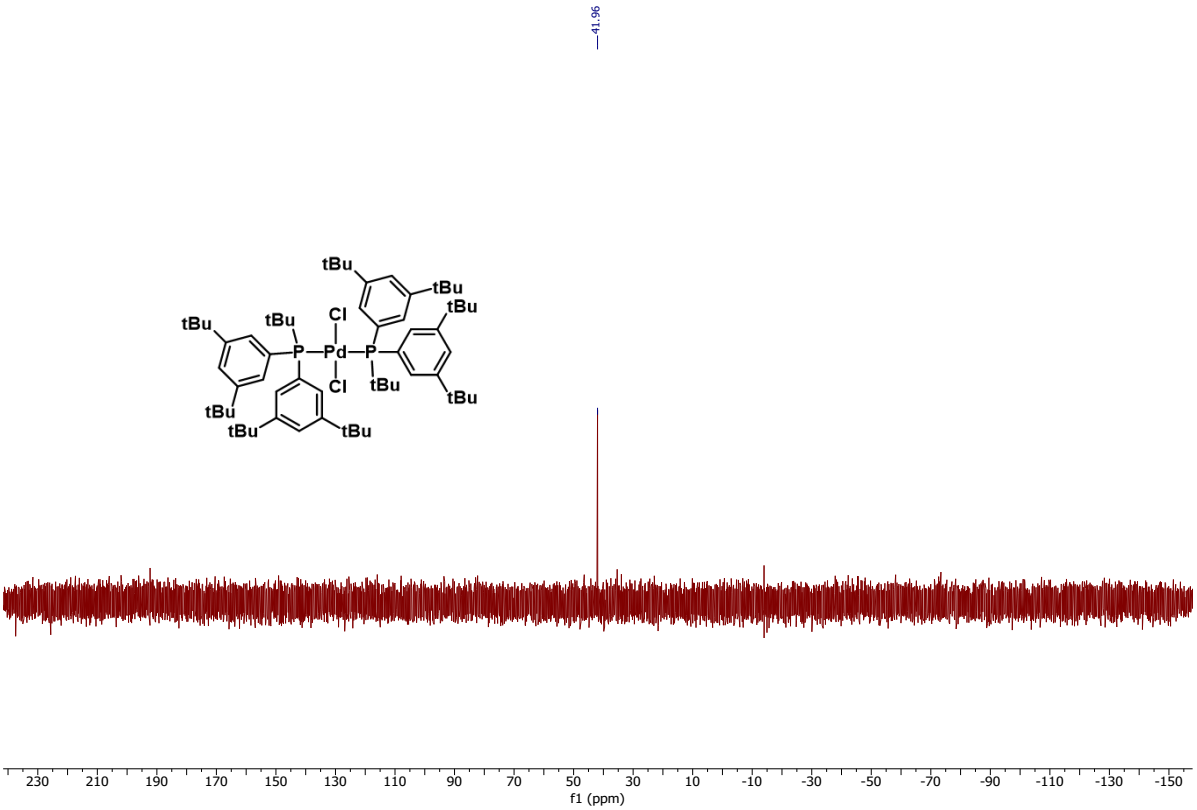

JF3-75_v1c2.1.fid — AV-300 Dual C-H probe proton starting parameters 7/23/03 RN.

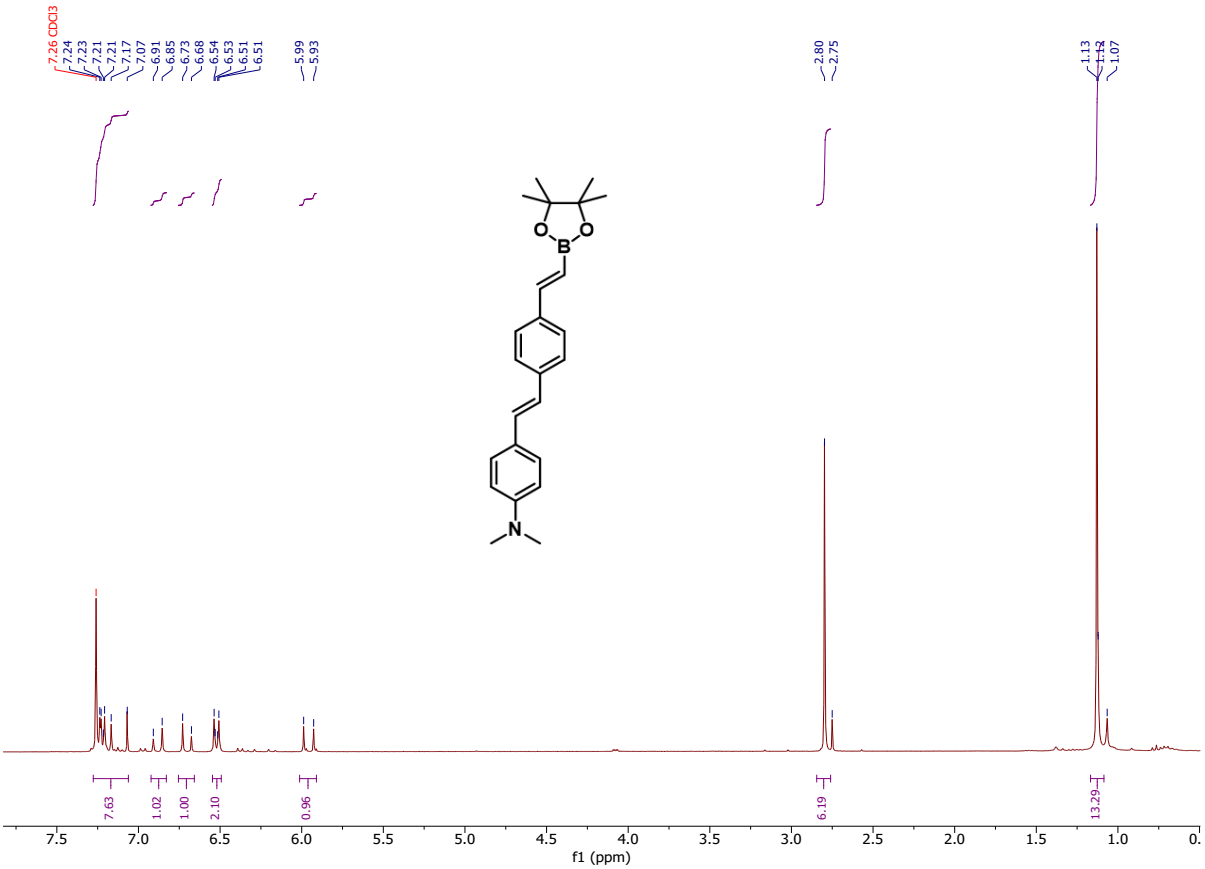

JF4-21_suzuki44-52.1.fid — AVQ-400 QNP Proton starting parameters. 7/16/03. Revised 7/22/03 RN

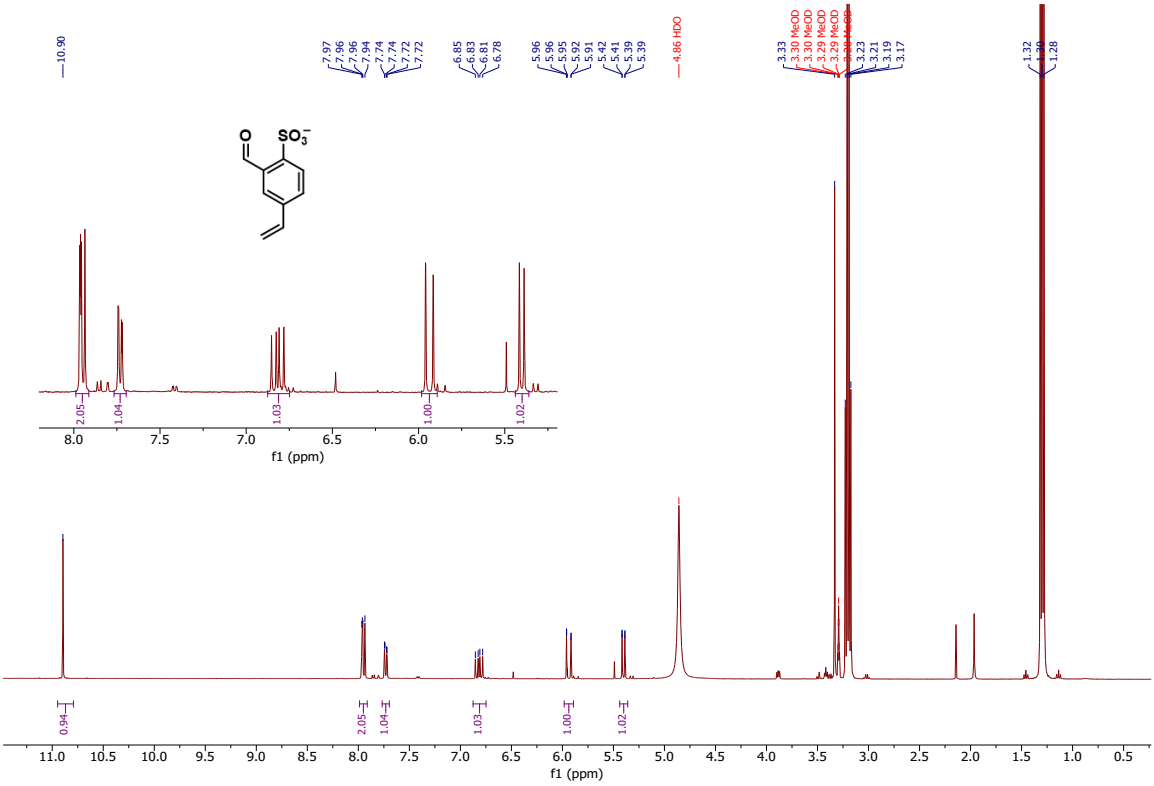

1 (2).1.fid — AV-300 Dual C-H probe proton starting parameters 7/23/03 RN.

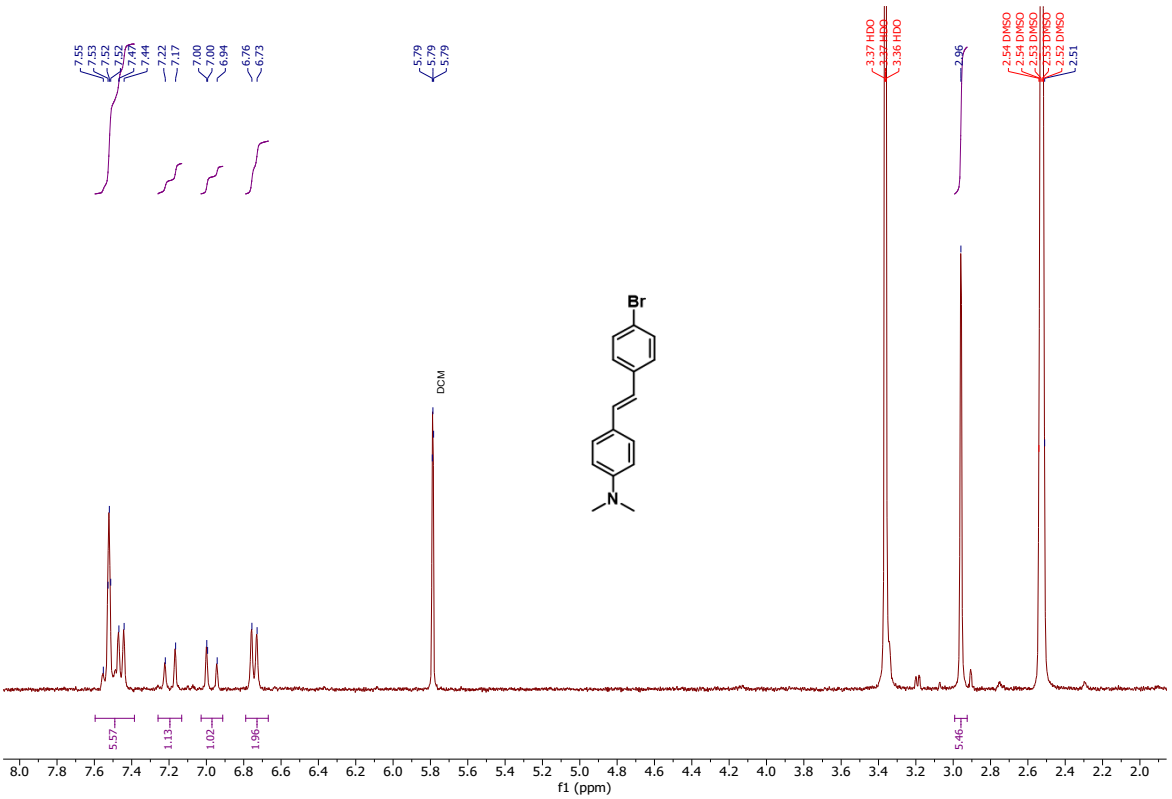

JF4-26_F23-31.1.fid — AV-500 TBI probe — 1H 1D NMR

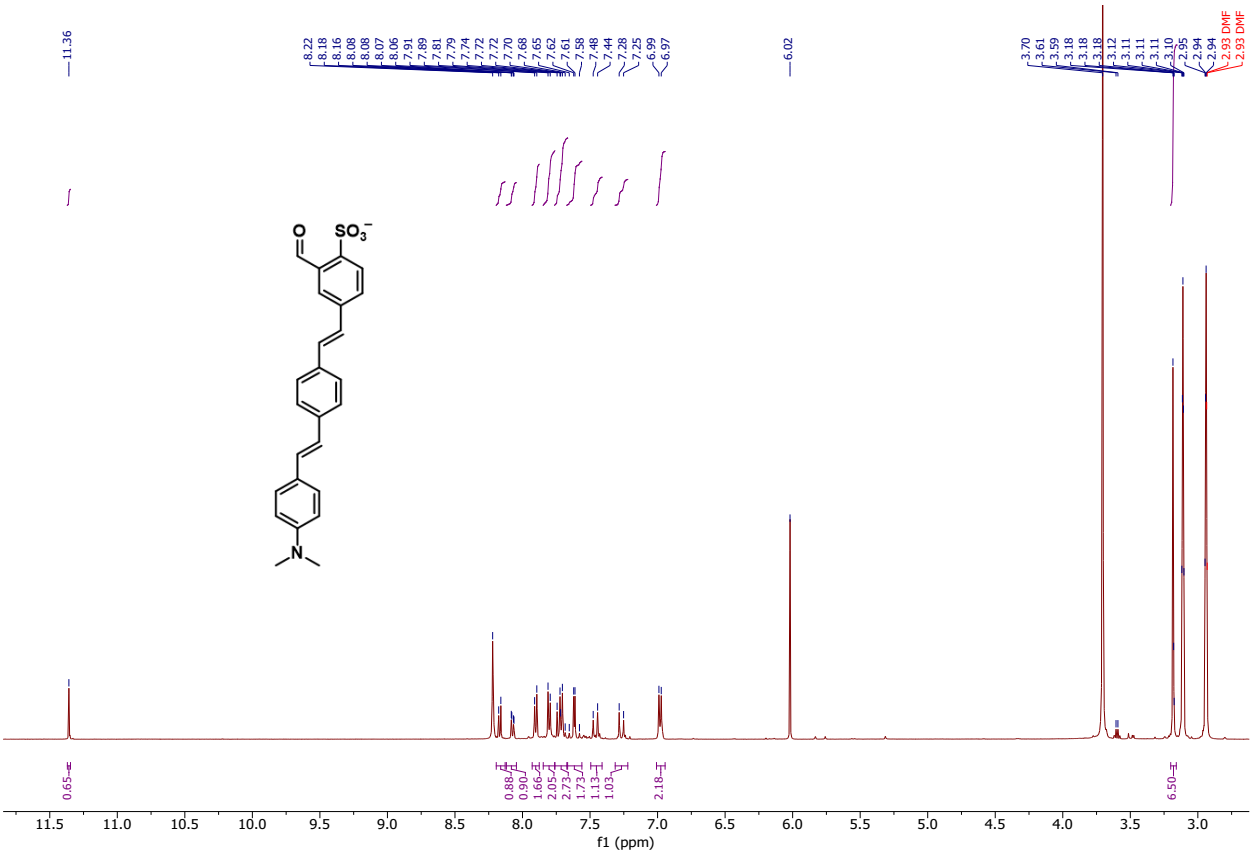

References

(1) DeVasher, R. B.; Moore, L. R.; Shaughnessy, K. H. Aqueous-Phase, Palladium-Catalyzed Cross-Coupling of Aryl Bromides under Mild Conditions, Using Water-Soluble, Sterically Demanding Alkylphosphines. *J. Org. Chem.* **2004**, *69* (23), 7919–7927.

(2) Moseley, J. D.; Murray, P. M.; Turp, E. R.; Tyler, S. N. G.; Burn, R. T. A Mild Robust Generic Protocol for the Suzuki Reaction Using an Air Stable Catalyst. *Tetrahedron* **2012**, *68*, 6010–6017.

(3) Reid, W. B.; Spillane, J. J.; Krause, S. B.; Watson, D. A. Direct Synthesis of Alkenyl Boronic Esters from Unfunctionalized Alkenes: A Boryl-Heck Reaction. *J. Am. Chem. Soc.* **2016**, *138* (17), 5539–5542.

(4) Uno, B. E.; Gillis, E. P.; Burke, M. D. Vinyl MIDA Boronate: A Readily Accessible and Highly Versatile Building Block for Small Molecule Synthesis. *Tetrahedron* **2008**, *65*, 3130–3138.

(5) Geoghegan, K. Selectivity in the Synthesis of Cyclic Sulfonamides: Application in the Synthesis of Natural Products, University College Dublin, Ireland, **2014**.

(6) Von Schenck, H.; Åkermark, B.; Svensson, M. Electronic Control of the Regiochemistry in the Heck Reaction. *J. Am. Chem. Soc.* **2003**, *125*, 3503–3508.

(7) Hayne, D. J.; North, A. J.; Fodero-Tavoletti, M.; White, J. M.; Hung, L. W.; Rigopoulos, A.; McLean, C. A.; Adlard, P. A.; Ackermann, U.; Tochon-Danguy, H.; et al. Rhenium and Technetium Complexes That Bind to Amyloid-β Plaques. *Dalt. Trans.* **2015**, *44* (11), 4933–4944.

(8) Chen, C.-C.; Sasaki, T.; Yamamoto, A.; Liu, J.-H.; Hisaki, I.; Miyata, M.; Tohnai, N. Acidic Proton Modulation of a Stilbene-Based Zwitterionic Sulfonic Acid in the Solid State: Mimicking a Biological Device. *Chem. Lett.* **2013**, *43* (3), 299–301.

(9) Hong, J. L.; Wang, L. Triethanolamine as an Efficient and Reusable Base, Ligand and Reaction Medium for Phosphane-Free Palladium-Catalyzed Heck Reactions. *European J. Org. Chem.* **2006**, No. 22, 5099–5102.

(10) Liu, Z.; Fang, Q.; Wang, D.; Cao, D.; Xue, G.; Yu, W.; Lei, H. Trivalent Boron as an Acceptor in Donor–π–Acceptor-Type Compounds for Single- and Two-Photon Excited Fluorescence. *Chem. - A Eur. J.* **2003**, *9* (20), 5074–5084.